PARTITIONED METHODS FOR COUPLED FLUID FLOW PROBLEMS

by

Hoang A. Tran

B.S. in Mathematics and Computer Sciences,

University of Natural Sciences, Ho Chi Minh City, Vietnam, 2006

France-Vietnam M.S. in Applied Mathematics,

Université d'Orléans, Orléans, France, 2008

Submitted to the Graduate Faculty of

the Department of Mathematics in partial fulfillment

of the requirements for the degree of

Doctor of Philosophy

University of Pittsburgh

2013

UNIVERSITY OF PITTSBURGH

MATHEMATICS DEPARTMENT

This dissertation was presented

by

Hoang A. Tran

It was defended on

April 4th 2013

and approved by

Prof. Catalin Trenchea, Dept. of Mathematics, University of Pittsburgh

Prof. William Layton, Dept. of Mathematics, University of Pittsburgh

Prof. Ivan Yotov, Dept. of Mathematics, University of Pittsburgh

Prof. Noel Walkington , Dept. of Mathematical Sciences, Carnegie Mellon University

Dissertation Advisors: Prof. Catalin Trenchea, Dept. of Mathematics, University of Pittsburgh,

Prof. William Layton, Dept. of Mathematics, University of Pittsburgh

PARTITIONED METHODS FOR COUPLED FLUID FLOW PROBLEMS

Hoang A. Tran, PhD

University of Pittsburgh, 2013

Many flow problems in engineering and technology are coupled in their nature. Plenty of turbulent flows are solved by legacy codes or by ones written by a team of programmers with great complexity. As knowledge of turbulent flows expands and new models are introduced, implementation of modern approaches in legacy codes and increasing their accuracy are of great concern. On the other hand, industrial flow models normally involve multi-physical process or multi-domains. Given the different nature of the physical processes of each sub-problem, they may require different meshes, time steps and methods. There is a natural desire to uncouple and solve such systems by solving each subphysics problem, to reduce the technical complexity and allow the use of optimized legacy sub-problems' codes.

The objective of this work is the development, analysis and validation of new modular, uncoupling algorithms for some coupled flow models, addressing both of the above problems. Particularly, this thesis studies: i) explicitly uncoupling algorithm for implementation of variational multiscale approach in legacy turbulence codes, ii) partitioned time stepping methods for magnetohydrodynamics flows, and iii) partitioned time stepping methods for groundwater-surface water flows. For each direction, we give comprehensive analysis of stability and derive optimal error estimates of our proposed methods. We discuss the advantages and limitations of uncoupling methods compared with monolithic methods, where the globally coupled problems are assembled and solved in one step. Numerical experiments are performed to verify the theoretical results.

TABLE OF CONTENTS

PREFACE . . . x

1.0 INTRODUCTION . . . 1

1.1 Explicitly uncoupled variational multiscale stabilization of fluid flows . . . 1

1.2 Partitioned time stepping methods for magnetohydrodynamic flows . . . 4

1.3 Partitioned time stepping methods for the evolutionary Stokes-Darcy problems 7

1.4 Analytical tools . . . 10

1.5 Thesis outline . . . 11

2.0 EXPLICITLY UNCOUPLED VARIATIONAL MULTISCALE STABILIZATION OF FLUID FLOWS . . . 13

2.1 Method descriptions . . . 13

2.2 Notation and Preliminaries . . . 14

2.3 The Postprocessed VMS Method . . . 17

2.3.1 Growth of Perturbations in the discrete scheme. . . . 29

2.4 Algorithms for Computing the Projection . . . 33

2.5 A Computationally Attractive Variant . . . 36

2.6 Numerical experiments . . . 40

2.6.1 Green-Taylor vortex. . . . 40

2.6.2 Test with an L-shaped discontinuity advected skew to mesh. . . . 41

2.6.3 Decaying Homogeneous Isotropic Turbulence. . . . 43

2.7 Conclusions . . . 49

3.0 PARTITIONED TIME STEPPING METHODS FOR MAGNETOHYDRODYNAMICS FLOWS . . . 51

3.1 Problem setting 51
3.1.1 Notation and preliminaries. 52
3.2 The partitioned time stepping schemes 54
3.3 Stability 55
3.4 Error analysis 59
3.5 Numerical experiments 67
3.5.1 Test 1: Convergence rates 67
3.5.2 Test 2: Stability. 70
3.6 Conclusion 72
4.0 IMPLICIT-EXPLICIT BASED PARTITIONED METHODS FOR THE EVOLUTIONARY STOKES-DARCY PROBLEMS 74
4.1 Introduction 74
4.2 The continuous problem and semi-discrete approximation 76
4.3 Discrete formulation 80
4.4 Long time stability 81
4.4.1 BEFE Stability. 81
4.4.2 BELF Stability. 85
4.5 Error analysis 91
4.6 Numerical experiments 96
4.6.1 Test 1: Convergence rates. 97
4.6.2 Test 2: Stability 98
4.7 Conclusion 103
5.0 SPLITTING BASED PARTITIONED METHODS FOR THE EVOLUTIONARY STOKES-DARCY PROBLEMS 104
5.1 Notations and preliminaries 104
5.2 Discrete formulation 107
5.3 Analysis of stability of SDsplit, BEsplit1/2 and CNsplit 109
5.3.1 SDsplit Stability. 110
5.3.2 BEsplit1 Stability. 113
5.3.3 BEsplit2 Stability. 118

5.3.4 CNsplit Stability. 121
5.4 Numerical experiments 124
5.4.1 Test 1: Convergence rates. 124
5.4.2 Test 2: Stability in case of small parameters. 126
5.5 Conclusion 127
6.0 CONCLUDING REMARKS AND FUTURE RESEARCH 133
6.1 Fast-slow wave splitting for atmospheric and ocean codes 134
BIBLIOGRAPHY 136

LIST OF TABLES

2.1 Error and convergence rate data for Uncoupled VMS where the projection term is solved iteratively. 41

2.2 Error and convergence rate data for Uncoupled VMS where the projection term is lagged. 42

2.3 Corresponding C* for different finite element large scale spaces. 45

3.1 The convergence performance for 1PARA. 68

3.2 The convergence performance for 2SEQU. 68

3.3 The convergence performance for Algorithm 1PARA: more oscillatory true solution. 69

3.4 The convergence performance for Algorithm 2SEQU: more oscillatory true solution. 69

3.5 Comparison of error of 1PARA, 2SEQU and corresponding monolithic methods. 70

4.1 Convergence rate for BEFE with $\Delta t = h$. 98

4.2 Convergence rate for BELF with $\Delta t = h$. 98

4.3 Convergence rate for BEFE with $\Delta t = h^2/5$. 99

4.4 Convergence rate for BELF with $\Delta t = h^2/5$. 99

4.5 Comparison of error of the fully coupled implicit method, BEFE and BELF. . 100

5.1 The convergence performance for SDsplit method. 125

5.2 The convergence performance for BEsplit1 method. 125

5.3 The convergence performance for BEsplit2 method. 126

5.4 The convergence performance for CNsplit method. 126

LIST OF FIGURES

2.1 Flow diagram of a numerical simulation with Uncoupled VMS algorithms . . 38

2.2 Advection of an L-shaped front: Problem description. 43

2.3 Advection of an L-shaped front: the solutions produced by using Backward Euler and Crank-Nicholson schemes in Step 1. 44

2.4 The decay of energy with time for different schemes. 46

2.5 Energy spectra observed with the Smagorinsky model in comparison to a postprocessed Smagorinsky step. 47

2.6 Energy spectra observed with 32^3 degrees of freedom for the velocity and the usual VMS model in comparison to a postprocessed VMS step, and a zoom into the plot on the right. 47

2.7 Energy spectra observed with 64^3 degrees of freedom for the velocity and the usual VMS model in comparison to a postprocessed VMS step. 48

2.8 Number of iterations in Uncoupled VMS where the projection term is solved iteratively and the decay of the L2-norm of the approximated solution. 49

3.1 The decay of system energy computed by 1PARA (left) and 2SEQU (right) with several different time steps chosen. 71

3.2 The decay of system energy computed by 1PARA (left) and 2SEQU (right) with several different time steps chosen and larger parameters 72

4.1 The decay of kinetic energy for different numerical methods. 100

4.2 Variation of kinetic energy with nu=1 and kmin=1.0e-6. 101

4.3 Variation of kinetic energy with nu=1.0e-1 and kmin=1.0e-6. 102

5.1 E^N using different time step sizes and splitting methods with kmin = 1 and S0 = 1.0e-12. 129
5.2 E^N using different time step sizes and splitting methods with kmin = 1.0e-12 and S0 = 1. 129
5.3 E^N using different time step sizes and splitting methods with kmin = 1.0e-3 and S0 = 1.0e-3. 130
5.4 E^N using different time step sizes and splitting methods with kmin = 1.0e-4 and S0 = 1.0e-4. 130
5.5 E^N using different time step sizes and splitting methods with kmin = 1.0e-4 and S0 = 1.0e-12. 131
5.6 E^N using different time step sizes and splitting methods with kmin = 1.0e-12 and S0 = 1.0e-4. 131
5.7 Stability of CNsplit at different small values of kmin and S0. 132

PREFACE

I would like to express my deep appreciation and gratitude to my advisor Dr. Catalin Trenchea. Throughout my years at University of Pittsburgh, he provided constant encouragement, sound advice, great patience and excellent teaching due to those this project was possible. With me, he is not only a great advisor but also a great friend, whose caring extends beyond research progress, and I have thoroughly enjoyed the time we spent to discuss both math and non-math topics.

I wish to thank my co-advisor Dr. William Layton for all his support, caring and inspiration. The confidence he has had in me and his invaluable guidance enabled me to carry out this thesis. He has done an excellent job in aiding me in understanding the deep concepts of fluid dynamics and turbulence models. I must also thank him for teaching me for many additional neccessary tools to build an academic career.

I am very grateful to Dr. Ivan Yotov for his stimulating and enthusiastic lectures, which gave me an insightful understanding of various topics in numerical analysis. My research significantly benefited from his class.

I also wish to thank Dr. Noel Walkington for the time he spent reading my thesis and for his valuable comments and suggestions.

I would like to thank Dr. Volker John at WIAS and Dr. Clayton Webster at ORNL for generously inviting me to visit their institutions, and involving me in the impressive works there.

A special thank to all of my passionate teachers, especially Nguyen Thanh Dung, Tran Nam Dung, Le Ba Khanh Trinh. Their classes nurtured my enthusiasm of mathematics and greatly influenced my decision to pursue a career in math.

Many thanks to my great friends and colleagues, in order of appearance: Tran Vinh

Hung, Nguyen Khac Dinh, Nguyen Tien Khai, Lars Röehe, Nick Hurl, Michaela Kubacki, Marina Moraiti, Xin Xiong, Nan Jiang, Martina Bukač for the wonderful time we studied and discussed mathematics together. I particularly thank Lars Röehe and Xin Xiong, from collaboration with whom I achieved the results appearing in Chapter 2 and 5 of this thesis.

I wish to thank my parents, Tran Van Loan and Dang Thi Viet for their unconditional love and for supporting me in whatever direction I choose. The completion of this work would not have been possible without the constant love, encouragement and understanding of my loving wife, Ha. Words are not enough to express how much grateful I am to her for sharing the past years with me. To her I dedicate this dissertation.

1.0 INTRODUCTION

The flow of liquids and gases occurs in many processes in nature and plays an important role in science and industry. Obtaining accurate, efficient and reliable prediction of quantities in fluid flows is crucial to understand and predict the related real-world phenomena. Many fluid flows in engineering and technology are solved by complex codes or coupled to other physical effects. The ability of fast refining these models when understanding is improved and using the legacy and best codes for subprocesses poses an important modeling problem. This thesis involves the development and testing of new numerical methods which help address the above difficulty in the modeling and simulation of some complex flows. In particular, we have studied

- new variational multiscale algorithms for implementation of modern turbulence models in legacy codes,
- partitioned methods to uncouple flows with electricity and magnetism in magnetohydrodynamics,
- partitioned methods for groundwater - surface water models.

The following sections will describe each of the topics in details.

1.1 EXPLICITLY UNCOUPLED VARIATIONAL MULTISCALE STABILIZATION OF FLUID FLOWS

Numerical simulation of turbulent flows generally requires extremely fine mesh size due to small characteristic size of these structures. This results in solving large systems of equations and large amounts of computing time and power. Clearly, a direct numerical simulation of many interesting and important flows is not practically possible at the present time. One alternative promising approach is large eddy simulation (LES). LES is motivated by the physical idea that the dynamics of the large and small structures of turbulent flows are quite different. The large structures (large eddies) evolve deterministically; in the meantime, the small eddies are sensitive on perturbations of the problem data. Their random character does, however, have universal features so that there is hope that their mean effects on the large eddies can be modelled. The goal of LES thus consists of accurately resolving the large scale features and modeling the effect of missing, unresolved scales on resolved scales. The dominant LES model over the years is Smagorinsky eddy viscosity model. This approach however is unable to successfully separate between large and small scales.

Introduced by Hughes in [61] and used first in turbulence modeling in [62], Variational Multiscale (VMS) method has proven to be a remarkably successful interpretation of the LES concept within a variational formulation of the Navier-Stokes equations. This method uses variational projection to differentiate scales and confines modeling to the small scale equation rather than all scales, overcoming many shortcomings of classical LES. Given the success of the VMS approach, there is a natural desire to introduce a VMS treatment of turbulence within legacy codes, in complex multi-physics applications and in other settings where reprogramming a new method from scratch is daunting. We propose, analyze and test herein (and also in [78]) a method to induce a VMS treatment of turbulence in an existing NSE discretization through an additional, modular and uncoupled projection step. An uncoupled method generally cannot be as accurate as a fully coupled one. We find in our analysis and first tests however that the uncoupled VMS method studied is consistent to a high level with the fully coupled implementation of the same VMS realization and not appreciably less accurate.

To introduce ideas, suppressing spatial discretization and the pressure, write the NSE as

$$\frac{\partial u}{\partial t} + NSE(u) = f.$$

The algorithm we developed adds a modular, uncoupled, projection-like Step 2 to a standard method, Step 1:

Step 1: Call for NSE solver to compute w^{n+1}. Given $u^n \simeq u(t^n)$, for the Crank-Nicholson method:

$$\frac{w^{n+1}-u^n}{\Delta t} + NSE\left(\frac{w^{n+1}+u^n}{2}\right) = \frac{f^{n+1}+f^n}{2}.$$

Step 2: Postprocess w^{n+1} to obtain u^{n+1}: $u^{n+1} = \Pi w^{n+1}$.

Eliminating Step 2 gives

$$\frac{u^{n+1}-u^n}{\Delta t} + NSE\left(\frac{w^{n+1}+u^n}{2}\right) + \boldsymbol{\frac{1}{\Delta t}(w^{n+1} - \Pi w^{n+1})} = \frac{f^{n+1}+f^n}{2}\,. \tag{1.1}$$

We defined the operator Π in Step 2 so that the extra, bold term in (1.1) is exactly a VMS eddy viscosity term acting on marginally resolved scales:

$$u^{n+1} = \Pi w^{n+1} \;\text{ satisfies, for all } v \text{ in the discrete velocity space,}$$
$$(\text{Extra Term}, v) = \frac{1}{\Delta t}(w^{n+1} - u^{n+1}, v) = (\nu_T(x,h)\,[I-P]\,\nabla \frac{w^{n+1}+u^{n+1}}{2}, [I-P]\,\nabla v),$$

where ν_T is the eddy viscosity coefficient and is assumed to be a known, positive, constant elementwise function. Also P is an L^2 projection that defines the VMS velocity gradient averages (so $[I-P]$ defines the fluctuations). The exact formulation of Step 2 does not depend on the time discretization used in Step 1. Therefore, the projection based stabilization in Step 2 is an uncoupled, independent second step and amenable to implementation in legacy codes.

The explicitly uncoupled variant of the VMS method presented in this thesis is based on ideas from filter based postprocessing in [44] and [77]. High *Re* flows have many difficulties including convection dominance and vortex stretching. The former can be studied in linear problems and is much better understood: many stabilized methods are available for convection dominance. In the context herein, these would be included in Step 1. Turbulence models, such as VMS, are directed at nonlinear behavior such as error stretching, backscatter (see [13]), equipartition of energy due to truncation of the energy cascade and so on. Projection based VMS methods give some stabilization for convection dominance, see [72]; they are known to reduce but do not eliminate oscillations near layers, [72, 73]. Properly tuned to mimic energy loss due to breakdown of eddies from resolved to unresolved scales, their added dissipation eliminates equipartition. It also helps control error growth from smaller to larger scales due to vortex stretching. Backscatter is a more complex issue. Within the VMS framework, $E_h u_h$ in (2.5) below is the approximation to $\overline{u}$ and $u_h - E_h u_h$ is the model for u'. Thus, the VMS method we study allows for backscatter from u' to $\overline{u}$ but not from completely unresolved scale to u'.

There is a wide range of methods adding numerical dissipation on all scales of a flow, like e.g. the residual based stabilization techniques [17]. One can find an overview in [106]. In LES modeling the aim is to simulate the large scales of a flow accurately, e.g., [14, 67]. In [61, 51] and [62], the VMS approach to LES was developed. In VMS modeling the velocity is decomposed into means, defined to be that which is resolvable on the given mesh, and the fluctuations being everything else. Only the equation for fluctuations is approximated and the resulting fluctuation model inserted exactly into the mean equation. Several fluctuation models have been used such as defining fluctuations using either a pair of FEM spaces of increasing local polynomial degree or with the same polynomial degree on a finer mesh (the cases considered herein); see [75], and [49, 68] for other work with these choices. The most common choice (that is not considered herein) is to define fluctuations using bubble functions which connects this development of the VMS idea with SUPG and other stabilized methods; see Bensow and Larson [13] and Hsu, Bazilev, Calo, Tezduyar and Hughes [58] for recent and interesting development of this VMS realization.

1.2 PARTITIONED TIME STEPPING METHODS FOR MAGNETOHYDRODYNAMIC FLOWS

The MHD equations describe the motion of electrically conducting, incompressible flows in the presence of a magnetic field. If an electrically conducting fluid moves in a magnetic field, the magnetic field exerts forces which may substantially modify the flow. Conversely, the flow itself gives rise to a second, induced field and thus modifies the magnetic field. Initiated by Alfven in 1942 [1], MHD models occur in astrophysics, geophysics as well as engineering. Understanding these flows is central to many important applications, e.g., liquid metal cooling of nuclear reactors [9, 55, 111], sea water propulsion [87], process metallurgy [34].

The magnetic Reynolds number R_m is an important parameter in MHD, being indicative of the relative strength of induced magnetic field and imposed magnetic field:

$$R_m = \frac{\text{Induced field}}{\text{Applied field}} = \mu\sigma u L.$$

Here μ is the permeability of free space, σ is the electrical conductivity, u and L are the characteristic velocity and length scale correspondingly. Large values of velocity and length scale are unreachable in most industrial and laboratory flows. Consequently, MHD flows in terrestrial applications typically occur at small magnetic Reynolds number. While the magnetic field considerably alters the fluid motion, the induced field is usually found to be negligible by comparison with the imposed field. Neglecting the induced magnetic field reduces MHD models to the reduced MHD system: Given body force $\mathbf{f}$ and external imposed magnetic field $\mathbf{B}$, find the fluid velocity $\mathbf{u}$, pressure p and electric potential ϕ such that:

$$\begin{aligned} \frac{1}{N}(\frac{\partial \mathbf{u}}{\partial t} + \mathbf{u}\cdot\nabla\mathbf{u}) - \frac{1}{M^2}\Delta\mathbf{u} + \nabla p &= \mathbf{f} + (\mathbf{B}\times\nabla\phi + \mathbf{B}\times(\mathbf{B}\times\mathbf{u}))\,, \\ \Delta\phi = \nabla\cdot(\mathbf{u}\times\mathbf{B}), &\text{ and } \nabla\cdot\mathbf{u} = 0. \end{aligned}$$

Here M, N are the Hartman number and interaction parameter given by

$$M = BL\sqrt{\frac{\sigma}{\rho\nu}}, \quad N = \sigma B^2 \frac{L}{\rho u}$$

where B is the characteristic magnetic field, ρ is the density, and ν is the kinematic viscosity, all assumed constant. Justification of using simplified MHD equations to model MHD flows in terrestrial applications can be found in [35, 74, 104]. There are several different, almost equivalent formulations for RMHD. The one we study in this thesis was also considered in [103, 53, 127].

MHD flows involve different physical processes: the motion of fluid is governed by hydrodynamics equations and the electric potential is governed by electrodynamics equations. Despite the importance of MHD in science and engineering and the large computational experience, numerical methods for MHD have not been well developed. The results on existence, uniqueness and finite element approximation of the steady-state MHD problems were developed through work in [125] (for two dimensional case), [103] (for small magnetic Reynolds number case) and [53] (for full MHD flows with perfectly conducting wall condition). In [92, 93, 84, 94], Meir et. al. studied variational methods and numerical approximation for solving stationary MHD equations under more physically realistic boundary conditions that account for the electromagnetic interaction of the fluid with the outside world. For further discussions on mathematical and numerical analysis of steady-state MHD flows, we refer to [52, 37].

There are much less works on time-dependent MHD. Schmidt [108] developed a formulation for evolutionary MHD and established the existence of global-in-time weak solutions via the Galerkin method. To the best of our knowledge, the first paper dealing with time discretization schemes of MHD problems was of Yuksel and Ingram [127], in which the authors studied the stability and error analysis of the fully coupled, monolithic Crank-Nicolson method for reduced MHD equations. In [117], Trenchea proposed a method that decouples of the evolutionary full MHD system in the Elsässer variables. Wilson, Labovsky and Trenchea developed that result by introducing a high-order accurate deferred correction method, which also decouples the MHD system, [124].

In this thesis (and also in [79], [80]), we propose two new implicit-explicit partitioned methods (based on uncoupling physical variables) for solving the evolutionary MHD equations at small magnetic Reynolds number. The methods we study include a first order, one step scheme consisting of implicit discretization of the subproblem terms and explicit discretization of coupling terms.

Algorithm. *Given* $\mathbf{u}^n, p^n, \phi^n$*, find* $\mathbf{u}^{n+1}, p^{n+1}, \phi^{n+1}$ *satisfying*

$$\begin{aligned}\frac{1}{N}\left(\frac{\mathbf{u}^{n+1}-\mathbf{u}^n}{\Delta t}+\mathbf{u}^{n+1}\cdot\nabla\mathbf{u}^{n+1}\right)-\frac{1}{M^2}\Delta\mathbf{u}^{n+1}+\nabla p^{n+1}&\\ =\mathbf{f}^{n+1}+\left(\mathbf{B}\times\nabla\phi^n+\mathbf{B}\times(\mathbf{B}\times\mathbf{u}^{n+1})\right)&,\\ \Delta\phi^{n+1}=\nabla\cdot(\mathbf{u}^n\times\mathbf{B})\ \textit{and}\ \nabla\cdot\mathbf{u}^{n+1}=0.&\end{aligned}$$

The second scheme we consider employs second order, three level backward differentiation formulas (BDF2) discretization for the subproblem terms. The coupling terms are treated by two step extrapolation in Navier-Stokes equation and by implicit method in Maxwell equation. Since one needs the updated value of u at current time level to compute ϕ, this method is uncoupled but sequential: $\phi^n \to \mathbf{u}^{n+1} \to \phi^{n+1}$.

Algorithm. *Given* $\mathbf{u}^{n-1}, \mathbf{u}^n, p^{n-1}, p^n, \phi^{n-1}, \phi^n$, *find* $\mathbf{u}^{n+1}, p^{n+1}, \phi^{n+1}$ *satisfying*

$$\frac{1}{N}\left(\frac{3\mathbf{u}^{n+1} - 4\mathbf{u}^n + \mathbf{u}^{n-1}}{2\Delta t} + \mathbf{u}^{n+1} \cdot \nabla \mathbf{u}^{n+1}\right) - \frac{1}{M^2}\Delta \mathbf{u}^{n+1} + \nabla p^{n+1}$$
$$= \mathbf{f}^{n+1} + \left(\mathbf{B} \times \nabla(2\phi^n - \phi^{n-1}) + \mathbf{B} \times (\mathbf{B} \times \mathbf{u}^{n+1})\right),$$
$$\Delta \phi^{n+1} = \nabla \cdot (\mathbf{u}^{n+1} \times \mathbf{B}) \text{ and } \nabla \cdot \mathbf{u}^{n+1} = 0.$$

We prove that these methods are stable over $0 \le t < \infty$ and convergent at first and second order respectively. In particular, we show that our first order partitioned method is long time stable *without* needing a restriction on time step size Δt, although we treat the coupling terms explicitly. The performance of our methods is compared with that of monolithic method by numerical tests.

1.3 PARTITIONED TIME STEPPING METHODS FOR THE EVOLUTIONARY STOKES-DARCY PROBLEMS

Groundwater, forming two-thirds of the world's fresh water, is vital to human activities. One serious global problem nowadays is groundwater contamination, which occurs when man-made pollutants are dissolved in lakes and rivers and get into the groundwater, making it unsafe and unfit for human use. To predict and control the spread of such contamination requires the accurate solution of coupling of groundwater flows with surface water flows (the Stokes-Darcy problem). The essential problems of estimation of the propagation of pollutants into groundwater are that (i) the different physical processes suggest that codes optimized for each sub-process need to be used for solution of the coupled problem, (ii) the large domains plus the need to compute for several turn-over times for reliable statistics require calculations over long time intervals and (iii) values of some system parameters, e.g., hydraulic conductivity and specific storage, are frequently very small. To address these issues, we study the stability and errors over long time intervals of uncoupled methods for the fully time dependent Stokes-Darcy problem. We are particularly interested in analyzing and comparing the performance of the studied methods for small parameters.

In this work (also in [81, 82]), we propose several implicit-explicit based and splitting based partitioned methods for uncoupling the evolutionary Stokes-Darcy problem. Suppressing technical complexities, write the Stokes-Darcy equation as

$$\begin{aligned}\frac{\partial u}{\partial t} + A_1 u + C\phi &= f,\\ \frac{\partial \phi}{\partial t} + A_2 \phi - C^T u &= g.\end{aligned}$$

where A_1, A_2 are symmetric positive definite (self-adjoint, maximal monotone and coercive) operators. The two equation are linked by exactly skew symmetric coupling. The methods we study herein include the first order **Backward Euler - Forward Euler (BEFE)**, which was also studied in [98]: Given u^n, ϕ^n, find u^{n+1}, ϕ^{n+1} satisfying

$$\begin{aligned}\frac{u^{n+1} - u^n}{\Delta t} + A_1 u^{n+1} + C\phi^n &= f^{n+1},\\ \frac{\phi^{n+1} - \phi^n}{\Delta t} + A_2 \phi^{n+1} - C^T u^n &= g^{n+1},\end{aligned}$$

and **Backward Euler - Leap Frog (BELF)**, a new two step partitioned scheme motivated by the form of the coupling: Given $u^{n-1}, u^n, \phi^{n-1}, \phi^n$, find u^{n+1}, ϕ^{n+1} such that

$$\begin{aligned}\frac{u^{n+1} - u^{n-1}}{2\Delta t} + A_1 u^{n+1} + C\phi^n &= f^{n+1},\\ \frac{\phi^{n+1} - \phi^{n-1}}{2\Delta t} + A_2 \phi^{n+1} - C^T u^n &= g^{n+1}.\end{aligned}$$

We prove the long time (over $0 \leq t < \infty$) stability of both methods and derive an optimal error estimate that is uniform in time over $0 \leq t < \infty$. For uncoupling a coupled problem, general experience with partitioned methods suggests that some price is inevitably paid. Our proposed methods with explicit coupling terms inherit restrictions on time step size Δt

$$\Delta t \leq C_0 \min\{k, S_0\}\, k \tag{1.2}$$

where S_0 is specific storage, k is hydraulic conductivity and C_0 is a generic positive constant independent of mesh size, time step and final time. The values of S_0 and k are frequently very small, see [11], [42], and in those cases, the dependence indicated in (1.2) becomes too pessimistic. To overcome this problem, we propose and analyze four novel uncoupling methods for Stokes-Darcy equations, which have stronger stability properties, using ideas from splitting methods. These methods include ones stable uniformly in S_0 for moderate k and uniformly in k for moderate S_0. They are thus good options when *one* of the parameters is small.

The literature on numerical analysis of methods for the Stokes-Darcy coupled problem has grown extensively since [38], [85]. See [41] for a recent survey and [12], [24], [101], [102], [107], [123] and [85] for theory of the continuum model. There is less work on the fully evolutionary Stokes-Darcy problem. One approach is monolithic discretization by an implicit method followed by iterative solution of the non-symmetric system where subregion uncoupling is attained by using a domain decomposition preconditioner; see, e.g., [24], [23], [22], [97], [20], [36], [40], [39], [60], [66], [95], [120]. Partitioned methods allow parallel, non-iterative uncoupling into one (SPD) Stokes and one (SPD) Darcy system per time step. The first such partitioned method was studied in 2010 by Mu and Zhu [98]. This has been followed by an asynchronous (allow different time steps in the two subregions) partitioned method in [110] and higher order partitioned methods in [21], [83]. In most of these works, stability and convergence were studied over bounded time intervals $0 \le t \le T < \infty$ and the estimates included $e^{\alpha T}$ multipliers.

Alternate approaches for coupling surface water flows with groundwater flows include Brinkman one-domain models, Angot [2], Ingram [64], which are a more accurate description of the physical processes. One-domain Brinkman models are also more computationally expensive. Monolithic quasi-static models (one domain evolutionary and the other assumed to instantly adjust back to equilibrium) have also been studied, e.g., [26]. While they are not considered herein in detail, the methods considered also give non-iterative, domain decomposition schemes for quasi-static models (e.g., set $S_0 \equiv 0$ in (4.7), (4.8) below).

Partitioned methods employ implicit discretizations of the sub-physics/ subdomain problems and explicit time discretizations of the coupling terms, e.g., [118], [98], [18], [19], [25], [32], [31], [30]. Thus there is a very strong connection between application-specific partitioned methods and more general IMEX (IMplicit - EXplicit) methods; the latter developed in, e.g., [121], [119], [5], [33], [45], [63], [45], [3], [32] and [122]. On the other hand, application-specific partitioned methods are often motivated by available codes for subproblems, [118]. Examples of partitioned methods include ones designed for fluid-structure interaction [18], [19], [25], Maxwell's equations, [122] and atmosphere-ocean coupling, [32], [31]. The idea used in our CNsplit scheme to compute in parallel two approximations and then average occurs in the Dyakunov splitting method, e.g., [91], [90], [126], [59].

Long time stable numerical schemes have also been introduced for related problems, especially for 2D Navier-Stokes equations. For such works, we refer to [116], [48], [115] and [71].

1.4 ANALYTICAL TOOLS

In this section, we state some well-known results and assumptions which will be utilized in the analysis throughout this thesis. Let Ω be an open, regular domain in $\mathbb{R}^d$ ($d = 2$ or 3). We denote the $L^2(\Omega)$ norm and inner product by $\|\cdot\|$ and $(\cdot,\cdot)$. Likewise, the $L^p(\Omega)$ norms and the Sobolev $W_p^k(\Omega)$ norms are denoted by $\|\cdot\|_{L^p}$ and $\|\cdot\|_{W_p^k}$, respectively. For the semi-norm in $W_p^k(\Omega)$ we use $|\cdot|_{W_p^k}$. H^k is used to represent the Sobolev space $W_2^k(\Omega)$, and $\|\cdot\|_k$ denotes the norm in H^k. The space H^{-k} denotes the dual space of H_0^k.

Theorem 1.4.1. *(the trace theorem) Let $\partial\Omega$ be a graph of a Lipschitz continuous function. If $u \in L^2(\Omega)$ and $\nabla u \in L^2(\Omega)$, then $u|_{\partial\Omega} \in L^2(\partial\Omega)$ and*

$$u|_{L^2(\partial\Omega)} \leq C\|u\|^{1/2}\left(\|u\|^2 + \|\nabla u\|^2\right)^{1/4}.$$

Theorem 1.4.2. *(the Poincaré inequality) There is a constant $C = C(\Omega)$ such that*

$$\|u\| \leq C\|\nabla u\|$$

for every $u \in H_0^1(\Omega)$.

Theorem 1.4.3. *For any $u, v, w \in H_0^1(\Omega)$, there is $C = C(\Omega)$ such that*

$$\left|\int_\Omega u \cdot \nabla v \cdot w dx\right| \leq C\sqrt{\|u\|\|\nabla u\|}\|\nabla v\|\|\nabla w\|. \tag{1.3}$$

For the proof, see [76].

Lemma 1.4.4. *(discrete Grönwall inequality) Let $D \geq 0$ and κ_n, A_n, B_n, $C_n \geq 0$ for any integer $n \geq 0$ and satisfy*

$$A_N + \Delta t \sum_{n=0}^{N} B_n \leq \Delta t \sum_{n=0}^{N} \kappa_n A_n + \Delta t \sum_{n=0}^{N} C_n + D \text{ for } N \geq 0.$$

Suppose that for all n, $\Delta t \kappa_n < 1$, and set $g_n = (1 - \Delta t \kappa_n)^{-1}$. Then,

$$A_N + \Delta t \sum_{n=0}^{N} B_n \leq exp\left(\Delta t \sum_{n=0}^{N} g_n \kappa_n\right) \left[\Delta t \sum_{n=0}^{N} C_n + D\right] \text{ for } N \geq 0.$$

For the details, see, e.g., [57].

1.5 THESIS OUTLINE

This thesis begins in Chapter 2 with a study of an algorithm for implementation of VMS approach in a legacy turbulence code. A complete stability and convergence analysis of this method is given in Section 2.3. In Section 2.4 we turn to the problem of actually computing the operator in Step 2 efficiently. A related VMS method (adding ideas from [3]) which is slightly less accurate but more efficient is given in Section 2.5. Numerical experiments are given in Section 2.6.

In Chapter 3, we discuss partitioned methods to uncouple conducting fluid flows with electricity and magnetism in magnetohydrodynamics. Our schemes are introduced in Section 3.2. We show in Section 3.3 that these formulations have a stable solution for long time periods. The main convergence results are presented in Theorem 3.4.1. The numerical experiments in Section 3.5 support these theoretical results.

Chapter 4 will be devoted for uncoupling algorithms for solving groundwater - surface water system. Section 4.3 presents two implicit-explicit based partitioned methods for Stokes-Darcy problem: BEFE and BELF. In Theorem 4.4.1 and 4.4.5, we prove that these methods are long time and uniformly in time stable. Section 4.5 (particularly, Theorem 4.5.1) gives a comprehensive error analysis and Section 4.6 follows with numerical tests which confirm the theory.

The study on partitioning the groundwater - surface water flow is extended in Chapter 5. We introduce four uncoupling schemes which are more stable in motivating applications involving small physical parameters. These algorithms are presented in Section 5.2. We analyze long time stability and derive the associated timestep restrictions in Section 5.3. In Section 5.4, we give computational experiments to verify the accuracy and stability of our methods.

2.0 EXPLICITLY UNCOUPLED VARIATIONAL MULTISCALE STABILIZATION OF FLUID FLOWS

2.1 METHOD DESCRIPTIONS

In this chapter, we develop a modular, postprocessing method to implement a variational multiscale method in complex (possibly legacy and possibly laminar) flow codes. Suppressing the pressure and spatial discretization, suppose the Navier-Stokes equations are written as

$$\frac{\partial u}{\partial t} + N(u) + \nu A u = f(t)\,.$$

Add one uncoupled, modular, projection-like step (Step 2) to the standard Crank-Nicolson Finite Element Method (Step 1): given $u^n \simeq u(t^n)$, compute u^{n+1} by

Step 1: Compute w^{n+1} via: $\dfrac{w^{n+1}-u^n}{\Delta t} + N\left(\dfrac{w^{n+1}+u^n}{2}\right) + \nu A\dfrac{w^{n+1}+u^n}{2} = f^{n+1/2}\,,$

Step 2: Postprocess w^{n+1} to obtain u^{n+1}: $u^{n+1} = \Pi w^{n+1}$,

where $f^{n+1/2} = (f^n + f^{n+1})/2$. We will develop theoretical results for the unstabilized Crank-Nicolson FEM in Step 1, but *the setting of Step 2 is independent of the time discretization, see Remark 2.3.4*. The deviations from previous work considered herein are that (1) the projection based stabilization is an uncoupled, independent second step and thus amenable to implementation in legacy codes, and (2) the projection in Step 2 is not a filter but constructed to recover the VMS eddy viscosity term.

Eliminating Step 2 gives

$$\frac{u^{n+1}-u^n}{\Delta t} + N\left(\frac{w^{n+1}+u^n}{2}\right) + \nu A\frac{w^{n+1}+u^n}{2} + \frac{\mathbf{1}}{\mathbf{\Delta t}}(\mathbf{w^{n+1}} - \mathbf{\Pi w^{n+1}}) = f^{n+1/2}\,, \tag{2.1}$$

which is a time relaxation discretization of the original problem with time relaxation coefficient $1/\Delta t$. We define the operator in Step 2 so that (see Section 2.4 for details) the extra, bold term in (2.1) is exactly a VMS eddy viscosity term acting on marginally resolved scales:

$$u^{n+1} = \Pi w^{n+1} \text{ satisfies, for all } v_h \text{ in the discrete velocity space,}$$
$$(\textbf{Extra Term}, v_h) = \frac{1}{\Delta t}(w^{n+1} - u^{n+1}, v_h) = (\nu_T(x,h)\,[I-P]\,\nabla \frac{w^{n+1}+u^{n+1}}{2}, [I-P]\,\nabla v_h).$$

The subscript $h = h(x)$ denotes the local meshwidth of a FEM mesh and P, defined precisely in (2.5), is an L^2 projection that defines the VMS velocity gradient averages (so $[I-P]$ defines the fluctuations). Full details are given in Section 2.3. Also $\nu_T(x,h)$ is the chosen eddy viscosity coefficient. We shall assume (motivated by the nonlinear case in which its value is often extrapolated from previous time levels) in this report that:

Condition 2.1.1. *$\nu_T = \nu_T(x,h)$ is a known, positive, bounded function which is constant elementwise.*

2.2 NOTATION AND PRELIMINARIES

We define the norms ($1 \le m < \infty$)

$$\|v\|_{\infty,k} \;:=\; EssSup_{[0,T]}\|v(t,\cdot)\|_k\,, \text{ and } \|v\|_{m,k} \;:=\; \left(\int_0^T \|v(t,\cdot)\|_k^m\,dt\right)^{1/m}.$$

for functions $v(x,t)$ defined on the entire time interval $(0,T)$. The Navier-Stokes equation with boundary and initial condition are: Given time $T > 0$, body force f, find velocity $u : [0,T]\times\Omega \to \mathbb{R}^d$, pressure $p : [0,T]\times\Omega \to \mathbb{R}$ satisfying

$$\begin{aligned} u_t + u\cdot\nabla u - \nu\Delta u + \nabla p = f(x) \text{ and } \nabla\cdot u = 0 \text{ in } \Omega,\ \text{for } 0 < t \le T \\ u(x,0) = u^0(x) \text{ in } \Omega,\ u = 0 \text{ on } \partial\Omega,\ \text{for } 0 < t \le T. \end{aligned} \tag{2.2}$$

The velocity and pressure spaces are

$$X := (H_0^1(\Omega))^d,\ Q := L_0^2(\Omega), \text{ with } \|v\|_X := \|\nabla v\|.$$

The space of divergence free functions is given by

$$V := \{v \in X : \ (\nabla \cdot v, q) = 0 \ \ \forall q \in Q\}.$$

A weak formulation of (2.2) is: Find $u : [0,T] \to X$, $p : [0,T] \to Q$ for a.e. $t \in (0,T]$ satisfying

$$(u_t, v) + (u \cdot \nabla u, v) - (p, \nabla \cdot v) + \nu(\nabla u, \nabla v) = (f, v) \ \ \forall v \in X \tag{2.3}$$

$$u(x,0) = u^0 \text{ in } X \text{ and } (\nabla \cdot u, q) = 0 \qquad \forall q \in Q. \tag{2.4}$$

We consider our analysis on the finite element method (FEM) for the spatial discretization (the results extend to many other variational methods). The finite element velocity and pressure spaces considered are built on a conforming, edge to edge triangulation with maximum triangle parameter denoted by a subscript "h". We assume that they satisfy the usual discrete inf-sup condition for div-stability. For a given selection of velocity and pressure elements, this can require enrichment by bubbles or impose implicitly a condition on the mesh. In our tests we have used the common Taylor-Hood pair of conforming quadratics for velocity and conforming linears for pressure. There are many cases where low order elements and very fine meshes are needed. These often require additional stabilizations for the incompressibility-pressure coupling. Extension of the methods herein to include such stabilizations is naturally an important problem that must be analyzed and tested on a case by case approach. We shall denote conforming velocity, pressure finite element spaces by

$$X_h \subset X, \ Q_h \subset Q.$$

We also must select a space of "well resolved" velocities and pressures, denoted by

$$X_H \subset X, \ Q_H \subset Q.$$

Three commonly seen examples of the definition of the well resolved spaces are:

- The fine space (containing means and fluctuations) X_h arises from augmentation of a given FEM space X_H with element bubble functions; see Hsu, Bazilev, Calo, Tezduyar and Hughes [58].

- A coarse mesh velocity and pressure space $X_H,\ Q_H$ (with meshwidth denoted by subscript $H \leq \sqrt{h}$) is constructed. If the meshes are nested and the space uses the same elements as the fine mesh space then $X_H \subset X_h \subset X,\ Q_H \subset Q_h \subset Q$; see [50, 89] for examples.
- The space of well refined velocities and pressures are defined on the same mesh but using finite element spaces of lower polynomial degree. In this case also $X_H \subset X_h \subset X,\ Q_H \subset Q_h \subset Q$; see [68, 105] for examples.

The first approach is most commonly seen and not considered herein. The second requires a code with only one element but pointers between the two meshes (as are commonly found with $h-$adaptive codes) while the third works only on one mesh but requires at least two velocity elements (such as in $p-$adaptive codes). We shall assume that $X_{H/h},\ Q_{H/h}$ satisfy the usual inf-sup condition necessary for the stability of the pressure, e.g. [54]. The discretely divergence free subspace of $X_{H/h}$ is

$$V_{H/h} = \{v_{H/h} \in X_{H/h} : (\nabla \cdot v_{H/h}, q_{H/h}) = 0 \ \ \forall q_{H/h} \in Q_{H/h}\}.$$

Note that $V_H \not\subseteq V_h$ in general. Taylor-Hood elements (see [16, 54]) are one common example of such a choice for $(X_h,\ Q_h)$, and are also the elements we use in our numerical experiments. Further, we denote the space of (typically discontinuous) coarse mesh velocity gradient tensors by

$$L_H := \nabla X_H = \{\nabla v_H : \text{ for all } v_H \in X_H\},$$

and analogously for L_h. The weighted L^2 and elliptic projections are defined as usual (in general and in this specific case following [14], Section 11.6) by

$$\begin{aligned} P_H \nabla u = G_H \in L_H \text{ satisfies } (\nu_T(x,h)\left[G_H - \nabla u\right], l_H) = 0, \forall\, l_H \in L_H, \\ E_H u = \widetilde{u} \in X_H \text{ satisfies } (\nu_T(x,h)\left[\nabla\widetilde{u} - \nabla u\right], \nabla v_H) = 0, \forall\, v_H \in X_H. \end{aligned} \tag{2.5}$$

The motivation for the definition in (2.5) is that means (and thus fluctuations) defined by elliptic projection are equivalent to means of deformations defined by L^2 projection (see [14], Lemma 11.10)

$$\overline{u} := E_H u,\ P_H \nabla u = \nabla E_H u.$$

Further, while computation of velocity means is global, when the means of deformation are defined by L^2 projection into a C^0 finite element space, $P_H\nabla u$ can be computed in parallel element by element.

Define the usual, explicitly skew symmetrized trilinear form

$$b(u,v,w) := \frac{1}{2}(u\cdot\nabla v, w) - \frac{1}{2}(u\cdot\nabla w, v).$$

Let $v(t^{n+1/2}) = v((t^{n+1}+t^n)/2)$ for a continuous function in time and $v^{n+1/2} = (v^{n+1}+v^n)/2$ for functions of time that are both continuous and discrete.

2.3 THE POSTPROCESSED VMS METHOD

In this section we will give a precise formulation of the method and prove stability and an a priori error estimate.

Definition 2.3.1. *Given w_h^{n+1}, $u_h^{n+1} = \Pi w_h^{n+1} \in V_h$ is the (unique) solution of*

$$\begin{aligned}\left(\frac{w_h^{n+1}-u_h^{n+1}}{\Delta t}, v_h\right) &= \left(\nu_T[I-P_H]\nabla\frac{w_h^{n+1}+u_h^{n+1}}{2}, [I-P_H]\nabla v_h\right)\\ &\quad + \left(\lambda_h^{n+1}, \nabla\cdot v_h\right) \text{ for all } v_h\in X_h \\ \left(\nabla\cdot u_h^{n+1}, q_h\right) &= 0 \text{ for all } q_h\in Q_h\end{aligned} \tag{2.6}$$

Step 2 requires taking a velocity on a mesh and from that solving Stokes like problems either on a different mesh followed by interpolation back to the mesh used for Step 1 or on the same mesh. Our analysis assumes Step 2 will be performed on the mesh used for Step 1. Extending the method and numerical analysis to the case of using Step 2 treating Step 1 as a black box solver requires this extra error (and other subtleties as well) to be understood. The form of the uncoupled projection step of Step 2 does not depend on the time discretization scheme used in Step 1.

Algorithm 2.3.2. *Given u_h^n compute u_h^{n+1} by*

Step 1: Compute $w_h^{n+1} \in V_h$ satisfying: for all $v_h \in V_h$

$$\left(\frac{w_h^{n+1} - u_h^n}{\Delta t}, v_h\right) + b\left(\frac{w_h^{n+1} + u_h^n}{2}, \frac{w_h^{n+1} + u_h^n}{2}, v_h\right) + \nu\left(\nabla\frac{w_h^{n+1} + u_h^n}{2}, \nabla v_h\right) = \left(f^{n+1/2}, v_h\right)$$

Step 2: Apply projection Π on w_h^{n+1} to obtain u_h^{n+1}

$$u_h^{n+1} = \Pi w_h^{n+1}.$$

Eliminating Step 2 gives

$$\left(\frac{u_h^{n+1} - u_h^n}{\Delta t}, v_h\right) + b\left(\frac{w_h^{n+1} + u_h^n}{2}, \frac{w_h^{n+1} + u_h^n}{2}, v_h\right) + \nu\left(\nabla\frac{w_h^{n+1} + u_h^n}{2}, \nabla v_h\right) + \left(\frac{w_h^{n+1} - \Pi w_h^{n+1}}{\Delta t}, v_h\right) = \left(f^{n+1/2}, v_h\right).$$

The last term on the left hand side is the additional term from Step 2. By definition (2.6), this term recovers the VMS eddy viscosity term and the projected velocity is discretely divergence free. The following lemma quantifies the eddy viscosity induced by Step 2.

Lemma 2.3.3. ***[Numerical Dissipation induced by Step 2]*** *Let ν_T fulfill Condition 2.1.1. Then, there holds*

$$\left\|w_h^{n+1}\right\|^2 = \left\|u_h^{n+1}\right\|^2 + 2\Delta t\left\|\sqrt{\nu_T}[I - P_H]\nabla\frac{w_h^{n+1} + u_h^{n+1}}{2}\right\|^2.$$

Proof. Set $v_h = \frac{w_h^{n+1} + u_h^{n+1}}{2}$ and $q_h = \lambda_h^{n+1}$ in (2.6) and obtain

$$\frac{1}{2\Delta t}\left(\| w_h^{n+1}\|^2 - \| u_h^{n+1}\|^2\right) = \left\|\sqrt{\nu_T}[I - P_H]\nabla\frac{w_h^{n+1} + u_h^{n+1}}{2}\right\|^2,$$

where we used that $w_h^{n+1} \in V_h$. This already proves the claim after rearranging. □

Remark 2.3.4. *The special choice in (2.6) used in Step 2 with the argument of the form*

$$\frac{w_h^{n+1} + u_h^{n+1}}{2} (\text{and not } \frac{w_h^{n+1} + u_h^{n}}{2})$$

does not depend on the time discretization scheme in Step 1. With a different discretization used in Step 1 we would get the same induced eddy dissipation terms in Step 2 within the proof of Lemma 2.3.3. This is why the explicitly uncoupled Step 2 of Algorithm 2.3.2 does not depend on the time discretization scheme in Step 1 and why Step 2 can be used with an arbitrary CFD code.

Lemma 2.3.3 is one key to prove stability of Algorithm 2.3.2.

Theorem 2.3.5. *Let ν_T satisfy Condition 2.1.1, then*

$$\frac{1}{2}\| u_h^N\|^2 + \Delta t \sum_{n=0}^{N-1}\left[\frac{\nu}{2}\left\|\nabla \frac{w_h^{n+1} + u_h^n}{2}\right\|^2 + \left\|\sqrt{\nu_T}[I - P_H]\nabla \frac{w_h^{n+1} + u_h^{n+1}}{2}\right\|^2\right]$$
$$\leq \frac{1}{2}\| u_h^0\|^2 + \frac{\Delta t}{2\nu}\sum_{n=0}^{N-1}\left\| f^{n+1/2}\right\|_{-1}^2 .$$

Proof. Set $v_h = \frac{w_h^{n+1} + u_h^n}{2}$ in Step 1 and obtain

$$\frac{1}{2\Delta t}\left(\| w_h^{n+1}\|^2 - \| u_h^n\|^2\right) + \nu\left\|\nabla \frac{w_h^{n+1} + u_h^n}{2}\right\|^2 = \left(f^{n+1/2}, \frac{w_h^{n+1} + u_h^n}{2}\right).$$

Application of Lemma 2.3.3 to this equation gives

$$\frac{1}{2\Delta t}\left(\| u_h^{n+1}\|^2 - \| u_h^n\|^2\right) + \left[\nu\left\|\nabla \frac{w_h^{n+1} + u_h^n}{2}\right\|^2 + \left\|\sqrt{\nu_T}[I - P_H]\nabla \frac{w_h^{n+1} + u_h^{n+1}}{2}\right\|^2\right]$$
$$= \left(f^{n+1/2}, \frac{w_h^{n+1} + u_h^n}{2}\right).$$

Summing this up from $n = 0$ to $n = N - 1$ results in

$$\frac{1}{2}\| u_h^N\|^2 + \Delta t \sum_{n=0}^{N-1}\left[\nu\left\|\nabla \frac{w_h^{n+1} + u_h^n}{2}\right\|^2 + \left\|\sqrt{\nu_T}[I - P_H]\nabla \frac{w_h^{n+1} + u_h^{n+1}}{2}\right\|^2\right]$$
$$= \frac{1}{2}\| u_h^0\|^2 + \Delta t \sum_{n=0}^{N-1}\left(f^{n+1/2}, \frac{w_h^{n+1} + u_h^n}{2}\right), \quad (2.7)$$

where we can apply Young's inequality to the right hand side inside the sum to see

$$\Delta t\left(f^{n+1/2}, \frac{w_h^{n+1} + u_h^n}{2}\right) \leq \frac{\Delta t}{2\nu}\left\| f^{n+1/2}\right\|_{-1}^2 + \frac{\nu\Delta t}{2}\left\|\nabla \frac{w_h^{n+1} + u_h^n}{2}\right\|^2 .$$

Hiding the last term on the left hand side of (2.7) proves the claim. ∎

Theorem 2.3.5 also gives a stability estimate for w_h^N. In particular, Corollary 2.3.6 shows that w_h^N is also not the usual CN approximation.

Corollary 2.3.6. *Let ν_T fulfill Condition 2.1.1, then*

$$\frac{1}{2}\left\| w_h^N\right\|^2 + \Delta t \sum_{n=0}^{N-1} \frac{\nu}{2}\left\|\nabla \frac{w_h^{n+1} + u_h^n}{2}\right\|^2 + \Delta t \sum_{n=0}^{N-2}\left\|\sqrt{\nu_T}[I - P_H]\nabla \frac{w_h^{n+1} + u_h^{n+1}}{2}\right\|^2$$
$$\leq \frac{1}{2}\left\| u_h^0\right\|^2 + \frac{\Delta t}{2\nu}\sum_{n=0}^{N-1}\left\| f^{n+1/2}\right\|_{-1}^2.$$

Proof. Apply Lemma 2.3.3 for $\|w_h^N\|^2$ to Theorem 2.3.5. □

As a next step we will give an a priori error estimate for the approximation scheme, Algorithm 2.3.2. Let $t^n = n\Delta t$, $n = 0, 1, 2, \ldots, N_T$, and $T := N_T \Delta t$. Also introduce the following discrete norms:

$$|||v|||_{\infty,k} := \max_{0\le n\le N_T} \|v^n\|_k\,, \qquad |||v_{1/2}|||_{\infty,k} := \max_{1\le n\le N_T} \|v^{n-1/2}\|_k\,,$$
$$|||v|||_{m,k} := \left(\sum_{n=0}^{N_T} \|v^n\|_k^m \Delta t\right)^{1/m}, \qquad |||v_{1/2}|||_{m,k} := \left(\sum_{n=1}^{N_T} \|v^{n-1/2}\|_k^m \Delta t\right)^{1/m}.$$

In order to establish the optimal asymptotic error estimates for the approximation we need to assume the following regularity of the true solution:

$$\begin{aligned} &u \in L^\infty(0,T;H^{k+1}(\Omega)) \cap H^1(0,T;H^{k+1}(\Omega)) \cap H^3(0,T;L^2(\Omega)) \cap W_4^2(0,T;H^1(\Omega)),\\ &p \in L^\infty(0,T;H^{s+1}(\Omega))\,, \text{ and } f \in H^2(0,T;L^2(\Omega)). \end{aligned} \tag{2.8}$$

For the error between $u^n - u_h^n$ we have the following theorem and corollary.

Theorem 2.3.7. *For u, p, and f satisfying (2.8), (2.3) and (2.4), and u_h^n, w_h^n given by Algorithm 2.3.2 we have that, for Δt sufficiently small,*

$$
\begin{aligned}
\frac{1}{2}\|u^N - u_h^N\|^2 + \frac{\Delta t}{4}\sum_{n=0}^{N-1}\Big(&\nu\|\nabla(u(t^{n+1/2}) - (w_h^{n+1} + u_h^n)/2)\|^2 \\
&+ \|\sqrt{\nu_T}[I - P_H]\nabla(u^{n+1} - (w_h^{n+1} + u_h^{n+1})/2)\|^2\Big) \\
\le Ch^{2k+2}|||u|||^2_{\infty,k+1} &+ C\nu h^{2k}|||u|||^2_{2,k+1} + C\nu_T h^{2k}|||u|||^2_{2,k+1} + C\nu_T H^{2k}|||u|||^2_{2,k+1} \\
&+ C\frac{h^{2k}}{\nu^2}|||u|||^2_{\infty,k+1} + C\frac{h^{2k+1}}{\nu}\left(|||u|||^4_{4,k+1} + |||\nabla u|||^4_{4,0}\right) + C\frac{h^{2s+2}}{\nu}|||p_{1/2}|||^2_{2,s+1} \\
&+ Ch^{2k+2}|||u_t|||^2_{2,k+1} + C(\Delta t)^4\Big(\frac{1}{\nu}|||\nabla u|||^4_{4,0} + \frac{1}{\nu}|||\nabla u_{1/2}|||^4_{4,0} \\
&+ |||u_{ttt}|||^2_{2,0} + \nu|||\nabla u_{tt}|||^2_{2,0} + \frac{1}{\nu}|||\nabla u_{tt}|||^4_{4,0} + |||f_{tt}|||^2_{2,0}\Big).
\end{aligned}
$$

For $k = 2$, $s = 1$ Taylor-Hood elements, i.e. C^0 piecewise quadratic velocity space X_h and C^0 piecewise linear pressure space Q_h, we have the following asymptotic estimate.

Corollary 2.3.8. *Under the assumptions of Theorem 2.3.7, with $\Delta t = Ch$, $\nu_T = h^2$, $H = \sqrt{h}$ and (X_h, Q_h) given by the Taylor-Hood approximation elements, we have*

$$
\begin{aligned}
\|u^N - u_h^N\|^2 + \frac{\Delta t}{2}\sum_{n=0}^{N-1}\Big(&\nu\|\nabla(u(t^{n+1/2}) - (w_h^{n+1} + u_h^n)/2)\|^2 \\
&+ \|\sqrt{\nu_T}[I - P_H]\nabla(u^{n+1} - (w_h^{n+1} + u_h^{n+1})/2)\|^2\Big) \le \; C\left((\Delta t)^4 + h^4\right).
\end{aligned}
$$

The rest of this section is devoted for proving Theorem 2.3.7. This proof is technical and exhibits the usual limitations in the final result that arise from employing the discrete Grönwall inequality of exponential error growth and the assumption that Δt is sufficiently small.

Proof. (of Theorem 2.3.7) Denote $\tilde{w}_h^{n+1/2} := \frac{w_h^{n+1}+u_h^n}{2}$. To begin the analysis we rewrite Algorithm 2.3.2. As the spaces X_h and Q_h satisfy the usual inf-sup condition, Algorithm

2.3.2 is equivalent to:

For $n = 0, 1, \dots, N_T - 1$ *find* w_h^{n+1}, $u_h^{n+1} \in V_h$ *such that*

$$(w_h^{n+1}, v_h) + \Delta t\, b(\tilde{w}_h^{n+1/2}, \tilde{w}_h^{n+1/2}, v_h) + \Delta t\, \nu(\nabla \tilde{w}_h^{n+1/2}, \nabla v_h) \\ = (u_h^n, v_h) + \Delta t\, (f^{n+1/2}, v_h), \ \forall v_h \in V_h, \qquad (2.9)$$

$$\frac{1}{\Delta t}(w_h^{n+1} - u_h^{n+1}, v_h) = (\nu_T\, [I - P_H]\, \nabla \frac{w_h^{n+1} + u_h^{n+1}}{2}, [I - P_H]\, \nabla v_h), \ \forall v_h \in V_h. \qquad (2.10)$$

To establish the optimal asymptotic error estimates for the approximation we assume true solution satisfies the regularity condition (2.8) from Section 2.3:

At time $t^{n+1/2} = (n + 1/2)\Delta t$ the true solution u of (2.3), (2.4) satisfies

$$(u^{n+1} - u^n, v_h) + \Delta t\, \nu(\nabla u^{n+1/2}, \nabla v_h) + \Delta t\, b(u^{n+1/2}, u^{n+1/2}, v_h) - \Delta t\, (p(t^{n+1/2}), \nabla \cdot v_h) \\ = \Delta t\, (f^{n+1/2}, v_h) + \Delta t\, Intp(u^{n+1}; v_h)\ , \qquad (2.11)$$

for all $v_h \in V_h$, where $Intp(u^{n+1}; v_h)$, representing the consistency error, denotes

$$Intp(u^{n+1}; v_h) = \big((u^{n+1} - u^n)/\Delta t - u_t(t^{n+1/2}), v_h\big) + \nu(\nabla u^{n+1/2} - \nabla u(t^{n+1/2}), \nabla v_h) \\ + b(u^{n+1/2}, u^{n+1/2}, v_h) - b(u(t^{n+1/2}), u(t^{n+1/2}), v_h) \\ + (f(t^{n+1/2}) - f^{n+1/2}, v_h)\,. \qquad (2.12)$$

We split the error into a Step 1 error ε_h according to (2.9), a Step 2 error e_h according to (2.10), and an approximation error Λ

$$\begin{aligned} u^{n+1} - w_h^{n+1} &= (u^{n+1} - I_h u^{n+1}) + (I_h u^{n+1} - w_h^{n+1}) =: \Lambda^{n+1} + \varepsilon_h^{n+1}, \\ u^{n+1} - u_h^{n+1} &= (u^{n+1} - I_h u^{n+1}) + (I_h u^{n+1} - u_h^{n+1}) =: \Lambda^{n+1} + e_h^{n+1}, \end{aligned} \qquad (2.13)$$

where $I_h u^{n+1} \in V_h$ will be an interpolation of u^{n+1} in V_h later in the proof but is an arbitrary element in V_h at this point. Now we subtract (2.9) from (2.11) and use $\frac{1}{2}(\varepsilon_h^{n+1} + e_h^n) \in V_h$ as test function v_h to obtain

$$\frac{1}{2}\left(\|\varepsilon_h^{n+1}\|^2 - \|e_h^n\|^2\right) + \Delta t\, \nu \|\nabla \frac{1}{2}(\varepsilon_h^{n+1} + e_h^n)\|^2 = \\ - (\Lambda^{n+1} - \Lambda^n, \frac{1}{2}(\varepsilon_h^{n+1} + e_h^n)) - \Delta t\, \nu(\nabla \Lambda^{n+1/2}, \nabla \frac{1}{2}(\varepsilon_h^{n+1} + e_h^n)) \\ - \Delta t\, b(u^{n+1/2}, u^{n+1/2}, \frac{1}{2}(\varepsilon_h^{n+1} + e_h^n)) + \Delta t\, b(\tilde{w}_h^{n+1/2}, \tilde{w}_h^{n+1/2}, \frac{1}{2}(\varepsilon_h^{n+1} + e_h^n)) \\ + \Delta t(p(t^{n+1/2}) - q_h^{n+1}, \nabla \cdot \frac{1}{2}(\varepsilon_h^{n+1} + e_h^n)) + \Delta t\, Intp(u^{n+1}; \frac{1}{2}(\varepsilon_h^{n+1} + e_h^n)). \qquad (2.14)$$

The key to this equation is that $\frac{1}{2}(\varepsilon_h^{n+1}+e_h^n)$ is discretely divergence free and hence a possible test function v_h. Next we estimate the terms on the RHS of (2.14) and get

$$
\begin{aligned}
&(\Lambda^{n+1}-\Lambda^n,\frac{1}{2}(\varepsilon_h^{n+1}+e_h^n)) \le \frac{1}{2}\Delta t\|\frac{\Lambda^{n+1}-\Lambda^n}{\Delta t}\|^2+\frac{1}{2}\Delta t\|\frac{1}{2}(\varepsilon_h^{n+1}+e_h^n)\|^2\\
&= \frac{1}{2}\Delta t\int_\Omega\left(\frac{1}{\Delta t}\int_{t^n}^{t^{n+1}}\Lambda_t\,dt\right)^2 d\Omega \;+\frac{1}{2}\Delta t\|\frac{1}{2}(\varepsilon_h^{n+1}+e_h^n)\|^2\\
&\le \frac{1}{2}\Delta t\int_\Omega\left(\frac{1}{\Delta t}\int_{t^n}^{t^{n+1}}|\Lambda_t|^2\,dt\right) d\Omega \;+\frac{1}{2}\Delta t\|\frac{1}{2}(\varepsilon_h^{n+1}+e_h^n)\|^2\\
&\le \frac{1}{2}\int_{t^n}^{t^{n+1}}\|\Lambda_t\|^2\,dt \;+\frac{1}{4}\Delta t\left(\|\varepsilon_h^{n+1}\|^2\;+\;\|e_h^n\|^2\right),
\end{aligned}
\tag{2.15}
$$

$$
\nu(\nabla\Lambda^{n+1/2},\nabla\frac{1}{2}(\varepsilon_h^{n+1}+e_h^n))\;\le\;\frac{\nu}{10}\|\nabla\frac{1}{2}(\varepsilon_h^{n+1}+e_h^n)\|^2\;+\;C\nu\,\|\nabla\Lambda^{n+1/2}\|^2\,. \tag{2.16}
$$

We rewrite $b(u^{n+1/2}\,,u^{n+1/2}\,,\,\frac{1}{2}(\varepsilon_h^{n+1}+e_h^n))\;-\;b(\tilde{w}_h^{n+1/2},\tilde{w}_h^{n+1/2},\frac{1}{2}(\varepsilon_h^{n+1}+e_h^n))$ as

$$
\begin{aligned}
&b(u^{n+1/2}\,,u^{n+1/2}\,,\,\frac{1}{2}(\varepsilon_h^{n+1}+e_h^n))\;-\;b(\tilde{w}_h^{n+1/2},\tilde{w}_h^{n+1/2},\frac{1}{2}(\varepsilon_h^{n+1}+e_h^n))\\
&=\;b(u^{n+1/2}\,,u^{n+1/2}\,,\,\frac{1}{2}(\varepsilon_h^{n+1}+e_h^n))\;-\;b(\tilde{w}_h^{n+1/2},u^{n+1/2},\frac{1}{2}(\varepsilon_h^{n+1}+e_h^n))\\
&\quad+\;b(\tilde{w}_h^{n+1/2},u^{n+1/2},\frac{1}{2}(\varepsilon_h^{n+1}+e_h^n))\;-\;b(\tilde{w}_h^{n+1/2},\tilde{w}_h^{n+1/2},\frac{1}{2}(\varepsilon_h^{n+1}+e_h^n))\\
&=\;b(\frac{1}{2}((u^{n+1}-w_h^{n+1})+(u^n-u_h^n))\,,u^{n+1/2}\,,\,\frac{1}{2}(\varepsilon_h^{n+1}+e_h^n))\\
&\quad+\;b(\tilde{w}_h^{n+1/2},\frac{1}{2}((u^{n+1}-w_h^{n+1})+(u^n-u_h^n)),\frac{1}{2}(\varepsilon_h^{n+1}+e_h^n))\\
&=\;b(\Lambda^{n+1/2}+\frac{1}{2}(\varepsilon_h^{n+1}+e_h^n)\,,u^{n+1/2}\,,\,\frac{1}{2}(\varepsilon_h^{n+1}+e_h^n))\\
&\quad+b(\tilde{w}_h^{n+1/2},\Lambda^{n+1/2}+\frac{1}{2}(\varepsilon_h^{n+1}+e_h^n)\,,\frac{1}{2}(\varepsilon_h^{n+1}+e_h^n))\\
&=\;b(\Lambda^{n+1/2},u^{n+1/2}\,,\,\frac{1}{2}(\varepsilon_h^{n+1}+e_h^n))\;+b(\frac{1}{2}(\varepsilon_h^{n+1}+e_h^n)\,,u^{n+1/2}\,,\,\frac{1}{2}(\varepsilon_h^{n+1}+e_h^n))\\
&\quad+b(\tilde{w}_h^{n+1/2},\Lambda^{n+1/2}\,,\frac{1}{2}(\varepsilon_h^{n+1}+e_h^n))\,,
\end{aligned}
\tag{2.17}
$$

where we used the skew symmetry of b. Using (1.3) and Young's inequality, we bound the terms on the RHS of (2.17) as follows.

$$
\begin{aligned}
b(\Lambda^{n+1/2}\,,u^{n+1/2}\,,\,\frac{1}{2}(\varepsilon_h^{n+1}+e_h^n)) &\le C\,\sqrt{\|\Lambda^{n+1/2}\|\,\|\nabla\Lambda^{n+1/2}\|}\,\|\nabla u^{n+1/2}\|\,\|\nabla\frac{1}{2}(\varepsilon_h^{n+1}+e_h^n)\|\\
&\le\frac{\nu}{10}\,\|\nabla\frac{1}{2}(\varepsilon_h^{n+1}+e_h^n)\|^2\;+\;C\,\nu^{-1}\,\|\Lambda^{n+1/2}\|\,\|\nabla\Lambda^{n+1/2}\|\,\|\nabla u^{n+1/2}\|^2
\end{aligned}
\tag{2.18}
$$

$$
\begin{aligned}
&b(\frac{1}{2}(\varepsilon_h^{n+1}+e_h^n)\,,u^{n+1/2}\,,\,\frac{1}{2}(\varepsilon_h^{n+1}+e_h^n))\leq C\,\|\frac{1}{2}(\varepsilon_h^{n+1}+e_h^n)\|^{1/2}\,\|\nabla\frac{1}{2}(\varepsilon_h^{n+1}+e_h^n)\|^{3/2}\,\|\nabla u^{n+1/2}\|\\
&\leq \frac{\nu}{10}\,\|\nabla\frac{1}{2}(\varepsilon_h^{n+1}+e_h^n)\|^2 \;+\; C\,\nu^{-3}\,\|\nabla u^{n+1/2}\|^4\,\|\frac{1}{2}(\varepsilon_h^{n+1}+e_h^n)\|^2\\
&\leq \frac{\nu}{10}\,\|\nabla\frac{1}{2}(\varepsilon_h^{n+1}+e_h^n)\|^2 \;+\; C\,\nu^{-3}\,\|\nabla u^{n+1/2}\|^4\,\left(\|\varepsilon_h^{n+1}\|^2\;+\;\|e_h^n\|^2\right)
\end{aligned}
\tag{2.19}
$$

$$
\begin{aligned}
b(\tilde{w}_h^{n+1/2}\,,\Lambda^{n+1/2}\,,\,\frac{1}{2}(\varepsilon_h^{n+1}+e_h^n)) &\leq C\,\|\nabla\tilde{w}_h^{n+1/2}\|\,\|\nabla\Lambda^{n+1/2}\|\,\|\nabla\frac{1}{2}(\varepsilon_h^{n+1}+e_h^n)\|\\
&\leq \frac{\nu}{10}\,\|\nabla\frac{1}{2}(\varepsilon_h^{n+1}+e_h^n)\|^2 \;+\; C\,\nu^{-1}\,\|\nabla\tilde{w}_h^{n+1/2}\|^2\,\|\nabla\Lambda^{n+1/2}\|^2
\end{aligned}
\tag{2.20}
$$

$$
\begin{aligned}
(p(t^{n+1/2})-q_h^{n+1},\nabla\cdot\frac{1}{2}(\varepsilon_h^{n+1}+e_h^n)) &\leq \|p(t^{n+1/2})-q_h^{n+1}\|\,\|\nabla\cdot\frac{1}{2}(\varepsilon_h^{n+1}+e_h^n)\|\\
&\leq \frac{\nu}{10}\|\nabla\frac{1}{2}(\varepsilon_h^{n+1}+e_h^n)\|^2 \;+\; C\,\nu^{-1}\,\|p(t^{n+1/2})-q_h^{n+1}\|^2\,.
\end{aligned}
\tag{2.21}
$$

The *consistency error term* $\Delta t|Intp(u^{n+1};\frac{1}{2}(\varepsilon_h^{n+1}+e_h^n))|$ in (2.14) can be bounded as follows.

Lemma 2.3.9. *Under the regularity assumption* (2.8) *from Section 2.3 there holds*

$$
\begin{aligned}
\Delta t|Intp(u^{n+1};\frac{1}{2}(\varepsilon_h^{n+1}+e_h^n))| \leq{}& \frac{\Delta t}{2}\left(\|\varepsilon_h^{n+1}\|^2+\|e_h^n\|^2\right)+\frac{\nu\Delta t}{4}\|\nabla\frac{1}{2}(\varepsilon_h^{n+1}+e_h^n)\|^2\\
&+\frac{C(\Delta t)^5}{\nu}\left(\|\nabla u^{n+1/2}\|^4+\|\nabla u(t^{n+1/2})\|^4\right)\\
&+C(\Delta t)^4\int_{t^n}^{t^{n+1}}\left(\|u_{ttt}\|^2+\nu\|\nabla u_{tt}\|^2+\frac{1}{\nu}\|\nabla u_{tt}\|^4+\|f_{tt}\|^2\right)dt.
\end{aligned}
$$

Proof. We want to estimate every term in the definition of $Intp(u^{n+1};v_h))$ from (2.12) and obtain

$$
\begin{aligned}
&((u^{n+1}-u^n)/\Delta t-u_t(t^{n+1/2}),\frac{1}{2}(\varepsilon_h^{n+1}+e_h^n))\\
\leq{}&\frac{1}{2}\|\frac{1}{2}(\varepsilon_h^{n+1}+e_h^n)\|^2+\frac{1}{2}\|(u^{n+1}-u^n)/\Delta t-u_t(t^{n+1/2})\|^2\\
\leq{}&\frac{1}{4}\|\varepsilon_h^{n+1}\|^2+\frac{1}{4}\|e_h^n\|^2+\frac{1}{2}\frac{(\Delta t)^3}{1280}\int_{t^n}^{t^{n+1}}\|u_{ttt}\|^2dt,
\end{aligned}
$$

$$
\begin{aligned}
&(f(t^{n+1/2}) - f^{n+1/2}, \frac{1}{2}(\varepsilon_h^{n+1} + e_h^n)) \le \frac{1}{2}\|\frac{1}{2}(\varepsilon_h^{n+1} + e_h^n)\|^2 + \frac{1}{2}\|f(t^{n+1/2}) - f^{n+1/2}\|^2 \\
&\le \frac{1}{4}\|\varepsilon_h^{n+1}\|^2 + \frac{1}{4}\|e_h^n\|^2 + \frac{1}{2}\frac{(\Delta t)^3}{48}\int_{t^n}^{t^{n+1}} \|f_{tt}\|^2 dt,
\end{aligned}
$$

$$
\begin{aligned}
&\nu(\nabla u^{n+1/2} - \nabla u(t^{n+1/2}), \nabla \frac{1}{2}(\varepsilon_h^{n+1} + e_h^n)) \\
&\le \frac{\nu}{8}\|\nabla \frac{1}{2}(\varepsilon_h^{n+1} + e_h^n)\|^2 + 2\nu\|\nabla u^{n+1/2} - \nabla u(t^{n+1/2})\|^2 \\
&\le \frac{\nu}{8}\|\nabla \frac{1}{2}(\varepsilon_h^{n+1} + e_h^n)\|^2 + 2\nu\frac{(\Delta t)^3}{48}\int_{t^n}^{t^{n+1}} \|\nabla u_{tt}\|^2 dt,
\end{aligned}
$$

where we used classical Cauchy-Schwarz inequality and Taylor expansion. Also with these inequalities we get an estimate of the terms of the nonlinearity

$$
\begin{aligned}
&\quad b(u^{n+1/2}, u^{n+1/2}, \frac{1}{2}(\varepsilon_h^{n+1} + e_h^n)) - b(u(t^{n+1/2}), u(t^{n+1/2}), \frac{1}{2}(\varepsilon_h^{n+1} + e_h^n)) \\
&= b(u^{n+1/2} - u(t^{n+1/2}), u^{n+1/2}, \frac{1}{2}(\varepsilon_h^{n+1} + e_h^n)) + b(u(t^{n+1/2}), u^{n+1/2} - u(t^{n+1/2}), \frac{1}{2}(\varepsilon_h^{n+1} + e_h^n)) \\
&\le C\|\nabla(u^{n+1/2} - u(t^{n+1/2}))\|\|\nabla\frac{1}{2}(\varepsilon_h^{n+1} + e_h^n)\| \left(\|\nabla u^{n+1/2}\| + \|\nabla u(t^{n+1/2})\|\right) \\
&\le \frac{\nu}{8}\|\nabla\frac{1}{2}(\varepsilon_h^{n+1} + e_h^n)\|^2 + C\nu^{-1}\|\nabla(u^{n+1/2} - u(t^{n+1/2}))\|^2 \left(\|\nabla u^{n+1/2}\|^2 + \|\nabla u(t^{n+1/2})\|^2\right) \\
&\le \frac{\nu}{8}\|\nabla\frac{1}{2}(\varepsilon_h^{n+1} + e_h^n)\|^2 + C\nu^{-1}\frac{(\Delta t)^3}{48}\left(\|\nabla u^{n+1/2}\|^2 + \|\nabla u(t^{n+1/2})\|^2\right)\int_{t^n}^{t^{n+1}} \|\nabla u_{tt}\|^2 dt \\
&\le \frac{\nu}{8}\|\nabla\frac{1}{2}(\varepsilon_h^{n+1} + e_h^n)\|^2 + C\nu^{-1}\frac{(\Delta t)^3}{48}\int_{t^n}^{t^{n+1}} \|\nabla u_{tt}\|^2 \left(\|\nabla u^{n+1/2}\|^2 + \|\nabla u(t^{n+1/2})\|^2\right) dt \\
&\le \frac{\nu}{8}\|\nabla\frac{1}{2}(\varepsilon_h^{n+1} + e_h^n)\|^2 \\
&\qquad\qquad + C\nu^{-1}\frac{(\Delta t)^3}{48}\left(\int_{t^n}^{t^{n+1}} \|\nabla u_{tt}\|^4 dt + \int_{t^n}^{t^{n+1}} \left(\|\nabla u^{n+1/2}\|^4 + \|\nabla u(t^{n+1/2})\|^4\right) dt\right) \\
&\le \frac{\nu}{8}\|\nabla\frac{1}{2}(\varepsilon_h^{n+1} + e_h^n)\|^2 + C\frac{(\Delta t)^3}{48\nu}\left(\Delta t\left(\|\nabla u^{n+1/2}\|^4 + \|\nabla u(t^{n+1/2})\|^4\right) + \int_{t^n}^{t^{n+1}} \|\nabla u_{tt}\|^4 dt\right).
\end{aligned}
$$

Combining all estimates yields the lemma. □

The application of Lemma 2.3.9 to (2.14) together with the estimates (2.15)–(2.21) gives

$$
\begin{aligned}
&\frac{1}{2}\left(\|\varepsilon_h^{n+1}\|^2 \,-\, \|e_h^n\|^2\right) + \Delta t\,\frac{\nu}{4}\|\nabla \frac{1}{2}(\varepsilon_h^{n+1} + e_h^n)\|^2 \\
&\quad \le\, C\Delta t\,(1+\nu^{-3}\|\nabla u^{n+1/2}\|^4)\left(\|\varepsilon_h^{n+1}\|^2 \,+\, \|e_h^n\|^2\right) \,+\, C\nu\Delta t\|\nabla\Lambda^{n+1/2}\|^2 \\
&+ \frac{C\Delta t}{\nu}\,\|\nabla \tilde{w}_h^{n+1/2}\|^2\,\|\nabla\Lambda^{n+1/2}\|^2 \,+\, \frac{C\Delta t}{\nu}\,\|\nabla u^{n+1/2}\|^2\|\Lambda^{n+1/2}\|\,\|\nabla\Lambda^{n+1/2}\| \\
&\quad + \frac{C\Delta t}{\nu}\|p(t^{n+1/2}) - q_h^{n+1}\|^2 + \frac{C(\Delta t)^5}{\nu}\left(\|\nabla u^{n+1/2}\|^4 + \|\nabla u(t^{n+1/2})\|^4\right) \\
&+ C\int_{t^n}^{t^{n+1}}\|\Lambda_t\|^2 dt + C(\Delta t)^4\int_{t^n}^{t^{n+1}}\left(\|u_{ttt}\|^2 + \nu\|\nabla u_{tt}\|^2 + \frac{1}{\nu}\|\nabla u_{tt}\|^4 + \|f_{tt}\|^2\right)dt.
\end{aligned}
\tag{2.22}
$$

As u_h^{n+1} and w_h^{n+1} are connected through the *variational multiscale* projection in Step 2, we next use that equation to obtain a relationship between $\|\varepsilon_h^n\|$ and $\|e_h^n\|$.

Lemma 2.3.10. *There holds*

$$
\begin{aligned}
\|\varepsilon_h^{n+1}\|^2 = \|e_h^{n+1}\|^2 \,+\, \frac{1}{2}\Delta t\|\sqrt{\nu_T}[I - P_H]\nabla(\varepsilon_h^{n+1} + e_h^{n+1})\|^2& \\
+\, \Delta t(\nu_T[I - P_H]\nabla(\Lambda^{n+1} - u^{n+1}), [I - P_H]\nabla(\varepsilon_h^{n+1} + e_h^{n+1}))&.
\end{aligned}
$$

Proof. From (2.10) we have

$$
\left(\frac{w_h^{n+1} - u_h^{n+1}}{\Delta t}, v_h\right) \;=\; \left(\nu_T[I - P_H]\nabla\frac{w_h^{n+1} + u_h^{n+1}}{2}, [I - P_H]\nabla v_h\right)
$$

and set $v_h = (w_h^{n+1} - I_h u^{n+1}) \,+\, (u_h^{n+1} \,-\, I_h u^{n+1}) \;=\; -(\varepsilon_h^{n+1} + e_h^{n+1})$. We obtain

$$
\begin{aligned}
&\left(\frac{-(\varepsilon_h^{n+1} - e_h^{n+1})}{\Delta t}, -(\varepsilon_h^{n+1} + e_h^{n+1})\right) = \\
&\qquad\qquad \left(\nu_T[I - P_H]\nabla\frac{-(\varepsilon_h^{n+1} + e_h^{n+1}) + 2I_h u^{n+1}}{2}, [I - P_H]\nabla(-(\varepsilon_h^{n+1} + e_h^{n+1}))\right).
\end{aligned}
$$

Hence

$$
\begin{aligned}
\frac{1}{\Delta t}(\|\varepsilon_h^{n+1}\|^2 - \|e_h^{n+1}\|^2) = \frac{1}{2}\left\|\sqrt{\nu_T}[I - P_H]\nabla(\varepsilon_h^{n+1} + e_h^{n+1})\right\|^2& \\
-\, (\nu_T[I - P_H]\nabla I_h u^{n+1}, [I - P_H]\nabla(\varepsilon_h^{n+1} + e_h^{n+1}))&
\end{aligned}
$$

and with $I_h u^{n+1} = u^{n+1} - \Lambda^{n+1}$ from (2.13) we conclude the proof. $\square$

Substituting Lemma 2.3.10 into (2.22), we obtain

$$\frac{1}{2}\left(\|e_h^{n+1}\|^2-\|e_h^n\|^2\right)+\frac{\Delta t}{4}\left(\nu\|\nabla\frac{1}{2}(\varepsilon_h^{n+1}+e_h^n)\|^2+\|\sqrt{\nu_T}[I-P_H]\nabla(\varepsilon_h^{n+1}+e_h^{n+1})\|^2\right)$$
$$\begin{aligned}\le\, & C\Delta t(1+\nu^{-3}\|\nabla u^{n+1/2}\|^4)\left(\|e_h^{n+1}\|^2+\|e_h^n\|^2\right)+C\nu\Delta t\|\nabla\Lambda^{n+1/2}\|^2\\
&+C(\Delta t)^2(1+\nu^{-3}\|\nabla u^{n+1/2}\|^4)\Big(\frac{1}{2}\|\sqrt{\nu_T}[I-P_H]\nabla(\varepsilon_h^{n+1}+e_h^{n+1})\|^2\\
&+(\nu_T[I-P_H]\nabla(\Lambda^{n+1}-u^{n+1}),[I-P_H]\nabla(\varepsilon_h^{n+1}+e_h^{n+1}))\Big)\\
&+\frac{\Delta t}{2}(\nu_T[I-P_H]\nabla(u^{n+1}-\Lambda^{n+1}),[I-P_H]\nabla(\varepsilon_h^{n+1}+e_h^{n+1}))\\
&+\frac{C\Delta t}{\nu}\|\nabla\tilde{w}_h^{n+1/2}\|^2\|\nabla\Lambda^{n+1/2}\|^2+\frac{C\Delta t}{\nu}\|\nabla u^{n+1/2}\|^2\|\Lambda^{n+1/2}\|\,\|\nabla\Lambda^{n+1/2}\|\\
&+\frac{C\Delta t}{\nu}\|p(t^{n+1/2})-q_h^{n+1}\|^2+\frac{C(\Delta t)^5}{\nu}\left(\|\nabla u^{n+1/2}\|^4+\|\nabla u(t^{n+1/2})\|^4\right)\\
&+C\int_{t^n}^{t^{n+1}}\|\Lambda_t\|^2dt+C(\Delta t)^4\int_{t^n}^{t^{n+1}}\left(\|u_{ttt}\|^2+\nu\|\nabla u_{tt}\|^2+\frac{1}{\nu}\|\nabla u_{tt}\|^4+\|f_{tt}\|^2\right)dt.\end{aligned}\tag{2.23}$$

Since we can estimate

$$\begin{aligned}&|(\nu_T[I-P_H]\nabla(\Lambda^{n+1}-u^{n+1}),[I-P_H]\nabla(\varepsilon_h^{n+1}+e_h^{n+1}))|\\
&\qquad\le\frac{1}{8}\|\sqrt{\nu_T}[I-P_H]\nabla(\varepsilon_h^{n+1}+e_h^{n+1})\|^2+C\|\sqrt{\nu_T}[I-P_H]\nabla(\Lambda^{n+1}-u^{n+1})\|^2,\end{aligned}$$

it is possible to choose Δt sufficiently small, i.e., $C\Delta t<\frac{1}{16}(1+\nu^{-3}\|\nabla u^{n+1/2}\|^4)^{-1}$ such that the terms stemming from the VMS method are hidden and after summing this up from $n=0$ to $n=N-1$ equation (2.23) results in

$$\frac{1}{2}\|e_h^N\|^2+\frac{\Delta t}{4}\sum_{n=0}^{N-1}\left(\nu\|\nabla\frac{1}{2}(\varepsilon_h^{n+1}+e_h^n)\|^2+\frac{1}{2}\|\sqrt{\nu_T}[I-P_H]\nabla(\varepsilon_h^{n+1}+e_h^{n+1})\|^2\right)$$
$$\begin{aligned}\le\sum_{n=0}^{N-1}\Bigg\{ & C\Delta t(1+\nu^{-3}\|\nabla u^{n+1/2}\|^4)(\|e_h^{n+1}\|^2+\|e_h^n\|^2)\\
&+C\nu\Delta t\|\nabla\Lambda^{n+1/2}\|^2+C\Delta t\left(\|\sqrt{\nu_T}[I-P_H]\nabla\Lambda^{n+1}\|^2+\|\sqrt{\nu_T}[I-P_H]\nabla u^{n+1}\|^2\right)\\
&+\frac{C\Delta t}{\nu}\|\nabla\tilde{w}_h^{n+1/2}\|^2\|\nabla\Lambda^{n+1/2}\|^2+\frac{C\Delta t}{\nu}\|\nabla u^{n+1/2}\|^2\|\Lambda^{n+1/2}\|\,\|\nabla\Lambda^{n+1/2}\|\\
&+\frac{C\Delta t}{\nu}\|p(t^{n+1/2})-q_h^{n+1}\|^2+\frac{C(\Delta t)^5}{\nu}\left(\|\nabla u^{n+1/2}\|^4+\|\nabla u(t^{n+1/2})\|^4\right)\\
&+C\int_{t^n}^{t^{n+1}}\|\Lambda_t\|^2dt+C(\Delta t)^4\int_{t^n}^{t^{n+1}}\left(\|u_{ttt}\|^2+\nu\|\nabla u_{tt}\|^2+\frac{1}{\nu}\|\nabla u_{tt}\|^4+\|f_{tt}\|^2\right)dt\Bigg\}.\end{aligned}$$

Now we choose the interpolation operator in V_h, constructed in [47, 4], and a usual interpolation operator for the pressure, which leads us to

$$\|u - I_h u\|_r \leq C h^{k+1-r} |u|_{k+1},$$

where $r \leq k$ and k is the polynomial degree of the corresponding FE space. Since P_H also fulfills the interpolation property, due to the regularity assumptions and Theorem 2.3.5 this gives

$$\begin{aligned}
&\frac{1}{2}\|e_h^N\|^2 + \frac{\Delta t}{4}\sum_{n=0}^{N-1}\left(\nu\|\nabla\frac{1}{2}(\varepsilon_h^{n+1}+e_h^n)\|^2 + \frac{1}{2}\|\sqrt{\nu_T}[I-P_H]\nabla(\varepsilon_h^{n+1}+e_h^{n+1})\|^2\right) \\
&\leq \sum_{n=0}^{N} C\Delta t\left(1+\nu^{-3}|||\nabla u|||_{\infty,0}^4\right)\|e_h^n\|^2 \\
&+ C\nu h^{2k}|||u|||_{2,k+1}^2 + C\nu_T h^{2k}|||u|||_{2,k+1}^2 + C\nu_T H^{2k}|||u|||_{2,k+1}^2 \\
&+ C\frac{h^{2k}}{\nu^2}|||u|||_{\infty,k+1}^2 + C\frac{h^{2k+1}}{\nu}\left(|||u|||_{4,k+1}^4 + |||\nabla u|||_{4,0}^4\right) + C\frac{h^{2s+2}}{\nu}|||p_{1/2}|||_{2,s+1}^2 \\
&+ Ch^{2k+2}|||u_t|||_{2,k+1}^2 + C(\Delta t)^4\Big(\frac{1}{\nu}|||\nabla u|||_{4,0}^4 + \frac{1}{\nu}|||\nabla u_{1/2}|||_{4,0}^4 \\
&+ |||u_{ttt}|||_{2,0}^2 + \nu|||\nabla u_{tt}|||_{2,0}^2 + \frac{1}{\nu}|||\nabla u_{tt}|||_{4,0}^4 + |||f_{tt}|||_{2,0}^2\Big).
\end{aligned}$$

The next step will be the application of Lemma 1.4.4, the discrete Grönwall inequality. Let Δt be sufficiently small, i.e., $C\Delta t < (1+\nu^{-3}|||\nabla u|||_{\infty,0}^4)^{-1}$, it is allowed to apply the lemma and we obtain

$$\begin{aligned}
&\frac{1}{2}\|e_h^N\|^2 + \frac{\Delta t}{4}\sum_{n=0}^{N-1}\left(\nu\|\nabla\frac{1}{2}(\varepsilon_h^{n+1}+e_h^n)\|^2 + \frac{1}{2}\|\sqrt{\nu_T}[I-P_H]\nabla(\varepsilon_h^{n+1}+e_h^{n+1})\|^2\right) \\
&\leq C\nu h^{2k}|||u|||_{2,k+1}^2 + C\nu_T h^{2k}|||u|||_{2,k+1}^2 + C\nu_T H^{2k}|||u|||_{2,k+1}^2 \\
&+ C\frac{h^{2k}}{\nu^2}|||u|||_{\infty,k+1}^2 + C\frac{h^{2k+1}}{\nu}\left(|||u|||_{4,k+1}^4 + |||\nabla u|||_{4,0}^4\right) + C\frac{h^{2s+2}}{\nu}|||p_{1/2}|||_{2,s+1}^2 \\
&+ Ch^{2k+2}|||u_t|||_{2,k+1}^2 + C(\Delta t)^4\Big(\frac{1}{\nu}|||\nabla u|||_{4,0}^4 + \frac{1}{\nu}|||\nabla u_{1/2}|||_{4,0}^4 \\
&+ |||u_{ttt}|||_{2,0}^2 + \nu|||\nabla u_{tt}|||_{2,0}^2 + \frac{1}{\nu}|||\nabla u_{tt}|||_{4,0}^4 + |||f_{tt}|||_{2,0}^2\Big).
\end{aligned}$$

Now we have an estimate for the model error e_h and it is left to find an error estimate for the whole error. We obtain

$$\begin{aligned}
&\frac{1}{2}\|u^N - u_h^N\|^2 + \frac{\Delta t}{4}\sum_{n=0}^{N-1}(\nu\|\nabla(u(t^{n+1/2}) - (w_h^{n+1} + u_h^n)/2)\|^2 \\
&\qquad\qquad + \|\sqrt{\nu_T}[I - P_H]\nabla(u(t^{n+1}) - (w_h^{n+1} + u_h^{n+1})/2)\|^2) \\
&\leq \|\Lambda^N\|^2 + \|e_h^N\|^2 + C\nu\Delta t\sum_{n=0}^{N-1}(\|\nabla(u^{n+1/2} - u(t^{n+1/2}))\|^2 + \|\nabla\Lambda^{n+1/2}\|^2 + \|\nabla\frac{1}{2}(\varepsilon_h^{n+1} + e_h^n)\|^2) \\
&\qquad + C\Delta t\sum_{n=0}^{N-1}(\|\sqrt{\nu_T}[I - P_H]\nabla\Lambda^{n+1}\|^2 + \|\sqrt{\nu_T}[I - P_H]\nabla\frac{1}{2}(\varepsilon_h^{n+1} + e_h^{n+1})\|^2),
\end{aligned}$$

where the upcoming new terms are either already contained in the RHS of the model error, or easy to handle like e.g. with Lemma 2.3.9. Combining all estimates from above we get Theorem 2.3.7 and (in the particular case) Corollary 2.3.8. □

2.3.1 Growth of Perturbations in the discrete scheme.

The question naturally arises of dependence of the constant C in Theorem 2.3.7 upon the final time T. This dependence is exponential (reflecting exponential stretching in the continuous NSE) and inevitably arising from the discrete Grönwall inequality. It is related to the maximal Lyapunov exponent in the discrete model given by Algorithm 2.3.2. In this subsection we derive an estimate for the Lyapunov exponent of this model and thus its error growth. To simplify the notation we will suppress the index h, although we only consider discrete solutions here. Let (u_1, w_1, f_1) and (u_2, w_2, f_2) be two solutions with different problem data from Algorithm 2.3.2. By subtracting the two corresponding equations in Step 1, we obtain

$$\begin{aligned}
&\frac{1}{\Delta t}\left((w_1^{n+1} - w_2^{n+1}) - (u_1^n - u_2^n), v\right) + \nu\left(\nabla\frac{(w_1^{n+1} - w_2^{n+1}) + (u_1^n - u_2^n)}{2}, \nabla v\right) \\
&+ b\left(\frac{w_1^{n+1} + u_1^n}{2}, \frac{w_1^{n+1} + u_1^n}{2}, v\right) - b\left(\frac{w_2^{n+1} + u_2^n}{2}, \frac{w_2^{n+1} + u_2^n}{2}, v\right) = \left(f_1^{n+1/2} - f_2^{n+1/2}, v\right)
\end{aligned}$$

for all functions $v \in V_h$. Setting $v = \frac{1}{2}[(w_1^{n+1} - w_2^{n+1}) + (u_1^n - u_2^n)]$ gives

$$
\begin{aligned}
\frac{1}{2\Delta t}\left(\|w_1^{n+1} - w_2^{n+1}\|^2 - \|u_1^n - u_2^n\|^2\right) + \nu \left\|\nabla \frac{(w_1^{n+1} - w_2^{n+1}) + (u_1^n - u_2^n)}{2}\right\|^2 = \\
b\left(\frac{w_2^{n+1} + u_2^n}{2}, \frac{w_2^{n+1} + u_2^n}{2}, \frac{(w_1^{n+1} - w_2^{n+1}) + (u_1^n - u_2^n)}{2}\right) \\
-b\left(\frac{w_1^{n+1} + u_1^n}{2}, \frac{w_1^{n+1} + u_1^n}{2}, \frac{(w_1^{n+1} - w_2^{n+1}) + (u_1^n - u_2^n)}{2}\right) \\
+\left(f_1^{n+1/2} - f_2^{n+1/2}, \frac{(w_1^{n+1} - w_2^{n+1}) + (u_1^n - u_2^n)}{2}\right).
\end{aligned}
\tag{2.24}
$$

As a next step we estimate all terms on the RHS and start with the easy one

$$
\begin{aligned}
&\left(f_1^{n+1/2} - f_2^{n+1/2}, \frac{(w_1^{n+1} - w_2^{n+1}) + (u_1^n - u_2^n)}{2}\right) \\
&\qquad \le \frac{\nu}{8}\left\|\nabla \frac{(w_1^{n+1} - w_2^{n+1}) + (u_1^n - u_2^n)}{2}\right\|^2 + \frac{2}{\nu}\left\|(f_1^{n+1/2} - f_2^{n+1/2})\right\|_{-1}^2.
\end{aligned}
$$

To bound the nonlinear term we use (1.3)

$$
\begin{aligned}
&\Bigg|b\left(\frac{w_2^{n+1} + u_2^n}{2}, \frac{w_2^{n+1} + u_2^n}{2}, \frac{(w_1^{n+1} - w_2^{n+1}) + (u_1^n - u_2^n)}{2}\right) \\
&\quad - b\left(\frac{w_1^{n+1} + u_1^n}{2}, \frac{w_1^{n+1} + u_1^n}{2}, \frac{(w_1^{n+1} - w_2^{n+1}) + (u_1^n - u_2^n)}{2}\right)\Bigg| \\
&= \Bigg|b\left(\frac{w_2^{n+1} + u_2^n}{2}, \frac{(w_2^{n+1} - w_1^{n+1}) + (u_2^n - u_1^n)}{2}, \frac{(w_1^{n+1} - w_2^{n+1}) + (u_1^n - u_2^n)}{2}\right) \\
&\quad + b\left(\frac{w_2^{n+1} + u_2^n}{2}, \frac{w_1^{n+1} + u_1^n}{2}, \frac{(w_1^{n+1} - w_2^{n+1}) + (u_1^n - u_2^n)}{2}\right) \\
&\quad - b\left(\frac{w_1^{n+1} + u_1^n}{2}, \frac{w_1^{n+1} + u_1^n}{2}, \frac{(w_1^{n+1} - w_2^{n+1}) + (u_1^n - u_2^n)}{2}\right)\Bigg| \\
&= \Bigg|b\left(\frac{(w_2^{n+1} - w_1^{n+1}) + (u_2^n - u_1^n)}{2}, \frac{w_1^{n+1} + u_1^n}{2}, \frac{(w_1^{n+1} - w_2^{n+1}) + (u_1^n - u_2^n)}{2}\right)\Bigg| \\
&\le C_*\sqrt{\left\|\frac{(w_1^{n+1} - w_2^{n+1}) + (u_1^n - u_2^n)}{2}\right\|}\left\|\nabla \frac{(w_1^{n+1} - w_2^{n+1}) + (u_1^n - u_2^n)}{2}\right\|^{3/2}\left\|\nabla \frac{w_1^{n+1} + u_1^n}{2}\right\| \\
&\le \frac{3\nu}{4}\left\|\nabla \frac{(w_1^{n+1} - w_2^{n+1}) + (u_1^n - u_2^n)}{2}\right\|^2 \\
&\qquad + \frac{C_*^4}{4\nu^3}\left\|\nabla \frac{w_1^{n+1} + u_1^n}{2}\right\|^4\left\|\frac{(w_1^{n+1} - w_2^{n+1}) + (u_1^n - u_2^n)}{2}\right\|^2,
\end{aligned}
$$

where the factor $\left\|\nabla\frac{w_1^{n+1}+u_1^n}{2}\right\|^4$ can also be replaced by $\min_{i=1,2}\left\|\nabla\frac{w_i^{n+1}+u_i^n}{2}\right\|^4$ when we apply the same steps for $w_2^{n+1}+u_2^n$ again and use both estimates. With this in mind (2.24) becomes

$$
\begin{aligned}
&\frac{1}{2\Delta t}\left(\|w_1^{n+1}-w_2^{n+1}\|^2-\|u_1^n-u_2^n\|^2\right)+\frac{\nu}{8}\left\|\nabla\frac{(w_1^{n+1}-w_2^{n+1})+(u_1^n-u_2^n)}{2}\right\|^2\\
&\leq\frac{C_*^4}{8\nu^3}\min_{i=1,2}\left\|\nabla\frac{w_i^{n+1}+u_i^n}{2}\right\|^4\left(\left\|w_1^{n+1}-w_2^{n+1}\right\|^2+\|u_1^n-u_2^n\|^2\right)+\frac{2}{\nu}\left\|(f_1^{n+1/2}-f_2^{n+1/2})\right\|_{-1}^2.
\end{aligned}
$$

To get a connection between u and w, we use a variant of Lemma 2.3.3 for the difference of the solutions and get

$$
\begin{aligned}
&\frac{1}{2\Delta t}\left(\|u_1^{n+1}-u_2^{n+1}\|^2-\|u_1^n-u_2^n\|^2\right)+\frac{\nu}{8}\left\|\nabla\frac{(w_1^{n+1}-w_2^{n+1})+(u_1^n-u_2^n)}{2}\right\|^2\\
&\qquad+\left\|\sqrt{\nu_T}[I-P_H]\nabla\frac{(w_1^{n+1}-w_2^{n+1})+(u_1^{n+1}-u_2^{n+1})}{2}\right\|^2\\
&\leq\frac{C_*^4}{8\nu^3}\min_{i=1,2}\left\|\nabla\frac{w_i^{n+1}+u_i^n}{2}\right\|^4\left(\left\|u_1^{n+1}-u_2^{n+1}\right\|^2+\|u_1^n-u_2^n\|^2\right)+\frac{2}{\nu}\left\|(f_1^{n+1/2}-f_2^{n+1/2})\right\|_{-1}^2\\
&\qquad+\frac{\Delta t C_*^4}{4\nu^3}\min_{i=1,2}\left\|\nabla\frac{w_i^{n+1}+u_i^n}{2}\right\|^4\left\|\sqrt{\nu_T}[I-P_H]\nabla\frac{(w_1^{n+1}-w_2^{n+1})+(u_1^{n+1}-u_2^{n+1})}{2}\right\|^2.
\end{aligned}
$$

At this point let us assume that

$$
\Delta t\leq\left(\frac{C_*^4}{3\nu^3}\min_{i=1,2}\left\|\nabla\frac{w_i^{n+1}+u_i^n}{2}\right\|^4\right)^{-1}
$$

to get

$$
\begin{aligned}
&\frac{1}{2\Delta t}\left(\|u_1^{n+1}-u_2^{n+1}\|^2-\|u_1^n-u_2^n\|^2\right)+\frac{\nu}{8}\left\|\nabla\frac{(w_1^{n+1}-w_2^{n+1})+(u_1^n-u_2^n)}{2}\right\|^2\\
&\qquad+\frac{1}{4}\left\|\sqrt{\nu_T}[I-P_H]\nabla\frac{(w_1^{n+1}-w_2^{n+1})+(u_1^{n+1}-u_2^{n+1})}{2}\right\|^2\\
&\leq\frac{C_*^4}{8\nu^3}\min_{i=1,2}\left\|\nabla\frac{w_i^{n+1}+u_i^n}{2}\right\|^4\left(\left\|u_1^{n+1}-u_2^{n+1}\right\|^2+\|u_1^n-u_2^n\|^2\right)+\frac{2}{\nu}\left\|(f_1^{n+1/2}-f_2^{n+1/2})\right\|_{-1}^2
\end{aligned}
$$

and sum up the inequalities from $n=0$ to $n=N-1$. It holds

$$
\begin{aligned}
&\frac{1}{2\Delta t}\|u_1^N-u_2^N\|^2+\sum_{n=0}^{N-1}\Big(\frac{\nu}{8}\left\|\nabla\frac{(w_1^{n+1}-w_2^{n+1})+(u_1^n-u_2^n)}{2}\right\|^2\\
&\qquad\qquad+\frac{1}{4}\left\|\sqrt{\nu_T}[I-P_H]\nabla\frac{(w_1^{n+1}-w_2^{n+1})+(u_1^{n+1}-u_2^{n+1})}{2}\right\|^2\Big)\\
&\quad\le\frac{1}{2\Delta t}\|u_1^0-u_2^0\|^2+\frac{C_*^4}{8\nu^3}\sum_{n=0}^{N-1}\min_{i=1,2}\left\|\nabla\frac{w_i^{n+1}+u_i^n}{2}\right\|^4\left(\left\|u_1^{n+1}-u_2^{n+1}\right\|^2+\|u_1^n-u_2^n\|^2\right)\\
&\quad+\frac{2}{\nu}\sum_{n=0}^{N-1}\left\|(f_1^{n+1/2}-f_2^{n+1/2})\right\|_{-1}^2=\sum_{n=0}^{N}\frac{\kappa_n}{2}\|u_1^n-u_2^n\|^2+\frac{2}{\nu}\sum_{n=0}^{N-1}\left\|(f_1^{n+1/2}-f_2^{n+1/2})\right\|_{-1}^2,
\end{aligned}
$$

where

$$
\kappa_n=\frac{C_*^4}{4\nu^3}\begin{cases}\frac{4\nu^3}{C_*^4\Delta t}+\min_{i=1,2}\left\|\nabla\frac{w_i^1+u_i^0}{2}\right\|^4 & \text{for } n=0\\ \min_{i=1,2}\left(\left\|\nabla\frac{w_i^n+u_i^{n-1}}{2}\right\|^4+\left\|\nabla\frac{w_i^{n+1}+u_i^n}{2}\right\|^4\right) & \text{for } n=1,\dots,N-1\\ \min_{i=1,2}\left\|\nabla\frac{w_i^N+u_i^{N-1}}{2}\right\|^4 & \text{for } n=N.\end{cases}
$$

When we now apply the discrete Grönwall inequality from Lemma 1.4.4, we get

$$
\begin{aligned}
&\|u_1^N-u_2^N\|^2+\Delta t\sum_{n=0}^{N-1}\Big(\frac{\nu}{4}\left\|\nabla\frac{(w_1^{n+1}-w_2^{n+1})+(u_1^n-u_2^n)}{2}\right\|^2\\
&\qquad\qquad+\frac{1}{2}\left\|\sqrt{\nu_T}[I-P_H]\nabla\frac{(w_1^{n+1}-w_2^{n+1})+(u_1^{n+1}-u_2^{n+1})}{2}\right\|^2\Big)\\
&\qquad\le\exp\left(\Delta t\sum_{n=1}^{N}g_n\kappa_n\right)\left\{\Delta t\kappa_0\left\|(u_1^0-u_2^0)\right\|^2+\frac{4\Delta t}{\nu}\sum_{n=0}^{N-1}\left\|(f_1^{n+1/2}-f_2^{n+1/2})\right\|_{-1}^2\right\},
\end{aligned}
$$

where $g_n=(1-\Delta t\kappa_n)^{-1}$ under the assumption that $\Delta t\kappa_n<1$. Now, we will look at the exponential multiplier. For clarity, let us define

$$
|w+u|_{1,\infty}^4:\ =\max_{n=0,\dots,N}\min_{i=1,2}\left\|\nabla\frac{w_i^n+u_i^{n-1}}{2}\right\|^4.
$$

Given in addition that $\Delta t\le\left(\frac{C_*^4}{\nu^3}\min_{i=1,2}\left\|\nabla\frac{w_i^{n+1}+u_i^n}{2}\right\|^4\right)^{-1}$ we can estimate

$$
\begin{aligned}
\exp\left(\Delta t\sum_{n=1}^{N}g_n\kappa_n\right)&\le\exp\left(\Delta t\frac{C_*^4}{2\nu^3}|w+u|_{1,\infty}^4(1-\Delta t\frac{C_*^4}{2\nu^3}|w+u|_{1,\infty}^4)^{-1}\sum_{n=1}^{N}1\right)\\
&\le\exp\left(N\Delta t\frac{C_*^4}{\nu^3}|w+u|_{1,\infty}^4\right)\le\exp\left(T\frac{C_*^4}{\nu^3}|w+u|_{1,\infty}^4\right).
\end{aligned}\tag{2.25}
$$

Remark 2.3.11. *The result in (2.25) is what one can expect from the discrete Grönwall inequality. Nevertheless it would be better to have an improvement of the factor* $\frac{C_*^4}{\nu^3}$ *to* $\frac{C_*^4}{(\nu+\nu_T)^3}$. *The analysis herein failed to produce this because of the mismatch in the arguments of the usual Galerkin terms in comparison to the term stemming from the VMS projection step. The Galerkin terms had an argument of the Crank-Nicolson time discretization scheme, i.e.* $w_i^n + u_i^{n-1}$, *where the terms from the VMS projection step had an argument* $w_i^n + u_i^n$. *Recall that the projection step does not depend on the time discretization, Remark 2.3.4.*

2.4 ALGORITHMS FOR COMPUTING THE PROJECTION

In Step 2 the action of Π must be computed. We consider two approaches to solving the linear system to compute the projection Πu in this section and one approach in Section 2.5 where the difficult term in (2.6) involving the operator P_H is simply lagged to the previous time level, reducing complexity to one Stokes solve and circumventing this possible difficulty. The simplest method is a fixed point iteration in which the terms involving P_H are in the RHS residual calculation. We prove convergence in Theorem 2.4.4. This method was used in our computable experiments in which convergence was seen in 15 steps or less. The proof of Theorem 2.4.4 can be adapted to give an estimate of the number of steps that is not in accord with the rapid convergence observed in our experiments. Step 2 involves solving a linear system with a mixed structure. Let RHS denote a right hand side known from previous values and let $\{\phi_1^h \cdots, \phi_N^h\}$ denote a basis for the velocity space X^h. Then we have the system

$$\begin{bmatrix} M + \frac{\Delta t}{2}A & C \\ C^t & 0 \end{bmatrix} \begin{bmatrix} u \\ \lambda \end{bmatrix} = \begin{bmatrix} RHS \\ 0 \end{bmatrix}, \text{ where} \tag{2.26}$$

$$(M + \frac{\Delta t}{2}A)_{ij} = B(\phi_i^h, \phi_j^h) := (\phi_i^h, \phi_j^h) + \frac{\Delta t}{2}(\nu_T[I - P_H]\nabla\phi_i^h, [I - P_H]\nabla\phi_j^h).$$

The $1,1$ block $M + \frac{\Delta t}{2}A$ is SPD. However, the difficulty in this system is that (for some common choices of P_H) if it is assembled it has a large bandwidth. For example, if P_H is the (weighted) L^2 projection onto a coarse mesh space, then it is very easy to compute it in a residual term but it couples fine mesh basis functions across the coarse mesh macro element. Our standard approach to mixed type systems is to solve the Schur complement system

$$C^T(M + \frac{\Delta t}{2}A)^{-1}C\lambda = C^T(RHS)$$

by an iterative method in which the inner action of $(M + \frac{\Delta t}{2}A)^{-1}$ is evaluated by another iterative method. We show in Proposition 2.4.2 that $cond(M + \frac{\Delta t}{2}A) = O(1)$ so this inner iteration is not challenging (and the action of P_H is computed in the residual calculation at each step). This suggests that alternate approaches (whose delineation is still an open question) are feasible.

To study the condition number of the $1,1$ block of (2.26), we make the following two assumptions on the velocity space which hold for many spaces on shape-regular meshes.

Condition 2.4.1 (Inverse Estimate and Norm Equivalence)**.** *(i) There is a C_{INV} such that for every $v^h \in X^h$ we have*

$$||\nabla v^h|| \leq C_{INV} h^{-1} ||v^h||.$$

(ii) There are positive constants C_1, C_2 such that for every $v^h \in X^h, v^h = \sum_{i=1}^N \alpha_i \phi_i^h$, we have

$$C_1 h^{-d} ||v^h||^2 \leq \sum_{i=1}^N \alpha_i^2 \leq C_2 h^{-d} ||v^h||^2.$$

Proposition 2.4.2. *Suppose the velocity space satisfies Condition 2.4.1 and $\nu_T = \nu_T(x, h)$. Then*

$$cond_2(M + \frac{\Delta t}{2}A) \leq \frac{C_2}{C_1}\left[1 + C_{INV}^2 \frac{\Delta t}{2h^2}\left(\max_x \nu_T(x,h)\right)\right].$$

Proof. First note that $M + \frac{\Delta t}{2}A$ is clearly SPD. Let $\overrightarrow{\alpha} = (\alpha_1, \cdots, \alpha_N)^t$ be an eigenvector of $M + \frac{\Delta t}{2}A$ and define $v^h := \sum_{i=1}^N \alpha_i \phi_i^h$. We have

$$\begin{aligned}\lambda|\overrightarrow{\alpha}|^2 &= \overrightarrow{\alpha}^t(M + \frac{\Delta t}{2}A)\overrightarrow{\alpha} = B(v^h, v^h) = \\ &= ||v^h||^2 + \frac{\Delta t}{2}(\nu_T[I - P_H]\nabla v^h, [I - P_H]\nabla v^h).\end{aligned}$$

If $\lambda = \lambda_{\min}$ then dropping $\frac{\Delta t}{2}(\nu_T[I-P_H]\nabla v^h, [I-P_H]\nabla v^h)$ and using norm equivalence we have

$$\lambda_{\min} = \frac{||v^h||^2 + \frac{\Delta t}{2}(\nu_T[I-P_H]\nabla v^h, [I-P_H]\nabla v^h)}{|\overrightarrow{\alpha}|^2} \geq C_2^{-1} h^d.$$

If $\lambda = \lambda_{\max}$ then majorizing $\frac{\Delta t}{2}(\nu_T[I-P_H]\nabla v^h, [I-P_H]\nabla v^h)$ and using the inverse estimate and norm equivalence we have

$$\begin{aligned}
\lambda_{\max} &= \frac{||v^h||^2 + \frac{\Delta t}{2}(\nu_T[I-P_H]\nabla v^h, [I-P_H]\nabla v^h)}{|\overrightarrow{\alpha}|^2} \leq \\
&\leq \frac{||v^h||^2 + \frac{\Delta t}{2}(\nu_T \nabla v^h, \nabla v^h)}{|\overrightarrow{\alpha}|^2} \leq C_1^{-1} h^d \frac{||v^h||^2 + \frac{\Delta t}{2}\left(\max_x \nu_T(x,h)\right)||\nabla v^h||^2}{||v^h||^2} \\
&\leq C_1^{-1} h^d \frac{||v^h||^2 + \frac{\Delta t}{2}\left(\max_x \nu_T(x,h)\right) C_{INV}^2 h^{-2} ||v^h||^2}{||v^h||^2} \\
&\leq C_1^{-1} h^d \left[1 + C_{INV}^2 \frac{\Delta t}{2h^2}\left(\max_x \nu_T(x,h)\right)\right].
\end{aligned}$$

The result follows by dividing these two estimates. $\square$

In many cases the dependence of $\nu_T(x,h)$ upon h scales like $O(h^2)$, implying (in these cases) that $cond_2(M + \frac{\Delta t}{2}A) = O(1)$.

Consider next the fixed point iteration for solving (2.26).

Algorithm 2.4.3. *Until convergence criteria are satisfied, given $\underline{u}_j \in V_h$ find $\underline{u}_{j+1} \in V_h$ satisfying*

$$\begin{aligned}
(\underline{u}_{j+1}, v_h) + \frac{\Delta t}{2}(\nu_T \nabla \underline{u}_{j+1}, \nabla v_h) &= \frac{\Delta t}{2}(\nu_T P_H \nabla \underline{u}_j, \nabla v_h) + (w_h^{n+1}, v_h) \\
&- \frac{\Delta t}{2}(\nu_T [I-P_H]\nabla w_h^{n+1}, \nabla v_h) \quad \textit{for all } v_h \in V_h.
\end{aligned}$$

Theorem 2.4.4. *Let $\{\underline{u}_j\}_{j\in N}$ be determined by Algorithm 2.4.3. Suppose that there exists a constant C such that $0 < \nu_T \leq C < \infty$. Then $\underline{u}_j \to \Pi w_h^{n+1}$ in X as $j \to \infty$.*

Proof. Subtracting the above equalities defining $\underline{u}_j$ and $\underline{u}_{j+1}$ yields

$$(\underline{u}_{j+1} - \underline{u}_j, v_h) + \frac{\Delta t}{2}(\nu_T \nabla(\underline{u}_{j+1} - \underline{u}_j), \nabla v_h) = \frac{\Delta t}{2}(\nu_T P_H \nabla(\underline{u}_j - \underline{u}_{j-1}), \nabla v_h).$$

Set $v_h = \underline{u}_{j+1} - \underline{u}_j$ and applying Young's inequality to the RHS give

$$\begin{aligned}
&\|\underline{u}_{j+1} - \underline{u}_j\|^2 + \frac{\Delta t}{2}\|\sqrt{\nu_T}\nabla(\underline{u}_{j+1} - \underline{u}_j)\|^2 \\
&\leq \frac{\Delta t}{4}\|\sqrt{\nu_T}P_H\nabla(\underline{u}_j - \underline{u}_{j-1})\|^2 + \frac{\Delta t}{4}\|\sqrt{\nu_T}\nabla(\underline{u}_{j+1} - \underline{u}_j)\|^2 \\
&\leq \frac{\Delta t}{4}\|\sqrt{\nu_T}\nabla(\underline{u}_j - \underline{u}_{j-1})\|^2 + \frac{\Delta t}{4}\|\sqrt{\nu_T}\nabla(\underline{u}_{j+1} - \underline{u}_j)\|^2.
\end{aligned}$$

Applying the inverse estimate $\|\underline{u}_{j+1} - \underline{u}_j\|^2 \geq C_{INV}^{-2}h^2\|\nabla(\underline{u}_{j+1} - \underline{u}_j)\|^2$, we obtain

$$C_{INV}^{-2}h^2\|\nabla(\underline{u}_{j+1} - \underline{u}_j)\|^2 + \frac{\Delta t}{4}\|\sqrt{\nu_T}\nabla(\underline{u}_{j+1} - \underline{u}_j)\|^2 \leq \frac{\Delta t}{4}\|\sqrt{\nu_T}\nabla(\underline{u}_j - \underline{u}_{j-1})\|^2.$$

Since ν_T is bounded from above by C we have

$$\frac{h^2}{C_{INV}^2 C}\|\sqrt{\nu_T}\nabla(\underline{u}_{j+1} - \underline{u}_j)\|^2 \leq C_{INV}^{-2}h^2\|\nabla(\underline{u}_{j+1} - \underline{u}_j)\|^2.$$

Therefore, $\left(\frac{h^2}{C_{INV}^2 C} + \frac{\Delta t}{4}\right)\|\sqrt{\nu_T}\nabla(\underline{u}_{j+1} - \underline{u}_j)\|^2 \leq \frac{\Delta t}{4}\|\sqrt{\nu_T}\nabla(\underline{u}_j - \underline{u}_{j-1})\|^2$. This implies (as a consequence of Contraction Mapping Theorem) both existence and uniqueness of a solution u to (2.26) and convergence. □

2.5 A COMPUTATIONALLY ATTRACTIVE VARIANT

The projector Π in Algorithm 2.3.2 is the solution of

$$\frac{1}{\Delta t}(w^{n+1} - u^{n+1}, v_h) = (\nu_T\,[I - P_H]\,\nabla\frac{w^{n+1} + u^{n+1}}{2}, [I - P_H]\,\nabla v_h).$$

The difficulty with this system for u^{n+1} is coupling across many fine mesh elements caused by the projection P_H. First note that the above is equivalent to

$$\frac{1}{\Delta t}(w^{n+1} - u^{n+1}, v_h) = (\nu_T\nabla\frac{w^{n+1} + u^{n+1}}{2}, \nabla v_h) - (\nu_T P_H\nabla\frac{w^{n+1} + u^{n+1}}{2}, \nabla v_h).$$

Thus the difficulty is given by the second term alone. We consider the modification of Step 2 in Algorithm 2.3.2 of just lagging this term to the previous time level with no iteration. The complexity of Step 2 is then one Stokes solve.

Step 2': Given $w^{n+1} \in V_h$, find $u^{n+1} \in V_h$ satisfying

$$\frac{1}{\Delta t}(w^{n+1} - u^{n+1}, v_h) = (\nu_T \nabla \frac{w^{n+1} + u^{n+1}}{2}, \nabla v_h) - (\nu_T P_H \nabla \frac{w^n + u^n}{2}, \nabla v_h), \forall v_h \in V_h. \tag{2.27}$$

In (2.27) the action of P_H is calculated for a known function and goes into the RHS of the linear system (2.27). Surprisingly, we show this to be unconditionally stable and second order accurate.

We thus consider the modification of Algorithm 2.3.2 below.

Algorithm 2.5.1. *Step 1: Given u_h^n find $w_h^{n+1} \in X_h, p_h^{n+1} \in Q_h$ satisfying*

$$\begin{aligned}(\frac{w_h^{n+1} - u_h^n}{\Delta t}, v_h) + b(\frac{w_h^{n+1} + u_h^n}{2}, \frac{w_h^{n+1} + u_h^n}{2}, v_h) + \nu(\nabla \frac{w_h^{n+1} + u_h^n}{2}, \nabla v_h) - (p_h^{n+1/2}, \nabla \cdot v_h)& \\ = (f^{n+1/2}, v_h), \ \textit{for all } v_h \in X_h,& \qquad (2.28)\\ (\nabla \cdot w_h^{n+1}, q_h) = 0, \ \textit{for all } q_h \in Q_h.&\end{aligned}$$

Step 2: $u_h^{n+1} := \Pi w_h^{n+1}$ where $(u_h^{n+1}, \lambda_h) \in X_h \times Q_h$ is the unique solution of

$$\begin{aligned}\frac{1}{\Delta t}(w_h^{n+1} - u_h^{n+1}, v_h) - (\lambda_h, \nabla \cdot v_h) = (\nu_T \nabla \frac{w_h^{n+1} + u_h^{n+1}}{2}, \nabla v_h) - (\nu_T P_H \nabla \frac{w_h^n + u_h^n}{2}, \nabla v_h),\\ (\nabla \cdot u_h^{n+1}, q_h) = 0, \qquad \forall v_h \in X_h, \ q_h \in Q_h.\end{aligned}$$

Figure 2.1 shows a flow diagram of algorithms proposed herein - Algorithm 2.3.2, 2.4.3 and 2.5.1.

Theorem 2.5.2. *Assume ν_T is constant in space at each time level. Consider Algorithm 2.5.1. It satisfies, for any $N > 0$, the following energy equality, implying stability,*

$$\begin{aligned}&\frac{1}{2}\left[||u_h^N||^2 + \Delta t||\sqrt{\nu_T} P_H \nabla \frac{w_h^N + u_h^N}{2}||^2\right] + \Delta t \sum_{n=0}^{N-1} \nu ||\nabla \frac{w_h^{n+1} + u_h^n}{2}||^2 \\ &+ \Delta t \sum_{n=0}^{N-1} \left(||\sqrt{\nu_T}[I - P_H]\nabla \frac{w_h^{n+1} + u_h^{n+1}}{2}||^2 + \frac{\Delta t^2}{8} ||\sqrt{\nu_T} P_H \nabla \left[\frac{w_h^{n+1} - w_h^n}{\Delta t} + \frac{u_h^{n+1} - u_h^n}{\Delta t}\right]||^2\right) \\ &= \frac{1}{2}\left[||u_h^0||^2 + \Delta t||\sqrt{\nu_T} P_H \nabla \frac{w_h^0 + u_h^0}{2}||^2\right] + \Delta t \sum_{n=0}^{N-1} \frac{1}{2}(f^{n+1/2}, w_h^{n+1} + u_h^n).\end{aligned}$$

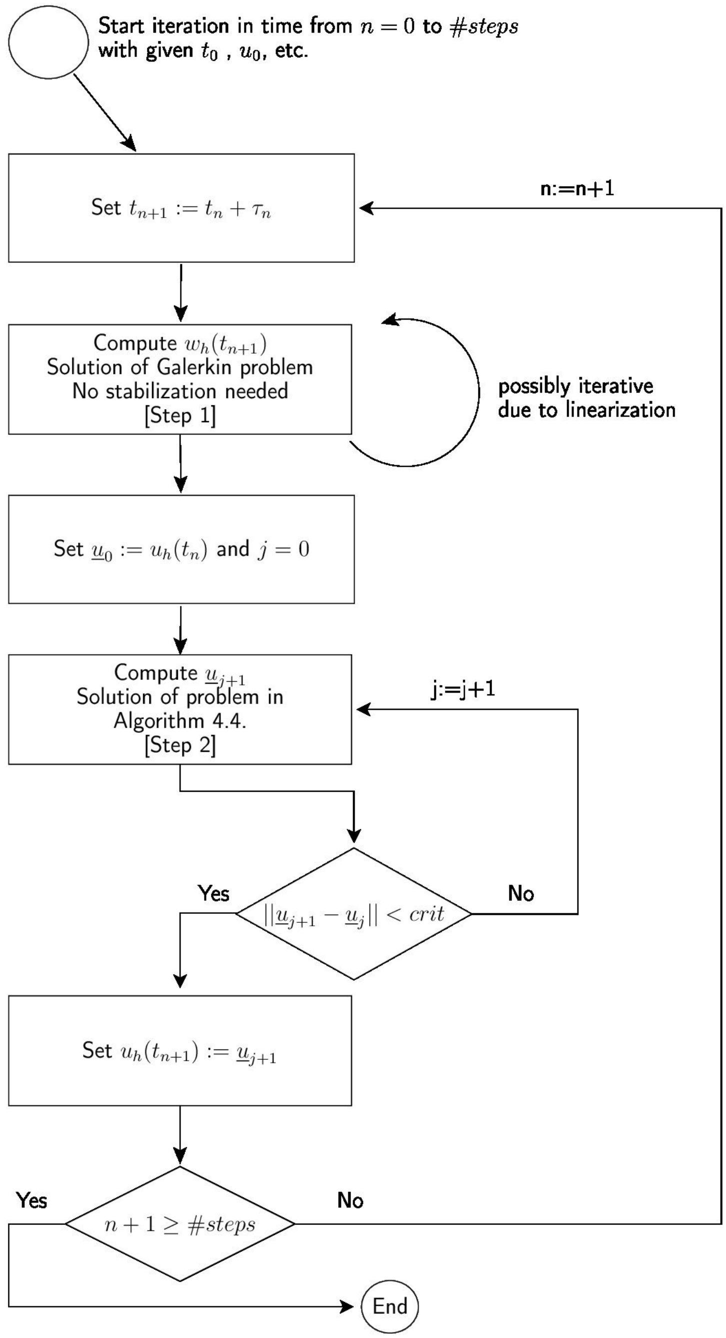

Figure 2.1: Flow diagram of a numerical simulation with Algorithm 2.3.2 and 2.4.3. The number *crit* is the stopping criterion of Algorithm 2.4.3. In Algorithm 2.5.1 we simply omit the iteration for Step 2 in the diagram.

Proof. Take the L^2 inner product of (2.28) with $(w_h^{n+1}+u_h^n)/2$. Rearranging the result gives

$$\frac{1}{2\Delta t}\left[\|u_h^{n+1}\|^2-\|u_h^n\|^2\right]+\nu\left\|\nabla\frac{w_h^{n+1}+u_h^n}{2}\right\|^2+\frac{1}{2\Delta t}\left[\|w_h^{n+1}\|^2-\|u_h^{n+1}\|^2\right]$$
$$=\frac{1}{2}(f^{n+1/2},w_h^{n+1}+u_h^n).$$

Now consider Step 2. Set $v_h=\left(w_h^{n+1}+u_h^{n+1}\right)/2$. This gives

$$\begin{aligned}
&\frac{1}{2\Delta t}\left[\|w_h^{n+1}\|^2-\|u_h^{n+1}\|^2\right]\\
&=\left\|\sqrt{\nu_T}\nabla\frac{w_h^{n+1}+u_h^{n+1}}{2}\right\|^2-\left(\nu_T P_H\nabla\frac{w_h^n+u_h^n}{2},\nabla\frac{w_h^{n+1}+u_h^{n+1}}{2}\right)\\
&=\left\|\sqrt{\nu_T}\nabla\frac{w_h^{n+1}+u_h^{n+1}}{2}\right\|^2-\left(\nu_T P_H\nabla\frac{w_h^n+u_h^n}{2},P_H\nabla\frac{w_h^{n+1}+u_h^{n+1}}{2}\right)\\
&=\left\|\sqrt{\nu_T}\nabla\frac{w_h^{n+1}+u_h^{n+1}}{2}\right\|^2-\left\{\frac{1}{2}\left\|\sqrt{\nu_T}P_H\nabla\frac{w_h^n+u_h^n}{2}\right\|^2\right.\\
&\quad\left.+\frac{1}{2}\left\|\sqrt{\nu_T}P_H\nabla\frac{w_h^{n+1}+u_h^{n+1}}{2}\right\|^2-\frac{1}{2}\left\|\sqrt{\nu_T}P_H\nabla\left[\frac{w_h^{n+1}+u_h^{n+1}}{2}-\frac{w_h^n+u_h^n}{2}\right]\right\|^2\right\}\\
&=\left\|\sqrt{\nu_T}(I-P_H)\nabla\frac{w_h^{n+1}+u_h^{n+1}}{2}\right\|^2+\frac{1}{2}\left\|\sqrt{\nu_T}P_H\nabla\left[\frac{w_h^{n+1}+u_h^{n+1}}{2}-\frac{w_h^n+u_h^n}{2}\right]\right\|^2\\
&\quad+\left\{\frac{1}{2}\left\|\sqrt{\nu_T}P_H\nabla\frac{w_h^{n+1}+u_h^{n+1}}{2}\right\|^2-\frac{1}{2}\left\|\sqrt{\nu_T}P_H\nabla\frac{w_h^n+u_h^n}{2}\right\|^2\right\}.
\end{aligned}$$

Now insert the above RHS in the energy estimate for the term $\frac{1}{2\Delta t}\left[\|w_h^{n+1}\|^2-\|u_h^{n+1}\|^2\right]$. This gives

$$\begin{aligned}
&\frac{1}{2\Delta t}\left[\|u_h^{n+1}\|^2-\|u_h^n\|^2\right]+\left\{\frac{1}{2}\left\|\sqrt{\nu_T}P_H\nabla\frac{w_h^{n+1}+u_h^{n+1}}{2}\right\|^2-\frac{1}{2}\left\|\sqrt{\nu_T}P_H\nabla\frac{w_h^n+u_h^n}{2}\right\|^2\right\}\\
&\quad+\nu\left\|\nabla\frac{w_h^{n+1}+u_h^n}{2}\right\|^2+\left\|\sqrt{\nu_T}(I-P_H)\nabla\frac{w_h^{n+1}+u_h^{n+1}}{2}\right\|^2\\
&+\frac{1}{2}\left\|\sqrt{\nu_T}P_H\nabla\left[\frac{w_h^{n+1}+u_h^{n+1}}{2}-\frac{w_h^n+u_h^n}{2}\right]\right\|^2=\frac{1}{2}(f^{n+1/2},w_h^{n+1}+u_h^n).
\end{aligned}$$

Summing from $n=0$ to $N-1$ yields the result. □

Remark 2.5.3. *The form of the kinetic energy and numerical diffusion induced by Algorithm 2.5.1 is*

$$
\begin{aligned}
Kinetic\ Energy &= \frac{1}{2}\left[\|u_h^N\|^2 + \Delta t \left\|\sqrt{\nu_T} P_H \nabla \frac{w_h^N + u_h^N}{2}\right\|^2\right],\\
Viscous\ Diffusion &= \nu \left\|\nabla \frac{w_h^{n+1} + u_h^n}{2}\right\|^2,\\
VMS\ Diffusion &= \left\|\sqrt{\nu_T}[I - P_H]\nabla \frac{w_h^{n+1} + u_h^{n+1}}{2}\right\|^2,\\
Additional\ Algorithmic\ Diffusion &= \frac{\Delta t^2}{8}\left\|\sqrt{\nu_T} P_H \nabla \left[\frac{w_h^{n+1} - w_h^n}{\Delta t} + \frac{u_h^{n+1} - u_h^n}{\Delta t}\right]\right\|^2.
\end{aligned}
$$

2.6 NUMERICAL EXPERIMENTS

We present numerical experiments to test the algorithms presented herein. Using the Green-Taylor vortex problem, we confirm the predicted convergence rates from the theory. Next, the effects of the methods as stabilization technique are tested with an advected L-shaped front. Further testing is then performed using the well-known benchmark of the decaying homogeneous isotropic turbulence to compare the algorithms presented herein to the usual approach where everything is applied in one step. We used *FreeFEM++* [56] for the Green-Taylor vortex and advection of L-shaped discontinuity and *deal.II* [6, 7] for the decaying homogeneous isotropic turbulence.

2.6.1 Green-Taylor vortex.

For the first test we select the velocity field given by the Green-Taylor vortex, [114], [113], which is used as a numerical test in many papers, e.g., Chorin [28], Tafti [112], John and Layton [69], Barbato, Berselli and Grisanti [8] and Berselli [15]. The exact velocity field is given by

$$
\begin{aligned}
&u_1(x,y,t) = -\cos(\omega\pi x)\sin(\omega\pi y)e^{-2\omega^2\pi^2 t/\tau},\ u_2(x,y,t) = \sin(\omega\pi x)\cos(\omega\pi y)e^{-2\omega^2\pi^2 t/\tau},\\
&p(x,y,t) = -\frac{1}{4}(\cos(2\omega\pi x) + \cos(2\omega\pi y))e^{-4\omega^2\pi^2 t/\tau}.
\end{aligned}
\tag{2.29}
$$

We take $\omega = 2$, $t = 1$, $\tau = Re = 500$, $\Omega = (0,1)^2$, $h = 1/m$, $\Delta t = h/10$, $H^2 = h$, where m is the number of subdivisions of the interval $(0,1)$. We utilize Taylor-Hood finite elements for the discretization. Newton iterations are applied to solve the nonlinear system with a $\|w_{(j+1)} - w_{(j)}\|_{H^1(\Omega)} < 10^{-10}$ as a stopping criterion. For the fixed point iteration in Algorithm 2.4.3, the convergence criterion is $\|\underline{u}_{(j+1)} - \underline{u}_{(j)}\|_{H^1(\Omega)} < 10^{-10}$. Convergence rates are calculated from the error at two successive values of h in the usual manner by postulating $e(h) = Ch^\beta$ and solving for β via $\beta = \ln(e(h_1)/e(h_2))/\ln(h_1/h_2)$. The boundary conditions could be taken to be periodic (the easier case). Instead we take the boundary condition on the problem to be inhomogeneous Dirichlet: $u_h = u_{exact}$, on $\partial\Omega$.

The errors and rates of convergence are presented in Table 2.1 and 2.2. From the tables, we see that the rates of convergence of both algorithms confirm the predicted convergence rates from theory. Algorithm 2.5.1 (in which the projected term in Step 2 is simply lagged to the previous time level) proves itself to be effective. While it does not utilize any iterative method in Step 2, the quality of its errors is as good as full solve VMS algorithm.

h	Δt	$\|u - u_h\|_{\infty,0}$	rate	$\|\nabla u - \nabla u_h\|_{2,0}$	rate
1/16	1/160	3.788e-2	−−	4.560e-1	−−
1/25	1/250	1.306e-2	2.39	2.009e-1	1.84
1/36	1/360	4.819e-3	2.73	8.627e-2	2.32
1/49	1/490	1.900e-3	3.02	3.975e-2	2.51
1/64	1/640	8.674e-4	2.94	1.931e-2	2.70
1/81	1/810	4.395e-4	2.89	1.009e-2	2.75
1/100	1/1000	2.642e-4	2.42	5.818e-3	2.61

Table 2.1: Error and convergence rate data for Algorithm 2.4.3

2.6.2 Test with an L-shaped discontinuity advected skew to mesh.

We also test and compare the performance of our uncoupled, partitioned approach to VMS with the usual, centered FEM without any stabilization for advection dominance on the

h	Δt	$\|u - u_h\|_{\infty,0}$	rate	$\|\nabla u - \nabla u_h\|_{2,0}$	rate
1/16	1/160	3.776e-2	$--$	4.546e-1	$--$
1/25	1/250	1.303e-2	2.38	2.007e-1	1.83
1/36	1/360	4.811e-3	2.73	8.624e-2	2.32
1/49	1/490	1.897e-3	3.02	3.974e-2	2.51
1/64	1/640	8.657e-4	2.94	1.931e-2	2.70
1/81	1/810	4.387e-4	2.89	1.009e-2	2.75
1/100	1/1000	2.638e-4	2.41	5.817e-3	2.61

Table 2.2: Error and convergence rate data for Algorithm 2.5.1

benchmark problem of advection of an L-shaped discontinuity from [10]; see [75], [72] and [73] for an analysis of projection based VMS for stabilization of advection. We solve

$$\begin{aligned} \phi_t + \mathbf{a} \cdot \nabla\phi - \nabla \cdot (\kappa \nabla \phi) = f \text{ on } \Omega, \\ \phi = g \text{ on } \partial\Omega, \end{aligned}$$

where f is the known source term, g is the prescribed boundary data, $\mathbf{a}$ is a solenoidal velocity field and κ is the diffusivity.

The problem setup is given in Figure 2.2. The domain is a unit square subdivided into triangle elements. The number of subdivisions in each side of the domain is 25. At the initial time, the value of ϕ is set to 1 in the interior of the L-shaped block located in the lower left-hand corner of the domain and 0 elsewhere. We choose the angle of advection to be 45° and the diffusivity $\kappa = 10^{-6}$. The solution is marched to $t = 0.5$ with time step $\Delta t = 0.025$. We utilize C^1-piecewise quadratic finite element in this test of three different approaches. The first approach is simply using a standard discretization scheme. The result is then compared with that of our proposed modular, postprocessing VMS approach. In the second test, the solution is computed by the Algorithm 2.4.3 and in the third test we use Algorithm 2.5.1. The results in [10] using bubble function based VMS and *quintic* smoothest splines were significantly better than all the results using projection based VMS and *quadratic* splines.

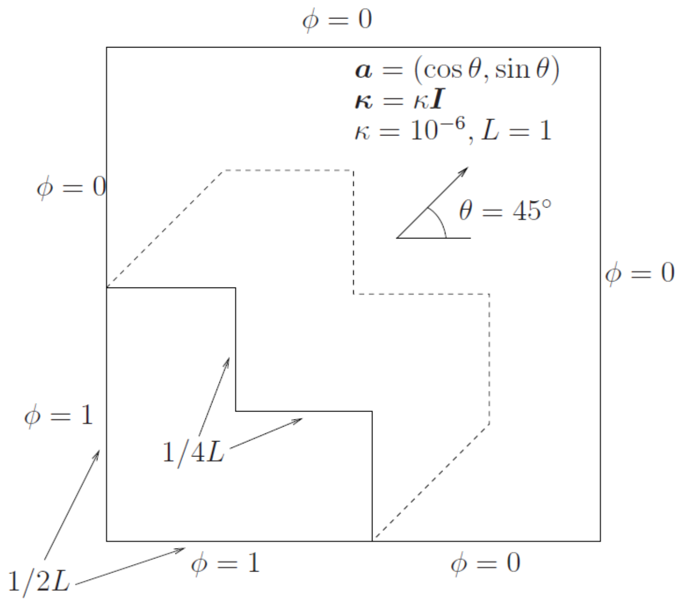

Figure 2.2: Advection of an L-shaped front. Problem description, from [10].

The performance of the mentioned methods is shown using two different approximation schemes in Step 1. In the first scheme, the numerical solutions in Step 1 are generated by Backward Euler discretization while in second scheme, we use Crank-Nicholson FEM. Results are shown in Figure 2.3 herein. We observe that in both case, the unstabilized solutions show the expected wiggles. The stabilized solutions are consistent with the results in [72] and [73]. There are less oscillations in solutions produced by the two later methods. In this test, the uncoupled VMS approach where the projected term is lagged again show its high consistence and competitiveness with the full solve VMS algorithm's solution.

2.6.3 Decaying Homogeneous Isotropic Turbulence.

Our next numerical illustration is for the three dimensional flow of the decaying, homogeneous, isotropic turbulence. The setting is a domain $\Omega = [0, 2\pi]^3$ with periodic boundary conditions on all sides of Ω and right hand side $f = 0$.

For comparison, we consider the experimental results of [29] which provide energy spectra

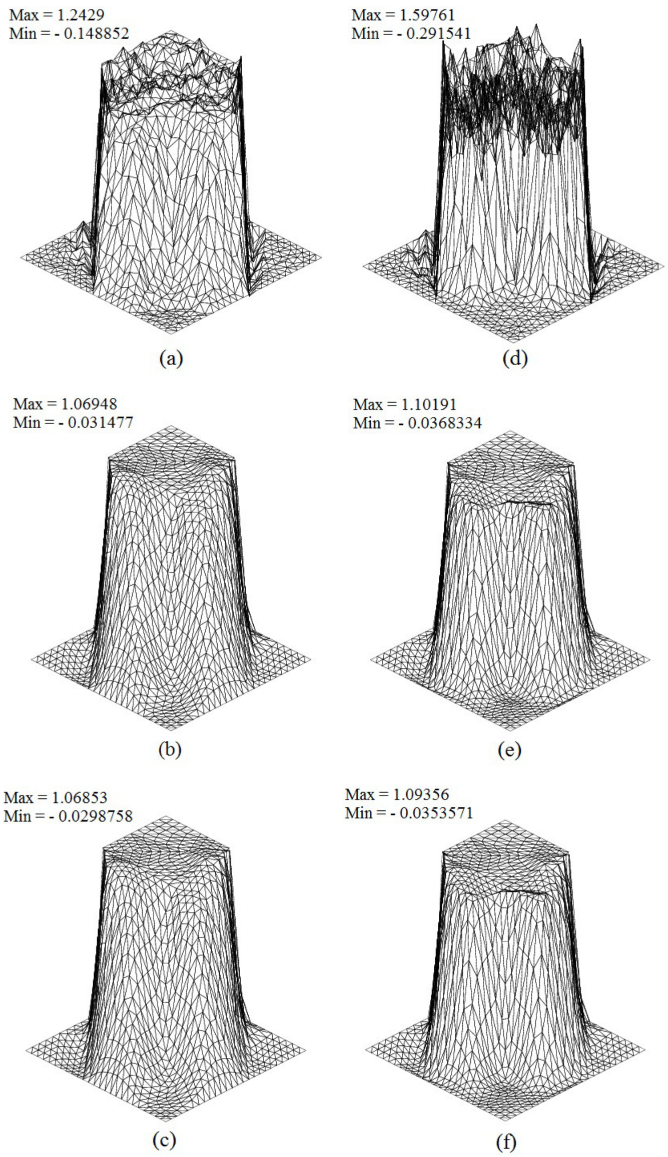

Figure 2.3: Advection of an L-shaped front. In the left is the solutions produced by using Backward Euler time discretization scheme in Step 1: (a) before stabilization, (b) after stabilized by Algorithm 2.4.3, (c) after stabilized by Algorithm 2.5.1. In the right is the solutions produced by using Crank-Nicholson time discretization scheme in Step 1: (d) before stabilization, (e) after stabilized by Algorithm 2.4.3, (f) after stabilized by Algorithm 2.5.1. The plotted solutions is at time $t = 0.5$ with time step $\Delta t = 0.025$.

at three different times. We take the first for calculating the turbulent initial data and compare the numerical solution to the remaining two energy spectra. Therefore we apply a Fourier transform $\hat{u}(k,t) = \int_\Omega u(x,t)e^{-ik\cdot x}dx$ and get the values of the energy spectrum of the numerical solution $E(k,t) = \frac{1}{2}\sum_{k-\frac{1}{2}\leq|k|\leq k+\frac{1}{2}} \hat{u}(k,t)\cdot\hat{u}(k,t)$ for a given time t. The experiment in [29] is prescribed by a Taylor scale Reynolds number $Re_\lambda = 150$ and $\nu = 1.494 \times 10^{-5}$ (Reynolds number for air).

For the simulations we apply the FE library *deal.II*, see [6, 7], with the one legged Crank-Nicolson time discretization scheme. The time-step size is taken as $\Delta t = 0.0174$, since smaller values showed no improvement. We apply the inf-sup stable Taylor-Hood element $\mathbb{Q}_2/\mathbb{Q}_1$ for the discretization of velocity and pressure in space. The nonlinearity is treated with the Picard iterative algorithm and there is no additional stabilization applied.

We will use this test case to have a fair comparison of the method developed within this paper to the usual VMS approach for this method. Therefore we choose ν_T to be as optimized for the usual VMS approach in [105]. The value of C_* in ν_T below was derived analytically based on arguments of Lilly [86]. We set ν_T to be cellwise constant and for every cell $K \subset \Omega$

$$\nu_T = C_*\Delta^2\|[I - P_H]\nabla u\|_{L^2(K)}.$$

The nonlinearity is iterated linearly within the Stokes iteration of Algorithm 2.4.3, i.e. $\nu_T = C_*\Delta^2\|[I - P_H]\nabla \underline{u}_{(j)}\|_{L^2(K)}$. The filter width is taken to be $\Delta = \frac{\min(\Delta x,\Delta y,\Delta z)}{2(q-1)}$, where $q \geq 2$ is the polynomial degree of the finite element space for the velocity and the parameter C_* is chosen like in Table 1 of [105], see Table 2.3 herein.

FE	$\mathbb{Q}_2/\mathbb{Q}_1$, $L_H = \{0\}$	$\mathbb{Q}_2/\mathbb{Q}_1$, $L_H = \mathbb{Q}_0^{disc}$
C_*	0.0942	0.2010

Table 2.3: Corresponding C_* for different finite element large scale spaces

To illustrate the behaviour of the decaying turbulence we show some results on the development of the kinetic energy, approximated by $\|u_h\|^2$, in Figure 2.4. The kinetic energy of the approximated solution is shown with 32^3 degrees of freedom for the pure Galerkin method without any additional stabilization etc. We observe that a turbulence model is really necessary, since the energy does not decay. The other lines correspond to the usual approaches of the variational multiscale method and the Smagorinsky in comparison to the Algorithms with an explicitly uncoupled postprocessing step developed herein. They are denoted by Exp. VMS, respectively Exp. Smagorinsky. We obtain that the additional postprocessing step induces additional numerical diffusion and that the Smagorinsky induces more diffusion than the VMS method.

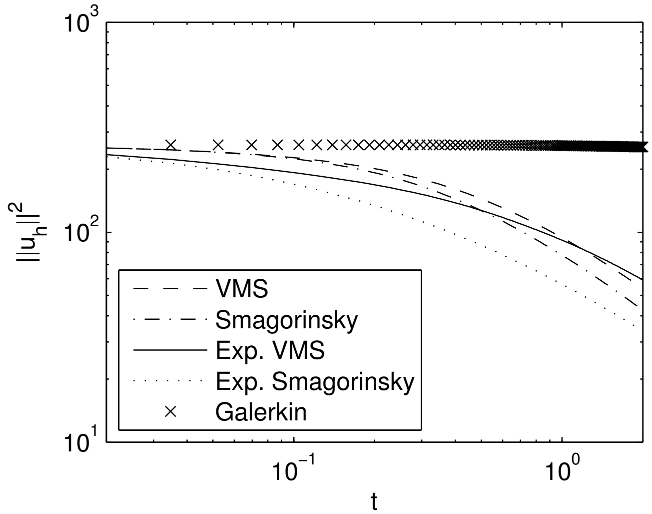

Figure 2.4: The decay of energy with time for different schemes.

Next, we look at the energy spectrum at different points in time. In Figure 2.5 we see results for the Smagorinsky model, i.e. $L_H = \{0\}$. With 32^3 and also 64^3 degrees of freedom for the velocity we obtain values of the energy spectrum in good agreement to the reference data. When we apply the Smagorinsky model in a postprocessing step we can see that more dissipation is induced. The plot also indicates that the Galerkin method without any turbulence model can not predict the energy spectra from [29] at the times $t = 0.87$ and $t = 2.0$.

Figure 2.6 illustrates a comparable behaviour as the explicitly uncoupled postprocessing step induces more dissipation to the system than the coupled, one step VMS approach. In this case the results of the postprocessed method with 32^3 degrees of freedom for the velocity are even closer to the reference data than the pure VMS results. On the left side of Figure

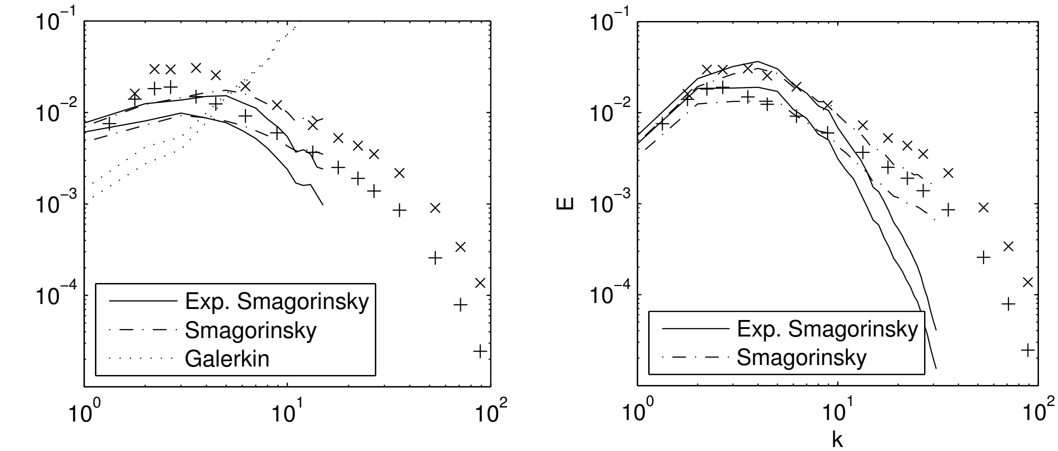

Figure 2.5: Energy spectra observed with the Smagorinsky model in comparison to a postprocessed Smagorinsky step, i.e. Algorithm 2.3.2 with $L_H = \{0\}$. 'x' and '+' denote the experimental data from Ref. [29].

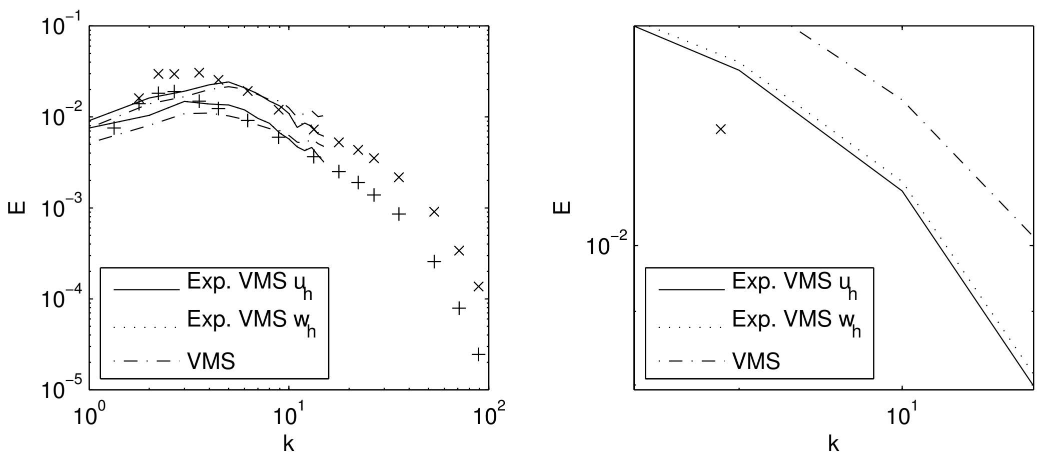

Figure 2.6: Energy spectra observed with 32^3 degrees of freedom for the velocity and the usual VMS model in comparison to a postprocessed VMS step, i.e. Algorithm 2.3.2 with $L_H = \mathbb{Q}_0^{disc}$, and a zoom into the plot on the right. 'x' and '+' denote the experimental data from Ref. [29].

2.6 the dotted line corresponding to the solution of Step 1 in Algorithm 2.3.2 is very hard to see. That is why we added a zoom into the plot on the right side, where one can see that the values for w_h are always very close to the values of u_h but always higher. This is exactly what one would expect, since the Step 2 is adding the numerical diffusion stemming from the VMS method in every time step.

When we look at the results with 64^3 degrees of freedom for the velocity in Figure 2.7 on the left, we see a similar behaviour as in the case of the Smagorinsky model. The postprocessing step induces more dissipation than the monolithic VMS method and this must be taken into account in the selection of C_*. On the right side of Figure 2.7 we see results for a different value of C_* in a better comparison to the experimental data.

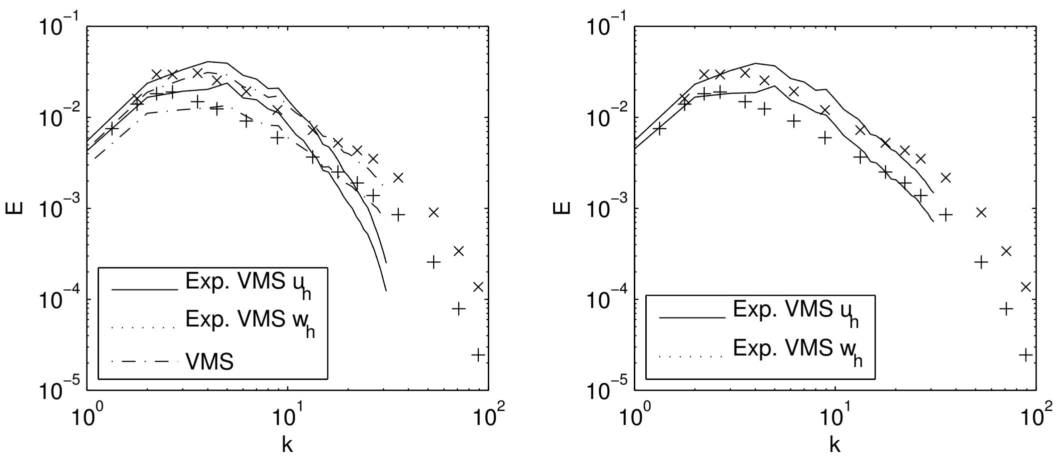

Figure 2.7: Energy spectra observed with 64^3 degrees of freedom for the velocity and the usual VMS model in comparison to a postprocessed VMS step, i.e. Algorithm 2.3.2 with $L_H = \mathbb{Q}_0^{disc}$ on the left. The postprocessed VMS step with a parameter $C_*/4$ on the right. 'x' and '+' denote the experimental data from Ref. [29].

In Figure 2.8 we present some observations concerning Algorithm 2.4.3 to compute the projection in Step 2 of Algorithm 2.3.2. Here we see that the number of iterations decays and that very few iterations are needed, except in the first steps. This decay might be related to the stopping criteria since the L^2-norm of the solution is decaying with the energy and the stopping criterion depends on the L^2-norm. Nevertheless, the results are very satisfying and in good agreement to the theory.

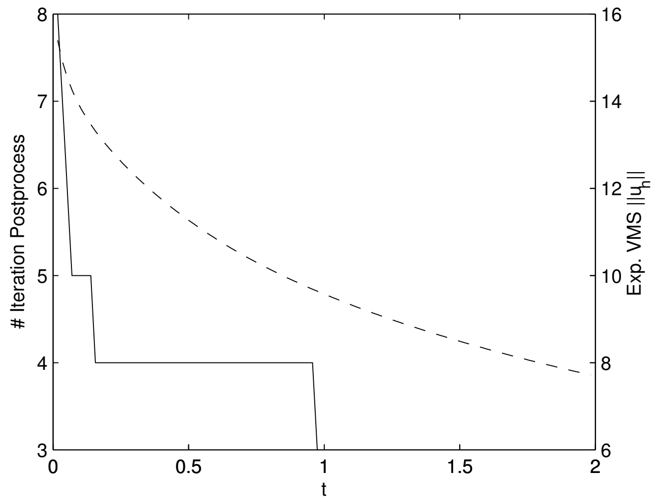

Figure 2.8: Number of iterations in Algorithm 2.4.3 with stopping criterion $\|\underline{u}_{(j+1)} - \underline{u}_{(j)}\| < 10^{-4}$ (solid line) and the decay of the L^2-norm of the approximated solution (dashed line).

2.7 CONCLUSIONS

The goal of any uncoupled, partitioned method is to give results not appreciably worse than the associated fully coupled approach (which is expected to be more accurate) by methods that have algorithmic advantages. The treatment of the variational multiscale method as an uncoupled postprocessing step is an effective method to introduce a modern approach to turbulence in a given fluid code. It is stable and accurate. The uncoupled method predicted the energy spectra of decaying homogeneous isotropic turbulence overall comparably to the full VMS approach. By this standard, this is a successful test for the method. To compute the projection with Algorithm 2.4.3 very few iterations are needed and the (preliminary) results from just lagging the troublesome term are also positive.

There are many open problems in elaborating this approach to VMS methods. These include extending the postprocessing VMS approach to the most common realization of VMS using bubble functions and understanding how to use Step 2 when Step 1 is the result from a black box flow code. This requires in particular understanding modifications in the algorithm and analysis necessary when different meshes are used for Steps 1 and 2. Further, general experience with partitioned methods suggests that some price is inevitably paid for uncoupling a coupled problem. Understanding if that is true for the methods herein and where the price is paid is another important open problem.

3.0 PARTITIONED TIME STEPPING METHODS FOR MAGNETOHYDRODYNAMICS FLOWS

3.1 PROBLEM SETTING

Incompressible flow of an electrically conducting fluid in the presence of a magnetic field at low R_m is modelled by the system, see, e.g., [103, 53, 127]: Given $\mathbf{f}$, $\mathbf{B}$ and time $T > 0$, find $\mathbf{u} : \Omega \times [0, T] \to \mathbb{R}^d$, $p : \Omega \times [0, T] \to \mathbb{R}$ and $\phi : \Omega \times [0, T] \to \mathbb{R}$ such that:

$$\begin{aligned} \frac{1}{N}(\mathbf{u}_t + \mathbf{u} \cdot \nabla \mathbf{u}) - \frac{1}{M^2}\Delta \mathbf{u} + \nabla p \;&=\; \mathbf{f} + (\mathbf{B} \times \nabla\phi + \mathbf{B} \times (\mathbf{B} \times \mathbf{u}))\,, \\ \Delta\phi = \nabla \cdot (\mathbf{u} \times \mathbf{B}),\ \text{ and }\ \nabla \cdot \mathbf{u} \;&=\; 0. \end{aligned} \tag{RMHD}$$

Here Ω is a bounded, Lipschitz domain in $\mathbb{R}^d$ ($d = 3$) and the body force $\mathbf{f}$ and the magnetic field $\mathbf{B}$ are assumed to be known with $\nabla \cdot \mathbf{B} = 0$. Further, $\mathbf{u}$ is the fluid velocity, p is pressure and ϕ is electric potential. M, N are the Hartman number and interaction parameter given by

$$M = BL\sqrt{\frac{\sigma}{\rho\nu}}, \quad N = \sigma B^2 \frac{L}{\rho u}$$

where u, B, L are the characteristic velocity, magnetic field and length, respectively. The other parameters appearing above are the density ρ, the kinematic viscosity ν, and the electrical conductivity σ, all assumed constant. The system (RMHD) is supplemented by the homogeneous Dirichlet boundary conditions

$$\mathbf{u} = 0,\ \ \phi = 0 \text{ on } \partial\Omega \times [0, T]$$

and the initial data

$$\mathbf{u}(x,0) = \mathbf{u}_0(x)\ \forall x \in \Omega. \tag{3.1}$$

Other boundary conditions and variable material parameters can be considered. However, constant parameters and simple boundary conditions allow us to focus on the physical coupling between u and ϕ and an algorithm allowing uncoupling of RMHD into physical subprocesses.

In this chapter, we propose and analyze the stability and errors of two partitioned methods for the evolutionary RMHD equations. The methods we study herein include a first order, one step scheme and a second order, two step scheme, both of which consist of implicit discretization of the subproblem terms and explicit discretization of coupling terms. These approaches solve the coupled problems by solving each sub-physics problem per time step (without iteration), allowing the use of optimized NSE codes and Ohm's law codes.

3.1.1 Notation and preliminaries.

In this chapter, we will use C_0 to represent a generic positive constant whose value may be different from place to place but which is independent of mesh size and time step. The velocity, pressure and potential spaces are $X = (H_0^1(\Omega))^d$, $Q = L_0^2(\Omega)$ and $S = H_0^1(\Omega)$, respectively. The space of divergence free functions is given by

$$V = \left\{\mathbf{v} \in X :\ (\nabla \cdot \mathbf{v}, q) = 0 \ \ \forall q \in Q\right\}.$$

A weak formulation of (RMHD) is: Find $\mathbf{u} : [0,T] \to X$, $p : [0,T] \to Q$ and $\phi : [0,T] \to S$ for a.e. $t \in (0,T]$ satisfying

$$\begin{aligned}
&\frac{1}{N}((\mathbf{u}_t,\mathbf{v}) + (\mathbf{u}\cdot\nabla\mathbf{u},\mathbf{v})) + \frac{1}{M^2}(\nabla\mathbf{u},\nabla\mathbf{v}) - (p,\nabla\cdot\mathbf{v}) \\
&\qquad\qquad + (\mathbf{u}\times\mathbf{B},\mathbf{v}\times\mathbf{B}) - (\nabla\phi,\mathbf{v}\times\mathbf{B}) = (\mathbf{f},\mathbf{v}) \ \ \forall \mathbf{v} \in X, \\
&(\nabla\cdot\mathbf{u}, q) = 0 \quad \forall q \in Q, \\
&-(\nabla\phi,\nabla\psi) + (\mathbf{u}\times\mathbf{B},\nabla\psi) = 0 \quad \forall \psi \in S,
\end{aligned} \tag{3.2}$$

with the initial condition (3.1) a.e. in Ω. Note that, setting $\mathbf{v}=\mathbf{u}$, $\psi=\phi$ and adding, the coupling terms exactly cancel in the monolithic sum and one verifies the energy equality of the continuous problem.

To make a spatial discretization of the RMHD system by the finite element method, we select finite element spaces

$$\text{velocity: } X^h \subset X, \text{ pressure: } Q^h \subset Q, \text{ and potential: } S^h \subset S$$

which are built on a conforming, edge to edge triangulation with maximum triangle parameter denoted by a subscript "h". We assume that $X^h \times Q^h$ satisfies the usual discrete inf-sup condition for the stability of the discrete pressure and X^h, Q^h, S^h satisfy approximation properties of piecewise polynomials on quasi-uniform meshes of local degrees $k, k-1, k$ respectively. The error analysis in [103, 127] indicates that the same order elements to be used for the velocity and electric potential. The discretely divergence free velocity space is denoted by

$$V^h := X^h \cap \{\mathbf{v}_h : (q_h, \nabla\cdot\mathbf{v}_h) = 0, \text{ for all } q_h \in Q^h\}.$$

Also define the usual, explicitly skew symmetrized trilinear form

$$b(\mathbf{u},\mathbf{v},\mathbf{w}) = \frac{1}{2}((\mathbf{u}\cdot\nabla\mathbf{v},\mathbf{w}) - (\mathbf{u}\cdot\nabla\mathbf{w},\mathbf{v})).$$

The monolithic, semi-discrete approximation of (3.2) (see [127]) are maps $(\mathbf{u}_h, p_h, \phi_h)$: $[0,T] \to X^h \times Q^h \times S^h$ satisfying for all $\mathbf{v}_h \in X^h, q_h \in Q^h, \psi_h \in S^h$

$$\begin{aligned}
&\frac{1}{N}((\mathbf{u}_{h,t},\mathbf{v}_h) + b(\mathbf{u}_h,\mathbf{u}_h,\mathbf{v}_h)) + \frac{1}{M^2}(\nabla\mathbf{u}_h,\nabla\mathbf{v}_h) - (p_h,\nabla\cdot\mathbf{v}_h)\\
&\qquad + (\mathbf{u}_h\times\mathbf{B},\mathbf{v}_h\times\mathbf{B}) - (\nabla\phi_h,\mathbf{v}_h\times\mathbf{B}) = (\mathbf{f},\mathbf{v}_h),\\
&(\nabla\cdot\mathbf{u}_h, q_h) = 0,\\
&-(\nabla\phi_h,\nabla\psi_h) + (\mathbf{u}_h\times\mathbf{B},\nabla\psi_h) = 0.
\end{aligned} \tag{3.3}$$

3.2 THE PARTITIONED TIME STEPPING SCHEMES

The methods we propose and analyze herein have the coupling terms lagged or extrapolated in a careful way that preserves stability. Thus the system at each time step uncouples into two subproblem solves. The first scheme we study is a combination of the backward Euler method with the coupling terms treated by the forward Euler method. It is *first* order accurate and solves two subproblems *parallely.* We call this scheme **1PARA**. We shall use the same time step in both subproblems. It reads

Algorithm 3.2.1 (First order scheme)**.** *Given* $\mathbf{u}_h^n \in X^h, p_h^n \in Q^h, \phi_h^n \in S^h$*, find* $\mathbf{u}_h^{n+1} \in X^h, p_h^{n+1} \in Q^h, \phi_h^{n+1} \in S^h$ *satisfying*

$$\begin{aligned}
&\frac{1}{N}\left(\left(\frac{\mathbf{u}_h^{n+1}-\mathbf{u}_h^n}{\Delta t}, \mathbf{v}_h\right) + b(\mathbf{u}_h^{n+1}, \mathbf{u}_h^{n+1}, \mathbf{v}_h)\right) + \frac{1}{M^2}(\nabla \mathbf{u}_h^{n+1}, \nabla \mathbf{v}_h) \\
&\qquad - (p_h^{n+1}, \nabla \cdot \mathbf{v}_h) + (\mathbf{u}_h^{n+1} \times \mathbf{B}, \mathbf{v}_h \times \mathbf{B}) - (\nabla \phi_h^n, \mathbf{v}_h \times \mathbf{B}) = (\mathbf{f}^{n+1}, \mathbf{v}_h), \\
&(\nabla \cdot \mathbf{u}_h^{n+1}, q_h) = 0, \\
&-(\nabla \phi_h^{n+1}, \nabla \psi_h) + (\mathbf{u}_h^n \times \mathbf{B}, \nabla \psi_h) = 0,
\end{aligned} \tag{1PARA}$$

for all $\mathbf{v}_h \in X^h, q_h \in Q^h$ *and* $\psi_h \in S^h$*.*

The second scheme we consider employs second order, three level BDF discretization for the subproblem terms. The coupling terms are treated by two step extrapolation in Navier-Stokes equation and by implicit method in Ohm's law. Since one needs the updated value of u_h at current time level to compute ϕ_h, this method is uncoupled but sequential: $\phi_h^n \to \mathbf{u}_h^{n+1} \to \phi_h^{n+1}$. Nevertheless, solving the subproblems sequentially may be an acceptable tradeoff for higher accuracy and preservation of stability. Computing time for the nonlinear equation of $\mathbf{u}_h$ is normally expected to dominate that for the Poisson solve for ϕ_h. We call this method **2SEQU**

Algorithm 3.2.2 (Second order scheme)**.** *Given* $\mathbf{u}_h^{n-1}, \mathbf{u}_h^n \in X^h, p_h^{n-1}, p_h^n \in Q^h, \phi_h^{n-1}, \phi_h^n \in S^h$, *find* $\mathbf{u}_h^{n+1} \in X^h, p_h^{n+1} \in Q^h, \phi_h^{n+1} \in S^h$ *satisfying*

$$\begin{aligned}
&\frac{1}{N}\left(\left(\frac{3\mathbf{u}_h^{n+1} - 4\mathbf{u}_h^n + \mathbf{u}_h^{n-1}}{2\Delta t}, \mathbf{v}_h\right) + b(\mathbf{u}_h^{n+1}, \mathbf{u}_h^{n+1}, \mathbf{v}_h)\right) + \frac{1}{M^2}(\nabla \mathbf{u}_h^{n+1}, \nabla \mathbf{v}_h) \\
&\qquad - (p_h^{n+1}, \nabla \cdot \mathbf{v}_h) + (\mathbf{u}_h^{n+1} \times \mathbf{B}, \mathbf{v}_h \times \mathbf{B}) - (\nabla(2\phi_h^n - \phi^{n-1}), \mathbf{v}_h \times \mathbf{B}) = (\mathbf{f}^{n+1}, \mathbf{v}_h), \\
&(\nabla \cdot \mathbf{u}_h^{n+1}, q_h) = 0, \qquad\qquad \text{(2SEQU)} \\
&- (\nabla \phi_h^{n+1}, \nabla \psi_h) + (\mathbf{u}_h^{n+1} \times \mathbf{B}, \nabla \psi_h) = 0,
\end{aligned}$$

for all $\mathbf{v}_h \in X^h, q_h \in Q^h$ *and* $\psi_h \in S^h$.

3.3 STABILITY

In this section, we establish stability of the approximations in Algorithms 1PARA and 2SEQU.

Theorem 3.3.1 (Unconditional stability of Algorithm 1PARA)**.** *Let* $(\mathbf{u}_h^n, p_h^n, \phi_h^n) \in X^h \times Q^h \times S^h$ *satisfy* (1PARA) *for each* $n \in \{1, 2, ..., \frac{T}{\Delta t}\}$. *Then*

$$\begin{aligned}
&\frac{1}{N}\|\mathbf{u}_h^n\|^2 + \frac{1}{N}\sum_{j=0}^{n-1}\|\mathbf{u}_h^{j+1} - \mathbf{u}_h^j\|^2 + \Delta t\|\nabla \phi_h^n\|^2 + \Delta t\|\mathbf{B} \times \mathbf{u}_h^n\|^2 + \frac{\Delta t}{M^2}\sum_{j=0}^{n-1}\|\nabla \mathbf{u}_h^{j+1}\|^2 \\
&\qquad + \Delta t\sum_{j=0}^{n-1}\left(\| - \nabla \phi_h^j + \mathbf{u}_h^{j+1} \times \mathbf{B}\|^2 + \| - \nabla \phi_h^{j+1} + \mathbf{u}_h^j \times \mathbf{B}\|^2\right) \qquad (3.4) \\
&\leq \frac{1}{N}\|\mathbf{u}_h^0\|^2 + \Delta t\|\nabla \phi_h^0\|^2 + \Delta t\|\mathbf{B} \times \mathbf{u}_h^0\|^2 + M^2\Delta t\sum_{j=0}^{n-1}\|\mathbf{f}^{j+1}\|_{-1}^2.
\end{aligned}$$

Proof. In (1PARA), setting $\mathbf{v}_h = \mathbf{u}_h^{j+1}, q_h = p_h^{j+1}, \psi_h = \phi_h^{j+1}$, we have

$$\begin{aligned}
&\frac{1}{2\Delta t}\cdot\frac{1}{N}\left(\|\mathbf{u}_h^{j+1}\|^2 - \|\mathbf{u}_h^j\|^2 + \|\mathbf{u}_h^{j+1} - \mathbf{u}_h^j\|^2\right) + \frac{1}{M^2}\|\nabla \mathbf{u}_h^{j+1}\|^2 + \|\mathbf{B} \times \mathbf{u}_h^{j+1}\|^2 \\
&\qquad = \left(\mathbf{u}_h^{j+1} \times \mathbf{B}, \nabla \phi_h^j\right) + (\mathbf{f}^{j+1}, \mathbf{u}_h^{j+1}), \qquad (3.5) \\
&\|\nabla \phi_h^{j+1}\|^2 = \left(\mathbf{u}_h^j \times \mathbf{B}, \nabla \phi_h^{j+1}\right).
\end{aligned}$$

Applying polarization identity $ab = \frac{1}{2}a^2 + \frac{1}{2}b^2 - \frac{1}{2}(a-b)^2$, it gives

$$\begin{aligned}\big(\mathbf{u}_h^{j+1}\times\mathbf{B}, \nabla\phi_h^j\big) &= \frac{1}{2}\|\mathbf{u}_h^{j+1}\times\mathbf{B}\|^2 + \frac{1}{2}\|\nabla\phi_h^j\|^2 - \frac{1}{2}\|-\nabla\phi_h^j + \mathbf{u}_h^{j+1}\times\mathbf{B}\|^2,\\ \big(\mathbf{u}_h^{j}\times\mathbf{B}, \nabla\phi_h^{j+1}\big) &= \frac{1}{2}\|\mathbf{u}_h^{j}\times\mathbf{B}\|^2 + \frac{1}{2}\|\nabla\phi_h^{j+1}\|^2 - \frac{1}{2}\|-\nabla\phi_h^{j+1} + \mathbf{u}_h^{j}\times\mathbf{B}\|^2.\end{aligned} \tag{3.6}$$

Inserting (3.6) into (3.5), adding (3.5), then multiplying by $2\Delta t$ and summing from $j=0$ to $n-1$ give

$$\begin{aligned}&\frac{1}{N}\|\mathbf{u}_h^n\|^2 + \frac{1}{N}\sum_{j=0}^{n-1}\|\mathbf{u}_h^{j+1} - \mathbf{u}_h^j\|^2 + \Delta t\|\nabla\phi_h^n\|^2 + \Delta t\|\mathbf{B}\times\mathbf{u}_h^n\|^2\\ &+ \frac{2\Delta t}{M^2}\sum_{j=0}^{n-1}\|\nabla\mathbf{u}_h^{j+1}\|^2 + \Delta t\sum_{j=0}^{n-1}\big(\|-\nabla\phi_h^j + \mathbf{u}_h^{j+1}\times\mathbf{B}\|^2 + \|-\nabla\phi_h^{j+1} + \mathbf{u}_h^j\times\mathbf{B}\|^2\big)\\ &\qquad = \frac{1}{N}\|\mathbf{u}_h^0\|^2 + \Delta t\|\nabla\phi_h^0\|^2 + \Delta t\|\mathbf{B}\times\mathbf{u}_h^0\|^2 + 2\Delta t\sum_{j=0}^{n-1}(\mathbf{f}^{j+1}, \mathbf{u}_h^{j+1}).\end{aligned}$$

Applying Young's inequality yields the result. □

Remark 3.3.2. *Besides the electric potential ϕ, the electric current density $\mathbf{J}$ defined by $\mathbf{J} = \sigma(-\nabla\phi + \mathbf{u}\times\mathbf{B})$ is another important electromagnetic quantity to be determined in MHD flows, see [104, 35]. For 1PARA, the stability of $\mathbf{J}$ comes directly from the boundedness of $\frac{1}{N}\sum_{j=0}^{n-1}\|\mathbf{u}_h^{j+1} - \mathbf{u}_h^j\|^2$ and $\Delta t\sum_{j=0}^{n-1}\|-\nabla\phi_h^{j+1} + \mathbf{u}_h^j\times\mathbf{B}\|^2$ in (3.4).*

Next, we turn to Algorithm 2SEQU. We prove that it is stable over $0 \le t < \infty$ with a condition related the time step and the problem data but independent of the spacial meshwidth.

Theorem 3.3.3 (Stability of Algorithm 2SEQU)**.** *Let $(\mathbf{u}_h^n, p_h^n, \phi_h^n) \in X^h \times Q^h \times S^h$ satisfy (2SEQU) for each $n \in \{1, 2, ..., \frac{T}{\Delta t}\}$. Under the time step restriction*

$$\Delta t < \frac{1}{2N\|\mathbf{B}\|_{L^\infty}^2(M^2C_P^2\|\mathbf{B}\|_{L^\infty}^2 + 1)} \tag{3.7}$$

Algorithm 2SEQU is stable

$$\begin{aligned}&\frac{1}{2N}\|\mathbf{u}_h^n\|^2 + \frac{1}{2N}\|2\mathbf{u}_h^n - \mathbf{u}_h^{n-1}\|^2 + \frac{\Delta t}{2M^2}\sum_{j=1}^{n-1}\|\nabla\mathbf{u}_h^{j+1}\|^2 + \frac{\Delta t}{\sigma^2}\sum_{j=1}^{n-1}\|2\mathbf{J}^j - \mathbf{J}^{j-1}\|^2\\ &\le \frac{1}{2N}\|\mathbf{u}_h^1\|^2 + \frac{1}{2N}\|2\mathbf{u}_h^1 - \mathbf{u}_h^0\|^2 + 2\Delta t M^2\sum_{j=1}^{n-1}\|\mathbf{f}^{j+1}\|_{-1}^2.\end{aligned} \tag{3.8}$$

Proof. Set $\mathbf{v}_h = \mathbf{u}_h^{j+1}$ in the first equation of (2SEQU) and use the identity

$$\frac{1}{4}[3a^2 - 4b^2 + c^2] + \frac{1}{2}(a-b)^2 - \frac{1}{2}(b-c)^2 + \frac{1}{4}(a-2b+c)^2 = \frac{1}{2}(3a-4b+c)a$$

with $a = \mathbf{u}_h^{j+1}, b = \mathbf{u}_h^j, c = \mathbf{u}_h^{j-1}$ to get

$$\begin{aligned}
&\frac{1}{4\Delta t}\cdot\frac{1}{N}\left(3\|\mathbf{u}_h^{j+1}\|^2 - 4\|\mathbf{u}_h^j\|^2 + \|\mathbf{u}_h^{j-1}\|^2\right)\\
&\quad + \frac{1}{2\Delta t}\cdot\frac{1}{N}\|\mathbf{u}_h^{j+1} - \mathbf{u}_h^j\|^2 - \frac{1}{2\Delta t}\cdot\frac{1}{N}\|\mathbf{u}_h^j - \mathbf{u}_h^{j-1}\|^2\\
&\quad + \frac{1}{4\Delta t}\cdot\frac{1}{N}\|\mathbf{u}_h^{j+1} - 2\mathbf{u}_h^j + \mathbf{u}_h^{j-1}\|^2 + \frac{1}{M^2}\|\nabla\mathbf{u}_h^{j+1}\|^2 + \frac{1}{2}\|\mathbf{B}\times\mathbf{u}_h^{j+1}\|^2\\
&\quad + \frac{1}{2}\| - \nabla(2\phi_h^j - \phi_h^{j-1}) + \mathbf{u}_h^{j+1}\times\mathbf{B}\|^2\\
&= \frac{1}{2}\|\nabla(2\phi_h^j - \phi_h^{j-1})\|^2 + (\mathbf{f}^{j+1}, \mathbf{u}_h^{j+1}).
\end{aligned} \tag{3.9}$$

The third equation of (2SEQU) gives

$$-(\nabla(2\phi_h^j - \phi_h^{j-1}), \nabla\psi_h) + ((2\mathbf{u}_h^j - \mathbf{u}_h^{j-1})\times\mathbf{B}, \nabla\psi_h) = 0.$$

Setting $\psi_h = 2\phi_h^j - \phi_h^{j-1}$, we have

$$\begin{aligned}
\|\nabla(2\phi_h^j - \phi_h^{j-1})\|^2 = &\|(2\mathbf{u}_h^j - \mathbf{u}_h^{j-1})\times\mathbf{B}\|^2\\
&- \|-\nabla(2\phi_h^j - \phi_h^{j-1}) + (2\mathbf{u}_h^j - \mathbf{u}_h^{j-1})\times\mathbf{B}\|^2.
\end{aligned} \tag{3.10}$$

Plugging (3.10) into (3.9) yields

$$\begin{aligned}
&\frac{1}{4\Delta t}\cdot\frac{1}{N}\left(3\|\mathbf{u}_h^{j+1}\|^2 - 4\|\mathbf{u}_h^j\|^2 + \|\mathbf{u}_h^{j-1}\|^2\right)\\
&\quad + \frac{1}{2\Delta t}\cdot\frac{1}{N}\|\mathbf{u}_h^{j+1} - \mathbf{u}_h^j\|^2 - \frac{1}{2\Delta t}\cdot\frac{1}{N}\|\mathbf{u}_h^j - \mathbf{u}_h^{j-1}\|^2\\
&\quad + \frac{1}{4\Delta t}\cdot\frac{1}{N}\|\mathbf{u}_h^{j+1} - 2\mathbf{u}_h^j + \mathbf{u}_h^{j-1}\|^2 + \frac{1}{M^2}\|\nabla\mathbf{u}_h^{j+1}\|^2 + \frac{1}{2}\|\mathbf{B}\times\mathbf{u}_h^{j+1}\|^2\\
&\quad + \frac{1}{2}\| - \nabla(2\phi_h^j - \phi_h^{j-1}) + \mathbf{u}_h^{j+1}\times\mathbf{B}\|^2 + \frac{1}{2}\|-\nabla(2\phi_h^j - \phi_h^{j-1}) + (2\mathbf{u}_h^j - \mathbf{u}_h^{j-1})\times\mathbf{B}\|^2\\
&= \frac{1}{2}\|(2\mathbf{u}_h^j - \mathbf{u}_h^{j-1})\times\mathbf{B}\|^2 + (\mathbf{f}^{j+1}, \mathbf{u}_h^{j+1}).
\end{aligned} \tag{3.11}$$

Next, observe that for an arbitrary $\epsilon > 0$

$$
\begin{aligned}
\|(2\mathbf{u}_h^j - \mathbf{u}_h^{j-1}) \times \mathbf{B}\|^2 &= \|(-\mathbf{u}_h^{j+1} + 2\mathbf{u}_h^j - \mathbf{u}_h^{j-1}) \times \mathbf{B}\|^2 + \|\mathbf{u}_h^{j+1} \times \mathbf{B}\|^2 \\
&\quad + 2((-\mathbf{u}_h^{j+1} + 2\mathbf{u}_h^j - \mathbf{u}_h^{j-1}) \times \mathbf{B}, \mathbf{u}_h^{j+1} \times \mathbf{B}) \\
&= \|(-\mathbf{u}_h^{j+1} + 2\mathbf{u}_h^j - \mathbf{u}_h^{j-1}) \times \mathbf{B}\|^2 + \|\mathbf{u}_h^{j+1} \times \mathbf{B}\|^2 + \frac{1}{\epsilon^2}\|(-\mathbf{u}_h^{j+1} + 2\mathbf{u}_h^j - \mathbf{u}_h^{j-1}) \times \mathbf{B}\|^2 \\
&\quad + \epsilon^2 \|\mathbf{u}_h^{j+1} \times \mathbf{B}\|^2 - \|(\frac{1}{\epsilon}(-\mathbf{u}_h^{j+1} + 2\mathbf{u}_h^j - \mathbf{u}_h^{j-1}) - \epsilon \mathbf{u}_h^{j+1}) \times \mathbf{B}\|^2 \\
&\leq \left(1 + \frac{1}{\epsilon^2}\right) \|\mathbf{B}\|_{L^\infty}^2 \|(-\mathbf{u}_h^{j+1} + 2\mathbf{u}_h^j - \mathbf{u}_h^{j-1})\|^2 + \|\mathbf{u}_h^{j+1} \times \mathbf{B}\|^2 \\
&\quad + \epsilon^2 C_P^2 \|\mathbf{B}\|_{L^\infty}^2 \|\nabla \mathbf{u}_h^{j+1}\|^2 - \|(\frac{1}{\epsilon}(-\mathbf{u}_h^{j+1} + 2\mathbf{u}_h^j - \mathbf{u}_h^{j-1}) - \epsilon \mathbf{u}_h^{j+1}) \times \mathbf{B}\|^2
\end{aligned} \tag{3.12}
$$

where C_P is the Poincaré constant.

From (3.12), we can hide $\frac{1}{2}\|(2\mathbf{u}_h^j - \mathbf{u}_h^{j-1}) \times \mathbf{B}\|^2$ in the left hand side of (3.11) to obtain

$$
\begin{aligned}
&\frac{1}{4\Delta t} \cdot \frac{1}{N} \left(3\|\mathbf{u}_h^{j+1}\|^2 - 4\|\mathbf{u}_h^j\|^2 + \|\mathbf{u}_h^{j-1}\|^2\right) \\
&\qquad + \frac{1}{2\Delta t} \cdot \frac{1}{N}\|\mathbf{u}_h^{j+1} - \mathbf{u}_h^j\|^2 - \frac{1}{2\Delta t} \cdot \frac{1}{N}\|\mathbf{u}_h^j - \mathbf{u}_h^{j-1}\|^2 \\
&\qquad + \left(\frac{1}{4\Delta t} \cdot \frac{1}{N} - \frac{1}{2}\left(1 + \frac{1}{\epsilon^2}\right)\|\mathbf{B}\|_{L^\infty}^2\right)\|\mathbf{u}_h^{j+1} - 2\mathbf{u}_h^j + \mathbf{u}_h^{j-1}\|^2 \\
&\quad + \frac{1}{2}\| - \nabla(2\phi_h^j - \phi_h^{j-1}) + \mathbf{u}_h^{j+1} \times \mathbf{B}\|^2 + \frac{1}{2}\| - \nabla(2\phi_h^j - \phi_h^{j-1}) + (2\mathbf{u}_h^j - \mathbf{u}_h^{j-1}) \times \mathbf{B}\|^2 \\
&\quad + \frac{1}{2}\|(\frac{1}{\epsilon}(-\mathbf{u}_h^{j+1} + 2\mathbf{u}_h^j - \mathbf{u}_h^{j-1}) - \epsilon \mathbf{u}_h^{j+1}) \times \mathbf{B}\|^2 + \left(\frac{1}{M^2} - \frac{1}{2}\epsilon^2 C_P^2 \|\mathbf{B}\|_{L^\infty}^2\right)\|\nabla \mathbf{u}_h^{j+1}\|^2 \\
&\leq (\mathbf{f}^{j+1}, \mathbf{u}_h^{j+1}).
\end{aligned} \tag{3.13}
$$

Let $\epsilon = (C_P M \|\mathbf{B}\|_{L^\infty})^{-1}$, under the condition (3.7), we have from (3.13)

$$
\begin{aligned}
&\frac{1}{4\Delta t} \cdot \frac{1}{N} \left(3\|\mathbf{u}_h^{j+1}\|^2 - 4\|\mathbf{u}_h^j\|^2 + \|\mathbf{u}_h^{j-1}\|^2\right) \\
&\qquad + \frac{1}{2\Delta t} \cdot \frac{1}{N}\|\mathbf{u}_h^{j+1} - \mathbf{u}_h^j\|^2 - \frac{1}{2\Delta t} \cdot \frac{1}{N}\|\mathbf{u}_h^j - \mathbf{u}_h^{j-1}\|^2 \\
&\quad + \frac{1}{2}\| - \nabla(2\phi_h^j - \phi_h^{j-1}) + \mathbf{u}_h^{j+1} \times \mathbf{B}\|^2 + \frac{1}{2}\| - \nabla(2\phi_h^j - \phi_h^{j-1}) + (2\mathbf{u}_h^j - \mathbf{u}_h^{j-1}) \times \mathbf{B}\|^2 \\
&\quad + \frac{1}{2}\|(\frac{1}{\epsilon}(-\mathbf{u}_h^{j+1} + 2\mathbf{u}_h^j - \mathbf{u}_h^{j-1}) - \epsilon \mathbf{u}_h^{j+1}) \times \mathbf{B}\|^2 + \frac{1}{2M^2}\|\nabla \mathbf{u}_h^{j+1}\|^2 \\
&\leq (\mathbf{f}^{j+1}, \mathbf{u}_h^{j+1}).
\end{aligned}
$$

Summing from $j = 1$ to $n-1$, multiply both sides by $2\Delta t$ and use the identity

$$\frac{3}{2}a^2 - \frac{1}{2}b^2 + (a-b)^2 = \frac{a^2}{2} + \left(a\sqrt{2} - \frac{b}{\sqrt{2}}\right)^2$$

we get

$$\begin{aligned}
&\frac{1}{2N}\|\mathbf{u}_h^n\|^2 + \frac{1}{2N}\|2\mathbf{u}_h^n - \mathbf{u}_h^{n-1}\|^2 + \frac{\Delta t}{M^2}\sum_{j=1}^{n-1}\|\nabla\mathbf{u}_h^{j+1}\|^2 \\
&\quad + \Delta t\sum_{j=1}^{n-1}\| - \nabla(2\phi_h^j - \phi_h^{j-1}) + \mathbf{u}_h^{j+1}\times\mathbf{B}\|^2 \\
&\quad + \Delta t\sum_{j=1}^{n-1}\|-\nabla(2\phi_h^j - \phi_h^{j-1}) + (2\mathbf{u}_h^j - \mathbf{u}_h^{j-1})\times\mathbf{B}\|^2 \\
&\leq \frac{1}{2N}\|\mathbf{u}_h^1\|^2 + \frac{1}{2N}\|2\mathbf{u}_h^1 - \mathbf{u}_h^0\|^2 + 2\Delta t\sum_{j=1}^{n-1}(\mathbf{f}^{j+1}, \mathbf{u}_h^{j+1}).
\end{aligned}$$

Applying Young's inequality for the term involving body force yields the energy estimate (3.8). □

3.4 ERROR ANALYSIS

We proceed to give an a priori error estimate for the partitioned methods 1PARA and 2SEQU. Due to the length and technicality of the proofs, for compactness, we only present the error of the first order uncoupling scheme, i.e. Algorithm 1PARA. With minor modifications (and greater length), the analogous convergence rates are obtained for Algorithm 2SEQU.

Let $t^j = j\Delta t$ and $\mathbf{u}^j := \mathbf{u}(t^j)$ (and similarly for other variables). To establish the optimal error estimate for the model, we introduce the following discrete norms

$$|||\omega|||_{\infty,k} := \max_{0\leq j\leq T/\Delta t}\|\omega^j\|_k, \quad |||\omega|||_{2,k} := \left(\sum_{j=0}^{T/\Delta t}\|\omega^j\|_k^2\Delta t\right)^{1/2}$$

and assume the following regularity of the true solution

$$\begin{aligned}
&\mathbf{u}\in L^\infty(0,T;(H^{k+1}(\Omega))^d)\cap H^1(0,T;(H^{k+1}(\Omega))^d)\cap H^2(0,T;(L^2(\Omega))^d), \\
&p\in L^2(0,T;H^{s+1}(\Omega)),\ \phi\in L^\infty(0,T;H^{k+1}(\Omega))\cap H^1(0,T;H^1(\Omega))
\end{aligned} \tag{3.14}$$

Denote the errors by $e_{\mathbf{u}}^j = \mathbf{u}^j - \mathbf{u}_h^j, e_\phi^j = \phi^j - \phi_h^j$ and $e_{\mathbf{J}}^j = -\nabla e_\phi^j + e_{\mathbf{u}}^j \times \mathbf{B}$. We have the following result.

Theorem 3.4.1. *For $\mathbf{u}, p, \phi$ satisfying the weak formulation (3.2) and regularity condition (3.14), and $\mathbf{u}_h^n, p_h^n, \phi_h^n$ given by Algorithm 1PARA with $n \in \{1, 2, ..., \frac{T}{\Delta t}\}$, we have for Δt sufficiently small*

$$
\begin{aligned}
&\|e_{\mathbf{u}}^n\|^2 + \sum_{j=0}^{n-1} \|e_{\mathbf{u}}^{j+1} - e_{\mathbf{u}}^j\|^2 + \frac{N\Delta t}{M^2} \sum_{j=0}^{n-1} \|\nabla e_{\mathbf{u}}^{j+1}\|^2 + N\Delta t \sum_{j=0}^{n-1} \|\nabla e_\phi^{j+1}\|^2 \\
&+ N\Delta t \sum_{j=0}^{n-1} \| - \nabla e_\phi^j + e_{\mathbf{u}}^{j+1} \times \mathbf{B}\|^2 + N\Delta t \sum_{j=0}^{n-1} \| - \nabla e_\phi^{j+1} + e_{\mathbf{u}}^j \times \mathbf{B}\|^2 \\
&\leq C_0 \Bigg(\|\mathbf{u}^0 - \mathbf{u}_h^0\|^2 + \|\nabla(\phi^0 - \phi_h^0)\|^2 + h^{2k+2} |||\mathbf{u}|||_{\infty,k+1}^2 + h^{2k} |||\phi|||_{\infty,k+1}^2 \\
&+ h^{2k+2} \|\mathbf{u}_t\|_{2,k+1}^2 + h^{2k} |||\mathbf{u}|||_{2,k+1}^2 + h^{4k} |||\mathbf{u}|||_{4,k+1}^4 + \Delta t^2 \|\phi_t\|_{2,1}^2 + h^{2s+2} |||p|||_{2,s+1}^2 \\
&+ \Delta t^2 \|\mathbf{u}_{tt}\|_{2,0}^2 + h^{2k} |||\phi|||_{2,k+1}^2 + h^{2k+2} |||\mathbf{u}|||_{2,k+1}^2 + \Delta t^2 \|\mathbf{u}_t\|_{2,0}^2 \Bigg).
\end{aligned} \tag{3.15}
$$

Proof. At time $t^{j+1} = (j+1)\Delta t$, the true solution $(\mathbf{u}, p, \phi)$ of (3.2) satisfies

$$
\begin{aligned}
&\frac{1}{N} \left(\left(\frac{\mathbf{u}^{j+1} - \mathbf{u}^j}{\Delta t}, \mathbf{v}_h \right) + b(\mathbf{u}^{j+1}, \mathbf{u}^{j+1}, \mathbf{v}_h) \right) + \frac{1}{M^2} (\nabla \mathbf{u}^{j+1}, \nabla \mathbf{v}_h) \\
&\quad - (p^{j+1}, \nabla \cdot \mathbf{v}_h) + (\mathbf{u}^{j+1} \times \mathbf{B}, \mathbf{v}_h \times \mathbf{B}) - (\nabla \phi^j, \mathbf{v}_h \times \mathbf{B}) = (\mathbf{f}^{j+1}, \mathbf{v}_h) \\
&\quad + (\nabla(\phi^{j+1} - \phi^j), \mathbf{v}_h \times \mathbf{B}) + \frac{1}{N} \left(\frac{\mathbf{u}^{j+1} - \mathbf{u}^j}{\Delta t} - u_t(t^{j+1}), \mathbf{v}_h \right) \quad \forall \mathbf{v}_h \in X_h, \\
&- (\nabla \phi^{j+1}, \nabla \psi_h) + (\mathbf{u}^j \times \mathbf{B}, \nabla \psi_h) = -((\mathbf{u}^{j+1} - \mathbf{u}^j) \times \mathbf{B}, \nabla \psi_h) \quad \forall \psi_h \in S_h.
\end{aligned} \tag{3.16}
$$

We construct the error equations for velocity and electric potential. Decompose the velocity error

$$
\mathbf{u}^{j+1} - \mathbf{u}_h^{j+1} = (\mathbf{u}^{j+1} - \tilde{\mathbf{u}}_h^{j+1}) + (\tilde{\mathbf{u}}_h^{j+1} - \mathbf{u}_h^{j+1}) =: \eta^{j+1} + \mathbf{U}_h^{j+1}
$$

and the electric potential error

$$
\phi^{j+1} - \phi_h^{j+1} = (\phi^{j+1} - \tilde{\phi}_h^{j+1}) + (\tilde{\phi}_h^{j+1} - \phi_h^{j+1}) =: \zeta^{j+1} + \Phi_h^{j+1}
$$

where $\tilde{\mathbf{u}}_h^{j+1}$ and $\tilde{\phi}_h^{j+1}$ will be the interpolation of $\mathbf{u}^{j+1}$ and ϕ^{j+1} in V_h and S_h, respectively.

Substract (3.16) from (1PARA) and set $\mathbf{v}_h = \mathbf{U}_h^{j+1}$ and $\psi_h = \Phi_h^{j+1}$ to obtain

$$
\begin{aligned}
&\frac{1}{2\Delta t}\cdot\frac{1}{N}\left(\|\mathbf{U}_h^{j+1}\|^2 - \|\mathbf{U}_h^{j}\|^2 + \|\mathbf{U}_h^{j+1} - \mathbf{U}_h^{j}\|^2\right) + \frac{1}{M^2}\|\nabla\mathbf{U}_h^{j+1}\|^2 + \|\mathbf{B}\times\mathbf{U}_h^{j+1}\|^2\\
&-(\nabla\Phi_h^j, \mathbf{U}_h^{j+1}\times\mathbf{B}) = -\frac{1}{N}\left(\frac{\eta^{j+1}-\eta^j}{\Delta t}, \mathbf{U}_h^{j+1}\right) - \frac{1}{N}b(\mathbf{U}_h^{j+1}, \mathbf{u}^{j+1}, \mathbf{U}_h^{j+1})\\
&\quad -\frac{1}{N}b(\mathbf{u}_h^{j+1}, \eta^{j+1}, \mathbf{U}_h^{j+1}) - \frac{1}{N}b(\eta^{j+1}, \mathbf{u}^{j+1}, \mathbf{U}_h^{j+1}) + (p^{j+1} - \lambda_h^{j+1}, \nabla\cdot\mathbf{U}_h^{j+1})\\
&\quad -\frac{1}{M^2}(\nabla\eta^{j+1}, \nabla\mathbf{U}_h^{j+1}) - (\eta^{j+1}\times\mathbf{B}, \mathbf{U}_h^{j+1}\times\mathbf{B}) + (\nabla\zeta^j, \mathbf{U}_h^{j+1}\times\mathbf{B})\\
&\quad +(\nabla(\phi^{j+1}-\phi^j), \mathbf{U}_h^{j+1}\times\mathbf{B}) + \frac{1}{N}\left(\frac{\mathbf{u}^{j+1}-\mathbf{u}^j}{\Delta t} - u_t(t^{j+1}), \mathbf{U}_h^{j+1}\right),
\end{aligned}
\tag{3.17}
$$

for every $\lambda_h^{j+1}\in Q^h$, and

$$
\begin{aligned}
-\|\nabla\Phi_h^{j+1}\|^2 + (\mathbf{U}_h^j\times\mathbf{B}, \nabla\Phi_h^{j+1}) &= (\nabla\zeta^{j+1}, \nabla\Phi_h^{j+1})\\
&\quad -(\eta^j\times\mathbf{B}, \nabla\Phi_h^{j+1}) - ((\mathbf{u}^{j+1}-\mathbf{u}^j)\times\mathbf{B}, \nabla\Phi_h^{j+1}).
\end{aligned}
\tag{3.18}
$$

We have from (3.18)

$$
\begin{aligned}
2\|\nabla\Phi_h^{j+1}\|^2 - (\mathbf{U}_h^j\times\mathbf{B}, \nabla\Phi_h^{j+1}) &= (\mathbf{U}_h^j\times\mathbf{B}, \nabla\Phi_h^{j+1}) - 2(\nabla\zeta^{j+1}, \nabla\Phi_h^{j+1})\\
&\quad + 2(\eta^j\times\mathbf{B}, \nabla\Phi_h^{j+1}) + 2((\mathbf{u}^{j+1}-\mathbf{u}^j)\times\mathbf{B}, \nabla\Phi_h^{j+1}).
\end{aligned}
\tag{3.19}
$$

Adding (3.17) and (3.19) and rearranging terms in the left hand side give

$$
\begin{aligned}
&\frac{1}{2\Delta t}\cdot\frac{1}{N}\left(\|\mathbf{U}_h^{j+1}\|^2 - \|\mathbf{U}_h^{j}\|^2 + \|\mathbf{U}_h^{j+1} - \mathbf{U}_h^{j}\|^2\right) + \frac{1}{M^2}\|\nabla\mathbf{U}_h^{j+1}\|^2\\
&\quad + \frac{1}{2}\|\mathbf{U}_h^{j+1}\times\mathbf{B}\|^2 - \frac{1}{2}\|\mathbf{U}_h^{j}\times\mathbf{B}\|^2 + \frac{1}{2}\|\nabla\Phi_h^{j+1}\|^2 - \frac{1}{2}\|\nabla\Phi_h^{j}\|^2\\
&+\frac{1}{2}\|-\nabla\Phi_h^j + \mathbf{U}_h^{j+1}\times\mathbf{B}\|^2 + \frac{1}{2}\|-\nabla\Phi_h^{j+1} + \mathbf{U}_h^{j}\times\mathbf{B}\|^2 + \|\nabla\Phi_h^{j+1}\|^2\\
&= -\frac{1}{N}\left(\frac{\eta^{j+1}-\eta^j}{\Delta t}, \mathbf{U}_h^{j+1}\right) - \frac{1}{N}b(\mathbf{U}_h^{j+1}, \mathbf{u}^{j+1}, \mathbf{U}_h^{j+1})\\
&-\frac{1}{N}b(\mathbf{u}_h^{j+1}, \eta^{j+1}, \mathbf{U}_h^{j+1}) - \frac{1}{N}b(\eta^{j+1}, \mathbf{u}^{j+1}, \mathbf{U}_h^{j+1}) + (p^{j+1} - \lambda_h^{j+1}, \nabla\cdot\mathbf{U}_h^{j+1})\\
&-\frac{1}{M^2}(\nabla\eta^{j+1}, \nabla\mathbf{U}_h^{j+1}) - (-\nabla\zeta^j + \eta^{j+1}\times\mathbf{B}, \mathbf{U}_h^{j+1}\times\mathbf{B}) + (\mathbf{U}_h^j\times\mathbf{B}, \nabla\Phi_h^{j+1})\\
&\quad +(\nabla(\phi^{j+1}-\phi^j), \mathbf{U}_h^{j+1}\times\mathbf{B}) + \frac{1}{N}\left(\frac{\mathbf{u}^{j+1}-\mathbf{u}^j}{\Delta t} - \mathbf{u}_t(t^{j+1}), \mathbf{U}_h^{j+1}\right)\\
&\quad -2(\nabla\zeta^{j+1}, \nabla\Phi_h^{j+1}) + 2(\eta^j\times\mathbf{B}, \nabla\Phi_h^{j+1}) + 2((\mathbf{u}^{j+1}-\mathbf{u}^j)\times\mathbf{B}, \nabla\Phi_h^{j+1}).
\end{aligned}
\tag{3.20}
$$

We proceed to bound each term on the right hand side of (3.20), absorb like-terms into the left hand side. For an arbitrary $\varepsilon > 0$,

$$-\frac{1}{N}\left(\frac{\eta^{j+1}-\eta^j}{\Delta t}, \mathbf{U}_h^{j+1}\right) \le \frac{1}{4\varepsilon N^2}\left\|\frac{\eta^{j+1}-\eta^j}{\Delta t}\right\|_{-1}^2 + \varepsilon\|\nabla \mathbf{U}_h^{j+1}\|^2. \tag{3.21}$$

The first nonlinear term can be bounded as

$$\begin{aligned}-\frac{1}{N}b(\mathbf{U}_h^{j+1}, \mathbf{u}^{j+1}, \mathbf{U}_h^{j+1}) &\le C_0\|\mathbf{U}_h^{j+1}\|\|\mathbf{u}^{j+1}\|_2\|\nabla \mathbf{U}_h^{j+1}\| \\ &\le \frac{C_0^2}{4\varepsilon}\|\mathbf{U}_h^{j+1}\|^2\|\mathbf{u}^{j+1}\|_2^2 + \varepsilon\|\nabla \mathbf{U}_h^{j+1}\|^2.\end{aligned} \tag{3.22}$$

We now give an estimation for $-\frac{1}{N}b(\mathbf{u}_h^{j+1}, \eta^{j+1}, \mathbf{U}_h^{j+1})$:

$$\begin{aligned}-\frac{1}{N}b(\mathbf{u}_h^{j+1}, \eta^{j+1}, \mathbf{U}_h^{j+1}) &= -\frac{1}{N}b(\mathbf{u}^{j+1}, \eta^{j+1}, \mathbf{U}_h^{j+1}) \\ &\quad + \frac{1}{N}b(\eta^{j+1}, \eta^{j+1}, \mathbf{U}_h^{j+1}) + \frac{1}{N}b(\mathbf{U}_h^{j+1}, \eta^{j+1}, \mathbf{U}_h^{j+1}),\end{aligned}$$

where terms in the right hand side can be controlled as

$$\begin{aligned}-\frac{1}{N}b(\mathbf{u}^{j+1}, \eta^{j+1}, \mathbf{U}_h^{j+1}) \le& C_0\|\nabla\mathbf{u}^{j+1}\|\|\nabla\eta^{j+1}\|\|\nabla \mathbf{U}_h^{j+1}\| \\ \le& \frac{C_0^2}{4\varepsilon}\|\mathbf{u}\|_{\infty,1}^2\|\nabla\eta^{j+1}\|^2 + \varepsilon\|\nabla \mathbf{U}_h^{j+1}\|^2,\end{aligned} \tag{3.23}$$

$$\frac{1}{N}b(\eta^{j+1}, \eta^{j+1}, \mathbf{U}_h^{j+1}) \le \frac{C_0^2}{4\varepsilon}\|\nabla\eta^{j+1}\|^4 + \varepsilon\|\nabla \mathbf{U}_h^{j+1}\|^2, \tag{3.24}$$

and

$$\begin{aligned}\frac{1}{N}b(\mathbf{U}_h^{j+1}, \eta^{j+1}, \mathbf{U}_h^{j+1}) &\le C_0\|\mathbf{U}_h^{j+1}\|^{1/2}\|\nabla\mathbf{U}_h^{j+1}\|^{1/2}\|\nabla\eta^{j+1}\|\|\nabla \mathbf{U}_h^{j+1}\| \\ &\le C_0h^{-1/2}\|\mathbf{U}_h^{j+1}\|\|\nabla\eta^{j+1}\|\|\nabla \mathbf{U}_h^{j+1}\| \le C_0h^{1/2}\|\mathbf{U}_h^{j+1}\|\|\mathbf{u}^{j+1}\|_2\|\nabla \mathbf{U}_h^{j+1}\| \\ &\le \frac{C_0^2}{4\varepsilon}h\|\mathbf{U}_h^{j+1}\|^2\|\mathbf{u}^{j+1}\|_2^2 + \varepsilon\|\nabla \mathbf{U}_h^{j+1}\|^2.\end{aligned} \tag{3.25}$$

The last nonlinear term can be bounded exactly like in (3.23). For the pressure term

$$(p^{j+1}-\lambda_h^{j+1}, \nabla\cdot\mathbf{U}_h^{j+1}) \le \frac{C_0^2}{4\varepsilon}\|p^{j+1}-\lambda_h^{j+1}\|^2 + \varepsilon\|\nabla \mathbf{U}_h^{j+1}\|^2. \tag{3.26}$$

We continue to deal with the remaining terms. First,

$$-\frac{1}{M^2}(\nabla\eta^{j+1}, \nabla\mathbf{U}_h^{j+1}) \le \frac{C_0^2}{4\varepsilon}\|\nabla\eta^{j+1}\|^2 + \varepsilon\|\nabla \mathbf{U}_h^{j+1}\|^2. \tag{3.27}$$

Next, we have

$$-(-\nabla\zeta^j+\eta^{j+1}\times\mathbf{B},\mathbf{U}_h^{j+1}\times\mathbf{B})\le\|-\nabla\zeta^j+\eta^{j+1}\times\mathbf{B}\|\|\mathbf{U}_h^{j+1}\times\mathbf{B}\| \tag{3.28}$$
$$\le C_0\|-\nabla\zeta^j+\eta^{j+1}\times\mathbf{B}\|^2+\|\mathbf{B}\|_{L^\infty}^2\|\mathbf{U}_h^{j+1}\|^2.$$

Also, observe that

$$(\mathbf{U}_h^j\times\mathbf{B},\nabla\Phi_h^{j+1})\le\|\mathbf{U}_h^j\times\mathbf{B}\|\|\nabla\Phi_h^{j+1}\|\le\frac{1}{4\varepsilon'}\|\mathbf{B}\|_{L^\infty}^2\|\mathbf{U}_h^j\|^2+\varepsilon'\|\nabla\Phi_h^{j+1}\|^2, \tag{3.29}$$

and

$$(\nabla(\phi^{j+1}-\phi^j),\mathbf{U}_h^{j+1}\times\mathbf{B})\le C_0\|\nabla(\phi^{j+1}-\phi^j)\|^2+\|\mathbf{B}\|_{L^\infty}^2\|\mathbf{U}_h^{j+1}\|^2. \tag{3.30}$$

Furthermore,

$$\frac{1}{N}\left(\frac{\mathbf{u}^{j+1}-\mathbf{u}^j}{\Delta t}-\mathbf{u}_t(t^{j+1}),\mathbf{U}_h^{j+1}\right)\le C_0\left\|\frac{\mathbf{u}^{j+1}-\mathbf{u}^j}{\Delta t}-\mathbf{u}_t(t^{j+1})\right\|\|\nabla\mathbf{U}_h^{j+1}\| \tag{3.31}$$
$$\le\frac{C_0^2}{4\varepsilon}\left\|\frac{\mathbf{u}^{j+1}-\mathbf{u}^j}{\Delta t}-\mathbf{u}_t(t^{j+1})\right\|^2+\varepsilon\left\|\nabla\mathbf{U}_h^{j+1}\right\|^2.$$

We also have

$$-2(\nabla\zeta^{j+1},\nabla\Phi_h^{j+1})\le2\|\nabla\zeta^{j+1}\|\|\nabla\Phi_h^{j+1}\|\le\frac{1}{\varepsilon'}\|\nabla\zeta^{j+1}\|^2+\varepsilon'\|\nabla\Phi_h^{j+1}\|^2. \tag{3.32}$$

Finally, it gives

$$2(\eta^j\times\mathbf{B},\nabla\Phi_h^{j+1})\le2\|\eta^j\times\mathbf{B}\|\|\nabla\Phi_h^{j+1}\|\le\frac{1}{\varepsilon'}\|\mathbf{B}\|_{L^\infty}^2\|\eta^j\|^2+\varepsilon'\|\nabla\Phi_h^{j+1}\|^2, \tag{3.33}$$

and

$$2((\mathbf{u}^{j+1}-\mathbf{u}^j)\times\mathbf{B},\nabla\Phi_h^{j+1})\le2\|(\mathbf{u}^{j+1}-\mathbf{u}^j)\times\mathbf{B}\|\|\nabla\Phi_h^{j+1}\| \tag{3.34}$$
$$\le\frac{1}{\varepsilon'}\|\mathbf{B}\|_{L^\infty}^2\|\mathbf{u}^{j+1}-\mathbf{u}^j\|^2+\varepsilon'\|\nabla\Phi_h^{j+1}\|^2.$$

Applying estimate (3.21)–(3.34) to (3.20) with $\varepsilon = \frac{1}{18M^2}$ and $\varepsilon' = \frac{1}{8}$ gives

$$
\begin{aligned}
&\frac{1}{2\Delta t}\cdot\frac{1}{N}\left(\|\mathbf{U}_h^{j+1}\|^2 - \|\mathbf{U}_h^{j}\|^2 + \|\mathbf{U}_h^{j+1}-\mathbf{U}_h^{j}\|^2\right) + \frac{1}{2M^2}\|\nabla\mathbf{U}_h^{j+1}\|^2 \\
&\quad + \frac{1}{2}\|\mathbf{U}_h^{j+1}\times\mathbf{B}\|^2 - \frac{1}{2}\|\mathbf{U}_h^{j}\times\mathbf{B}\|^2 + \frac{1}{2}\|\nabla\Phi_h^{j+1}\|^2 - \frac{1}{2}\|\nabla\Phi_h^{j}\|^2 \\
&\quad + \frac{1}{2}\|-\nabla\Phi_h^{j} + \mathbf{U}_h^{j+1}\times\mathbf{B}\|^2 + \frac{1}{2}\|-\nabla\Phi_h^{j+1} + \mathbf{U}_h^{j}\times\mathbf{B}\|^2 + \frac{1}{2}\|\nabla\Phi_h^{j+1}\|^2 \\
&\le \left(\frac{9}{2}C_0^2M^2\|\mathbf{u}^{j+1}\|_2^2(1+h) + 2\|\mathbf{B}\|_{L^\infty}^2\right)\|\mathbf{U}_h^{j+1}\|^2 + 2\|\mathbf{B}\|_{L^\infty}^2\|\mathbf{U}_h^{j}\|^2 \\
&\quad + \frac{9M^2}{2N^2}\left\|\frac{\eta^{j+1}-\eta^j}{\Delta t}\right\|_{-1}^2 + 9C_0^2M^2\|\mathbf{u}\|_{\infty,1}^2\|\nabla\eta^{j+1}\|^2 + \frac{9}{2}C_0^2M^2\|\nabla\eta^{j+1}\|^4 \\
&\quad + \frac{9}{2}C_0^2M^2\|p^{j+1}-\lambda_h^{j+1}\|^2 + \frac{9}{2}C_0^2M^2\|\nabla\eta^{j+1}\|^2 + C_0\|-\nabla\zeta^j + \eta^{j+1}\times\mathbf{B}\|^2 \\
&\quad + C_0\|\nabla(\phi^{j+1}-\phi^j)\|^2 + \frac{9}{2}C_0^2M^2\left\|\frac{\mathbf{u}^{j+1}-\mathbf{u}^j}{\Delta t} - \mathbf{u}_t(t^{j+1})\right\|^2 \\
&\quad + 8\|\nabla\zeta^{j+1}\|^2 + 8\|\mathbf{B}\|_{L^\infty}^2\|\eta^j\|^2 + 8\|\mathbf{B}\|_{L^\infty}^2\|\mathbf{u}^{j+1}-\mathbf{u}^j\|^2.
\end{aligned}
\tag{3.35}
$$

Let $\kappa = 9C_0^2M^2N\|\mathbf{u}\|_{\infty,2}^2(1+h) + 8\|\mathbf{B}\|_{L^\infty}^2N$, summing from $j=0$ to $j=n-1$ and applying the discrete Grönwall lemma (Lemma 1.4.4) yield

$$
\begin{aligned}
&\|\mathbf{U}_h^n\|^2 + \sum_{j=0}^{n-1}\|\mathbf{U}_h^{j+1}-\mathbf{U}_h^j\|^2 + \frac{N\Delta t}{M^2}\sum_{j=0}^{n-1}\|\nabla\mathbf{U}_h^{j+1}\|^2 + N\Delta t\sum_{j=0}^{n-1}\|\nabla\Phi_h^{j+1}\|^2 \\
&\quad + N\Delta t\sum_{j=0}^{n-1}\|-\nabla\Phi_h^j + \mathbf{U}_h^{j+1}\times\mathbf{B}\|^2 + N\Delta t\sum_{j=0}^{n-1}\|-\nabla\Phi_h^{j+1} + \mathbf{U}_h^{j}\times\mathbf{B}\|^2 \\
&\le \exp\left((n+1)\frac{\Delta t\kappa}{1-\Delta t\kappa}\right)\Bigg(\|\mathbf{U}_h^0\|^2 + N\Delta t\|\mathbf{U}_h^0\times\mathbf{B}\|^2 + N\Delta t\|\nabla\Phi_h^0\|^2 \\
&\quad + \Delta t\frac{9M^2}{N}\sum_{j=0}^{n-1}\left\|\frac{\eta^{j+1}-\eta^j}{\Delta t}\right\|_{-1}^2 + 2N\Delta t\left(9C_0^2M^2\|\mathbf{u}\|_{\infty,1}^2 + \frac{9}{2}C_0^2M^2\right)\sum_{j=0}^{n-1}\|\nabla\eta^{j+1}\|^2 \\
&\quad + 9\Delta tC_0^2M^2N\sum_{j=0}^{n-1}\|\nabla\eta^{j+1}\|^4 + 9\Delta tC_0^2M^2N\sum_{j=0}^{n-1}\|p^{j+1}-\lambda_h^{j+1}\|^2 \\
&\quad + 2N\Delta tC_0\sum_{j=0}^{n-1}\|\nabla(\phi^{j+1}-\phi^j)\|^2 + 9\Delta tC_0^2M^2N\sum_{j=0}^{n-1}\left\|\frac{\mathbf{u}^{j+1}-\mathbf{u}^j}{\Delta t} - \mathbf{u}_t(t^{j+1})\right\|^2 \\
&\quad + 2N\Delta t(2C_0+8)\sum_{j=0}^{n}\|\nabla\zeta^j\|^2 + 2N\Delta t(2C_0+8)\|\mathbf{B}\|_{L^\infty}^2\sum_{j=0}^{n}\|\eta^j\|^2 \\
&\quad + 16N\Delta t\|\mathbf{B}\|_{L^\infty}^2\sum_{j=0}^{n-1}\|\mathbf{u}^{j+1}-\mathbf{u}^j\|^2\Bigg)
\end{aligned}
\tag{3.36}
$$

provided that $\Delta t < 1/\kappa$.

We next bound the right hand side of (3.36). First,

$$
\begin{aligned}
&\|\mathbf{U}_h^0\|^2 + N\Delta t\|\mathbf{U}_h^0 \times \mathbf{B}\|^2 + N\Delta t\|\nabla\Phi_h^0\|^2 \\
\le\, & 2\|\mathbf{u}^0 - \mathbf{u}_h^0\|^2 + 2\|\eta^0\|^2 + 2N\Delta t\|(\mathbf{u}^0 - \mathbf{u}_h^0)\times\mathbf{B}\|^2 + 2N\Delta t\|\eta^0 \times \mathbf{B}\|^2 \\
&\qquad + 2N\Delta t\|\nabla(\phi^0 - \phi_h^0)\|^2 + 2N\Delta t\|\nabla\zeta^0\|^2 \qquad (3.37)\\
\le\, & (2 + 2N\Delta t\|\mathbf{B}\|_{L^\infty}^2)\|\mathbf{u}^0 - \mathbf{u}_h^0\|^2 + 2N\Delta t\|\nabla(\phi^0 - \phi_h^0)\|^2 \\
&\qquad + C_0(2 + 2N\Delta t\|\mathbf{B}\|_{L^\infty}^2)h^{2k+2}|||\mathbf{u}|||_{\infty,k+1}^2 + 2N\Delta t C_0 h^{2k}|||\phi|||_{\infty,k+1}^2 \\
\le\, & C_0\|\mathbf{u}^0 - \mathbf{u}_h^0\|^2 + C_0\|\nabla(\phi^0 - \phi_h^0)\|^2 + C_0 h^{2k+2}|||\mathbf{u}|||_{\infty,k+1}^2 + C_0 h^{2k}|||\phi|||_{\infty,k+1}^2.
\end{aligned}
$$

The next term can be controlled as follows

$$
\Delta t\frac{9M^2}{N}\sum_{j=0}^{n-1}\left\|\frac{\eta^{j+1}-\eta^j}{\Delta t}\right\|_{-1}^2 \le C_0\sum_{j=0}^{n-1}\int_{t^j}^{t^{j+1}}\|\eta_t\|^2 dt \le C_0 h^{2k+2}\|\mathbf{u}_t\|_{2,k+1}^2. \qquad (3.38)
$$

We also have

$$
\begin{aligned}
&9N\Delta t C_0^2 M^2\big(2\|\mathbf{u}\|_{\infty,1}^2+1\big)\sum_{j=0}^{n-1}\|\nabla\eta^{j+1}\|^2 \\
&\qquad \le C_0\Delta t\sum_{j=0}^{n-1}h^{2k}\|\mathbf{u}^{j+1}\|_{k+1}^2 = C_0 h^{2k}|||\mathbf{u}|||_{2,k+1}^2. \qquad (3.39)
\end{aligned}
$$

Observe that

$$
9\Delta t C_0^2 M^2 N\sum_{j=0}^{n-1}\|\nabla\eta^{j+1}\|^4 \le C_0\Delta t\sum_{j=0}^{n-1}h^{4k}\|\mathbf{u}^{j+1}\|_{k+1}^4 = C_0 h^{4k}|||\mathbf{u}|||_{4,k+1}^4, \qquad (3.40)
$$

and

$$
2N\Delta t C_0\sum_{j=0}^{n-1}\|\nabla(\phi^{j+1}-\phi^j)\|^2 \le C_0\Delta t^2\sum_{j=0}^{n-1}\int_{t^j}^{t^{j+1}}\|\nabla\phi_t\|^2 dt \le C_0\Delta t^2\|\phi_t\|_{2,1}^2. \qquad (3.41)
$$

Let λ_h^{j+1} be the interpolation of p^{j+1} in Q_h, we have

$$
9\Delta t C_0^2 M^2 N\sum_{j=0}^{n-1}\|p^{j+1}-\lambda_h^{j+1}\|^2 \le C_0 h^{2s+2}|||p|||_{2,s+1}^2. \qquad (3.42)
$$

Moreover, it gives

$$9\Delta t C_0^2 M^2 N \sum_{j=0}^{n-1} \left\| \frac{\mathbf{u}^{j+1} - \mathbf{u}^j}{\Delta t} - \mathbf{u}_t(t^{j+1}) \right\|^2 \leq C_0 \Delta t^2 \sum_{j=0}^{n-1} \int_{t^j}^{t^{j+1}} \|\mathbf{u}_{tt}\|^2 dt = C_0 \Delta t^2 \|\mathbf{u}_{tt}\|_{2,0}^2. \quad (3.43)$$

On the other hand, we can see that

$$2N\Delta t(2C_0+8) \sum_{j=0}^{n} \|\nabla \zeta^j\|^2 \leq C_0 \Delta t \sum_{j=0}^{n} h^{2k} \|\phi^j\|_{k+1}^2 = C_0 h^{2k} \||\phi|\|_{2,k+1}^2. \quad (3.44)$$

Finally, we have

$$2N\Delta t(2C_0+8)\|\mathbf{B}\|_{L^\infty}^2 \sum_{j=0}^{n} \|\eta^j\|^2 \leq C_0 \Delta t \sum_{j=0}^{n} h^{2k+2} \|\mathbf{u}^j\|_{k+1}^2 = C_0 h^{2k+2} \||\mathbf{u}|\|_{2,k+1}^2, \quad (3.45)$$

and

$$16N\Delta t \|\mathbf{B}\|_{L^\infty}^2 \sum_{j=0}^{n-1} \|\mathbf{u}^{j+1} - \mathbf{u}^j\|^2 \leq C_0 \Delta t^2 \sum_{j=0}^{n-1} \int_{t^j}^{t^{j+1}} \|\mathbf{u}_t\|^2 dt \leq C_0 \Delta t^2 \|\mathbf{u}_t\|_{2,0}^2. \quad (3.46)$$

Combining (3.36)–(3.46) gives

$$\begin{aligned} &\|\mathbf{U}_h^n\|^2 + \sum_{j=0}^{n-1} \|\mathbf{U}_h^{j+1} - \mathbf{U}_h^j\|^2 + \frac{N\Delta t}{M^2} \sum_{j=0}^{n-1} \|\nabla \mathbf{U}_h^{j+1}\|^2 + N\Delta t \sum_{j=0}^{n-1} \|\nabla \Phi_h^{j+1}\|^2 \qquad (3.47) \\ &\quad + N\Delta t \sum_{j=0}^{n-1} \| -\nabla \Phi_h^j + \mathbf{U}_h^{j+1} \times \mathbf{B}\|^2 + N\Delta t \sum_{j=0}^{n-1} \| -\nabla \Phi_h^{j+1} + \mathbf{U}_h^j \times \mathbf{B}\|^2 \\ &\leq C_0 \Bigg(\|\mathbf{u}^0 - \mathbf{u}_h^0\|^2 + \|\nabla(\phi^0 - \phi_h^0)\|^2 + h^{2k+2} \||\mathbf{u}|\|_{\infty,k+1}^2 + h^{2k} \||\phi|\|_{\infty,k+1}^2 \\ &\quad + h^{2k+2} \|\mathbf{u}_t\|_{2,k+1}^2 + h^{2k} \||\mathbf{u}|\|_{2,k+1}^2 + h^{4k} \||\mathbf{u}|\|_{4,k+1}^4 + \Delta t^2 \|\phi_t\|_{2,1}^2 + h^{2s+2} \||p|\|_{2,s+1}^2 \\ &\quad + \Delta t^2 \|\mathbf{u}_{tt}\|_{2,0}^2 + h^{2k} \||\phi|\|_{2,k+1}^2 + h^{2k+2} \||\mathbf{u}|\|_{2,k+1}^2 + \Delta t^2 \|\mathbf{u}_t\|_{2,0}^2 \Bigg). \end{aligned}$$

To obtain the error estimate given in (3.15), we add both sides of (3.47) with

$$\begin{aligned} Extra\_terms &= \|\eta^n\|^2 + \sum_{j=0}^{n-1} \|\eta^{j+1} - \eta^j\|^2 + \frac{N\Delta t}{M^2} \sum_{j=0}^{n-1} \|\nabla \eta^{j+1}\|^2 + N\Delta t \sum_{j=0}^{n-1} \|\nabla \zeta^{j+1}\|^2 \\ &\quad + N\Delta t \sum_{j=0}^{n-1} \| -\nabla \zeta^j + \eta^{j+1} \times \mathbf{B}\|^2 + N\Delta t \sum_{j=0}^{n-1} \| -\nabla \zeta^{j+1} + \eta^j \times \mathbf{B}\|^2, \end{aligned}$$

and apply the triangle inequality for the left hand side, noticing that the upcoming new terms are already contained in the right hand side of the model. □

Consequently, for Taylor-Hood elements, i.e. $k = 2$, $s = 1$, we have the following result.

Corollary 3.4.2. *Consider Algorithm 1PARA. Under the assumptions of Theorem 3.4.1, suppose that (X^h, Q^h) is given by P2-P1 Taylor-Hood approximation elements and S^h is P2 finite element. Then, there is a positive constant C_0 such that*

$$|||e_{\mathbf{u}}|||_{\infty,0}^2 + |||\nabla e_{\mathbf{u}}|||_{2,0}^2 + |||\nabla e_{\phi}|||_{2,0}^2 + |||e_{\mathbf{J}}|||_{2,0}^2 \leq C_0(\Delta t^2 + h^4).$$

3.5 NUMERICAL EXPERIMENTS

We present two numerical experiments to test the algorithms proposed herein. First, given exact solutions, we verify the convergence rates of our methods. Second, we will test the stability in case the Hartman number M and the interaction parameter N are large. The code was implemented using the software package *FreeFEM++*.

3.5.1 Test 1: Convergence rates

We consider true solution $(\mathbf{u}, p, \phi)$ from [127] is given by

$$\begin{aligned}
&\mathbf{u}(x, y, t) = (2\cos(2x)\sin(2y), -2\sin(2x)\cos(2y))e^{-5t},\\
&p(x, y, t) = 0,\\
&\phi(x, y, t) = (\cos(2x)\cos(2y) + x^2 - y^2)e^{-5t}.
\end{aligned}$$

defined on the domain $\Omega = [0, \pi]^2$, satisfying $\Delta\phi = \nabla\cdot(\mathbf{u}\times\mathbf{B})$. Take the time interval $0 \leq t \leq 1$ and set $M = 20, N = 16$. The imposed magnetic field is $\mathbf{B} = (0, 0, 1)$. We utilize piecewise quadratic for velocity and piecewise linear for pressure for the Navier-Stokes equation and continuous piecewise quadratic finite elements for the Ohm's law. The boundary condition on the problem is inhomogeneous Dirichlet: $\mathbf{u}_h = \mathbf{u}$ on $\partial\Omega$. The initial data and source terms are chosen to correspond the exact solution. Convergence rates are computed using linear regression. We denote $\|\cdot\|_\infty = \|\cdot\|_{L^\infty(0,T;L^2(\Omega))}$ and $\|\cdot\|_2 = \|\cdot\|_{L^2(0,T;L^2(\Omega))}$. From the tables 3.1 and 3.2, 1PARA is first order and 2SEQU is second order.

h	Δt	$\|\mathbf{u}-\mathbf{u}_h\|_\infty$	$\|\nabla\mathbf{u}-\nabla\mathbf{u}_h\|_2$	$\|\nabla\cdot(p-p_h)\|_\infty$	$\|\phi-\phi_h\|_\infty$	$\|\nabla\phi-\nabla\phi_h\|_2$
1/5	1/40	1.047e+0	2.921e+0	1.956e+0	5.760e-1	9.764e-1
1/10	1/80	7.406e-1	2.062e+0	1.005e+0	3.913e-1	6.764e-1
1/20	1/160	4.338e-1	1.214e+0	5.094e-1	2.277e-1	3.952e-1
1/40	1/320	2.348e-1	6.522e-1	2.564e-1	1.237e-1	2.137e-1
1/80	1/640	1.223e-1	3.374e-1	1.286e-1	6.459e-2	1.113e-1
Rate of conv.		0.7853	0.7889	0.9825	0.7975	0.7928

Table 3.1: The convergence performance for Algorithm 1PARA.

h	Δt	$\|\mathbf{u}-\mathbf{u}_h\|_\infty$	$\|\nabla\mathbf{u}-\nabla\mathbf{u}_h\|_2$	$\|\nabla\cdot(p-p_h)\|_\infty$	$\|\phi-\phi_h\|_\infty$	$\|\nabla\phi-\nabla\phi_h\|_2$
1/5	1/40	3.217e-1	1.108e+0	2.837e-1	1.634e-1	3.206e-1
1/10	1/80	4.633e-2	3.670e-1	6.676e-2	2.374e-2	6.380e-2
1/20	1/160	8.973e-3	8.325e-2	1.614e-2	4.694e-3	1.519e-2
1/40	1/320	2.081e-3	1.533e-2	4.003e-3	1.096e-3	3.806e-3
1/80	1/640	5.118e-4	3.104e-3	1.001e-3	2.698e-4	9.577e-4
Rate of conv.		2.1747	2.1541	2.0353	2.2922	2.0841

Table 3.2: The convergence performance for Algorithm 2SEQU.

A more oscillatory true solution is also tested:

$$\begin{aligned}
&\mathbf{u}(x,y,t) = (5\cos(5x)\sin(5y), -5\sin(5x)\cos(5y), 0)e^{-5t},\\
&p(x,y,t) = 0, \\
&\phi(x,y,t) = (\cos(5x)\cos(5y) + x^2 - y^2)e^{-5t}.
\end{aligned} \tag{3.48}$$

Convergence rates are calculated from the errors at two successive values of h in the usual manner by postulating $e(h) = Ch^\beta$ and solving for β via $\beta = \ln(e(h_1)/e(h_2))/\ln(h_1/h_2)$. The errors and convergence rates for this case are shown in Table 3.3 and 3.4.

h	Δt	$\|\mathbf{u}-\mathbf{u}_h\|_\infty$	Rate	$\|\nabla\mathbf{u}-\nabla\mathbf{u}_h\|_2$	Rate	$\|\nabla\phi-\nabla\phi_h\|_2$	Rate
1/20	1/160	9.196*e*-1	–	5.361*e*+0	–	8.046*e*-1	–
1/40	1/320	5.307*e*-1	0.793	2.856*e*+0	0.908	4.455*e*-1	0.853
1/60	1/480	3.644*e*-1	0.927	1.935*e*+0	0.960	3.031*e*-1	0.950
1/80	1/640	2.769*e*-1	0.955	1.462*e*+0	0.974	2.293*e*-1	0.970
1/120	1/960	1.870*e*-1	0.968	9.826*e*-1	0.980	1.542*e*-1	0.979

Table 3.3: The convergence performance for Algorithm 1PARA: more oscillatory true solution.

h	Δt	$\|\mathbf{u}-\mathbf{u}_h\|_\infty$	Rate	$\|\nabla\mathbf{u}-\nabla\mathbf{u}_h\|_2$	Rate	$\|\nabla\phi-\nabla\phi_h\|_2$	Rate
1/20	1/160	1.209*e*-1	–	1.725*e*+0	–	2.137*e*-1	–
1/40	1/320	1.187*e*-2	3.348	4.147*e*-1	2.056	5.227*e*-2	2.032
1/60	1/480	3.417*e*-3	3.071	1.769*e*-1	2.101	2.338*e*-2	1.984
1/80	1/640	1.516*e*-3	2.825	9.738*e*-2	2.075	1.321*e*-2	1.985
1/120	1/960	5.782*e*-4	2.377	4.253*e*-2	2.043	5.897*e*-3	1.989

Table 3.4: The convergence performance for Algorithm 2SEQU: more oscillatory true solution.

The performance of numerical methods we studied herein is also compared with the monolithic, fully implicit methods (same discretization of subdomain terms but *implicit* discretization of coupling terms). Specifically, using the test problem (3.48), Table 3.5 compares the errors $\|\mathbf{u}-\mathbf{u}_h\|_\infty + \|\phi-\phi_h\|_\infty$ produced by 1PARA and Backward Euler method (BE), and compares those errors of 2SEQU and second order, implicit BDF method (BDF).

h	Δt	1PARA	BE	2SEQU	BDF
1/20	1/160	1.073e+0	9.573e-2	1.407e-1	1.238e-1
1/40	1/320	6.195e-1	4.295e-2	1.372e-2	1.339e-2
1/60	1/480	4.254e-1	3.104e-2	3.942e-3	3.873e-3
1/80	1/640	3.233e-1	2.376e-2	1.758e-3	1.597e-3
1/120	1/960	2.183e-1	1.602e-2	6.710e-4	4.592e-4

Table 3.5: Comparison of error $\|u-u_h\|_\infty+\|\phi-\phi_h\|_\infty$ of 1PARA, 2SEQU and corresponding monolithic methods.

3.5.2 Test 2: Stability.

Many important applications of MHD in laboratory and industry involve large Hartmann number and interaction parameter, see, e.g., [104, 35]. The theory shows that Algorithm 1PARA is unconditionally stable. However, the time step condition for stability of Algorithm 2SEQU looks pessimistic in these cases. In the following experiment, we test and compare the performance of our methods for such flows. We confirm the unconditional stability of Algorithm 1PARA and show that Algorithm 2SEQU to be stable for much larger time steps than predicted by Theorem 3.3.3.

Let $\Omega = [0, 10^{-1}]^2$ and $\mathbf{B} = (0, 0, 1)$. We consider the flow of liquid aluminium at 700°C:

$$\sigma = 4.1 \cdot 10^6 \text{ mho/m}, \qquad \rho = 2400 \text{ kg/m}^3,$$
$$\nu = 6 \cdot 10^{-7} \text{ m}^2/\text{s}, \qquad \eta = 1.94 \cdot 10^{-1} \text{ m}^2/\text{s}.$$

We take the characteristic values of length, velocity and magnetic field to be $L = 0.1$m, $u = 0.1$m/s, $B = 1$T, typical for laboratory and industrial flows. The Reynolds number, magnetic Reynolds number, Hartmann number and interaction parameter are then $Re = 16667$, $R_m = 0.051496$, $M = 5336$, $N = 1708$ correspondingly.

We take the source term $\mathbf{f}$ and the boundary condition to be 0 and the initial condition is given by

$$\mathbf{u}_0(x,y) = (10\pi\cos(10\pi x)\sin(10\pi y), -10\pi\sin(10\pi x)\cos(10\pi y)),$$
$$\phi_0(x,y) = (\cos(10\pi x)\cos(10\pi y) + x^2 - y^2).$$

In absence of external energy exchange and body forces, the system energy decays over time. The energy $E^j = \|\mathbf{u}_h^j\|^2 + \|\phi_h^j\|^2$ is computed using two different methods studied herein, on $h = 1/10$. For each algorithm, the time step is chosen purposely to give us an estimate of practical restriction on time step for the stability of the method. The results are shown in Figure 3.1.

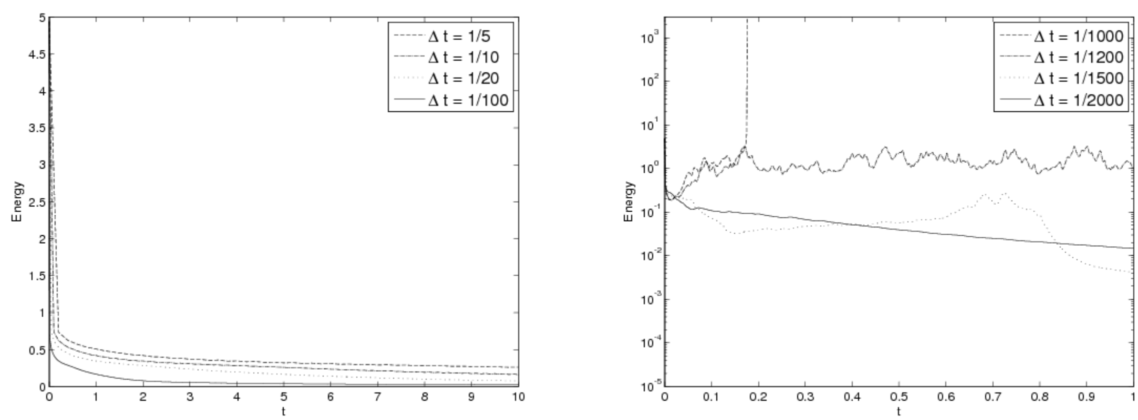

Figure 3.1: The decay of system energy computed by 1PARA (left) and 2SEQU (right) with several different time steps chosen.

Next, we consider the flow of liquid sodium at 100°C, which involves larger M and N:

$$\sigma = 1.03 \cdot 10^7 \text{ mho/m}, \qquad \rho = 928 \text{ kg/m}^3,$$
$$\nu = 7.39 \cdot 10^{-7} \text{ m}^2/\text{s}, \qquad \eta = 7.72 \cdot 10^{-2} \text{ m}^2/\text{s}.$$

The characteristic values of length, velocity and magnetic field are now assigned as follows: $L = 0.1$m, $u = 0.05$m/s, $B = 1$T. The Reynolds number, magnetic Reynolds number, Hartmann number and interaction parameter are then $Re = 6766$, $R_m = 0.064736$, $M = 12255$, $N = 22198$ correspondingly.

With the same source term, boundary and initial condition, the results are shown in Figure 3.2.

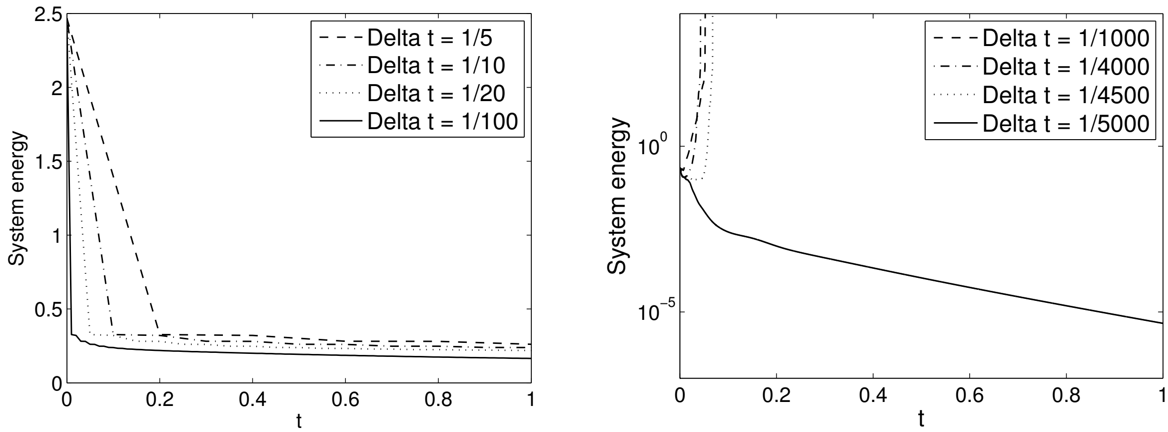

Figure 3.2: The decay of system energy computed by 1PARA (left) and 2SEQU (right) with several different time steps chosen and larger parameters.

Figures 3.1 and 3.2 confirm the unconditional stability of 1PARA established in Theorem 3.3.1. They also indicate that the experimental stability condition for 2SEQU is $\Delta t \lesssim 1/2000$ for the first test and $\Delta t \lesssim 1/5000$ for the second test, which, while still restrictive, are significantly better than the condition in Theorem 3.3.3.

3.6 CONCLUSION

We give a complete analysis on stability and errors of a promising approach to solving the MHD problems at low magnetic Reynolds numbers. Our algorithms lag or extrapolate the coupling terms to previous time levels at which their values are known; therefore, at each time step, the multi-physics problem is uncoupled and solved non-iteratively. Compared to monolithic methods, our methods allow the use of legacy and optimized codes for subproblems.

Normally, for uncoupling a coupled problem, the price to be paid is stability. The first order scheme is, surprisingly, unconditionally stable. However, the time step condition of second order scheme, while independent of h, may be too restrictive in some applications involving small or large physical parameters. Open problems in elaborating this approach to MHD flows include higher order partitioned methods that are long time stable with *improved time step restrictions* with respect to the physical parameters. Another important question which naturally arises is developing partitioned methods for general MHD flows, which occur in both astrophysics and terrestrial applications and whose coupling terms are nonlinear.

4.0 IMPLICIT-EXPLICIT BASED PARTITIONED METHODS FOR THE EVOLUTIONARY STOKES-DARCY PROBLEMS

4.1 INTRODUCTION

In this chapter, we give a complete analysis of the stability and errors over long time intervals of partitioned methods (which require only one uncoupled Stokes and one Darcy subdomain solve per time step) for the coupled, fully time dependent Stokes-Darcy problem. This builds upon recent studies of partitioned methods over bounded time intervals (with constants $C(T) \sim e^{aT}$) of Mu and Zhu [98] who studied the first (first order) partitioned method for the Stokes-Darcy coupling. The method was extended to allow different time steps in the two subregions [110]. These works used Grönwall's inequality in an essential way for analyzing both stability and convergence. Thus, the stability and error behaviour over the required long time intervals is important for both algorithm development and analysis.

We analyze the *stability and error behaviour over long time intervals* $(0 \leq t < \infty)$ of two *implicit-explicit based* partitioned methods for uncoupling the evolutionary Stokes-Darcy problem. The first method we study is the first order method of [98] consisting of first order implicit discretization of subdomain terms and explicit discretization of coupling terms. The stability regions of the explicit method used for the anti-symmetric coupling terms suggest that exponential growth of errors and perturbations is inevitable for the combination. Surprisingly, we show that this is not the case: the method is stable and optimally convergent uniformly over $0 \leq t < \infty$. The second method we study is a new, two step partitioned scheme motivated by the form of the coupling. It involves first order implicit discretization of the subdomain terms and leap frog discretization of the exactly skew symmetric coupling terms. We prove that this combination has superior stability properties and is optimally accurate and convergent uniformly over $0 \leq t < \infty$. We also present numerical experiments verifying the numerical analysis and comparing the accuracy of the two approaches.

To specify the problem considered, let the two domains be denoted by Ω_f, Ω_p and lie across an interface I from each other. The fluid velocity and porous media piezometric head (Darcy pressure) satisfy

$$
\begin{aligned}
u_t - \nu\Delta u + \nabla p = \mathbf{f}_f, \nabla \cdot u = 0, \quad \text{in} \;\; \Omega_f, \\
S_0\phi_t - \nabla \cdot (\mathcal{K}\nabla\phi) = f_p, \;\; \text{in} \;\; \Omega_p, \\
\phi(x,0) = \phi_0, \;\; \text{in } \Omega_p \text{ and } u(x,0) = u_0, \;\; \text{in } \Omega_f, \\
\phi(x,t) = 0, \;\; \text{in } \partial\Omega_p \backslash I \text{ and } u(x,t) = 0, \;\; \text{in } \partial\Omega_f \backslash I, \\
+ \text{ coupling conditions across } I.
\end{aligned}
$$

The exact boundary conditions chosen above on the exterior boundaries ($\partial\Omega_{f/p}\backslash I$) are not essential to either the analysis or algorithms studied herein. Let $\widehat{n}_{f/p}$ denote the indicated, outward pointing, unit normal vector on I. The coupling conditions are conservation of mass and balance of forces on I

$$
\begin{aligned}
u \cdot \widehat{n}_f - \mathcal{K}\nabla\phi \cdot \widehat{n}_p = 0, \;\; \text{on I}, \\
p - \nu \; \widehat{n}_f \cdot \nabla u \cdot \widehat{n}_f = g\phi \;\; \text{ on I}.
\end{aligned}
$$

The last condition needed is a tangential condition on the fluid region's velocity on the interface. The most correct condition is not completely understood (possibly due to matching a pointwise velocity in the fluid region with an averaged or homogenized velocity in the porous region). We take the Beavers-Joseph-Saffman (-Jones) interfacial coupling

$$
-\nu \; \widehat{\tau}_i \cdot \nabla u \cdot \widehat{n}_f = \alpha_{BJ}\sqrt{\frac{\nu g}{\widehat{\tau}_i \cdot \mathcal{K} \cdot \widehat{\tau}_i}} u \cdot \widehat{\tau}_i, \;\; \text{on } I \text{ for any } \widehat{\tau}_i \text{ tangent vector on } I.^{1}
$$

[1] Since $\mathcal{K} = \frac{\Pi g}{\nu}$ where Π is the intrinsic permeability, this form of the interface condition is equivalent to $-\nu \; \widehat{\tau}_i \cdot \nabla u \cdot \widehat{n}_f = \frac{\alpha_{BJ}\nu}{\sqrt{\widehat{\tau}_i \cdot \Pi \cdot \widehat{\tau}_i}} u \cdot \widehat{\tau}_i$, which was derived in [12], [107], [65].

This is a simplification of the original and more physically realistic Beavers-Joseph conditions (in $u \cdot \widehat{\tau}_i$ which is replaced by $(u - \mathbf{u}_p) \cdot \widehat{\tau}_i$), studied in [24], [23]. Here α_{BJ} is a dimensionless, experimentally determined constant and

$$
\begin{aligned}
\phi &= \text{Darcy pressure + elevation induced pressure = piezometric head,} \\
p &= \text{kinematic pressure in fluid region, } \Omega_f, \\
u &= \text{fluid velocity in Stokes region, } \Omega_f, \\
\mathbf{f}_f, f_p &= \text{body forces in fluid region and source in porous region,} \\
\mathcal{K} &= \text{hydraulic conductivity tensor,} \\
\nu &= \text{kinematic viscosity of fluid,} \\
S_0 &= \text{specific mass storativity coefficient,} \\
g &= \text{gravitational acceleration constant.}
\end{aligned}
$$

We shall assume that all material and fluid parameters above are positive and $O(1)$, in particular, $\mathcal{K}$ is a symmetric positive definite (SPD) matrix with the smallest eigenvalue $k_{\min} > 0$.

4.2 THE CONTINUOUS PROBLEM AND SEMI-DISCRETE APPROXIMATION

We denote the $L^2(I)$ norm by $\|\cdot\|_I$ and the $L^2(\Omega_{f/p})$ norms by $\|\cdot\|_{f/p}$, respectively; the corresponding inner products are denoted by $(\cdot,\cdot)_{f/p}$. Define

$$
\begin{aligned}
X_f &= \{v \in \left(H^1(\Omega_f)\right)^d : v = 0 \text{ on } \partial\Omega_f \backslash I\},\ Q_f = L^2(\Omega_f), \\
X_p &= \{\psi \in H^1(\Omega_p) : \psi = 0 \text{ on } \partial\Omega_p \backslash I\}.
\end{aligned}
$$

Throughout this chapter, we will use C_0 to denote a generic positive constant whose value may be different from place to place but which is independent of mesh size, time step and final time. We will use the combined trace, interpolation and Poincaré inequality

$$\|\phi\|_I \leq C(\Omega_p)\sqrt{\|\phi\|_p\|\nabla\phi\|_p} \text{ and } \|u\|_I \leq C(\Omega_f)\sqrt{\|u\|_f\|\nabla u\|_f}$$

where, by a scaling argument, $C(\Omega_{f/p}) = O(\sqrt{L_{f/p}}), L_{f/p} = diameter(\Omega_{f/p})$.

Define the bilinear forms

$$\begin{aligned} a_f(u,v) &= (\nu\nabla u, \nabla v)_f + \sum_i \int_I \alpha_{BJ}\sqrt{\frac{\nu g}{\widehat{\tau}_i \cdot \mathcal{K} \cdot \widehat{\tau}_i}}(u\cdot\widehat{\tau}_i)(v\cdot\widehat{\tau}_i)ds, \\ a_p(\phi,\psi) &= g(\mathcal{K}\nabla\phi, \nabla\psi)_p, \text{ and } c_I(u,\phi) = g\int_I \phi u \cdot \widehat{n}_f ds. \end{aligned}$$

The bilinear forms $a_{f/p}(\cdot,\cdot)$ are continuous and coercive. The key to uncoupling the problem is the treatment of coupling term through the bilinear form $c_I(u,\phi)$. Let $C_{P,f}$ and $C_{P,p}$ be the Poincaré constants of the indicated domains. Define three parameter-dependent constants

$$\begin{aligned} &C_1 = \frac{g^{3/2}\left[C(\Omega_f)C(\Omega_p)\right]^2}{4\sqrt{\nu k_{\min}}}, \quad C_2 = \frac{1}{\nu^2}C_{P,f}^2[gC(\Omega_f)C(\Omega_p)]^4, \\ &C_3 = \frac{1}{k_{\min}^2}C_{P,p}^2 g^2[C(\Omega_f)C(\Omega_p)]^4. \end{aligned}$$

Lemma 4.2.1. *We have for $(u,\phi) \in X_f \times X_p$ and all ε_1, ε_2, $\varepsilon_3 > 0$*

$$|c_I(u,\phi)| \leq \frac{\nu}{4\varepsilon_1}\|\nabla u\|_f^2 + \frac{gk_{\min}}{4\varepsilon_1}\|\nabla\phi\|_p^2 + \varepsilon_1 C_1\left(\|u\|_f^2 + \|\phi\|_p^2\right), \tag{4.1}$$

$$|c_I(u,\phi)| \leq \frac{1}{4\varepsilon_2}\|\phi\|_p^2 + \varepsilon_2 C_2\|\nabla\phi\|_p^2 + \frac{\nu}{4}\|\nabla u\|_f^2, \tag{4.2}$$

$$|c_I(u,\phi)| \leq \frac{1}{4\varepsilon_3}\|u\|_f^2 + \varepsilon_3 C_3\|\nabla u\|_f^2 + \frac{gk_{\min}}{4}\|\nabla\phi\|_p^2. \tag{4.3}$$

Proof. Using basic estimates we obtain

$$\begin{aligned}
c_I(u,\phi) &= g\int_I \phi u\cdot\widehat{n}ds \\
&\le gC(\Omega_f)C(\Omega_p)\sqrt{\|\phi\|_p\|\nabla\phi\|_p}\cdot\sqrt{\|u\|_f\|\nabla u\|_f} \\
&\le \frac{\nu}{4\varepsilon_1}\|\nabla u\|_f^2+\frac{gk_{\min}}{4\varepsilon_1}\|\nabla\phi\|_p^2+\varepsilon_1 C_1\left(\|u\|_f^2+\|\phi\|_p^2\right).
\end{aligned}$$

For (4.2), observe that

$$\begin{aligned}
&c_I(u,\phi) = g\int_I \phi u\cdot\widehat{n}ds \le gC(\Omega_f)C(\Omega_p)\sqrt{\|\phi\|_p\|\nabla\phi\|_p}\cdot\sqrt{\|u\|_f\|\nabla u\|_f} \\
&\le \left(\frac{1}{\varepsilon_2^{1/4}}\|\phi\|_p^{1/2}\right)\left(gC(\Omega_f)C(\Omega_p)\varepsilon_2^{1/4}\left(\frac{2}{\nu}\right)^{1/2}C_{P,f}^{1/2}\|\nabla\phi\|_p^{1/2}\right)\left(\left(\frac{\nu}{2}\right)^{1/2}\|\nabla u\|_f\right) \\
&\le \frac{1}{4\varepsilon_2}\|\phi\|_p^2+\varepsilon_2 C_2\|\nabla\phi\|_p^2+\frac{\nu}{4}\|\nabla u\|_f^2.
\end{aligned}$$

Finally, (4.3) comes from a similar argument. □

A (monolithic) variational formulation of the coupled problem is to find $(u,p,\phi):[0,\infty)\to X_f\times Q_f\times X_p$ satisfying the given initial conditions and, for all $v\in X_f, q\in Q_f, \psi\in X_p$

$$\begin{aligned}
(u_t,v)_f+a_f(u,v)-(p,\nabla\cdot v)_f+c_I(v,\phi) &= (\mathbf{f}_f,v)_f, \\
(q,\nabla\cdot u)_f &= 0, \\
gS_0(\phi_t,\psi)_p+a_p(\phi,\psi)-c_I(u,\psi) &= g(f_p,\psi)_p.
\end{aligned} \tag{4.4}$$

Note that, setting $v=u,\psi=\phi$ and adding, the coupling terms exactly cancel in the monolithic sum yielding the energy estimate for the coupled system.

To discretize the Stokes-Darcy problem in space by the finite element method, we select finite element spaces

$$\text{velocity: } X_f^h\subset X_f,\ \text{Darcy pressure: } X_p^h\subset X_p,\ \text{Stokes pressure: } Q_f^h\subset Q_f$$

based on a conforming FEM triangulation with maximum triangle diameter denoted by ”h”. No mesh compatibility or interdomain continuity at the interface I between the FEM meshes in the two subdomains is assumed. It is known that provided a minimum angle condition holds functions in piecewise polynomial finite element spaces including X_f^h, X_p^h and even Q_f^h (for the elementwise gradient) satisfy an inverse inequality[2]:

$$||\nabla v_h|| \leq C_{INV} h^{-1} ||v_h||, \;\; h = \text{minimum meshwidth.} \tag{4.5}$$

The Stokes velocity-pressure FEM spaces are assumed to satisfy the usual discrete inf-sup condition for stability of the discrete pressure, e.g., [46], and X_f^h, X_p^h, Q_f^h satisfy approximation properties of piecewise polynomials on quasi-uniform meshes of local degrees $k, k, k-1$ respectively. We denote the discretely divergence free velocities by

$$V^h := X_f^h \cap \{v_h : (q_h, \nabla \cdot v_h)_f = 0, \text{ for all } q_h \in Q_f^h\}.$$

The $H_{DIV}(\Omega_f)$ norm is given by

$$||u||_{DIV} := \sqrt{||u||_f^2 + ||\nabla \cdot u||_f^2}.$$

Note that if $d = \dim(\Omega_f)$, then $||\nabla \cdot u||_f \leq \sqrt{d} ||\nabla u||_f$. The semi-discrete approximations are maps $(u_h, p_h, \phi_h) : [0, \infty) \to X_f^h \times Q_f^h \times X_p^h$ satisfying the given initial conditions and, for all $v_h \in X_f^h$, $q_h \in Q_f^h, \psi_h \in X_p^h$

$$\begin{aligned} (u_{h,t}, v_h)_f + a_f(u_h, v_h) - (p_h, \nabla \cdot v_h)_f + c_I(v_h, \phi_h) &= (\mathbf{f}_f, v_h)_f, \\ (q_h, \nabla \cdot u_h)_f &= 0, \\ gS_0(\phi_{h,t}, \psi_h)_p + a_p(\phi_h, \psi_h) - c_I(u_h, \psi_h) &= g(f_p, \psi_h)_p. \end{aligned} \tag{4.6}$$

Note in particular the exactly skew symmetric coupling between the Stokes and the Darcy sub-problems.

[2]The constant C_{INV} depends upon the angles in the finite element mesh but not on the domain size. The analysis must either use $h_{\min}$ in stability restrictions and $h_{\max}$ in the interpolation inequalities or assume a quasi-uniform mesh. For notational simplicity we do the latter.

4.3 DISCRETE FORMULATION

In this section, we consider two implicit-explicit based partitioned methods. The first method we analyze is **BEFE = Backward Euler - Forward Euler**, the original method of Mu and Zhu [98]. Since we focus on the long time error and stability, we shall use the same time step in both subdomains. Let $t^n := n\Delta t$ and let superscripts denote the time level of the approximation. The BEFE partitioned approximations are maps $(u_h^n, p_h^n, \phi_h^n) \in X_f^h \times Q_f^h \times X_p^h$ for $n \geq 1$ satisfying, for all $v_h \in X_f^h, q_h \in Q_f^h, \psi_h \in X_p^h$

$$
\begin{aligned}
(\frac{u_h^{n+1} - u_h^n}{\Delta t}, v_h)_f + a_f(u_h^{n+1}, v_h) - (p_h^{n+1}, \nabla \cdot v_h)_f + c_I(v_h, \phi_h^n) = (\mathbf{f}_f^{n+1}, v_h)_f, \\
(q_h, \nabla \cdot u_h^{n+1})_f = 0, \\
gS_0(\frac{\phi_h^{n+1} - \phi_h^n}{\Delta t}, \psi_h)_p + a_p(\phi_h^{n+1}, \psi_h) - c_I(u_h^n, \psi_h) = g(f_p^{n+1}, \psi_h)_p.
\end{aligned}
\tag{4.7}
$$

The second method we consider is **BELF = Backward Euler - Leap Frog**, a combination of the three level implicit method with the coupling terms treated by the explicit Leap-Frog method. We shall use the same time step, Δt, in both sub domains; extension to asynchronous time stepping, e.g. [110], is an important open problem. The BELF partitioned approximations are maps $(u_h^n, p_h^n, \phi_h^n) \in X_f^h \times Q_f^h \times X_p^h$ for $n \geq 2$ satisfying, for all $v_h \in X_f^h, q_h \in Q_f^h, \psi_h \in X_p^h$

$$
\begin{aligned}
(\frac{u_h^{n+1} - u_h^{n-1}}{2\Delta t}, v_h)_f + a_f(u_h^{n+1}, v_h) - (p_h^{n+1}, \nabla \cdot v_h)_f + c_I(v_h, \phi_h^n) = (\mathbf{f}_f^{n+1}, v_h)_f, \\
(q_h, \nabla \cdot u_h^{n+1})_f = 0, \\
gS_0(\frac{\phi_h^{n+1} - \phi_h^{n-1}}{2\Delta t}, \psi_h)_p + a_p(\phi_h^{n+1}, \psi_h) - c_I(u_h^n, \psi_h) = g(f_p^{n+1}, \psi_h)_p.
\end{aligned}
\tag{4.8}
$$

BELF is a 3 level method and approximations are needed at the first two time steps to begin. We shall suppose these are computed to appropriate accuracy, such as by BEFE (the first method above). See Verwer [121] for subtle effects that depend on the starting values. The stability region of the usual Leap-Frog time discretization for $y' = \lambda y$ is exactly the interval of the imaginary axis $-1 \leq Im(\Delta t \lambda) \leq +1$. Thus, LF is unstable for every problem except for ones which are exactly skew symmetric such as the coupling herein, see [43]. For them, as with any explicit scheme, it inherits a time step restriction.

4.4 LONG TIME STABILITY

We analyze the *long time stability* of the proposed methods over $0 \leq t^n < \infty$. We derive the restriction needed as the time step, of the form $\Delta t \leq C(\textit{physical parameter})$ under which

1. the approximate solutions are convergent uniformly over $0 < t < \infty$,
2. if $\mathbf{f}_f = f_p = 0$, $u^n, \phi^n \to 0$ as $t^n \to \infty$ (thus, if $(i = 1, 2)$ u_i^n, ϕ_i^n are two solutions with the same RHS and different initial conditions, then $u_1^n - u_2^n, \phi_1^n - \phi_2^n \to 0$ as $n \to \infty$), and
3. if $\|\mathbf{f}_f(t)\|$, $\|f_p(t)\|$ are uniformly bounded in time then $\sup_{t^n} (\|u^n\| + \|\phi^n\|) < \infty$.

4.4.1 BEFE Stability.

The analysis of Mu and Zhu includes (inside the error estimation) a proof (which also extends to BELF as well) of stability over bounded time intervals of the form: for any Δt and $0 \leq t^n < T < \infty$

$$\|u_h^n\|_f^2 + \|\phi_h^n\|_p^2 \leq C(T) \left[\sup_{0 \leq t_n \leq T} \left\{ \|\mathbf{f}_f(t_n)\|_f^2 + \|f_p(t_n)\|_p^2 \right\} + \|u_h^0\|_{H^1(\Omega_f)}^2 + \|\phi_h^0\|_{H^1(\Omega_p)}^2 \right]$$

where $C(T)$ arises from Gronwall's inequality and thus grows exponentially with T. We begin by proving uniform in time stability of the BEFE partitioned approximation (4.7) under the time step restriction

$$\Delta t \leq \Delta t_{BEFE} := \min \left\{ \frac{k_{\min}}{C_{P,p}^2}, \frac{S_0 \nu}{C_{P,f}^2} \right\} \frac{\nu k_{\min}}{8 g^2 (C(\Omega_f) C(\Omega_p))^4}. \tag{4.9}$$

Note that the RHS of (4.9) is independent of h so that, in the usual terminology of numerical PDEs, BEFE is unconditionally stable. Our experiments in Section 4.6 with $k_{\min} = 10^{-6}$ show that there is some dependence of Δt_{BEFE} on $k_{\min}$ but the dependence indicated in (4.9) is likely not sharp.

Theorem 4.4.1. *(BEFE long time stability) Consider BEFE method (4.7). Under the time step condition (4.9) it is long time and uniformly in time stable*

$$\begin{aligned}
&\frac{1}{2}\|u_h^N\|_f^2 + \frac{gS_0}{2}\|\phi_h^N\|_p^2 + \Delta t\sum_{n=0}^{N-1}\left(\frac{\nu}{4}\|\nabla u_h^{n+1}\|_f^2 + \frac{gk_{\min}}{4}\|\nabla\phi_h^{n+1}\|_p^2\right)\\
&\quad + \frac{\Delta t\nu}{8}\|\nabla u_h^N\|_f^2 + \frac{\Delta t g k_{\min}}{8}\|\nabla\phi_h^N\|_p^2\\
&\le \frac{1}{2}\|u_h^0\|_f^2 + \frac{gS_0}{2}\|\phi_h^0\|_p^2 + \Delta t\sum_{n=0}^{N-1}\left(\frac{C_{P,f}^2}{\nu}\|\mathbf{f}_f^{n+1}\|_f^2 + \frac{gC_{P,p}^2}{k_{\min}}\|f_p^{n+1}\|_p^2\right)\\
&\quad + \frac{\Delta t\nu}{8}\|\nabla u_h^0\|_f^2 + \frac{\Delta t g k_{\min}}{8}\|\nabla\phi_h^0\|_p^2.
\end{aligned} \tag{4.10}$$

There is a $C_0 < \infty$ such that if $\mathbf{f}_f \in L^\infty(L^2(\Omega_f))$, $f_p \in L^\infty(L^2(\Omega_p))$ then

$$\begin{aligned}
\sup_{0\le N\le\infty}\left\{\|u_h^N\|_f^2 + gS_0\|\phi_h^N\|_p^2\right\} \le C_0\Bigg(&\sup_{0\le N\le\infty}\left\{\|\mathbf{f}_f^N\|_f^2 + \|f_p^N\|_p^2\right\}\\
&+ \|u_h^0\|_{H^1(\Omega_f)}^2 + \|\phi_h^0\|_{H^1(\Omega_p)}^2\Bigg),
\end{aligned} \tag{4.11}$$

and if $\mathbf{f}_f \equiv 0$, $f_p \equiv 0$ then

$$u_h^N \to 0, \ \ \phi_h^N \to 0 \tag{4.12}$$

in $H^1(\Omega_f)$ and $H^1(\Omega_p)$ respectively as $N \to \infty$.

Proof. In (4.7), set $v_h = u_h^{n+1}$ and $\psi_h = \phi_h^{n+1}$ and add. This gives

$$\begin{aligned}
&\frac{1}{2\Delta t}\|u_h^{n+1}\|_f^2 - \frac{1}{2\Delta t}\|u_h^n\|_f^2 + \frac{1}{2\Delta t}\|u_h^{n+1}-u_h^n\|_f^2 + \frac{gS_0}{2\Delta t}\|\phi_h^{n+1}\|_p^2 - \frac{gS_0}{2\Delta t}\|\phi_h^n\|_p^2\\
&+ \frac{gS_0}{2\Delta t}\|\phi_h^{n+1}-\phi_h^n\|_p^2 + a_f(u_h^{n+1},u_h^{n+1}) + a_p(\phi_h^{n+1},\phi_h^{n+1}) + c_I(u_h^{n+1}-u_h^n,\phi_h^{n+1})\\
&- c_I(u_h^{n+1},\phi_h^{n+1}-\phi_h^n) = (\mathbf{f}_f^{n+1},u_h^{n+1}) + g(f_p^{n+1},\phi_h^{n+1}).
\end{aligned}$$

Applying (4.2) and (4.3) with $\varepsilon_2 = \frac{\Delta t}{2gS_0}$ and $\varepsilon_3 = \frac{\Delta t}{2}$, if (4.9) occurs, we have

$$\begin{aligned}
&c_I(u_h^{n+1}-u_h^n,\phi_h^{n+1}) - c_I(u_h^{n+1},\phi_h^{n+1}-\phi_h^n)\\
\ge\ & -\frac{gS_0}{2\Delta t}\|\phi_h^{n+1}-\phi_h^n\|_p^2 - \frac{\Delta t}{2gS_0}C_2\|\nabla(\phi_h^{n+1}-\phi_h^n)\|_p^2 - \frac{\nu}{4}\|\nabla u_h^{n+1}\|_f^2\\
&-\frac{1}{2\Delta t}\|u_h^{n+1}-u_h^n\|_f^2 - \frac{\Delta t}{2}C_3\|\nabla(u_h^{n+1}-u_h^n)\|_f^2 - \frac{gk_{\min}}{4}\|\nabla\phi_h^{n+1}\|_p^2\\
\ge\ & -\frac{gS_0}{2\Delta t}\|\phi_h^{n+1}-\phi_h^n\|_p^2 - \frac{gk_{\min}}{8}(\|\nabla\phi_h^{n+1}\|_p^2 + \|\nabla\phi_h^n\|_p^2) - \frac{\nu}{4}\|\nabla u_h^{n+1}\|_f^2\\
&-\frac{1}{2\Delta t}\|u_h^{n+1}-u_h^n\|_f^2 - \frac{\nu}{8}(\|\nabla u_h^{n+1}\|_f^2 + \|\nabla u_h^n\|_f^2) - \frac{gk_{\min}}{4}\|\nabla\phi_h^{n+1}\|_p^2.
\end{aligned}$$

Furthermore, a combination of Schwarz inequality and Poincaré inequality yields

$$
\begin{aligned}
&(\mathbf{f}_f^{n+1}, u_h^{n+1}) + g(f_p^{n+1}, \phi_h^{n+1}) \\
\leq\ & \frac{C_{P,f}^2}{\nu}\|\mathbf{f}_f^{n+1}\|_f^2 + \frac{\nu}{4}\|\nabla u_h^{n+1}\|_f^2 + \frac{gC_{P,p}^2}{k_{\min}}\|f_p^{n+1}\|_p^2 + \frac{gk_{\min}}{4}\|\nabla\phi_h^{n+1}\|_p^2.
\end{aligned}
$$

Thus

$$
\begin{aligned}
&\frac{1}{2\Delta t}\|u_h^{n+1}\|_f^2 - \frac{1}{2\Delta t}\|u_h^n\|_f^2 + \frac{gS_0}{2\Delta t}\|\phi_h^{n+1}\|_p^2 - \frac{gS_0}{2\Delta t}\|\phi_h^n\|_p^2 \\
&+ \frac{\nu}{4}\|\nabla u_h^{n+1}\|_f^2 + \frac{gk_{\min}}{4}\|\nabla\phi_h^{n+1}\|_p^2 + \frac{\nu}{8}\left(\|\nabla u_h^{n+1}\|_f^2 - \|\nabla u_h^n\|_f^2\right) \\
&+ \frac{gk_{\min}}{8}\left(\|\nabla\phi_h^{n+1}\|_p^2 - \|\nabla\phi_h^n\|_p^2\right) \leq\ \frac{C_{P,f}^2}{\nu}\|\mathbf{f}_f^{n+1}\|_f^2 + \frac{gC_{P,p}^2}{k_{\min}}\|f_p^{n+1}\|_p^2.
\end{aligned} \tag{4.13}
$$

Summing this up from $n = 0$ to $n = N - 1$ results in

$$
\begin{aligned}
&\frac{1}{2}\|u_h^N\|_f^2 + \frac{gS_0}{2}\|\phi_h^N\|_p^2 + \frac{\Delta t\nu}{8}\|\nabla u_h^N\|_f^2 + \frac{\Delta t g k_{\min}}{8}\|\nabla\phi_h^N\|_p^2 \\
&\qquad + \Delta t\sum_{n=0}^{N-1}\left(\frac{\nu}{4}\|\nabla u_h^{n+1}\|_f^2 + \frac{gk_{\min}}{4}\|\nabla\phi_h^{n+1}\|_p^2\right) \\
\leq\ &\frac{1}{2}\|u_h^0\|_f^2 + \frac{gS_0}{2}\|\phi_h^0\|_p^2 + \frac{\Delta t\nu}{8}\|\nabla u_h^0\|_f^2 + \frac{\Delta t g k_{\min}}{8}\|\nabla\phi_h^0\|_p^2 \\
&\qquad + \Delta t\sum_{n=0}^{N-1}\left(\frac{C_{P,f}^2}{\nu}\|\mathbf{f}_f^{n+1}\|_f^2 + \frac{gC_{P,p}^2}{k_{\min}}\|f_p^{n+1}\|_p^2\right).
\end{aligned}
$$

For the second part, let

$$
Q(\Delta t) = \min\left\{\frac{2\nu}{4C_{P,f}^2 + \nu\Delta t}, \frac{2k_{\min}}{4S_0C_{P,p}^2 + k_{\min}\Delta t}\right\}\Delta t.
$$

After simple calculations and applying Poincaré inequality

$$
\begin{aligned}
\frac{\nu}{4}\|\nabla u_h^{n+1}\|_f^2 &\geq Q(\Delta t)\left(\frac{1}{2\Delta t}\|u_h^{n+1}\|_f^2 + \frac{\nu}{8}\|\nabla u_h^{n+1}\|_f^2\right), \\
\frac{gk_{\min}}{4}\|\nabla\phi_h^{n+1}\|_p^2 &\geq Q(\Delta t)\left(\frac{gS_0}{2\Delta t}\|\phi_h^{n+1}\|_p^2 + \frac{gk_{\min}}{8}\|\nabla\phi_h^{n+1}\|_p^2\right).
\end{aligned} \tag{4.14}
$$

Denote

$$
\begin{aligned}
s_{n+1} &= \frac{1}{2\Delta t}\|u_h^{n+1}\|_f^2 + \frac{\nu}{8}\|\nabla u_h^{n+1}\|_f^2 + \frac{gS_0}{2\Delta t}\|\phi_h^{n+1}\|_p^2 + \frac{gk_{\min}}{8}\|\nabla\phi_h^{n+1}\|_p^2 \\
\text{and}\quad P &= \frac{C_{P,f}^2}{\nu}\sup_{0\leq N\leq\infty}\|\mathbf{f}_f^N\|_f^2 + \frac{gC_{P,p}^2}{k_{\min}}\sup_{0\leq N\leq\infty}\|f_p^N\|_p^2.
\end{aligned}
$$

From (4.13) and (4.14), we have

$$(1+Q(\Delta t))s_{n+1}-s_n \le P,$$

which yields

$$s_{n+1} \le \frac{P}{Q(\Delta t)} + \frac{1}{(1+Q(\Delta t))^{n+1}} s_0.$$

Inserting the expression defining s_{n+1} gives

$$\frac{1}{2\Delta t}\|u_h^{n+1}\|_f^2 + \frac{gS_0}{2\Delta t}\|\phi_h^{n+1}\|_p^2 \le \frac{P}{Q(\Delta t)} + \frac{1}{(1+Q(\Delta t))^{n+1}} s_0.$$

Hence, (4.11) follows since

$$\begin{aligned}
&\|u_h^{n+1}\|_f^2 + gS_0\|\phi_h^{n+1}\|_p^2 \le \frac{2\Delta t P}{Q(\Delta t)} + 2\Delta t s_0 \\
&\le \max\left\{\frac{4C_{P,f}^2}{\nu} + \Delta t, \frac{4C_{P,p}^2 S_0}{k_{\min}} + \Delta t\right\} P + 2\Delta t s_0 \\
&\le \max\left\{\frac{4C_{P,f}^2}{\nu} + \Delta t_{BEFE}, \frac{4C_{P,p}^2 S_0}{k_{\min}} + \Delta t_{BEFE}\right\} P \\
&\qquad + \|u_h^0\|_f^2 + \frac{\nu \Delta t_{BEFE}}{4}\|\nabla u_h^0\|_f^2 + gS_0\|\phi_h^0\|_p^2 + \frac{g k_{\min}\Delta t_{BEFE}}{4}\|\nabla \phi_h^0\|_p^2.
\end{aligned}$$

Finally, if $\mathbf{f}_f \equiv 0$, $f_p \equiv 0$, from (4.10), the series

$$\sum_{n=0}^{\infty}\left(\frac{\nu}{4}\|\nabla u_h^{n+1}\|_f^2 + \frac{g k_{\min}}{4}\|\nabla \phi_h^{n+1}\|_p^2\right)$$

is convergent and conclusion (4.12) follows. □

Remark 4.4.2 (Asymptotic stability of BEFE)**.** *Since the problem is linear, the stability result in Theorem 4.4.1 implies asymptotic stability in the classical sense. Indeed, let u_h^n, ϕ_h^n denote the difference between two solutions of BEFE with the same right hand side and different initial conditions. Then, by linearity, the differences u_h^n, ϕ_h^n satisfy BEFE with RHS identically zero. Let $y^n := ||u_h^n||^2 + ||\phi_h^n||^2$. Then by the Poincaré inequality,* (4.10) *implies*

$$y^N + \Delta t \sum_{n=1}^{N} y^n \le C(y^0) < \infty, \ C \text{ independent of } N.$$

Hence $\sum_{n=1}^{\infty} y^n$ converges, $y^n \to 0$ and BEFE is asymptotically stable. By a longer but still standard argument, exponential asymptotic stability can also be shown.

4.4.2 BELF Stability.

As noted above, stability over bounded time intervals (allowing exponential growth in time) follows for BELF as for BEFE without any time step restriction. We thus turn to long time stability. First, under time step condition

$$\Delta t \leq \Delta t_{BELF_1} := \frac{2\sqrt{\nu k_{\min}}\min\{1, gS_0\}}{\left[C(\Omega_f)C(\Omega_p)\right]^2 g^{3/2}}, \tag{4.15}$$

we prove a stability result of BELF, which does not include e^{aT} multiplier.

Theorem 4.4.3. *(A first stability bound for BELF) Under the time step condition (4.15) above, BELF method (4.8) is stable:*

$$\begin{aligned} &\|u_h^N\|_f^2 + \|u_h^{N-1}\|_f^2 + gS_0\|\phi_h^N\|_p^2 + gS_0\|\phi_h^{N-1}\|_p^2 \\ &+ \Delta t\sum_{n=1}^{N-1}\left[\nu\|\nabla\left(u_h^{n+1}+u_h^{n-1}\right)\|_f^2 + gk_{\min}\|\nabla\left(\phi_h^{n+1}+\phi_h^{n-1}\right)\|_p^2\right] \\ &\leq 4\Delta t\sum_{n=1}^{N-1}\left(\frac{C_{P,f}^2}{\nu}\left\|\mathbf{f}_f^{n+1}\right\|_f^2 + \frac{gC_{P,p}^2}{k_{\min}}\left\|f_p^{n+1}\right\|_p^2\right) + 2\|u_h^1\|_f^2 + 2\|u_h^0\|_f^2 \\ &+ 2gS_0\|\phi_h^1\|_p^2 + 2gS_0\|\phi_h^0\|_p^2 + 2\Delta t\left(a_f(u_h^1,u_h^1) + a_p(\phi_h^1,\phi_h^1) + a_f(u_h^0,u_h^0) + a_p(\phi_h^0,\phi_h^0)\right) \\ &+ 4\Delta t g\int_I\left(\phi_h^0 u_h^1\cdot\widehat{n}_f - \phi_h^1 u_h^0\cdot\widehat{n}_f\right)ds. \end{aligned} \tag{4.16}$$

Proof. Define the system energy $E^n := \frac{1}{2}\|u_h^n\|_f^2 + \frac{gS_0}{2}\|\phi_h^n\|_p^2$. In (4.8) set $v_h = u_h^{n+1}+u_h^{n-1}$, $q_h = p_h^{n+1}$, $\psi_h = \phi_h^{n+1}+\phi_h^{n-1}$ respectively and add

$$\begin{aligned} \frac{1}{\Delta t}\left(E^{n+1}-E^{n-1}\right) &+ a_f(u_h^{n+1}, u_h^{n+1}+u_h^{n-1}) + a_p(\phi_h^{n+1},\phi_h^{n+1}+\phi_h^{n-1}) \\ &+ c_I(u_h^{n+1}+u_h^{n-1},\phi_h^n) - c_I(u_h^n,\phi_h^{n+1}+\phi_h^{n-1}) \\ &= (\mathbf{f}_f^{n+1}, u_h^{n+1}+u_h^{n-1})_f + g(f_p^{n+1},\phi_h^{n+1}+\phi_h^{n-1})_p. \end{aligned}$$

Since $a_f(\cdot,\cdot)$ and $a_p(\cdot,\cdot)$ are symmetric we have

$$\begin{aligned} a_f(u_h^{n+1}, u_h^{n+1}+u_h^{n-1}) &= \frac{1}{2}a_f(u_h^{n+1},u_h^{n+1}) - \frac{1}{2}a_f(u_h^{n-1},u_h^{n-1}) \\ &+\frac{1}{2}a_f(u_h^{n+1}+u_h^{n-1}, u_h^{n+1}+u_h^{n-1}), \\ a_p(\phi_h^{n+1},\phi_h^{n+1}+\phi_h^{n-1}) &= \frac{1}{2}a_p(\phi_h^{n+1},\phi_h^{n+1}) - \frac{1}{2}a_p(\phi_h^{n-1},\phi_h^{n-1}) \\ &+\frac{1}{2}a_p(\phi_h^{n+1}+\phi_h^{n-1},\phi_h^{n+1}+\phi_h^{n-1}). \end{aligned} \tag{4.17}$$

Let us denote

$$A^n = \frac{1}{2}a_f(u_h^n, u_h^n) + \frac{1}{2}a_p(\phi_h^n, \phi_h^n),$$
$$B^n = \frac{1}{2}a_f(u_h^{n+1} + u_h^{n-1}, u_h^{n+1} + u_h^{n-1}) + \frac{1}{2}a_p(\phi_h^{n+1} + \phi_h^{n-1}, \phi_h^{n+1} + \phi_h^{n-1}),$$
$$C^{n+1/2} = c_I(u_h^{n+1}, \phi_h^n) - c_I(u_h^n, \phi_h^{n+1}).$$

Adding and subtracting E^n and $\Delta t A^n$ in the first two terms below and rearranging the remainder gives

$$\begin{aligned}
&\left[E^{n+1} + E^n + \Delta t A^{n+1} + \Delta t A^n + \Delta t C^{n+1/2}\right] \\
&- \left[E^{n-1} + E^n + \Delta t A^n + \Delta t A^{n-1} + \Delta t C^{n-1/2}\right] \\
&+\Delta t B^n = \ \Delta t \left(\ (\mathbf{f}_f^{n+1}, u_h^{n+1} + u_h^{n-1})_f + g(f_p^{n+1}, \phi_h^{n+1} + \phi_h^{n-1})_p \right).
\end{aligned}$$

Summing this up from $n = 1$ to $n = N - 1$ results in

$$\begin{aligned}
& E^N + E^{N-1} + \Delta t(A^N + A^{N-1}) + \Delta t C^{N-1/2} + \Delta t \sum_{n=1}^{N-1} B^n \\
= \ & E^1 + E^0 + \Delta t(A^1 + A^0) + \Delta t C^{1-1/2} \\
& +\Delta t \sum_{n=1}^{N-1} (\mathbf{f}_f^{n+1}, u_h^{n+1} + u_h^{n-1})_f + \Delta t \sum_{n=1}^{N-1} g(f_p^{n+1}, \phi_h^{n+1} + \phi_h^{n-1})_p.
\end{aligned}$$

We note that

$$\begin{aligned}
A^n &\geq \frac{\nu}{2}\|\nabla u_h^n\|_f^2 + \frac{gk_{\min}}{2}\|\nabla \phi_h^n\|_p^2, \\
B^n &\geq \frac{\nu}{2}\|\nabla \left(u_h^{n+1} + u_h^{n-1}\right)\|_f^2 + \frac{gk_{\min}}{2}\|\nabla \left(\phi_h^{n+1} + \phi_h^{n-1}\right)\|_p^2.
\end{aligned}$$

Applying (4.1) with $\varepsilon_1 = \frac{1}{2}$ yields

$$\begin{aligned}
C^{n-1/2} \ \geq \ & -\frac{\nu}{2}\|\nabla u_h^n\|_f^2 - \frac{\nu}{2}\|\nabla u_h^{n-1}\|_f^2 - \frac{gk_{\min}}{2}\|\nabla \phi_h^n\|_p^2 - \frac{gk_{\min}}{2}\|\nabla \phi_h^{n-1}\|_p^2 \\
& -\frac{1}{2}C_1 \left(\|u_h^n\|_f^2 + \|u_h^{n-1}\|_f^2 + \|\phi_h^n\|_p^2 + \|\phi_h^{n-1}\|_p^2\right).
\end{aligned}$$

Applying the last three inequalities into the energy estimate, bounding the RHS by Schwarz and Poincaré inequalities, summing and rearranging terms yield the result. $\square$

Remark 4.4.4 (Asymptotic stability of BELF does not follow from Theorem 4.4.3)**.** *Asymptotic stability for BELF does not follow from Theorem 4.4.3. Following the last remark, the proof here fails since $\|\nabla(u_h^{n+1} + u_h^{n-1})\|^2$ is not coercive due to the unstable mode of Leap Frog.*

Interestingly, our proof of long time stability of BELF requires an additional time step condition. We impose the following time step condition

$$\Delta t \leq \Delta t_{BELF} := \min\{2\Delta t_{BEFE}, \Delta t_{BELF_1}\} \tag{4.18}$$

to prove long time stability of BELF.

Theorem 4.4.5. *(BELF long time stability) Consider BELF method (4.8). Assume $\Delta t < 1$ and the time step condition (4.18) hold, then*

$$\begin{aligned}
&\|u_h^N\|_f^2 + gS_0\|\phi_h^N\|_p^2 + \Delta t \sum_{n=1}^{N-1} \nu \|\nabla u_h^{n+1}\|_f^2 + \Delta t \sum_{n=1}^{N-1} g k_{\min} \|\nabla \phi_h^{n+1}\|_p^2 \\
&\leq 2\|u_h^1\|_f^2 + 2gS_0\|\phi_h^1\|_p^2 + 2\|u_h^0\|_f^2 + 2gS_0\|\phi_h^0\|_p^2 + 4\Delta t g \int_I (\phi_h^0 u_h^1 \cdot \widehat{n}_f - \phi_h^1 u_h^0 \cdot \widehat{n}_f) ds \\
&\quad + \Delta t \nu (2\|\nabla u_h^1\|_f^2 + \|\nabla u_h^0\|_f^2) + \Delta t g k_{\min}(2\|\nabla \phi_h^1\|_p^2 + \|\nabla \phi_h^0\|_p^2) \\
&\quad + 4\Delta t \sum_{n=1}^{N-1} \frac{C_{P,f}^2}{\nu} \|\mathbf{f}_f^{n+1}\|_f^2 + 4\Delta t \sum_{n=1}^{N-1} \frac{g C_{P,p}^2}{k_{\min}} \|f_p^{n+1}\|_p^2.
\end{aligned} \tag{4.19}$$

There is a $C_0 < \infty$ such that if $\mathbf{f}_f \in L^\infty(L^2(\Omega_f))$, $f_p \in L^\infty(L^2(\Omega_p))$ then

$$\begin{aligned}
\sup_{0\leq N\leq\infty} \left\{\|u_h^N\|_f^2 + gS_0\|\phi_h^N\|_p^2\right\} \leq C_0 \Bigg(&\sup_{0\leq N\leq\infty} \left\{\|\mathbf{f}_f^N\|_f^2 + \|f_p^N\|_p^2\right\} \\
&+ \|u_h^0\|_{H^1(\Omega_f)}^2 + \|\phi_h^0\|_{H^1(\Omega_p)}^2 + \|u_h^1\|_{H^1(\Omega_f)}^2 + \|\phi_h^1\|_{H^1(\Omega_p)}^2 \Bigg).
\end{aligned} \tag{4.20}$$

Also, if $\mathbf{f}_f \equiv 0, f_p \equiv 0$ then

$$u_h^N \to 0, \phi_h^N \to 0 \tag{4.21}$$

in $H^1(\Omega_f)$ and $H^1(\Omega_p)$ respectively as $N \to \infty$.

Proof. In (4.8) set $v_h = u_h^{n+1}, q_h = p_h^{n+1}$, $\psi_h = \phi_h^{n+1}$ respectively and add

$$\begin{aligned}\frac{1}{2\Delta t}\left(E^{n+1}-E^{n-1}\right)+\frac{1}{4\Delta t}\|u_h^{n+1}-u_h^{n-1}\|_f^2+\frac{gS_0}{4\Delta t}\|\phi_h^{n+1}-\phi_h^{n-1}\|_p^2 \\ +2A^{n+1}+c_I(u_h^{n+1},\phi_h^n)-c_I(u_h^n,\phi_h^{n+1})\le(\mathbf{f}_f^{n+1},u_h^{n+1})_f+g(f_p^{n+1},\phi_h^{n+1})_p.\end{aligned} \tag{4.22}$$

Denote the LHS and RHS of (4.22) by L and R correspondingly. Write

$$\begin{aligned}c_I(u_h^{n+1},\phi_h^n)&=\frac{1}{2}c_I(u_h^{n+1},\phi_h^n)+\frac{1}{2}c_I(u_h^{n-1},\phi_h^n)+\frac{1}{2}c_I(u_h^{n+1}-u_h^{n-1},\phi_h^n),\\ c_I(u_h^n,\phi_h^{n+1})&=\frac{1}{2}c_I(u_h^n,\phi_h^{n+1})+\frac{1}{2}c_I(u_h^n,\phi_h^{n-1})+\frac{1}{2}c_I(u_h^n,\phi_h^{n+1}-\phi_h^{n-1}).\end{aligned}$$

Adding and subtracting E^n and rearranging the remainder gives

$$\begin{aligned}L=&\frac{1}{2\Delta t}\left[E^{n+1}+E^n+\Delta tC^{n+1/2}\right]-\frac{1}{2\Delta t}\left[E^n+E^{n-1}+\Delta tC^{n-1/2}\right]\\ &+\frac{1}{4\Delta t}\|u_h^{n+1}-u_h^{n-1}\|_f^2+\frac{gS_0}{4\Delta t}\|\phi_h^{n+1}-\phi_h^{n-1}\|_p^2+2A^{n+1}\\ &+\frac{1}{2}c_I(u_h^{n+1}-u_h^{n-1},\phi_h^n)-\frac{1}{2}c_I(u_h^n,\phi_h^{n+1}-\phi_h^{n-1})\end{aligned}$$

Applying (4.2) and (4.3) with $\varepsilon_2=\frac{\Delta t}{2gS_0}$ and $\varepsilon_3=\frac{\Delta t}{2}$, since $\Delta t\le 2\Delta t_{BEFE}$ we have

$$\begin{aligned}&\frac{1}{2}c_I(u_h^{n+1}-u_h^{n-1},\phi_h^n)-\frac{1}{2}c_I(u_h^n,\phi_h^{n+1}-\phi_h^{n-1})\\ \ge&-\frac{gS_0}{4\Delta t}\|\phi_h^{n+1}-\phi_h^{n-1}\|_p^2-\frac{\Delta t}{4gS_0}C_2\|\nabla(\phi_h^{n+1}-\phi_h^{n-1})\|_p^2-\frac{\nu}{8}\|\nabla u_h^n\|_f^2\\ &-\frac{1}{4\Delta t}\|u_h^{n+1}-u_h^{n-1}\|_f^2-\frac{\Delta t}{4}C_3\|\nabla(u_h^{n+1}-u_h^{n-1})\|_f^2-\frac{gk_{\min}}{8}\|\nabla\phi_h^n\|_p^2\\ \ge&-\frac{gS_0}{4\Delta t}\|\phi_h^{n+1}-\phi_h^{n-1}\|_p^2-\frac{gk_{\min}}{8}(\|\nabla\phi_h^{n+1}\|_p^2+\|\nabla\phi_h^{n-1}\|_p^2)-\frac{\nu}{8}\|\nabla u_h^n\|_f^2\\ &-\frac{1}{4\Delta t}\|u_h^{n+1}-u_h^{n-1}\|_f^2-\frac{\nu}{8}(\|\nabla u_h^{n+1}\|_f^2+\|\nabla u_h^{n-1}\|_f^2)-\frac{gk_{\min}}{8}\|\nabla\phi_h^n\|_p^2.\end{aligned}$$

Denote $D^n=\nu\|\nabla u_h^n\|_f^2+gk_{\min}\|\nabla\phi_h^n\|_p^2$, there follows

$$\begin{aligned}L\ge&\frac{1}{2\Delta t}\left[E^{n+1}+E^n+\Delta tC^{n+1/2}\right]-\frac{1}{2\Delta t}\left[E^n+E^{n-1}+\Delta tC^{n-1/2}\right]\\ &+\frac{5}{8}D^{n+1}+\frac{1}{8}(D^{n+1}-D^n)+\frac{1}{8}(D^{n+1}-D^{n-1})\\ =&\frac{1}{2\Delta t}\left[E^{n+1}+E^n+\Delta tC^{n+1/2}+\frac{\Delta t}{4}(2D^{n+1}+D^n)\right]\\ &\qquad-\frac{1}{2\Delta t}\left[E^n+E^{n-1}+\Delta tC^{n-1/2}+\frac{\Delta t}{4}(2D^n+D^{n-1})\right]+\frac{5}{8}D^{n+1}\end{aligned}$$

Applying Schwarz inequality and Poincaré inequality to the RHS, summing the whole expression from $n=1$ to $n=N-1$ and multiplying by $2\Delta t$ results in

$$\begin{aligned} E^N + E^{N-1} + \Delta t C^{N-1/2} + \frac{\Delta t}{2} D^N + \frac{\Delta t}{4} D^{N-1} + \frac{5\Delta t}{4} \sum_{n=1}^{N-1} D^{n+1} \\ \leq E^1 + E^0 + \Delta t C^{1/2} + \frac{\Delta t}{2} D^1 + \frac{\Delta t}{4} D^0 + \Delta t \sum_{n=1}^{N-1} D^{n+1} \\ + \Delta t \sum_{n=1}^{N-1} \frac{C_{P,f}^2}{\nu} \|\mathbf{f}_f^{n+1}\|_f^2 + \Delta t \sum_{n=1}^{N-1} \frac{g C_{P,p}^2}{k_{\min}} \|f_p^{n+1}\|_p^2. \end{aligned} \tag{4.23}$$

Applying (4.1), since $\Delta t \leq \Delta t_{BELF_1}$ we have

$$\begin{aligned} C^{N-1/2} \geq & -\frac{\nu}{2}\|\nabla u_h^N\|_f^2 - \frac{\nu}{4}\|\nabla u_h^{N-1}\|_f^2 - \frac{g k_{\min}}{2}\|\nabla \phi_h^N\|_p^2 - \frac{g k_{\min}}{4}\|\nabla \phi_h^{N-1}\|_p^2 \\ & - \frac{C_1}{2}\left(\|u_h^N\|_f^2 + \|\phi_h^N\|_p^2\right) - C_1(\|u_h^{N-1}\|_f^2 + \|\phi_h^{N-1}\|_p^2) \\ \geq & -\frac{D^N}{2} - \frac{D^{N-1}}{4} - \frac{E^N}{2\Delta t} - \frac{E^{N-1}}{\Delta t}. \end{aligned} \tag{4.24}$$

Inserting this inequality into the energy estimate (4.23) and multiplying by 4 yields (4.19).

For the second part, denote $H^n = E^n + E^{n-1} + \Delta t C^{n-1/2} + \frac{\Delta t}{4}(2D^n + D^{n-1})$, we will prove that $H^n \leq \beta(D^n + D^{n-1})$, where

$$\beta = \max\left\{ \frac{C_{P,f}^2 + g C(\Omega_f) C(\Omega_p) C_{P,f}^{1/2} C_{P,p}^{1/2} + \nu}{2\nu}, \frac{S_0 C_{P,p}^2 + C(\Omega_f) C(\Omega_p) C_{P,f}^{1/2} C_{P,p}^{1/2} + k_{\min}}{2k_{\min}} \right\}.$$

Indeed, by the Poincaré inequality

$$\begin{aligned} E^n + E^{n-1} \leq & \frac{C_{P,f}^2}{2\nu}(\nu\|\nabla u_h^n\|_f^2 + \nu\|\nabla u_h^{n-1}\|_f^2) \\ & + \frac{S_0 C_{P,p}^2}{2k_{\min}}(g k_{\min}\|\nabla \phi_h^n\|_p^2 + g k_{\min}\|\nabla \phi_h^{n-1}\|_p^2). \end{aligned}$$

Since $\Delta t < 1$, we have $\frac{2\Delta t}{4} D^n + \frac{\Delta t}{4} D^{n-1} \leq \frac{1}{2}(D^n + D^{n-1})$. Applying the trace, Poincaré and Schwarz inequalities, we get

$$\begin{aligned} \Delta t C^{n-1/2} = & \Delta t c_I(u_h^n, \phi_h^{n-1}) - \Delta t c_I(u_h^{n-1}, \phi_h^n) \\ \leq & g C(\Omega_f) C(\Omega_p) C_{P,f}^{1/2} C_{P,p}^{1/2} \left(\|\nabla u_h^n\|_f \|\nabla \phi_h^{n-1}\|_p + \|\nabla u_h^{n-1}\|_f \|\nabla \phi_h^n\|_p\right) \\ \leq & \frac{g C(\Omega_f) C(\Omega_p) C_{P,f}^{1/2} C_{P,p}^{1/2}}{2\nu}(\nu\|\nabla u_h^n\|_f^2 + \nu\|\nabla u_h^{n-1}\|_f^2) \\ & + \frac{C(\Omega_f) C(\Omega_p) C_{P,f}^{1/2} C_{P,p}^{1/2}}{2k_{\min}}(g k_{\min}\|\nabla \phi_h^n\|_p^2 + g k_{\min}\|\nabla \phi_h^{n-1}\|_p^2). \end{aligned}$$

The last three inequalities give $H^n \leq \beta(D^n + D^{n-1})$. There follows

$$\begin{aligned} L &\geq \frac{1}{2\Delta t}H^{n+1} - \frac{1}{2\Delta t}H^n + \frac{5}{8}D^{n+1} \\ &\geq \frac{1}{2\Delta t}H^{n+1} - \frac{1}{2\Delta t}H^n + \frac{5}{8}D^{n+1} + \frac{1}{32\beta}H^n - \frac{1}{32}(D^n + D^{n-1}) \\ &\geq \frac{1}{2\Delta t}H^{n+1} - \frac{1}{2\Delta t}\gamma H^n + \frac{5}{8}D^{n+1} - \frac{1}{32}(D^n + D^{n-1}), \end{aligned} \tag{4.25}$$

where $\gamma = \left(1 - \frac{\Delta t}{16\beta}\right) < 1$.

As $\Delta t < 1$ and $\beta > \frac{1}{2}$, we have $\gamma > \frac{7}{8} > \frac{\sqrt{2}}{2}$. Thus,

$$-\frac{1}{32}(D^n + D^{n-1}) \geq -\frac{\gamma}{16}D^n - \frac{\gamma^2}{16}D^{n-1}.$$

Combining this with (4.25) yields

$$\begin{aligned} L &\geq \frac{1}{2\Delta t}H^{n+1} - \frac{1}{2\Delta t}\gamma H^n + \frac{1}{8}(D^{n+1} - \gamma D^n) + \frac{\gamma}{16}(D^n - \gamma D^{n-1}) + \frac{1}{2}D^{n+1} \\ &= \frac{1}{2\Delta t}M^{n+1} - \frac{\gamma}{2\Delta t}M^n + \frac{1}{2}D^{n+1}, \end{aligned} \tag{4.26}$$

where $M^n = H^n + \frac{\Delta t}{4}D^n + \frac{\gamma\Delta t}{8}D^{n-1}$.

Meanwhile, for every $n = 1, 2, ..., N-1$

$$\begin{aligned} R &\leq \frac{C_{P,f}^2}{2\nu}\|f_f^{n+1}\|_f^2 + \frac{gC_{P,p}^2}{2k_{\min}}\|f_p^{n+1}\|_p^2 + \frac{1}{2}D^{n+1} \\ &\leq C_0 \sup_{0\leq N\leq\infty}\{\|\mathbf{f}_f^N\|_f^2 + \|f_p^N\|_p^2\} + \frac{1}{2}D^{n+1} =: I + \frac{1}{2}D^{n+1}. \end{aligned} \tag{4.27}$$

Combining (4.26) and (4.27) gives: for every $n = 1, 2, ..., N-1$

$$M^{n+1} \leq \gamma M^n + 2\Delta t I. \tag{4.28}$$

Applying (4.28) recursively, we have $M^N \leq \gamma^{N-1}M^1 + 32\beta I$. On the other hand, from (4.24)

$$M^N \geq H^N \geq \frac{1}{2}E^N.$$

Thus, $\frac{1}{2}E^N \leq \gamma^{N-1}M^1 + 32\beta I$ and the second assertion follows.

If $\mathbf{f}_f \equiv 0$ and $f_p \equiv 0$, the third assertion of Theorem 4.4.5 follows from the convergence of series $\sum_{n=1}^{\infty}\nu\|\nabla u_h^{n+1}\|_f^2 + \sum_{n=1}^{\infty}gk_{\min}\|\nabla\phi_h^{n+1}\|_p^2$, given by (4.19). $\square$

Remark 4.4.6 (Asymptotic stability of BELF)**.** *Asymptotic stability for BELF does follow from Theorem 4.4.5 (under a different time step condition than Theorem 4.4.3) by the argument outlined for BEFE.*

4.5 ERROR ANALYSIS OVER $0 \le T^N < \infty$.

For compactness, we only present the analysis of error of BELF. With minor modifications in our proof, we will get the analogous results of convergence rates and long time behaviour for BEFE. Recall that our FEM spaces are assumed to satisfy the usual approximation properties and the Stokes velocity-pressure spaces satisfy the discrete inf-sup condition. Also

$$V^h := X_f^h \cap \{v_h : (q_h, \nabla \cdot v_h)_f = 0, \text{ for all } q_h \in Q_f^h\}.$$

Let $t^n = n\Delta t$, $T = N\Delta t$ (if $T = \infty$ then $N = \infty$), and $u^n := u(t^n)$ (and similarly for other variables).

To establish the optimal error estimates for the approximation we assume

$$\begin{aligned}
&u \in L^\infty(0,T;H^{k+1}(\Omega_f)),\ u_t \in L^\infty(0,T;H^{k+1}(\Omega_f)),\ u_{tt} \in L^\infty(0,T;L^2(\Omega_f)),\\
&\phi \in L^\infty(0,T;H^{k+1}(\Omega_p)),\ \phi_t \in L^\infty(0,T;H^{k+1}(\Omega_p),\ \phi_{tt} \in L^\infty(0,T;L^2(\Omega_p)),\\
&p \in L^\infty(0,T;H^{s+1}(\Omega_f)).
\end{aligned} \tag{4.29}$$

We denote the following continuous and discrete norms by

$$\|v\|_{p,k,r} := \|v\|_{L^p(0,T;H^k(\Omega_r))},\ |||v|||_{\infty,k,r} := \sup_{0\le n\le N} \|v^n\|_{H^k(\Omega_r)}, \quad r \in \{f,p\}.$$

Denote the errors by $e_f^n := u^n - u_h^n$, $e_p^n := \phi^n - \phi_h^n$. The variational formulation of the continuous problem is first rewritten as the discrete problem driven by consistency errors as: for all $v_h \in V^h$, $\psi_h \in X_p^h$ and any $\lambda_h^{n+1} \in Q_f^h$,

$$\begin{aligned}
&(\frac{u^{n+1} - u^{n-1}}{2\Delta t}, v_h)_f + a_f(u^{n+1}, v_h) - (p^{n+1} - \lambda_h^{n+1}, \nabla \cdot v_h)_f + c_I(v_h, \phi^n)\\
&\qquad = (\mathbf{f}_f^{n+1}, v_h)_f + \varepsilon_f^{n+1}(v_h),\\
&gS_0(\frac{\phi^{n+1} - \phi^{n-1}}{2\Delta t}, \psi_h)_p + a_p(\phi^{n+1}, \psi_h) - c_I(u^n, \psi_h)\\
&\qquad = g(f_p^{n+1}, \psi_h)_p + \varepsilon_p^{n+1}(\psi_h).
\end{aligned} \tag{4.30}$$

The consistency errors, $\varepsilon_f^{n+1}(v_h), \varepsilon_p^{n+1}(\psi_h)$, are defined, as usual, by

$$\begin{aligned}
\varepsilon_f^{n+1}(v_h) \ &: = (\frac{u^{n+1} - u^{n-1}}{2\Delta t} - u_t^{n+1}, v_h)_f + c_I(v_h, \phi^n - \phi^{n+1}),\\
\varepsilon_p^{n+1}(\psi_h) \ &: = gS_0(\frac{\phi^{n+1} - \phi^{n-1}}{2\Delta t} - \phi_t^{n+1}, \psi_h)_p - c_I(u^n - u^{n+1}, \psi_h).
\end{aligned}$$

Subtraction gives the error equations: for all $v_h \in V^h$, $\psi_h \in X_p^h$ and any $\lambda_h^{n+1} \in Q_f^h$,

$$
\begin{aligned}
(\frac{e_f^{n+1}-e_f^{n-1}}{2\Delta t}, v_h)_f + a_f(e_f^{n+1}, v_h) + c_I(v_h, e_p^n) &= \varepsilon_f^{n+1}(v_h) + (p^{n+1}-\lambda_h^{n+1}, \nabla\cdot v_h)_f, \\
gS_0(\frac{e_p^{n+1}-e_p^{n-1}}{2\Delta t}, \psi_h)_p + a_p(e_p^{n+1}, \psi_h) - c_I(e_f^n, \psi_h) &= \varepsilon_p^{n+1}(\psi_h).
\end{aligned} \tag{4.31}
$$

Theorem 4.5.1. *(Long time error estimate) Consider BELF method (4.8). Suppose $\Delta t < 1$ and the time step condition (4.18) holds and u, ϕ and p satisfy regularity condition (4.29). Then, for any $0 \le t^N < \infty$, there is a positive constant C_0 such that*

$$
\begin{aligned}
&\|e_f^N\|_f^2 + gS_0\|e_p^N\|_p^2 \\
&\le C_0\Big\{ \left\|u^1-u_h^1\right\|_f^2 + \left\|u^0-u_h^0\right\|_f^2 + gS_0\left\|\phi^1-\phi_h^1\right\|_p^2 + gS_0\left\|\phi^0-\phi_h^0\right\|_p^2 \\
&+ \Delta t\Big(\left\|\nabla\left(u^1-u_h^1\right)\right\|_f^2 + \left\|\nabla\left(u^0-u_h^0\right)\right\|_f^2 + \left\|\nabla\left(\phi^1-\phi_h^1\right)\right\|_p^2 + \left\|\nabla\left(\phi^0-\phi_h^0\right)\right\|_p^2 \Big) \\
&+ h^{2k}\left(|||u|||_{\infty,k+1,f}^2 + |||\phi|||_{\infty,k+1,p}^2\right) + h^{2k+2}\left(\|u_t\|_{\infty,k+1,f}^2 + \|\phi_t\|_{\infty,k+1,p}^2\right) \\
&+ \Delta t^2\left(\|u_{tt}\|_{\infty,0,f}^2 + \|\phi_{tt}\|_{\infty,0,p}^2\right) + \Delta t^2\left(\|u_t\|_{\infty,1,f}^2 + \|\phi_t\|_{\infty,1,p}^2\right) + h^{2s+2}|||p|||_{\infty,s+1,f}^2 \Big\}.
\end{aligned} \tag{4.32}
$$

Proof. Let U^{n+1}, Φ^{n+1} be the interpolation of u^{n+1} and ϕ^{n+1} in V^h and X_p^h correspondingly. Denote

$$
\begin{aligned}
e_f^{n+1} &= (u^{n+1}-U^{n+1}) + (U^{n+1}-u_h^{n+1}) =: \eta_f^{n+1} + \xi_f^{n+1}, \\
e_p^{n+1} &= (\phi^{n+1}-\Phi^{n+1}) + (\Phi^{n+1}-\phi_h^{n+1}) =: \eta_p^{n+1} + \xi_p^{n+1}.
\end{aligned}
$$

Rearranging terms of the error equations (4.31) gives

$$
\begin{aligned}
\frac{1}{2\Delta t}\left(\xi_f^{n+1}-\xi_f^{n-1}, v_h\right)_f + a_f(\xi_f^{n+1}, v_h) + c_I(v_h, \xi_p^n) &= -\frac{1}{2\Delta t}\left(\eta_f^{n+1}-\eta_f^{n-1}, v_h\right)_f \\
-a_f(\eta_f^{n+1}, v_h) - c_I(v_h, \eta_p^n) &+ \varepsilon_f^{n+1}(v_h) + (p^{n+1}-\lambda_h^{n+1}, \nabla\cdot v_h)_f, \\
\frac{gS_0}{2\Delta t}\left(\xi_p^{n+1}-\xi_p^{n-1}, \psi_h\right)_p + a_p(\xi_p^{n+1}, \psi_h) - c_I(\xi_f^n, \psi_h) &= -\frac{gS_0}{2\Delta t}\left(\eta_p^{n+1}-\eta_p^{n-1}, \psi_h\right)_p \\
&- a_p(\eta_p^{n+1}, \psi_h) + c_I(\eta_f^n, \psi_h) + \varepsilon_p^{n+1}(\psi_h),
\end{aligned} \tag{4.33}
$$

for every $v_h \in V_h, \psi_h \in X_p^h$ and $\lambda_h^{n+1} \in Q_f^h$.

Choosing $v_h = \xi_f^{n+1}$ and $\psi_h = \xi_p^{n+1}$ and denoting

$$\mathcal{A}^n = \frac{1}{2}a_f(\xi_f^n, \xi_f^n) + \frac{1}{2}a_p(\xi_p^n, \xi_p^n), \quad \mathcal{C}^{n+1/2} = c_I(\xi_f^{n+1}, \xi_p^n) - c_I(\xi_f^n, \xi_p^{n+1}),$$
$$\mathcal{D}^n = \nu\|\nabla\xi_f^n\|_f^2 + gk_{\min}\|\nabla\xi_p^n\|_p^2, \quad \mathcal{E}^n = \frac{1}{2}\|\xi_f^n\|_f^2 + \frac{gS_0}{2}\|\xi_p^n\|_p^2.$$

After adding (4.33) sides by sides

$$\begin{aligned}
&\frac{1}{2\Delta t}(\mathcal{E}^{n+1} + \mathcal{E}^n + \Delta t\mathcal{C}^{n+1/2}) - \frac{1}{2\Delta t}(\mathcal{E}^n + \mathcal{E}^{n-1} + \Delta t\mathcal{C}^{n-1/2}) + \frac{1}{4\Delta t}\|\xi_f^{n+1} - \xi_f^{n-1}\|_f^2 \\
&+ \frac{gS_0}{4\Delta t}\|\xi_p^{n+1} - \xi_p^{n-1}\|_p^2 + 2\mathcal{A}^{n+1} + \frac{1}{2}c_I(\xi_f^{n+1} - \xi_f^{n-1}, \xi_p^n) - \frac{1}{2}c_I(\xi_f^n, \xi_p^{n+1} - \xi_p^{n-1}) \\
&= -\frac{1}{2\Delta t}\left(\eta_f^{n+1} - \eta_f^{n-1}, \xi_f^{n+1}\right)_f - \frac{gS_0}{2\Delta t}\left(\eta_p^{n+1} - \eta_p^{n-1}, \xi_p^{n+1}\right)_p \\
&\quad - a_f(\eta_f^{n+1}, \xi_f^{n+1}) - a_p(\eta_p^{n+1}, \xi_p^{n+1}) - c_I(\xi_f^{n+1}, \eta_p^n) \\
&\quad + c_I(\eta_f^n, \xi_p^{n+1}) + \varepsilon_f^{n+1}(\xi_f^{n+1}) + \varepsilon_p^{n+1}(\xi_p^{n+1}) + (p^{n+1} - \lambda_h^{n+1}, \nabla\cdot\xi_f^{n+1})_f.
\end{aligned} \tag{4.34}$$

Denote the left and right hand side of (4.34) by $\mathcal{L}$ and $\mathcal{R}$ correspondingly. Also, denote $\mathcal{M} = \mathcal{E}^n + \mathcal{E}^{n-1} + \Delta t\mathcal{C}^{n-1/2} + \frac{3\Delta t}{4}\mathcal{D}^n + \left(\frac{\Delta t}{4} + \frac{\gamma\Delta t}{8}\right)\mathcal{D}^{n-1}$. By the argument outlined in Theorem 4.4.5, using the same definition for β and γ, we have

$$\mathcal{L} \geq \frac{1}{2\Delta t}\mathcal{M}^{n+1} - \frac{\gamma}{2\Delta t}\mathcal{M}^n + \frac{1}{2}\mathcal{D}^{n+1}. \tag{4.35}$$

Next, we derive a bound for $\mathcal{R}$. We first note

$$\begin{aligned}
-\frac{1}{2\Delta t}\left(\eta_f^{n+1} - \eta_f^{n-1}, \xi_f^{n+1}\right)_f - \frac{gS_0}{2\Delta t}\left(\eta_p^{n+1} - \eta_p^{n-1}, \xi_p^{n+1}\right)_p &\leq \frac{5C_{P,f}^2}{2\nu}\left\|\frac{\eta_f^{n+1} - \eta_f^{n-1}}{2\Delta t}\right\|_f^2 \\
+\frac{\nu}{10}\|\nabla\xi_f^{n+1}\|_f^2 + \frac{2C_{P,p}^2 gS_0^2}{k_{\min}}\left\|\frac{\eta_p^{n+1} - \eta_p^{n-1}}{2\Delta t}\right\|_p^2 &+ \frac{gk_{\min}}{8}\left\|\nabla\xi_p^{n+1}\right\|_p^2.
\end{aligned} \tag{4.36}$$

The next terms can be controlled as follows

$$\begin{aligned}
&- a_f(\eta_f^{n+1}, \xi_f^{n+1}) - a_p(\eta_p^{n+1}, \xi_p^{n+1}) \\
&\leq C_0\left(\|\nabla\eta_f^{n+1}\|_f^2 + \|\nabla\eta_p^{n+1}\|_p^2\right) + \frac{\nu}{10}\|\nabla\xi_f^{n+1}\|_f^2 + \frac{gk_{\min}}{8}\|\nabla\xi_p^{n+1}\|_p^2.
\end{aligned} \tag{4.37}$$

Using the trace inequality, Young's inequality and Poincaré's inequality, we obtain

$$
\begin{aligned}
&-c_I(\xi_f^{n+1}, \eta_p^n) + c_I(\eta_f^n, \xi_p^{n+1}) \\
&\le C_0\|\nabla \eta_p^n\|_p^2 + C_0\|\nabla \eta_f^n\|_f^2 + \frac{\nu}{10}\|\nabla \xi_f^{n+1}\|_f^2 + \frac{gk_{\min}}{8}\|\nabla \xi_p^{n+1}\|_p^2.
\end{aligned} \tag{4.38}
$$

The consistency errors are bounded as follows:

$$
\begin{aligned}
|\varepsilon_f^{n+1}(\xi_f^{n+1})| &\le C_0 \left\| u_t^{n+1} - \frac{u^{n+1}-u^{n-1}}{2\Delta t} \right\|_f^2 + C_0\|\nabla(\phi^{n+1}-\phi^n)\|_p^2 + \frac{\nu}{10}\|\nabla \xi_f^{n+1}\|_f^2, \\
|\varepsilon_p^{n+1}(\xi_p^{n+1})| &\le C_0 \left\| \phi_t^{n+1} - \frac{\phi^{n+1}-\phi^{n-1}}{2\Delta t} \right\|_p^2 + C_0\|\nabla(u^{n+1}-u^n)\|_f^2 + \frac{gk_{\min}}{8}\|\nabla \xi_p^{n+1}\|_p^2.
\end{aligned} \tag{4.39}
$$

Lastly, we bound the pressure term by

$$
(p^{n+1} - \lambda_h^{n+1}, \nabla \cdot \xi_f^{n+1})_f \le C_0\|p^{n+1} - \lambda_h^{n+1}\|_f^2 + \frac{\nu}{10}\|\nabla \xi_f^{n+1}\|_f^2. \tag{4.40}
$$

From (4.36)–(4.40), for every $n = 1, 2, ..., N-1$

$$
\begin{aligned}
\mathcal{R} \le & \frac{5C_{P,f}^2}{2\nu} \sup_{1\le n\le N-1} \left\| \frac{\eta_f^{n+1}-\eta_f^{n-1}}{2\Delta t} \right\|_f^2 + \frac{2C_{P,p}^2 g S_0^2}{k_{\min}} \sup_{1\le n\le N-1} \left\| \frac{\eta_p^{n+1}-\eta_p^{n-1}}{2\Delta t} \right\|_p^2 \\
&+ C_0 \sup_{1\le n\le N-1} \left\| u_t^{n+1} - \frac{u^{n+1}-u^{n-1}}{2\Delta t} \right\|_f^2 + C_0 \sup_{1\le n\le N-1} \left\| \phi_t^{n+1} - \frac{\phi^{n+1}-\phi^{n-1}}{2\Delta t} \right\|_p^2 \\
&+ C_0 \left(\sup_{1\le n\le N-1} \|\nabla(u^{n+1}-u^n)\|_f^2 + \sup_{1\le n\le N-1} \|\nabla(\phi^{n+1}-\phi^n)\|_p^2 \right) \\
&+ C_0 \left(\sup_{1\le n\le N} \|\nabla \eta_f^n\|_f^2 + \sup_{1\le n\le N} \|\nabla \eta_p^n\|_p^2 \right) + C_0 \sup_{1\le n\le N-1} \|p^{n+1} - \lambda_h^{n+1}\|_f^2 + \frac{1}{2}\mathcal{D}^{n+1}.
\end{aligned} \tag{4.41}
$$

Applying Taylor's theorem and interpolation error estimates gives

$$
\begin{aligned}
&\frac{5C_{P,f}^2}{2\nu} \sup_{1\le n\le N-1} \left\| \frac{\eta_f^{n+1}-\eta_f^{n-1}}{2\Delta t} \right\|_f^2 + \frac{2C_{P,p}^2 g S_0^2}{k_{\min}} \sup_{1\le n\le N-1} \left\| \frac{\eta_p^{n+1}-\eta_p^{n-1}}{2\Delta t} \right\|_p^2 \\
&\le C_0 \sup_{1\le n\le N-1} \left(\sup_{t^{n-1}\le t\le t^{n+1}} \|\eta_{f,t}(t)\|_f^2 \right) + C_0 \sup_{1\le n\le N-1} \left(\sup_{t^{n-1}\le t\le t^{n+1}} \|\eta_{p,t}(t)\|_p^2 \right) \\
&\le C_0 \left(\|\eta_{f,t}\|_{\infty,0,f}^2 + \|\eta_{p,t}\|_{\infty,0,p}^2 \right) \le C_0 h^{2k+2} \left(\|u_t\|_{\infty,k+1,f}^2 + \|\phi_t\|_{\infty,k+1,p}^2 \right).
\end{aligned} \tag{4.42}
$$

The remaining terms in (4.41) requiring bounds are treated in the same way. First,

$$\begin{aligned}
&C_0 \sup_{1\le n\le N-1}\left\| u_t^{n+1} - \frac{u^{n+1}-u^{n-1}}{2\Delta t}\right\|_f^2 + C_0 \sup_{1\le n\le N-1}\left\| \phi_t^{n+1} - \frac{\phi^{n+1}-\phi^{n-1}}{2\Delta t}\right\|_p^2 \\
&\le C_0\Delta t^2 \left[\sup_{1\le n\le N-1}\left(\sup_{t^{n-1}\le t\le t^{n+1}} \|u_{tt}(t)\|_f^2 \right) + \sup_{1\le n\le N-1}\left(\sup_{t^{n-1}\le t\le t^{n+1}} \|\phi_{tt}(t)\|_p^2 \right)\right] \\
&\le C_0\Delta t^2 \left(\|u_{tt}\|_{\infty,0,f}^2 + \|\phi_{tt}\|_{\infty,0,p}^2 \right).
\end{aligned} \tag{4.43}$$

The next term requires interpolation error estimates to bound as

$$C_0(\sup_{1\le n\le N} \|\nabla \eta_f^n\|_f^2 + \sup_{1\le n\le N} \|\nabla \eta_p^n\|_p^2) \le C_0 h^{2k} \left(|||u|||_{\infty,k+1,f}^2 + |||\phi|||_{\infty,k+1,p}^2 \right). \tag{4.44}$$

Also,

$$\begin{aligned}
&C_0(\sup_{1\le n\le N-1} \|\nabla(u^{n+1}-u^n)\|_f^2 + \sup_{1\le n\le N-1} \|\nabla(\phi^{n+1}-\phi^n)\|_p^2) \\
&\le C_0\Delta t^2 \left[\sup_{1\le n\le N-1}\left(\sup_{t^{n}\le t\le t^{n+1}} \|\nabla(u_t(t))\|_f^2 \right) + \sup_{1\le n\le N-1}\left(\sup_{t^{n}\le t\le t^{n+1}} \|\nabla(\phi_t(t))\|_p^2 \right)\right] \\
&\le C_0\Delta t^2 \left(\|u_t\|_{\infty,1,f}^2 + \|\phi_t\|_{\infty,1,p}^2 \right).
\end{aligned} \tag{4.45}$$

Let λ_h^{n+1} be the interpolation of p^{n+1} in Q_h^f, we have

$$C_0 \sup_{1\le n\le N-1} \|p^{n+1} - \lambda_h^{n+1}\|_f^2 \le C_0 h^{2s+2} |||p|||_{\infty,s+1,f}^2. \tag{4.46}$$

From (4.41)–(4.46), it follows that

$$\begin{aligned}
\mathcal{R} &\le C_0 h^{2k+2} \left(\|u_t\|_{\infty,k+1,f}^2 + \|\phi_t\|_{\infty,k+1,p}^2 \right) \\
&+ C_0\Delta t^2 \left(\|u_{tt}\|_{\infty,0,f}^2 + \|\phi_{tt}\|_{\infty,0,p}^2 \right) + C_0 h^{2k} \left(|||u|||_{\infty,k+1,f}^2 + |||\phi|||_{\infty,k+1,p}^2 \right) \\
&+ C_0\Delta t^2 \left(\|u_t\|_{\infty,1,f}^2 + \|\phi_t\|_{\infty,1,p}^2 \right) + C_0 h^{2s+2} |||p|||_{\infty,s+1,f}^2 + \frac{1}{2}\mathcal{D}^{n+1} \\
&=: \mathcal{I} + \frac{1}{2}\mathcal{D}^{n+1}.
\end{aligned} \tag{4.47}$$

Combining (4.35) and (4.47) and multiplying by $2\Delta t$ yields

$$\mathcal{M}^{n+1} \le \gamma \mathcal{M}^n + 2\Delta t \mathcal{I}, \quad \forall n = 1, 2, ..., N-1. \tag{4.48}$$

Using the same argument as in Theorem 4.4.5 gives

$$\frac{1}{2}\mathcal{E}^N \leq \gamma^{N-1}\mathcal{M}^1 + 32\beta\mathcal{I}. \tag{4.49}$$

Bound for $\mathcal{M}^1$ can be derived from interpolation error estimates

$$\begin{aligned}
\mathcal{M}^1 &= \mathcal{E}^1 + \mathcal{E}^0 + \frac{3\Delta t}{4}\mathcal{D}^1 + \left(\frac{\Delta t}{4} + \frac{\gamma \Delta t}{8}\right)\mathcal{D}^0 + \Delta t \mathcal{C}^{1/2} \\
&\leq \left\|u^1 - u_h^1\right\|_f^2 + \left\|u^0 - u_h^0\right\|_f^2 + gS_0\left\|\phi^1 - \phi_h^1\right\|_p^2 + gS_0\left\|\phi^0 - \phi_h^0\right\|_p^2 \\
&\quad + C_0\Delta t\Big(\left\|\nabla\left(u^1 - u_h^1\right)\right\|_f^2 + \left\|\nabla\left(u^0 - u_h^0\right)\right\|_f^2 + \left\|\nabla\left(\phi^1 - \phi_h^1\right)\right\|_p^2 \\
&\quad + \left\|\nabla\left(\phi^0 - \phi_h^0\right)\right\|_p^2\Big) + C_0 h^{2k}\Big(|||u|||_{\infty,k+1,f}^2 + |||\phi|||_{\infty,k+1,p}^2\Big).
\end{aligned} \tag{4.50}$$

The estimate given in (4.32) follows from (4.49)–(4.50) and the triangle inequality with the notice that the upcoming new terms are already contained in the right hand side of the model. □

For Taylor-Hood elements, i.e. $k = 2$, $s = 1$, we have the following long time estimate.

Corollary 4.5.2. *Consider BELF method (4.8). Under the assumptions of Theorem 4.5.1 with $T = \infty$, suppose that (X_f^h, Q_f^h) is given by P2-P1 Taylor-Hood approximation elements and X_p^h is P2 finite element. Then, there is a positive constant C_0 such that*

$$\sup_{1\leq N\leq\infty}\left\{\|e_f^N\|_f^2 + gS_0\|e_p^N\|_p^2\right\} \leq C_0(\Delta t^2 + h^4).$$

4.6 NUMERICAL EXPERIMENTS

We present numerical experiments to test the algorithms presented in this chapter. First, using the exact solutions introduced in [98], we confirm the predicted convergence rates from the theory. Second, we will look at errors over longer time intervals and small values of $k_{\min}$ to see the long time stability of our proposed methods for $k_{\min}$ smaller than covered by the theory. The code was implemented using the software package *FreeFEM++* [56].

4.6.1 Test 1: Convergence rates.

For the first test we select the velocity and pressure field given in [98]. Let the domain Ω be composed of $\Omega_f = (0,1) \times (1,2)$ and $\Omega_p = (0,1) \times (0,1)$ with the interface $I = (0,1) \times \{1\}$. The exact velocity field is given by

$$
\begin{aligned}
u_1(x,y,t) &= (x^2(y-1)^2 + y)\cos t\,,\\
u_2(x,y,t) &= \left(-\frac{2}{3}x(y-1)^3 + 2 - \pi\sin(\pi x)\right)\cos t\,,\\
p(x,y,t) &= (2-\pi\sin(\pi x))\sin\left(\frac{\pi}{2}y\right)\cos t\,,\\
\phi(x,y,t) &= (2-\pi\sin(\pi x))(1-y-\cos(\pi y))\cos t.
\end{aligned}
$$

We take the time interval $0 \le t \le 3$ and all the physical parameters $\eta, \rho, g, \nu, K, S_0$ and α are simply set to 1. We utilize Taylor-Hood P2-P1 finite elements for the Stokes equations and continuous piecewise quadratic finite element for the Darcy equation. The boundary condition on the problem is inhomogeneous Dirichlet: $u_h = u_{exact}$ on $\partial\Omega$. The initial data and source terms are chosen to correspond the exact solution.

For convenience, we denote $\|.\|_\infty = \|.\|_{\infty,0,f|p}$ and $\|.\|_2 = \|.\|_{2,0,f|p}$. The rates of convergence are computed using linear regression. Table 4.1–4.4 summarize the convergence rates with different order combinations of h and Δt. In particular, Table 4.3 and 4.4 confirm the convergence rates provided in Corollary 3.4.2.

The performance of numerical methods we studied herein is also compared with the monolithic, coupled implicit method. Using the same test problem, the errors $\|u-u_h\|_\infty + \|\phi-\phi_h\|_\infty$ produced by three methods (Fully coupled Backward Euler, BEFE and BELF) are shown in Table 4.5.

Next let the source terms $\mathbf{f}_f \equiv 0$, $f_p \equiv 0$ and the initial condition is given by

$$
\begin{aligned}
&u_1(x,y,0) = (x^2(y-1)^2 + y)\,, u_2(x,y,0) = \left(-\frac{2}{3}x(y-1)^3 + 2 - \pi\sin(\pi x)\right)\,,\\
&p(x,y,0) = (2-\pi\sin(\pi x))\sin\left(\frac{\pi}{2}y\right)\,, \phi(x,y,0) = (2-\pi\sin(\pi x))(1-y-\cos(\pi y)).
\end{aligned}
$$

We take $h = \frac{1}{20}$, $\Delta t = \frac{1}{20}$, $T = 2.0$ and compute $E^n = \|u_h^n\|_f^2 + \|\phi_h^n\|_p^2$ for each $n = 0, ..., N$ using three methods: fully coupled implicit method, BEFE and BELF. The variation of

h	Δt	$\|u-u_h\|_\infty$	$\|\nabla u-\nabla u_h\|_2$	$\|p-p_h\|_2$	$\|\phi-\phi_h\|_\infty$	$\|\nabla\phi-\nabla\phi_h\|_2$
1/5	1/5	3.565e-3	1.230e-1	9.863e-2	1.142e-2	2.050e-1
1/10	1/10	1.814e-3	3.563e-2	4.760e-2	5.760e-3	6.172e-2
1/20	1/20	9.113e-4	1.359e-2	2.354e-2	2.891e-3	2.42e-2
1/40	1/40	4.560e-4	6.166e-3	1.176e-2	1.448e-3	1.125e-2
1/80	1/80	2.280e-4	2.989e-3	5.882e-3	7.248e-4	5.506e-3
Rate of conv.		0.9926	1.3256	1.0152	0.9946	1.2891

Table 4.1: Convergence rate for BEFE with $\Delta t = h$.

h	Δt	$\|u-u_h\|_\infty$	$\|\nabla u-\nabla u_h\|_2$	$\|p-p_h\|_2$	$\|\phi-\phi_h\|_\infty$	$\|\nabla\phi-\nabla\phi_h\|_2$
1/5	1/5	4.484e-3	1.176e-1	1.334e-1	1.210e-2	1.937e-1
1/10	1/10	1.947e-3	3.680e-2	6.842e-2	6.038e-2	6.121e-2
1/20	1/20	9.805e-4	1.481e-2	3.473e-2	3.026e-3	2.451e-2
1/40	1/40	4.922e-4	6.883e-3	1.753e-2	1.515e-3	1.146e-2
1/80	1/80	2.467e-4	3.367e-3	8.812e-3	7.578e-4	5.615e-3
Rate of conv.		1.0352	1.2672	0.9805	0.9988	1.2634

Table 4.2: Convergence rate for BELF with $\Delta t = h$.

approximated kinetic energy E^n from 0.0 to 2.0 is shown in Figure 4.1. For the exact solution, we solve the problem with a small time step and mesh size ($h = \frac{1}{100}$, $\Delta t = \frac{1}{200}$) and use the solution obtained as reference. We note that all methods predict that $E^n \to 0$ as $t^n \to \infty$, which is completely consistent with our theoretical results when $\mathbf{f}_f, f_p \equiv 0$.

4.6.2 Test 2: Stability

Stokes-Darcy flows with very small hydraulic conductivity tensor $\mathcal{K}$ are of special interest in some applications, see [42]. We test herein and compare the performance of our two proposed

h	Δt	$\|u-u_h\|_\infty$	$\|\nabla u-\nabla u_h\|_2$	$\|p-p_h\|_2$	$\|\phi-\phi_h\|_\infty$	$\|\nabla\phi-\nabla\phi_h\|_2$
1/5	1/5	3.565e-3	1.230e-1	1.024e-1	1.142e-2	2.050e-1
1/10	1/20	9.086e-4	3.143e-2	2.532e-2	2.894e-3	4.978e-2
1/20	1/80	2.279e-4	7.356e-3	6.282e-3	7.251e-4	1.202e-2
1/40	1/320	5.702e-5	1.822e-3	1.563e-3	1.814e-4	3.017e-3
1/80	1/1280	1.426e-5	4.673e-4	3.923e-4	4.532e-5	7.631e-4
Rate of conv.		1.9926	2.0189	2.0074	1.9950	2.0183

Table 4.3: Convergence rate for BEFE with $\Delta t = h^2/5$.

h	Δt	$\|u-u_h\|_\infty$	$\|\nabla u-\nabla u_h\|_2$	$\|p-p_h\|_2$	$\|\phi-\phi_h\|_\infty$	$\|\nabla\phi-\nabla\phi_h\|_2$
1/5	1/5	4.484e-3	1.176e-1	1.359e-1	1.210e-2	1.937e-1
1/10	1/20	1.004e-3	3.153e-2	3.597e-2	3.035e-3	4.926e-2
1/20	1/80	2.479e-4	7.492e-3	9.085e-3	7.584e-4	1.203e-2
1/40	1/320	6.188e-5	1.862e-3	2.273e-3	1.896e-4	3.027e-3
1/80	1/1280	1.547e-5	4.773e-4	5.699e-4	4.738e-5	7.661e-4
Rate of conv.		2.0378	1.9971	1.9779	1.9994	1.9989

Table 4.4: Convergence rate for BELF with $\Delta t = h^2/5$.

methods with that of the fully implicit method for such flows. In the following numerical experiment, we keep all initial condition, boundary condition, source data and parameters unchanged from the last test, except $k_{\min}$ is now set to be 10^{-6} and final time T is switched to 5.0, for a clearer representation of behavior of kinetic energy E^n over a longer time. Let $h = 1/10$, we plot E^n with four different time steps $\Delta t = 1/5, 1/8, 1/10, 1/20$ (Figure 4.6.2).

We observe that the fully implicit method is stable with no restriction on Δt. However, BELF and BEFE are already as stable as the implicit method for $\Delta t = 1/10$, which is a very mild constraint and far better than predicted by the theory.

h	Δt	Fully coupled implicit method	BEFE	BELF
1/5	1/5	9.305e-3	1.499e-2	1.658e-2
1/10	1/10	2.083e-3	7.574e-3	7.985e-3
1/20	1/20	9.604-4	3.802e-3	4.007e-3
1/40	1/40	4.797e-4	1.904e-3	2.007e-3
1/80	1/80	2.463e-4	9.528e-4	1.005e-3

Table 4.5: Comparison of error $\|u-u_h\|_\infty + \|\phi-\phi_h\|_\infty$ of the fully coupled implicit method, BEFE and BELF.

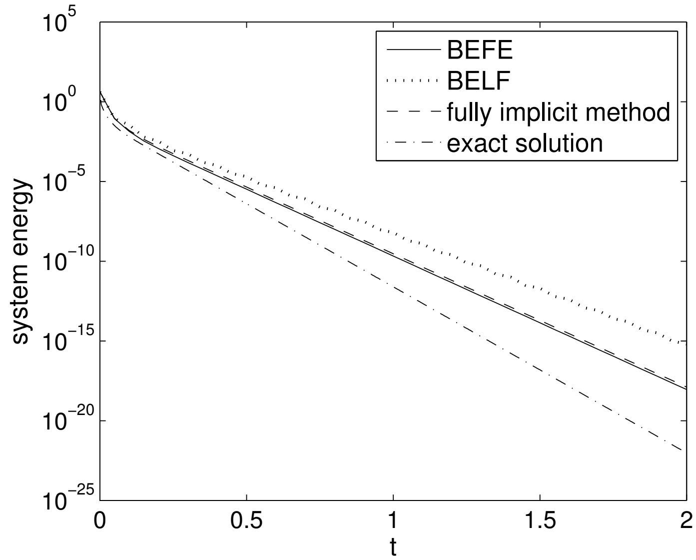

Figure 4.1: The decay of kinetic energy for different numerical methods.

Finally, we repeat the above experiment with ν and $k_{\min}$ set to be 10^{-1} and 10^{-6} correspondingly. We present the results for various values of Δt, purposely chosen to show the difference of the studied methods.

We see that the fully coupled Backward Euler method is the most stable, followed by BELF and then BEFE, as expected. We also note that BELF is already stable for $\Delta t = 1/30$

and so is BEFE for $\Delta t = 1/50$, again far better than conditions derived in the theory. The problem of optimizing the time step conditions for the long time stability of BEFE and BELF is thus an open question.

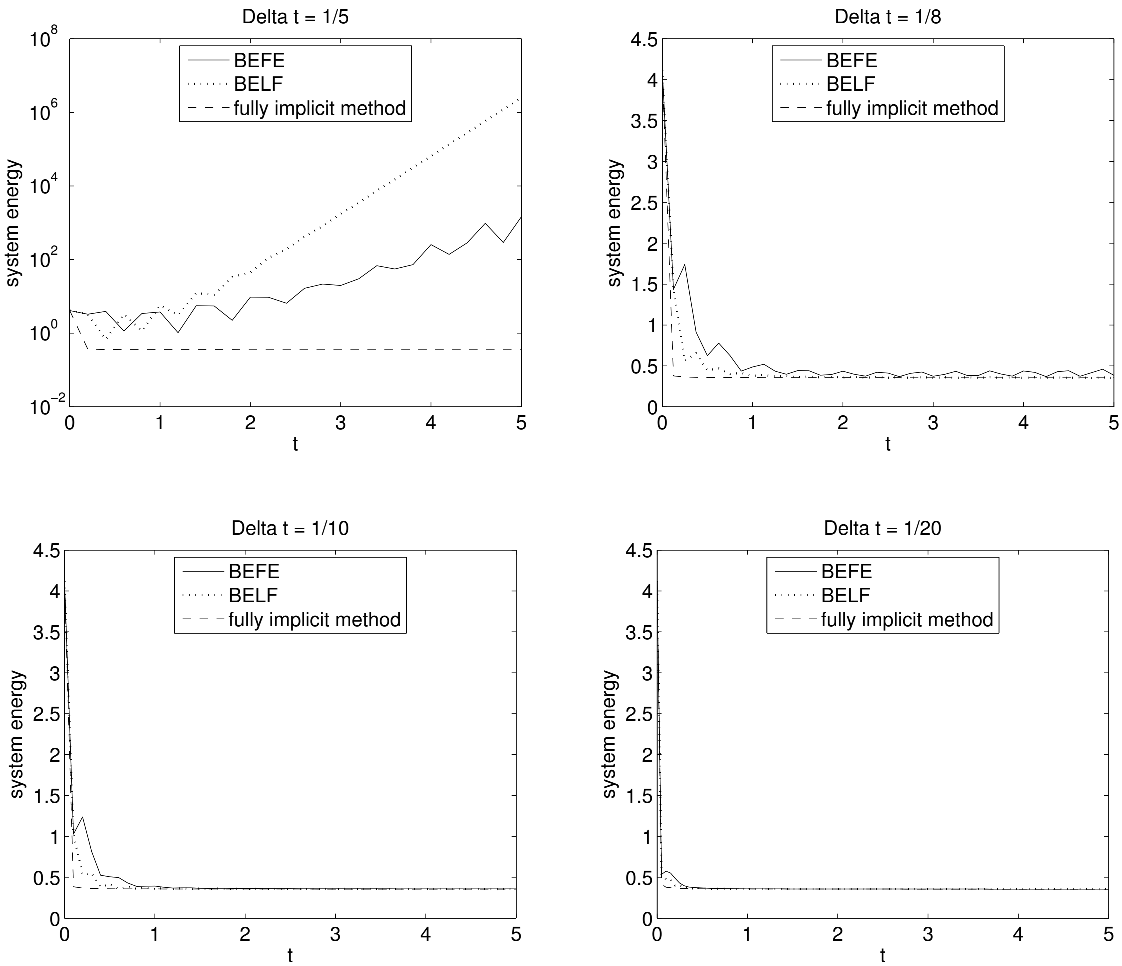

Figure 4.2: Variation of kinetic energy with $\nu = 1$ and $k_{\min} = 10^{-6}$.

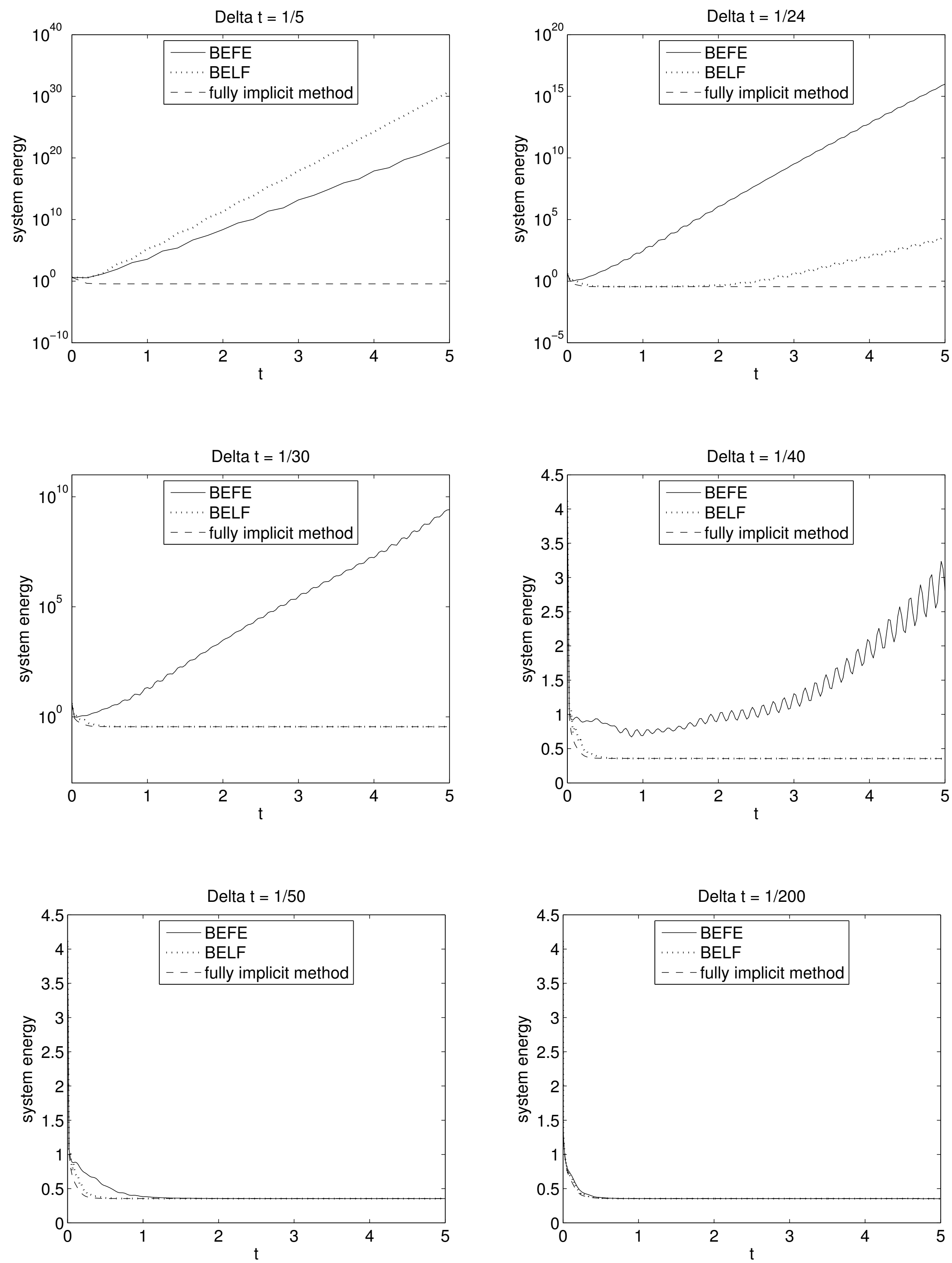

Figure 4.3: Variation of kinetic energy with $\nu = 10^{-1}$ and $k_{\min} = 10^{-6}$.

4.7 CONCLUSION

The evolutionary coupled Stokes-Darcy problem is a complex and high impact problem for which detailed numerical analysis can have a direct impact on algorithm development and solution strategies. Partitioned methods, which require one (per subdomain) solve of SPD system per time step are very attractive in computational complexity compared to monolithic methods (requiring one coupled, non symmetric system of roughly double in size). However, because the coupling is exactly skew symmetric, care must be taken in devising an appropriate uncoupling strategy. We have analyzed two first order partitioned methods which are also comparable in stability and accuracy to fully coupled, monolithic methods. Many open questions remain such as higher order partitioned methods that are long time stable and the severity of the time step restriction in motivating applications where $k_{\min}$ small and S_0 small. We will address both of the issues in next chapter.

5.0 SPLITTING BASED PARTITIONED METHODS FOR THE EVOLUTIONARY STOKES-DARCY PROBLEMS

5.1 NOTATIONS AND PRELIMINARIES

Partitioned methods for the evolutionary Stokes-Darcy problem confront small values of hydraulic conductivity $k_{\min}$ (ranging from 10^{-12} for sands to 10^{-15} for clay, see [11]) and the storativity coefficient S_0 (ranging from 10^{-2} in unconfined aquifers to 10^{-5} in confined aquifers, [70]). In this chapter, we study stability vs. the severity of the induced time step restriction for small $k_{\min}$, S_0 and long time intervals for four *splitting based* partitioned methods. Our estimates and tests suggest that these methods are stable for larger timesteps than the IMEX based partitioned methods mentioned in Chapter 4 and in [98], [83], [81], [109]. In particular, stability analysis and numerical tests herein indicate that splitting based partitioned methods are a very good option when either $k_{\min}$ or S_0 is small. Since the Stokes-Darcy problem and the methods we consider are linear, their error satisfies the same equations as the approximate solution with the body force replaced by a consistency error. Thus, for errors also, stability over long time intervals for small $S_0, k_{\min}$ is the key to a method with good error behavior.

For the continuous model, notations and preliminaries, we refer to Section 4.1 and 4.2. We only state new assumptions and estimations necessary for the analysis herein. In this chapter, we shall assume that the domains $\Omega_{f/p}$ are such that the following trace inequality holds:

$$\left|\int_I \phi u \cdot \widehat{n} ds\right| \leq C||u||_{DIV}||\phi||_{H^1(\Omega_p)}, \text{ for all } u \in X_f, \phi \in X_p. \qquad \text{(HDIV trace)}$$

This inequality is standard if $\Omega_p = \Omega_f$ and $I = \partial\Omega_p$ and holds with $C = 1$ in that case, e.g., [46]. It also holds if Ω_p is contained in Ω_f and $I = \partial\Omega_p$ and visa versa. The most general domains and shared boundaries I which satisfy this inequality do not seem to be known. However, Moraiti [96] shows that it holds in many cases directly (without extra assumptions like $\phi \in H_{00}^{1/2}(I)$) such as when one domain is an image under a smooth map of the other. For example, we have the following special case of Moraiti [96].

Lemma 5.1.1. *Suppose $\Omega_{f/p}$ are open connected, regular sets in $\mathbb{R}^d$ sharing a boundary portion I which is an open connected set with $I \subset \{x = (x_1, \cdots, x_d) : x_d = 0\}$. Suppose Ω_p is the reflection of Ω_f across I, i.e., $(x_1, \cdots, x_d) \in \Omega_p$ if and only if $(x_1, \cdots, -x_d) \in \Omega_f$. Then (HDIV trace) holds with $C = 1$.*

Proof. We have that $\phi(x_1, \cdots, x_d) \in X_p$ means $\phi^* := \phi(x_1, \cdots, -x_d)$ is a well defined function on Ω_f with the same regularity, norms and boundary conditions. Since $\phi^* = \phi$ on I we have

$$\begin{aligned}\int_I \phi u \cdot \widehat{n} ds &= \int_I \phi^* u \cdot \widehat{n} ds = \int_{\Omega_f} \nabla \cdot (u\phi^*)\, dx = \\ &= \int_{\Omega_f} (\nabla \cdot u)\, \phi^* dx + \int_{\Omega_f} u \cdot \nabla \phi^* dx.\end{aligned}$$

Thus, by the Cauchy-Schwarz inequality

$$\left| \int_I \phi u \cdot \widehat{n} ds \right| \leq ||u||_{DIV} ||\phi^*||_{H^1(\Omega_f)} = ||u||_{DIV} ||\phi||_{H^1(\Omega_p)}.$$

$\square$

On the other hand, we include grad-div stabilization (the term $(\nabla \cdot u, \nabla \cdot v)_f$), an idea developed by [88], [99], [100], with coefficient (normally $O(1)$) chosen to be $1/\rho$. To input this term to the scheme, we re-define the bilinear form $a_f(\cdot, \cdot)$:

$$a_f(u, v) = (\nu \nabla u, \nabla v)_f + \frac{1}{\rho} (\nabla \cdot u, \nabla \cdot v)_f + \sum_i \int_I \alpha_{BJ} \sqrt{\frac{\nu g}{\widehat{\tau}_i \cdot \mathcal{K} \cdot \widehat{\tau}_i}} (u \cdot \widehat{\tau}_i)(v \cdot \widehat{\tau}_i) ds,$$

The key to the problem is again the coupling term. The following lemma gives several estimates for this term, which will be used in our next analysis.

Lemma 5.1.2. *If (HDIV trace) holds we have for $u, \phi \in X_f, X_p$*

$$\begin{aligned}
|c_I(u,\phi)| &\leq \frac{\nu}{2}||\nabla u||_f^2 + \frac{gk_{\min}}{2}||\nabla \phi||_p^2 + \frac{[C(\Omega_f)C(\Omega_p)]^2 g^{3/2}}{4\sqrt{\nu k_{\min}}}||u||_f||\phi||_p, \\
|c_I(u,\phi)| &\leq \frac{\nu}{2}||\nabla u||_f^2 + \frac{gk_{\min}}{2}||\nabla \phi||_p^2 + \frac{1}{2}||u||_f^2 + \frac{[C(\Omega_f)C(\Omega_p)]^4 g^3}{32\nu k_{\min}}||\phi||_p^2, \\
& \textit{and} \\
|c_I(u,\phi)| &\leq \frac{gk_{\min}}{2}||\nabla \phi||_p^2 + \frac{g(1+C_{P,p}^2)}{2k_{\min}}\left(||u||_j^2 + ||\nabla \cdot u||_f^2\right).
\end{aligned}$$

In the discrete case, if the inverse estimate (4.5) holds we have for all $u^h, \phi^h \in X_f^h, X_p^h$

$$|c_I(u^h,\phi^h)| \leq gC(\Omega_f)C(\Omega_p)C_{INV}h^{-1}\left(\frac{1}{2}||u^h||_f^2 + \frac{1}{2}||\phi^h||_p^2\right).$$

Proof. Using (2.2) and the Cauchy-Schwarz inequality twice we obtain

$$\begin{aligned}
c_I(u,\phi) = g\int_I \phi u \cdot \widehat{n} ds &\leq g||u||_I||\phi||_I \\
&\leq gC(\Omega_f)C(\Omega_p)||\phi||_p^{1/2}||\nabla\phi||_p^{1/2}||u||_f^{1/2}||\nabla u||_f^{1/2} \\
&\leq \frac{\nu}{2}||\nabla u||_f^2 + \frac{gk_{\min}}{2}||\nabla \phi||_p^2 + \frac{[C(\Omega_f)C(\Omega_p)]^2 g^{3/2}}{4\sqrt{\nu k_{\min}}}||u||_f||\phi||_p.
\end{aligned}$$

The second follows from the first by another application of the Cauchy-Schwarz inequality. For the third estimate we use (HDIV trace) and the Poincaré inequality

$$\begin{aligned}
|c_I(u,\phi)| \leq g||u||_{DIV}||\phi||_{H^1(\Omega_p)} &\leq g||u||_{DIV}\sqrt{1+C_{P,p}^2}||\nabla\phi||_p \\
&\leq \frac{gk_{\min}}{2}||\nabla\phi||_p^2 + \frac{g(1+C_{P,p}^2)}{2k_{\min}}||u||_{DIV}^2.
\end{aligned}$$

The fourth follows similarly using the inverse estimate:

$$\begin{aligned}
|c_I(u^h,\phi^h)| \leq g||u^h||_I||\phi^h||_I &\leq gC(\Omega_f)||u||_f^{1/2}||\nabla u||_f^{1/2}C(\Omega_p)||\phi^h||_p^{1/2}||\nabla\phi^h||_p^{1/2} \\
\leq gC(\Omega_f)C(\Omega_p)C_{INV}h^{-1}||u^h||_f||\phi^h||_p &\leq gC(\Omega_f)C(\Omega_p)C_{INV}h^{-1}\left(\frac{1}{2}||u^h||_f^2 + \frac{1}{2}||\phi^h||_p^2\right).
\end{aligned}$$

□

5.2 DISCRETE FORMULATION

We consider four uncoupling methods. BEsplit1 and 2 methods have superior stability properties in different cases of small physical parameters. The fourth method is second order accurate. The first method is a translation of the method from [121] to the Stokes-Darcy problem.

Method 1: SDsplit = a Stokes-Darcy time-split method. SDsplit is a first order accurate, three sub-step method adapted from [121]. The **SDsplit** approximations are: given (u_h^n, p_h^n, ϕ_h^n), find $(u_h^{n+1}, p_h^{n+1}, \phi_h^{n+1/2}) \in X_f^h \times Q_f^h \times X_p^h$ and $\phi_h^{n+1} \in X_p^h$ satisfying, for all $v_h \in X_f^h$, $q_h \in Q_f^h$, $\psi_h \in X_p^h$:

$$gS_0(\frac{\phi_h^{n+1/2} - \phi_h^n}{\Delta t}, \psi_h)_p + \frac{1}{2}a_p(\phi_h^{n+1/2}, \psi_h) - \frac{1}{2}c_I(u_h^n, \psi_h) = \frac{1}{2}g(f_p^{n+1/2}, \psi_h)_p,$$
$$(\frac{u_h^{n+1} - u_h^n}{\Delta t}, v_h)_f + a_f(u_h^{n+1}, v_h) - (p_h^{n+1}, \nabla \cdot v_h)_f$$
$$+c_I(v_h, \phi_h^{n+1/2}) = (f_f^{n+1}, v_h)_f, \quad \text{and} \quad (q_h, \nabla \cdot u_h^{n+1})_f = 0, \tag{SDsplit}$$
$$gS_0(\frac{\phi_h^{n+1} - \phi_h^{n+1/2}}{\Delta t}, \psi_h)_p + \frac{1}{2}a_p(\phi_h^{n+1}, \psi_h) - \frac{1}{2}c_I(u_h^{n+1}, \psi_h) = \frac{1}{2}g(f_f^{n+1}, \psi_h)_p.$$

SDsplit is uncoupled but sequential: $u_h^n \to \phi_h^{n+1/2} \to u_h^{n+1} \to \phi_h^{n+1}$.

Method 2: BEsplit1 = a Backward Euler time-split method. The BEsplit approximations are: given (u_h^n, p_h^n, ϕ_h^n) find $(u_h^{n+1}, p_h^{n+1}, \phi_h^{n+1}) \in X_f^h \times Q_f^h \times X_p^h$ satisfying, for all $v_h \in X_f^h$, $q_h \in Q_f^h$, $\psi_h \in X_p^h$,

$$(\frac{u_h^{n+1} - u_h^n}{\Delta t}, v_h)_f + a_f(u_h^{n+1}, v_h) - (p_h^{n+1}, \nabla \cdot v_h)_f + c_I(v_h, \phi_h^n) = (f_f^{n+1}, v_h)_f,$$
$$(q_h, \nabla \cdot u_h^{n+1})_f = 0, \tag{BEsplit1}$$
$$gS_0(\frac{\phi_h^{n+1} - \phi_h^n}{\Delta t}, \psi_h)_p + a_p(\phi_h^{n+1}, \psi_h) - c_I(u_h^{n+1}, \psi_h) = g(f_p^{n+1}, \psi_h)_p.$$

The coupling term in the ϕ equation is evaluated at the newly computed value u_h^{n+1} so we compute $\phi_h^n \to u_h^{n+1} \to \phi_h^{n+1}$.

Method 3: BEsplit2. The order of cycling through the equations alters the computed results. **BEsplit2** is the previous method in the opposite order. It is given by: given

(u_h^n, p_h^n, ϕ_h^n) find $(u_h^{n+1}, p_h^{n+1}, \phi_h^{n+1}) \in X_f^h \times Q_f^h \times X_p^h$ satisfying, for all $v_h \in X_f^h$, $q_h \in Q_f^h$, $\psi_h \in X_p^h$,

$$
\begin{aligned}
gS_0(\frac{\phi_h^{n+1} - \phi_h^n}{\Delta t}, \psi_h)_p + a_p(\phi_h^{n+1}, \psi_h) - c_I(u_h^n, \psi_h) = g(f_p^{n+1}, \psi_h)_p \\
(\frac{u_h^{n+1} - u_h^n}{\Delta t}, v_h)_f + (\nabla \cdot \frac{u_h^{n+1} - u_h^n}{\Delta t}, \nabla \cdot v_h)_f + a_f(u_h^{n+1}, v_h) \\
-(p_h^{n+1}, \nabla \cdot v_h)_f + c_I(v_h, \phi_h^{n+1}) = (f_f^{n+1}, v_h)_f, \\
(q_h, \nabla \cdot u_h^{n+1})_f = 0.
\end{aligned}
\tag{BEsplit2}
$$

Our initial analysis revealed that control was needed for a term $||u_h^{n+1} - u_h^n||_{DIV}$. This led to the idea of inserting the grad-div stabilization term $(\nabla \cdot \left(u_h^{n+1} - u_h^n\right)/\Delta t, \nabla \cdot v_h)_f$ acting on the time discretization of u_t. This term is exactly zero for the continuous problem so it does not increase the method's consistency error.

Method 4: CNsplit= a Crank-Nicolson time-split method. CNsplit is second order accurate. It computes *in parallel*[1] two partitioned approximations $(\widehat{u}_h^{n+1}, \widehat{p}_h^{n+1}, \widehat{\phi}_h^{n+1})$ and $(\widetilde{u}_h^{n+1}, \widetilde{p}_h^{n+1}, \widetilde{\phi}_h^{n+1}) \in X_f^h \times Q_f^h \times X_p^h$ whereupon *the new approximation to each variable is the average of the two computed approximations*:

$$
(u_h^{n+1}, p_h^{n+1}, \phi_h^{n+1}) = \frac{1}{2}[(\widehat{u}_h^{n+1}, \widehat{p}_h^{n+1}, \widehat{\phi}_h^{n+1}) + (\widetilde{u}_h^{n+1}, \widetilde{p}_h^{n+1}, \widetilde{\phi}_h^{n+1})]. \tag{CNsplit}
$$

The two individual approximations satisfy, for all $v_h \in X_f^h$, $q_h \in Q_f^h$, $\psi_h \in X_p^h$

$$
\begin{aligned}
(\frac{\widehat{u}_h^{n+1} - \widehat{u}_h^n}{\Delta t}, v_h)_f + a_f(\frac{\widehat{u}_h^{n+1} + \widehat{u}_h^n}{2}, v_h) - (\frac{\widehat{p}_h^{n+1} + \widehat{p}_h^n}{2}, \nabla \cdot v_h)_f \\
+c_I(v_h, \widehat{\phi}_h^n) = (f_f^{n+1/2}, v_h)_f, \text{ and } (q_h, \nabla \cdot \widehat{u}_h^{n+1})_f = 0, \\
gS_0(\frac{\widehat{\phi}_h^{n+1} - \widehat{\phi}_h^n}{\Delta t}, \psi_h)_p + a_p(\frac{\widehat{\phi}_h^{n+1} + \widehat{\phi}_h^n}{2}, \psi_h) - c_I(\widehat{u}_h^{n+1}, \psi_h) = g(f_p^{n+1/2}, \psi_h)_p
\end{aligned}
\tag{CNsplit-a}
$$

and

$$
\begin{aligned}
gS_0(\frac{\widetilde{\phi}_h^{n+1} - \widetilde{\phi}_h^n}{\Delta t}, \psi_h)_p + a_p(\frac{\widetilde{\phi}_h^{n+1} + \widetilde{\phi}_h^n}{2}, \psi_h) - c_I(\widetilde{u}_h^n, \psi_h) = g(f_p^{n+1/2}, \psi_h)_p. \\
(\frac{\widetilde{u}_h^{n+1} - \widetilde{u}_h^n}{\Delta t}, v_h)_f + a_f(\frac{\widetilde{u}_h^{n+1} + \widetilde{u}_h^n}{2}, v_h) - (\frac{\widetilde{p}_h^{n+1} + \widetilde{p}_h^n}{2}, \nabla \cdot v_h)_f \\
+c_I(v_h, \widetilde{\phi}_h^{n+1}) = (f_f^{n+1/2}, v_h)_f, \text{ and } (q_h, \nabla \cdot \widetilde{u}_h^{n+1})_f = 0.
\end{aligned}
\tag{CNsplit-b}
$$

[1] Two processors can be working simultaneously with waiting only due to the different speeds of solving the subdomain problems.

The calculation can proceed as follows

Step 1: Pass previous values across the interface to the other domains

solve, in parallel for $\widehat{u}_h^{n+1}, \widetilde{\phi}_h^{n+1}$

Step 2: Pass each of $\widehat{u}_h^{n+1}, \widetilde{\phi}_h^{n+1}$ across the interface to the other domains

solve, in parallel, for $\widetilde{u}_h^{n+1}, \widehat{\phi}_h^{n+1}$.

Step 3: Average the two approximations on each domain

Averaging the equations of the two approximations shows that the averages u_h^n and ϕ_h^n satisfy

$$
\begin{aligned}
&(\frac{u_h^{n+1}-u_h^n}{\Delta t}, v_h)_f + a_f(\frac{u_h^{n+1}+u_h^n}{2}, v_h) - (\frac{p_h^{n+1}+p_h^n}{2}, \nabla\cdot v_h)_f \\
&+c_I(v_h, \frac{\widetilde{\phi}_h^{n+1}+\widehat{\phi}_h^n}{2}) = (f_f^{n+1/2}, v_h)_f, \text{ and } (q_h, \nabla\cdot u_h^{n+1})_f = 0, \\
&gS_0(\frac{\phi_h^{n+1}-\phi_h^n}{\Delta t}, \psi_h)_p + a_p(\frac{\phi_h^{n+1}+\phi_h^n}{2}, \psi_h) - c_I(\frac{\widehat{u}_h^{n+1}+\widetilde{u}_h^n}{2}, \psi_h) = g(f_p^{n+1/2}, \psi_h)_p
\end{aligned}
\tag{5.1}
$$

To assess consistency errors, the residual is estimated when the true solution $u(t), \phi(t)$ is inserted for all variables u, $\widetilde{u}$, $\widehat{u}$, ϕ, $\widetilde{\phi}$ and $\widehat{\phi}$ in (5.1). As this eliminates the differences between the "hat" and the "tilde" variables, it shows that CNsplit has the same consistency error as the (monolithic / fully coupled) Crank-Nicolson time discretization.

5.3 ANALYSIS OF STABILITY OF SDSPLIT, BESPLIT1/2 AND CNSPLIT

This section gives a stability proof by energy methods in the form that implies stability over long time intervals and elucidates the timestep restriction required for the four methods.

5.3.1 SDsplit Stability.

We prove conditional stability (with a timestep restriction linked to the spacial meshwidth) of SDsplit in this subsection. The timestep restriction is of the form

$$\Delta t < C \min\left\{S_0, k_{min}\right\} h.$$

To be precise, define

$$\Delta T_0 := \frac{2}{g[C(\Omega_f)C(\Omega_p)]^2 C_{INV}} \min\left\{\frac{S_0\nu}{C_{P,f}}, \frac{k_{min}}{C_{P,p}}\right\} h.$$

Theorem 5.3.1. *Suppose that for some α, $0 < \alpha < 1$,*

$$\Delta t \leq (1-\alpha)\Delta T_0. \tag{5.2}$$

Then SDsplit is stable:

$$\begin{aligned}
&\frac{1}{2}\left[||u_h^N||_f^2 + gS_0||\phi_h^N||_p^2\right] + \Delta t\sum_{n=0}^{N-1}\Delta t\frac{gS_0}{2}||\frac{\phi_h^{n+1/2}-\phi_h^n}{\Delta t}||_p^2 \\
&+\frac{\alpha g S_0}{2}\Delta t\sum_{n=0}^{N-1}\Delta t||\frac{\phi_h^{n+1/2}-\phi_h^{n+1}}{\Delta t}||_p^2 + \frac{\alpha}{2}\Delta t\sum_{n=0}^{N-1}\Delta t||\frac{u_h^{n+1}-u_h^n}{\Delta t}||_f^2 \\
&\leq \frac{1}{2}\left[||u_h^0||_f^2 + gS_0||\phi_h^0||_p^2\right] + \frac{gC_{P,p}^2}{2k_{min}}\Delta t\sum_{n=0}^{N-1}||f_p^{n+1/2}||_p^2 \\
&+\frac{C_{P,f}^2}{2\nu}\Delta t\sum_{n=0}^{N-1}||f_f^{n+1}||_f^2 + \frac{gC_{P,p}^2}{4k_{min}}\Delta t\sum_{n=0}^{N-1}||f_p^{n+1}||_p^2.
\end{aligned} \tag{5.3}$$

Proof. In the first 1/3 step of SDsplit, take $\psi = \Delta t\phi_h^{n+1/2}$. This gives

$$\begin{aligned}
&\frac{1}{2}gS_0(||\phi_h^{n+1/2}||_p^2 - ||\phi_h^n||_p^2 + ||\phi_h^{n+1/2}-\phi_h^n||_p^2) + \frac{\Delta t}{2}a_p(\phi_h^{n+1/2}, \phi_h^{n+1/2}) \\
&= \frac{\Delta t}{2}g(f_p^{n+1/2}, \phi_h^{n+1/2})_p + \frac{\Delta t}{2}c_I(u_h^n, \phi_h^{n+1/2}).
\end{aligned}$$

Take $v = \Delta t u_h^{n+1}, q = p_h^{n+1}$ in the 2/3 step and add. This gives

$$\begin{aligned}
&\frac{1}{2}(||u_h^{n+1}||_f^2 - ||u_h^n||_f^2 + ||u_h^{n+1}-u_h^n||_f^2) + \Delta t a_f(u_h^{n+1}, u_h^{n+1}) \\
&= \Delta t(f_f^{n+1}, u_h^{n+1})_f - \Delta t c_I(u_h^{n+1}, \phi_h^{n+1/2}).
\end{aligned}$$

In the 3/3 step, take $\psi = \Delta t \phi_h^{n+1}$:

$$\frac{1}{2}gS_0(||\phi_h^{n+1}||_p^2 - ||\phi_h^{n+1/2}||_p^2 + ||\phi_h^{n+1} - \phi_h^{n+1/2}||_p^2) + \frac{\Delta t}{2}a_p(\phi_h^{n+1}, \phi_h^{n+1})$$
$$= \frac{\Delta t}{2}g(f_p^{n+1}, \phi_h^{n+1})_p + \frac{\Delta t}{2}c_I(u_h^{n+1}, \phi_h^{n+1}).$$

Adding, we obtain:

$$\begin{aligned}
&\frac{1}{2}gS_0(||\phi_h^{n+1}||_p^2 - ||\phi_h^{n}||_p^2) + \frac{1}{2}(||u_h^{n+1}||_f^2 - ||u_h^{n}||_f^2)\\
&+\frac{1}{2}gS_0(||\phi_h^{n+1/2} - \phi_h^{n}||_p^2 + ||\phi_h^{n+1} - \phi_h^{n+1/2}||_p^2) + \frac{1}{2}||u_h^{n+1} - u_h^{n}||_f^2\\
&+\frac{\Delta t}{2}a_p(\phi_h^{n+1/2}, \phi_h^{n+1/2}) + \frac{\Delta t}{2}a_p(\phi_h^{n+1}, \phi_h^{n+1}) + \Delta t a_f(u_h^{n+1}, u_h^{n+1})\\
&= \frac{\Delta t}{2}g(f_p^{n+1/2}, \phi_h^{n+1/2})_p + \Delta t(f_f^{n+1}, u_h^{n+1})_f + \frac{\Delta t}{2}g(f_p^{n+1}, \phi_h^{n+1})_p\\
&+\frac{\Delta t}{2}c_I(u_h^{n}, \phi_h^{n+1/2}) - \Delta t c_I(u_h^{n+1}, \phi_h^{n+1/2}) + \frac{\Delta t}{2}c_I(u_h^{n+1}, \phi_h^{n+1}).
\end{aligned}$$

Consider the interface terms (the last line):

$$\text{Interface Terms} = \frac{\Delta t}{2}c_I(u_h^{n}, \phi_h^{n+1/2}) - \Delta t c_I(u_h^{n+1}, \phi_h^{n+1/2}) + \frac{\Delta t}{2}c_I(u_h^{n+1}, \phi_h^{n+1}).$$

Rewrite the interface term as a difference by splitting the middle term. This gives

$$\begin{aligned}
\text{Interface Terms} &= \frac{\Delta t}{2}c_I(u_h^{n}, \phi_h^{n+1/2}) - \frac{\Delta t}{2}c_I(u_h^{n+1}, \phi_h^{n+1/2})\\
&-\frac{\Delta t}{2}c_I(u_h^{n+1}, \phi_h^{n+1/2}) + \frac{\Delta t}{2}c_I(u_h^{n+1}, \phi_h^{n+1})\\
&= \frac{\Delta t}{2}c_I(u_h^{n} - u_h^{n+1}, \phi_h^{n+1/2}) - \frac{\Delta t}{2}c_I(u_h^{n+1}, \phi_h^{n+1/2} - \phi_h^{n+1}).
\end{aligned}$$

Lemma 5.1.2, the Poincaré inequality and inverse inequality (4.5) give the two bounds

$$\begin{aligned}
&\frac{\Delta t}{2}|c_I(u^n - u^{n+1}, \phi^{n+1/2})|\\
&\leq \frac{g\Delta t}{4}||\mathcal{K}^{1/2}\nabla\phi_h^{n+1/2}||_p^2 + \frac{g[C(\Omega_f)C(\Omega_p)]^2 C_{INV}C_{P,p}h^{-1}\Delta t}{4k_{min}}||u_h^n - u_h^{n+1}||_f^2,
\end{aligned}$$

$$\begin{aligned}
&\frac{\Delta t}{2}|c_I(u_h^{n+1}, \phi_h^{n+1/2} - \phi_h^{n+1})|\\
&\leq \frac{\nu\Delta t}{4}||\nabla u_h^{n+1}||_f^2 + \frac{g^2[C(\Omega_f)C(\Omega_p)]^2 C_{INV}C_{P,f}h^{-1}\Delta t}{4\nu}||\phi_h^{n+1/2} - \phi_h^{n+1}||_p^2.
\end{aligned}$$

Next, we bound the right-hand side in a standard way:

$$\begin{aligned}
\frac{\Delta t}{2} g(f_p^{n+1/2}, \phi_h^{n+1/2}) &\leq \frac{g\Delta t}{8}||K^{1/2}\nabla\phi_h^{n+1/2}||_p^2 + \frac{gC_{P,p}^2\Delta t}{2k_{min}}||f_p^{n+1/2}||_p^2, \\
\Delta t(f_f^{n+1}, u_h^{n+1}) &\leq \frac{C_{P,f}^2\Delta t}{2\nu}||f_f^{n+1}||_f^2 + \frac{\nu\Delta t}{2}||\nabla u_h^{n+1}||_f^2, \\
\frac{\Delta t}{2} g(f_p^{n+1}, \phi_h^{n+1}) &\leq \frac{g\Delta t}{4}||K^{1/2}\nabla\phi_h^{n+1}||_p^2 + \frac{gC_{P,p}^2\Delta t}{4k_{min}}||f_p^{n+1}||_p^2.
\end{aligned}$$

For the left side, apply coercivity:

$$\begin{aligned}
\frac{\Delta t}{2} a_p(\phi_h^{n+1/2}, \phi_h^{n+1/2}) &\geq \frac{g\Delta t}{2}||K^{1/2}\nabla\phi_h^{n+1/2}||_p^2, \\
\Delta t a_f(u_h^{n+1}, u_h^{n+1}) &\geq \nu\Delta t||\nabla u_h^{n+1}||_f^2, \\
\frac{\Delta t}{2} a_p(\phi_h^{n+1}, \phi_h^{n+1}) &\geq \frac{g\Delta t}{2}||K^{1/2}\nabla\phi_h^{n+1}||_p^2.
\end{aligned}$$

Combine, we arrive at:

$$\begin{aligned}
&\frac{1}{2}gS_0(||\phi_h^{n+1}||_p^2 - ||\phi_h^n||_p^2) + \frac{1}{2}(||u_h^{n+1}||_f^2 - ||u_h^n||_f^2) + \frac{1}{2}gS_0||\phi_h^{n+1/2} - \phi_h^n||_p^2 \\
&\quad + (\frac{1}{2}gS_0 - \frac{g^2[C(\Omega_f)C(\Omega_p)]^2 C_{INV} C_{P,f} h^{-1}\Delta t}{4\nu})||\phi_h^{n+1/2} - \phi_h^{n+1}||_p^2 \\
&\quad + (\frac{1}{2} - \frac{g[C(\Omega_f)C(\Omega_p)]^2 C_{INV} C_{P,p} h^{-1}\Delta t}{4k_{min}})||u_h^{n+1} - u_h^n||_f^2 \\
&\leq \frac{gC_{P,p}^2\Delta t}{2k_{min}}||f_p^{n+1/2}||_p^2 + \frac{C_{P,f}^2\Delta t}{2\nu}||f_f^{n+1}||_f^2 + \frac{gC_{P,p}^2\Delta t}{4k_{min}}||f_p^{n+1}||_p^2.
\end{aligned}$$

Sum this over $n = 0, 1, \cdots, N-1$. We have:

$$\begin{aligned}
&\frac{1}{2}\left[||u_h^N||_f^2 + gS_0||\phi_h^N||_p^2\right] + \frac{1}{2}gS_0\sum_{n=0}^{N-1}||\phi_h^{n+1/2} - \phi_h^n||_p^2 \\
&+ (\frac{1}{2}gS_0 - \frac{g^2[C(\Omega_f)C(\Omega_p)]^2 C_{INV} C_{P,f} h^{-1}\Delta t}{4\nu})\sum_{n=0}^{N-1}||\phi_h^{n+1/2} - \phi_h^{n+1}||_p^2 \\
&+ (\frac{1}{2} - \frac{g[C(\Omega_f)C(\Omega_p)]^2 C_{INV} C_{P,p} h^{-1}\Delta t}{4k_{min}})\sum_{n=0}^{N-1}||u_h^{n+1} - u_h^n||_f^2 \\
&\leq \frac{1}{2}\left[||u_h^0||_f^2 + gS_0||\phi_h^0||_p^2\right] + \frac{gC_{P,p}^2\Delta t}{2k_{min}}\sum_{n=0}^{N-1}||f_p^{n+1/2}||_p^2 \\
&+ \frac{C_{P,f}^2\Delta t}{2\nu}\sum_{n=0}^{N-1}||f_f^{n+1}||_f^2 + \frac{gC_{P,p}^2\Delta t}{4k_{min}}\sum_{n=0}^{N-1}||f_p^{n+1}||_p^2.
\end{aligned}$$

Stability follows under the two conditions below, which are equivalent to the time step restriction $\Delta t \leq (1-\alpha)\Delta T_0$:

$$\frac{1}{2}gS_0 - \frac{g^2[C(\Omega_f)C(\Omega_p)]^2 C_{INV}C_{P,f}h^{-1}\Delta t}{4\nu} \geq \alpha\frac{gS_0}{2},$$
$$\frac{1}{2} - \frac{g[C(\Omega_f)C(\Omega_p)]^2 C_{INV}C_{P,p}h^{-1}\Delta t}{4k_{min}} \leq \alpha\frac{1}{2}.$$

□

5.3.2 BEsplit1 Stability.

Define

$$\begin{aligned}
\Delta T_1 &:= 2\min\{\nu k_{\min} S_0 \frac{16}{[C(\Omega_f)C(\Omega_p)]^4 g^2}, 1\},\\
\Delta T_2 &:= \frac{2\min\{1, gS_0\}}{gC(\Omega_f)C(\Omega_p)C_{INV}}h,\\
\Delta T_3 &:= 2gS_0\nu h[gC(\Omega_f)C(\Omega_p)]^{-2}(C_{INV}C_{P,f})^{-1},\\
\Delta T_4 &:= \frac{2\min\{1,\rho\}}{\rho g(1+C_{P,p}^2)}k_{\min},\\
Parameters &:= (1+C_{P,p}^2)(C_{P,f}^2+d)\frac{g}{k_{\min}\nu}.
\end{aligned}$$

Note that ΔT_1 and ΔT_4 are independent of h but depend on $k_{\min}$ and S_0 as $\Delta T_1 \simeq S_0 k_{\min}$ and $\Delta T_4 \simeq k_{\min}$. ΔT_2 and ΔT_3 are independent of $k_{\min}$ but depend on h and S_0 as $\Delta T_{2/3} \simeq S_0 h$. The combination of physical parameters $Parameters$ is independent of h and S_0 but depends on all the other physical parameters. When $\nu = O(1)$, the meshwidth h in the porous medium is moderate and $k_{\min}$, S_0 are small the above restrictions mean either $\Delta t \leq C\max\{k_{\min}, S_0 k_{\min}, S_0 h\}$ or $C\sqrt{\nu k_{\min}} \geq 1$.

Theorem 5.3.2 (Uniform in time stability of BEsplit1)**.** *Suppose either the problem parameters satisfy*

$$Parameters \leq 1$$

or there is an $0<\alpha<1$ *such that* Δt *satisfies the time step restriction*

$$\Delta t \leq (1-\alpha)\max\{\Delta T_1, \Delta T_2, \Delta T_3, \Delta T_4\}.$$

Then, (BEsplit1) is stable uniformly in time. Specifically, if the timestep restriction with ΔT_3 is active then:

$$\frac{1}{2}\left[||u_h^N||_f^2 + gS_0||\phi_h^N||_p^2\right] + \Delta t \sum_{n=0}^{N-1}[\frac{\Delta t}{2}||\frac{u_h^{n+1} - u_h^n}{\Delta t}||_f^2 + \alpha a_f(u_h^{n+1}, u_h^{n+1}) + a_p(\phi_h^{n+1}, \phi_h^{n+1})]$$
$$\leq \frac{1}{2}\left[||u_h^0||_f^2 + gS_0||\phi_h^0||_p^2\right] + \Delta t \sum_{n=0}^{N-1}\left[(f_f^{n+1}, u_h^{n+1})_f + g(f_p^{n+1}, \phi_h^{n+1})_p\right].$$

If any of the other timestep restrictions are active then for any $N > 0$, there holds

$$\alpha\left[||u_h^N||_f^2 + gS_0||\phi_h^N||_p^2\right] + \frac{\Delta t}{2}\sum_{n=0}^{N-1}[a_f(u_h^{n+1} + u_h^n, u_h^{n+1} + u_h^n) + a_p(\phi_h^{n+1} + \phi_h^n, \phi_h^{n+1} + \phi_h^n)]$$
$$\leq \alpha\left[||u_h^0||_f^2 + gS_0||\phi_h^0||_p^2\right] + \Delta t \sum_{n=0}^{N-1}\left[(f_f^{n+1}, u_h^{n+1} + u_h^n)_f + g(f_p^{n+1}, \phi_h^{n+1} + \phi_h^n)_p\right].$$

Proof. In (BEsplit1) set $v_h = u_h^{n+1} + u_h^n, q_h = p_h^{n+1}$, average the incompressibility condition at successive time levels and add. We use

$$a_f(u_h^{n+1}, u_h^{n+1} + u_h^n) = \frac{1}{2}a_f(u_h^{n+1}, u_h^{n+1}) - \frac{1}{2}a_f(u_h^n, u_h^n) + \frac{1}{2}a_f(u_h^{n+1} + u_h^n, u_h^{n+1} + u_h^n). \quad (5.4)$$

This gives:

$$\frac{1}{2}\left[2||u_h^{n+1}||_f^2 + \Delta t a_f(u_h^{n+1}, u_h^{n+1})\right] - \frac{1}{2}\left[2||u_h^n||_f^2 + \Delta t a_f(u_h^n, u_h^n)\right] \quad (5.5)$$
$$+\frac{\Delta t}{2}a_f(u_h^{n+1} + u_h^n, u_h^{n+1} + u_h^n) + \Delta t c_I(\phi_h^n, u_h^{n+1} + u_h^n) = \Delta t(f_f^{n+1}, u_h^{n+1} + u_h^n)_f.$$

Similarly, in the porous media equation, set $\psi_h = \phi_h^{n+1} + \phi_h^n$. We use here

$$a_p(\phi_h^{n+1}, \phi_h^{n+1} + \phi_h^n) = \frac{1}{2}a_p(\phi_h^{n+1}, \phi_h^{n+1}) - \frac{1}{2}a_p(\phi_h^n, \phi_h^n) + \frac{1}{2}a_p(\phi_h^{n+1} + \phi_h^n, \phi_h^{n+1} + \phi_h^n).$$

This gives

$$\frac{1}{2}\left[2gS_0||\phi_h^{n+1}||_p^2 + \Delta t a_p(\phi_h^{n+1}, \phi_h^{n+1})\right] - \frac{1}{2}\left[2gS_0||\phi_h^n||_p^2 + \Delta t a_p(\phi_h^n, \phi_h^n)\right] \quad (5.6)$$
$$+\frac{\Delta t}{2}a_p(\phi_h^{n+1} + \phi_h^n, \phi_h^{n+1} + \phi_h^n) - \Delta t c_I(\phi_h^{n+1} + \phi_h^n, u_h^{n+1}) = \Delta t g(f_p^{n+1}, \phi_h^{n+1} + \phi_h^n)_p.$$

Add (5.5) and (5.6). Consider the sum of the two coupling terms that results

$$\begin{aligned} Coupling &= \Delta t \left[c_I(\phi_h^n, u_h^{n+1} + u_h^n) - c_I(\phi_h^{n+1} + \phi_h^n, u_h^{n+1}) \right] = \\ &= \Delta t \left[c_I(\phi_h^n, u_h^n) - c_I(\phi_h^{n+1}, u_h^{n+1}) \right]. \end{aligned}$$

Let us denote $C^n = c_I(\phi_h^n, u_h^n)$ and

$$\begin{aligned} E^n &= \frac{1}{2}\left[2||u_h^n||_f^2 + 2gS_0||\phi_h^n||_p^2 + \Delta t a_f(u_h^n, u_h^n) + \Delta t a_p(\phi_h^n, \phi_h^n)\right], \\ D^n &= \frac{1}{2}a_f(u_h^{n+1} + u_h^n, u_h^{n+1} + u_h^n) + \frac{1}{2}a_p(\phi_h^{n+1} + \phi_h^n, \phi_h^{n+1} + \phi_h^n). \end{aligned}$$

Adding the two energy estimates and using the above reduction of the coupling term reduces the total energy estimate to

$$\begin{aligned} \left[E^{n+1} - \Delta t C^{n+1}\right] - \left[E^n - \Delta t C^n\right] + \\ +\Delta t D^n = \ \Delta t \left((f_f^{n+1}, u_h^{n+1} + u_h^n)_f + g(f_p^{n+1}, \phi_h^{n+1} + \phi_h^n)_p \right). \end{aligned}$$

Summing this up from $n = 0$ to $n = N - 1$ results in

$$\begin{aligned} \left[E^N - \Delta t C^N\right] + \Delta t \sum_{n=0}^{N-1} D^n = \left[E^0 - \Delta t C^0\right] \\ + \Delta t \sum_{n=0}^{N-1} \left[(f_f^{n+1}, u_h^{n+1} + u_h^n)_f + g(f_p^{n+1}, \phi_h^{n+1} + \phi_h^n)_p\right]. \end{aligned}$$

Stability and the stated energy inequality thus follows provided

$$E^N - \Delta t C^N > 0 \ \text{ for every } N.$$

We have already shown that

$$\begin{aligned} D^n &\geq \frac{\nu}{2}||\nabla\left(u_h^{n+1} + u_h^n\right)||_f^2 + \frac{gk_{\min}}{2}||\nabla\left(\phi_h^{n+1} + \phi_h^n\right)||_p^2, \\ |C^n| &\leq \frac{\nu}{2}||\nabla u_h^n||_f^2 + \frac{gk_{\min}}{2}||\nabla\phi_h^n||_p^2 + \frac{1}{2}||u_h^n||_f^2 + \frac{[C(\Omega_f)C(\Omega_p)]^4 g^3}{32\nu k_{\min}}||\phi_h^n||_p^2. \end{aligned}$$

Thus,

$$\begin{aligned} E^n - \Delta t C^n \geq ||u_h^n||_f^2 + gS_0||\phi_h^n||_p^2 + \frac{\Delta t}{2}\left(\nu||\nabla u_h^n||_f^2 + gk_{\min}||\nabla\phi_h^n||_p^2\right) \\ -\Delta t[\frac{\nu}{2}||\nabla u_h^n||_f^2 + \frac{gk_{\min}}{2}||\nabla\phi_h^n||_p^2 + \frac{1}{2}||u_h^n||_f^2 + \frac{[C(\Omega_f)C(\Omega_p)]^4 g^3}{32\nu k_{\min}}||\phi_h^n||_p^2]. \end{aligned} \tag{5.7}$$

Thus stability follows provided

$$\Delta t \frac{[C(\Omega_f)C(\Omega_p)]^4 g^3}{32\nu k_{\min}} \leq (1-\alpha) g S_0, \text{ or}$$
$$\Delta t \leq (1-\alpha)\nu k_{\min} S_0 \frac{32}{[C(\Omega_f)C(\Omega_p)]^4 g^2} \equiv (1-\alpha)\Delta T_1.$$

Alternate conditions are obtained using different estimates of the coupling / interface term. Indeed, using Lemma 5.1.2

$$|C^n| = |c_I(u_h^n, \phi_h^n)| \leq g C(\Omega_f) C(\Omega_p) C_{INV} h^{-1} \left(\frac{1}{2}||u_h^n||_f^2 + \frac{1}{2}||\phi_h^n||_p^2\right).$$

Thus stability follows provided

$$\begin{aligned} \frac{\Delta t}{h} g C(\Omega_f) C(\Omega_p) C_{INV} &\leq 2(1-\alpha)\min\{1, gS_0\}, \text{ or} \\ \Delta t &\leq (1-\alpha)\frac{2\min\{1, gS_0\}}{gC(\Omega_f)C(\Omega_p)C_{INV}} h \equiv (1-\alpha)\Delta T_2, \end{aligned}$$

which is the second condition.

For the condition $Parameters \leq 1$, that by Lemma 5.1.2

$$\begin{aligned} |C^n| &\leq \frac{g k_{\min}}{2}||\nabla \phi_h^n||_p^2 + \frac{g(1+C_{P,p}^2)}{2k_{\min}}||u_h^n||_{DIV}^2 \\ &\leq \frac{g k_{\min}}{2}||\nabla \phi_h^n||_p^2 + \frac{g(1+C_{P,p}^2)}{2k_{\min}}(||u_h^n||_f^2 + d||\nabla u_h^n||_f^2) \\ &\leq \frac{g k_{\min}}{2}||\nabla \phi_h^n||_p^2 + \frac{g(1+C_{P,p}^2)}{2k_{\min}}(C_{P,f}^2 + d)||\nabla u_h^n||_f^2 \end{aligned}$$

Thus the method is also stable if the problem data satisfies

$$\frac{g(1+C_{P,p}^2)}{2k_{\min}}(C_{P,f}^2 + d) \leq \frac{\nu}{2} \text{ or}$$
$$Parameters = (1+C_{P,p}^2)(C_{P,f}^2 + d)\frac{g}{k_{\min}\nu} \leq 1$$

The condition involving ΔT_3 requires a separate stability proof. In (BEsplit1) set $v_h = u_h^{n+1}, q_h = p_h^{n+1}$ and add. We use

$$(u_h^{n+1} - u_h^n, u_h^{n+1})_f = \frac{1}{2}\left[||u_h^{n+1}||_f^2 - ||u_h^n||_f^2\right] + \frac{1}{2}||u_h^{n+1} - u_h^n||_f^2,$$

and similarly for ϕ. This gives:

$$\frac{1}{2}\left[||u_h^{n+1}||_f^2 - ||u_h^n||_f^2\right] + \frac{1}{2}||u_h^{n+1} - u_h^n||_f^2 + \Delta t a_f(u_h^{n+1}, u_h^{n+1}) +$$
$$+\Delta t c_I(\phi_h^n, u_h^{n+1}) = \Delta t(f_f^{n+1}, u_h^{n+1})_f.$$

Similarly, in the porous media equation, set $\psi_h = \phi_h^{n+1}$, we get

$$\frac{1}{2}\left[gS_0||\phi_h^{n+1}||_p^2 - gS_0||\phi_h^n||_p^2 + gS_0||\phi_h^{n+1} - \phi_h^n||_p^2\right] + \Delta t a_p(\phi_h^{n+1}, \phi_h^{n+1})$$
$$-\Delta t c_I(\phi_h^{n+1}, u_h^{n+1}) = \ \Delta t g(f_p^{n+1}, \phi_h^{n+1})_p.$$

Add these two equations and consider the sum of the two coupling terms that result:

$$|Coupling| = \Delta t|c_I(\phi_h^n, u_h^{n+1}) - c_I(\phi_h^{n+1}, u_h^{n+1})| = \Delta t|c_I(\phi_h^{n+1} - \phi_h^n, u_h^{n+1})|.$$

The following bound holds by an analogous proof as that of in Lemma 5.1.2:

$$\begin{aligned}
|Coupling| &\leq \frac{gS_0}{2}||\phi_h^{n+1} - \phi_h^n||_p^2 \\
&+\Delta t\left[\frac{\Delta t}{2gS_0}\left(gC(\Omega_f)C(\Omega_p)\right)^2 C_{INV}h^{-1}||u_h^{n+1}||_f||\nabla u_h^{n+1}||_f\right] \\
&\leq \frac{gS_0}{2}||\phi_h^{n+1} - \phi_h^n||_p^2 \\
&+\Delta t\left[\frac{\Delta t}{2gS_0\nu}\left(gC(\Omega_f)C(\Omega_p)\right)^2 C_{INV}h^{-1}C_{P,f}a_f(u_h^{n+1}, u_h^{n+1})\right].
\end{aligned}$$

The remainder of the proof follows the above pattern and is complete, provided

$$\frac{\Delta t}{2gS_0\nu}\left(gC(\Omega_f)C(\Omega_p)\right)^2 C_{INV}h^{-1}C_{P,f} \leq 1-\alpha, \text{ or}$$
$$\Delta t < (1-\alpha)\frac{2gS_0\nu}{\left(gC(\Omega_f)C(\Omega_p)\right)^2 C_{INV}C_{P,f}}h \equiv (1-\alpha)\Delta T_3.$$

For the ΔT_4 condition, we exploit the added grad-div stabilization. By the third inequality of Lemma 5.1.2

$$|Coupling| \leq \Delta t\frac{gk_{\min}}{2}||\nabla\phi||_p^2 + \Delta t\frac{g(1+C_{P,p}^2)}{2k_{\min}}||u||^2 + \Delta t\frac{g(1+C_{P,p}^2)}{2k_{\min}}||\nabla \cdot u||^2.$$

The last term can be subsumed into the grad-div stabilization term provided

$$\Delta t \frac{g(1+C_{P,p}^2)}{2k_{\min}} \leq \frac{1}{\rho}.$$

The other two terms are subsumed into the system energy. Stability thus follows provided

$$||u_h^n||_f^2 + gS_0||\phi_h^n||_p^2 + \frac{\Delta t}{2}\left(\nu||\nabla u_h^n||_f^2 + gk_{\min}||\nabla \phi_h^n||_p^2\right)$$
$$-\left[\Delta t \frac{gk_{\min}}{2}||\nabla \phi||_p^2 + \Delta t \frac{g(1+C_{P,p}^2)}{2k_{\min}}||u||^2\right] > 0.$$

This requires

$$\Delta t \frac{g(1+C_{P,p}^2)}{2k_{\min}} \leq 1$$

Thus, stability follows under these two conditions, i.e., if $\Delta t \leq \min\{1,\rho\}\frac{2k_{\min}}{\rho g(1+C_{P,p}^2)} = \Delta T_4$. The rest of the proof follows by summing. □

5.3.3 BEsplit2 Stability.

Due to the similarity of the analysis for BEsplit2 to BEsplit1, we present the aspects of the proof that differ only. Define

$$\begin{aligned}
\Delta T_5 &: = \frac{2k_{\min}h}{g[C(\Omega_f)C(\Omega_p)]^2 C_{P,p}C_{INV}} \\
\Delta T_6 &: = \frac{2}{g\left(1+C_{P,p}^2\right)}k_{\min}.
\end{aligned}$$

We prove uniform in time stability under a time step restriction of the form that occurred in BEsplit1 with ΔT_3 replaced by ΔT_5 and ΔT_4 replaced by ΔT_6. Thus, for small S_0 the active constraint is expected to be

$$\Delta t < \Delta T_6 \simeq Ck_{\min}$$

which is independent of both h and S_0. Thus, BEsplit1/2 are promising for the quasi-static approximation and for problems with very small S_0 and moderate $k_{\min}$.

Theorem 5.3.3 (Uniform in time and S_0 stability)**.** *Consider the method (BEsplit2). Suppose that there is an $\alpha, 0 < \alpha < 1$, such that either the problem parameters satisfy*

$$Parameters \leq 1 - \alpha,$$

or Δt satisfies the time step restriction

$$\Delta t \leq (1-\alpha)\max\{\Delta T_1, \Delta T_2, \Delta T_5, \Delta T_6\}.$$

Then, BEsplit2 is stable uniformly in time and uniformly in S_0. Specifically, for any $N > 0$ we have the energy inequality (which also proves stability)

$$\begin{aligned}
&\frac{1}{2}\left[||u_h^N||_f^2 + ||\nabla \cdot u_h^N||_f^2 + gS_0||\phi_h^N||_p^2\right] \\
&+\Delta t \sum_{n=0}^{N-1}\left[\frac{\Delta t}{2} gS_0 ||\frac{\phi_h^{n+1} - \phi_h^n}{\Delta t}||_p^2 + a_f(u_h^{n+1}, u_h^{n+1}) + \alpha a_p(\phi_h^{n+1}, \phi_h^{n+1})\right] \\
&\leq \frac{1}{2}\left[||u_h^0||_f^2 + ||\nabla \cdot u_h^0||_f^2 + gS_0||\phi_h^0||_p^2\right] + \Delta t \sum_{n=0}^{N-1}\left[(f_f^{n+1}, u_h^{n+1})_f + g(f_p^{n+1}, \phi_h^{n+1})_p\right].
\end{aligned}$$

Proof. The derivation of the stability conditions involving $Parameters$ and ΔT_1, ΔT_2 is very similar to the case of BEsplit1. We therefore move to the condition involving ΔT_5 and ΔT_6.

In (BEsplit2) set $\psi_h = \phi_h^{n+1}, v_h = u_h^{n+1}, q_h = p_h^{n+1}$, and add. We use

$$-(u_h^n, u_h^{n+1})_f = -\frac{1}{2}(u_h^n, u_h^n)_f - \frac{1}{2}(u_h^{n+1}, u_h^{n+1})_f + \frac{1}{2}(u_h^{n+1} - u_h^n, u_h^{n+1} - u_h^n)_f,$$

and similarly for the $(\nabla \cdot u_h^n, \nabla \cdot u_h^{n+1})_f$ terms and the analogous terms in the ϕ equation. This gives:

$$\begin{aligned}
&\frac{1}{2}\left[||u_h^{n+1}||_f^2 + ||\nabla \cdot u_h^{n+1}||_f^2 + gS_0||\phi_h^{n+1}||_p^2\right] - \frac{1}{2}\left[||u_h^n||_f^2 + ||\nabla \cdot u_h^n||_f^2 + gS_0||\phi_h^n||_p^2\right] \\
&+\frac{1}{2}\left[||u_h^{n+1} - u_h^n||_f^2 + ||\nabla \cdot (u_h^{n+1} - u_h^n)||_f^2 + gS_0||\phi_h^{n+1} - \phi_h^n||_p^2\right] \\
&+\Delta t\left[a_f(u_h^{n+1}, u_h^{n+1}) + a_p(\phi_h^{n+1}, \phi_h^{n+1})\right] \\
&+\Delta t c_I(\phi_h^{n+1}, u_h^{n+1} - u_h^n) = \Delta t(f_f^{n+1}, u_h^{n+1})_f + \Delta t g(f_p^{n+1}, \phi_h^{n+1})_p.
\end{aligned}$$

Consider the sum of the two coupling terms

$$Coupling = \Delta t c_I(\phi_h^{n+1}, u_h^{n+1} - u_h^n).$$

For the condition involving ΔT_5,

$$\begin{aligned}
|Coupling| &\leq \Delta t g C(\Omega_f) C(\Omega_p) C_{P,p}^{\frac{1}{2}} (C_{INV} h^{-1})^{\frac{1}{2}} ||\nabla \phi_h^{n+1}||_p ||u_h^{n+1} - u_h^n||_f \\
&\leq \frac{1}{2} ||u_h^{n+1} - u_h^n||_f^2 + \frac{g[C(\Omega_f)C(\Omega_p)]^2 C_{P,p} C_{INV} h^{-1} \Delta t^2}{2k_{min}} a_p(\phi_h^{n+1}, \phi_h^{n+1})
\end{aligned}$$

Subsuming the above two terms in the obvious places, the method is stable if

$$\Delta t \leq \frac{2k_{min} h}{g[C(\Omega_f)C(\Omega_p)]^2 C_{P,p} C_{INV}} = \Delta T_5.$$

For the stability condition involving ΔT_6, we have, using Lemma 5.1.2 and $a_p(\phi_h^{n+1}, \phi_h^{n+1}) \geq g k_{\text{min}} ||\nabla \phi_h^{n+1}||_p$,

$$\begin{aligned}
|Coupling| &\leq \Delta t g ||\phi_h^{n+1}||_{H^1(\Omega_p)} ||u_h^{n+1} - u_h^n||_{DIV} \\
&\leq \Delta t g \sqrt{1 + C_{P,p}^2} ||\nabla \phi_h^{n+1}||_p ||u_h^{n+1} - u_h^n||_{DIV} \\
&\leq \frac{1}{2} \left[||u_h^{n+1} - u_h^n||_f^2 + ||\nabla \cdot (u_h^{n+1} - u_h^n)||_f^2 \right] \\
&+ \frac{1}{2} \Delta t^2 \frac{g}{k_{\text{min}}} \left(1 + C_{P,p}^2\right) a_p(\phi_h^{n+1}, \phi_h^{n+1}).
\end{aligned}$$

Thus

$$\begin{aligned}
\frac{1}{2} \left[||u_h^{n+1}||_f^2 + ||\nabla \cdot u_h^{n+1}||_f^2 + g S_0 ||\phi_h^{n+1}||_p^2 \right] - \frac{1}{2} \left[||u_h^n||_f^2 + ||\nabla \cdot u_h^n||_f^2 + g S_0 ||\phi_h^n||_p^2 \right] \\
+ \frac{1}{2} g S_0 ||\phi_h^{n+1} - \phi_h^n||_p^2 + \Delta t [a_f(u_h^{n+1}, u_h^{n+1}) \\
+ (1 - \frac{1}{2} \Delta t g \left(1 + C_{P,p}^2\right) k_{\text{min}}^{-1}) a_p(\phi_h^{n+1}, \phi_h^{n+1})] \\
\leq \Delta t (f_f^{n+1}, u_h^{n+1})_f + \Delta t g (f_p^{n+1}, \phi_h^{n+1})_p.
\end{aligned}$$

Stability then follows under the timestep restriction

$$(1 - \frac{1}{2} \Delta t g \left(1 + C_{P,p}^2\right) k_{\text{min}}^{-1}) \geq \alpha > 0$$

which is equivalent to

$$\Delta t \leq (1 - \alpha) \frac{2}{g \left(1 + C_{P,p}^2\right)} k_{\text{min}} \equiv (1 - \alpha) \Delta T_6.$$

$\square$

5.3.4 CNsplit Stability.

CNsplit computes two partitioned approximations $(\widehat{u}_h^n, \widehat{p}_h^n, \widehat{\phi}_h^n)$ and $(\widetilde{u}_h^n, \widetilde{p}_h^n, \widetilde{\phi}_h^n) \in X_f^h \times Q_f^h \times X_p^h$ for $n \geq 1$ whereupon

$$(u_h^{n+1}, p_h^{n+1}, \phi_h^{n+1}) = \frac{1}{2}[(\widehat{u}_h^{n+1}, \widehat{p}_h^{n+1}, \widehat{\phi}_h^{n+1}) + (\widetilde{u}_h^{n+1}, \widetilde{p}_h^{n+1}, \widetilde{\phi}_h^{n+1})], \tag{CNsplit}$$

that is, *the new approximation to each variable is the average of the two computed approximations.* Since the unit ball in a Hilbert space is convex, stability of $(u_h^{n+1}, p_h^{n+1}, \phi_h^{n+1})$ follows from stability of $(\widehat{u}_h^{n+1}, \widehat{p}_h^{n+1}, \widehat{\phi}_h^{n+1})$ and $(\widetilde{u}_h^{n+1}, \widetilde{p}_h^{n+1}, \widetilde{\phi}_h^{n+1})$. We thus prove stability of the two individual sub-problems. Define

$$\Delta T_6 := \frac{\sqrt{2S_0}}{\sqrt{g}C(\Omega_f)C(\Omega_p)C_{INV}} h$$

We prove long time stability under a time step condition of the form

$$\Delta t < C\sqrt{S_0}h.$$

Theorem 5.3.4 (Stability of one step of CNsplit)**.** *Consider (CNsplit-a) one step of the **CNsplit** method. Suppose there is an $0 < \alpha < 1/2$ such that Δt satisfies the time step restriction*

$$\Delta t \leq (1-\alpha)\Delta T_6$$

Then, (CNsplit-a) is stable uniformly in time over possibly long time intervals. Specifically, for every $N \geq 1$

$$\begin{aligned}
\alpha \left[||\widehat{u}_h^N||_f^2 + gS_0||\widehat{\phi}_h^N||_p^2\right] + \Delta t \sum_{n=0}^{N-1} \frac{1}{2}\left[a_f(\widehat{u}_h^{n+1} + \widehat{u}_h^n, \widehat{u}_h^{n+1} + \widehat{u}_h^n) + a_p(\widehat{\phi}_h^{n+1} + \widehat{\phi}_h^n, \widehat{\phi}_h^{n+1} + \widehat{\phi}_h^n)\right] \\
\leq ||\widehat{u}_h^0||_f^2 + gS_0||\widehat{\phi}_h^0||_p^2 - \Delta t c_I(\widehat{\phi}_h^0, \widehat{u}_h^0) \\
+ \Delta t \sum_{n=0}^{N-1} \left[(f_f^{n+1/2}, \widehat{u}_h^{n+1} + \widehat{u}_h^n)_f + g(f_p^{n+1/2}, \widehat{\phi}_h^{n+1} + \widehat{\phi}_h^n)_p\right].
\end{aligned}$$

Proof. In (CNsplit-a) set $v_h = \widehat{u}_h^{n+1} + \widehat{u}_h^n, q_h = \widehat{p}_h^{n+1}$, average the incompressibility condition at successive time levels and add. This gives:

$$\begin{aligned}&||\widehat{u}_h^{n+1}||_f^2 - ||\widehat{u}_h^n||_f^2 + \frac{\Delta t}{2} a_f(\widehat{u}_h^{n+1} + \widehat{u}_h^n, \widehat{u}_h^{n+1} + \widehat{u}_h^n)\\ &+\Delta t c_I(\widehat{\phi}_h^n, \widehat{u}_h^{n+1} + \widehat{u}_h^n) = \Delta t(f_f^{n+1/2}, \widehat{u}_h^{n+1} + \widehat{u}_h^n)_f.\end{aligned}$$

Similarly, in the porous media equation, set $\psi_h = \widehat{\phi}_h^{n+1} + \widehat{\phi}_h^n$. This gives

$$\begin{aligned}&gS_0||\widehat{\phi}_h^{n+1}||_p^2 - gS_0||\widehat{\phi}_h^n||_p^2 + \frac{\Delta t}{2} a_p(\widehat{\phi}_h^{n+1} + \widehat{\phi}_h^n, \widehat{\phi}_h^{n+1} + \widehat{\phi}_h^n)\\ &-\Delta t c_I(\widehat{\phi}_h^{n+1} + \widehat{\phi}_h^n, \widehat{u}_h^{n+1}) = \Delta t g(f_p^{n+1/2}, \widehat{\phi}_h^{n+1} + \widehat{\phi}_h^n).\end{aligned}$$

Add and consider the sum of the two coupling terms

$$\begin{aligned}Coupling &= \Delta t \left[c_I(\widehat{\phi}_h^n, \widehat{u}_h^{n+1} + \widehat{u}_h^n) - c_I(\widehat{\phi}_h^{n+1} + \widehat{\phi}_h^n, \widehat{u}_h^{n+1})\right]\\ &= \Delta t \left[c_I(\widehat{\phi}_h^n, \widehat{u}_h^n) - c_I(\widehat{\phi}_h^{n+1}, \widehat{u}_h^{n+1})\right].\end{aligned}$$

Let us denote $C^n = c_I(\widehat{\phi}_h^n, \widehat{u}_h^n)$ and

$$\begin{aligned}E^n &= ||\widehat{u}_h^n||_f^2 + gS_0||\widehat{\phi}_h^n||_p^2,\\ D^n &= \frac{1}{2} a_f(\widehat{u}_h^{n+1} + \widehat{u}_h^n, \widehat{u}_h^{n+1} + \widehat{u}_h^n) + \frac{1}{2} a_p(\widehat{\phi}_h^{n+1} + \widehat{\phi}_h^n, \widehat{\phi}_h^{n+1} + \widehat{\phi}_h^n).\end{aligned}$$

Adding the two energy estimates and using the above reduction of the coupling term reduces the total energy estimate to

$$\begin{aligned}&\left[E^{n+1} - \Delta t C^{n+1}\right] - [E^n - \Delta t C^n]\\ &+\Delta t D^n = \Delta t \Big((f_f^{n+1/2}, \widehat{u}_h^{n+1} + \widehat{u}_h^n)_f + g(f_p^{n+1/2}, \widehat{\phi}_h^{n+1} + \widehat{\phi}_h^n)_p \Big).\end{aligned}$$

Sum this inequality from $n = 0$ to $N - 1$. The energy inequality thus follows provided

$$E^N - \Delta t C^N \geq \alpha E^N \quad \text{for every } N.$$

Consider $\Delta t C^N$. Dropping super and subscripts and applying Lemma 5.1.2 gives

$$\begin{aligned}\Delta t|C^N| &\leq \Delta t g C(\Omega_f) C(\Omega_p) C_{INV} h^{-1} ||u||_f ||\phi||_p \\ &\leq \frac{gS_0}{2}||\phi||_p^2 + \frac{\Delta t^2}{2gS_0}\left[gC(\Omega_f)C(\Omega_p)C_{INV}h^{-1}\right]^2 ||u||_f^2.\end{aligned}$$

We thus have stability provided

$$\frac{\Delta t^2}{2gS_0}\left[gC(\Omega_f)C(\Omega_p)C_{INV}h^{-1}\right]^2 < 1 \text{ or } \Delta t < \Delta T_6.$$

Under the timestep restriction $\Delta t \leq \sqrt{1-\alpha}\Delta T_6$ which is implied by $\Delta t \leq (1-\alpha)\Delta T_6$ we have

$$||\widehat{u}_h^{n+1}||_f^2 + gS_0||\widehat{\phi}_h^{n+1}||_p^2 - \Delta t c_I(\widehat{\phi}_h^{n+1}, \widehat{u}_h^{n+1}) \geq \alpha\left[||\widehat{u}_h^{n+1}||_f^2 + gS_0||\widehat{\phi}_h^{n+1}||_p^2\right].$$

This proves stability of the first half step. $\square$

Now we consider the second half step.

Theorem 5.3.5 (Stability of one step of CNsplit)**.** *Consider (CNsplit-b). Suppose there is an $\alpha, 0 < \alpha < 1$, such that Δt satisfies the time step restriction*

$$\Delta t \leq (1-\alpha)\Delta T_6$$

Then, it is stable over long time intervals. Specifically, for every $N \geq 1$

$$\begin{aligned}&\alpha\left[||\widetilde{u}_h^N||_f^2 + gS_0||\widetilde{\phi}_h^N||_p^2\right] + \Delta t\sum_{n=0}^{N-1}\frac{1}{2}\left[a_f(\widetilde{u}_h^{n+1}+\widetilde{u}_h^n, \widetilde{u}_h^{n+1}+\widetilde{u}_h^n) + a_p(\widetilde{\phi}_h^{n+1}+\widetilde{\phi}_h^n, \widetilde{\phi}_h^{n+1}+\widetilde{\phi}_h^n)\right] \\ &\leq \left[||\widetilde{u}_h^0||_f^2 + gS_0||\widetilde{\phi}_h^0||_p^2 + \Delta t c_I(\widetilde{\phi}_h^0, \widetilde{u}_h^0)\right] \\ &\qquad + \Delta t\sum_{n=0}^{N-1}\left[(f_f^{n+1/2}, \widetilde{u}_h^{n+1}+\widetilde{u}_h^n)_f + g(f_p^{n+1/2}, \widetilde{\phi}_h^{n+1}+\widetilde{\phi}_h^n)_p\right].\end{aligned}$$

The proof is essentially the same as for the first half-step and is thus omitted.

5.4 NUMERICAL EXPERIMENTS

We present numerical experiments to test the algorithms proposed in this chapter. First, using the exact solution introduced in [98], we test accuracy. One new aspect is that we also test mass conservation errors across the interface I, the last columns of Tables 5.1 through 5.4. While mixed methods are expected to have better conservation properties than the non-mixed formulation we use, we find the mass conservation errors are quite acceptable in this limited test. Second, we test stability over longer time intervals and small values of $k_{\min}$ and S_0. In these tests the splitting based partitioned methods appear to be stable for larger timestep sizes than the IMEX based partitioned methods tested previously in Chapter 4 and that good partitioned methods are available when one parameter is small. When both are small, a very small timestep is required for stability for the four methods. The code was implemented using the software package *FreeFEM++*.

5.4.1 Test 1: Convergence rates.

For the first test we select the velocity and pressure field given in [98]. Let the domain Ω be composed of $\Omega_f = (0,1) \times (1,2)$ and $\Omega_p = (0,1) \times (0,1)$ with the interface $\Gamma = (0,1) \times \{1\}$. The exact velocity field is given by

$$
\begin{aligned}
u_1(x,y,t) &= (x^2(y-1)^2 + y)\cos t\,,\\
u_2(x,y,t) &= \left(-\frac{2}{3}x(y-1)^3 + 2 - \pi\sin(\pi x)\right)\cos t\,,\\
p(x,y,t) &= (2-\pi\sin(\pi x))\sin\left(\frac{\pi}{2}y\right)\cos t\,,\\
\phi(x,y,t) &= (2-\pi\sin(\pi x))(1-y-\cos(\pi y))\cos t.
\end{aligned}
$$

To check the rates of convergence, take the time interval $0 \le t \le 1$ and in this first test the physical parameters ρ, g, μ, K, S_0 and α are simply set to 1. We utilize Taylor-Hood $P2-P1$ finite elements for the Stokes subdomain and continuous piecewise quadratic finite element for the Darcy subdomain. The boundary conditions on the exterior boundaries (not including the interface I) are inhomogeneous Dirichlet: $u_h = u_{exact}, \phi_h = \phi_{exact}$ on the exterior boundaries. The initial data and source terms are chosen to correspond the exact solution.

For convenience, we denote $\|\cdot\|_I = \|\cdot\|_{L^2(0,T;L^2(I))}$, $\|\cdot\|_\infty = \|\cdot\|_{L^\infty(0,T;L^2(\Omega_{f|p}))}$ and $\|\cdot\|_2 = \|\cdot\|_{L^2(0,T;L^2(\Omega_{f|p}))}$. We show below in Table 5.1–5.4 the errors of approximated velocity and Darcy pressure in several different norms. In the last columns of the tables are the errors in mass conservation on I.

From the tables, we see that SDsplit, BEsplit1 and BEsplit2 are first order methods while CNsplit is second order accuracy, as predicted. Further, the error levels of the first order methods seem quite acceptable as are the mass conservation errors across I.

h	$\|u-u_h\|_\infty$	$\|\nabla u-\nabla u_h\|_2$	$\|\phi-\phi_h\|_\infty$	$\|\phi-\phi_h\|_I$	$\|(u_h^f-u_h^p)\cdot\mathbf{n}\|_I$
1/5	2.921e-3	7.194e-2	4.030e-3	4.626e-3	2.280e-1
1/10	8.954e-4	2.181e-2	1.183e-2	1.661e-3	4.070e-2
1/20	4.198e-4	5.751e-3	6.367e-4	9.080e-4	9.566e-3
1/40	2.105e-4	1.959e-3	3.399e-4	4.977e-4	2.376e-3
1/80	1.057e-4	8.328e-4	1.771e-4	2.668e-4	5.047e-4

Table 5.1: The convergence performance for SDsplit method. The time step Δt is set to be equal to mesh size h.

h	$\|u-u_h\|_\infty$	$\|\nabla u-\nabla u_h\|_2$	$\|\phi-\phi_h\|_\infty$	$\|\phi-\phi_h\|_I$	$\|(u_h^f-u_h^p)\cdot\mathbf{n}\|_I$
1/5	3.448e-3	7.371e-2	4.289e-3	4.766e-3	2.278e-1
1/10	1.657e-3	2.343e-2	1.163e-3	1.665e-3	4.694e-2
1/20	8.405e-4	7.200e-3	5.409e-4	8.126e-3	9.531e-3
1/40	4.239e-4	2.923e-3	2.705e-4	4.081e-4	2.369e-3
1/80	2.128e-4	1.367e-3	1.356e-4	2.046e-4	5.035e-4

Table 5.2: The convergence performance for BEsplit1 method. The time step Δt is set to be equal to mesh size h.

h	$\|u-u_h\|_\infty$	$\|\nabla u-\nabla u_h\|_2$	$\|\phi-\phi_h\|_\infty$	$\|\phi-\phi_h\|_I$	$\|(u_h^f-u_h^p)\cdot\mathbf{n}\|_I$
1/5	2.768e-3	7.130e-2	9.738e-3	1.649e-2	2.547e-1
1/10	9.282e-4	2.164e-2	4.833e-3	8.441e-3	7.087e-2
1/20	4.390e-4	5.610e-3	2.447e-3	4.231e-3	2.722e-2
1/40	2.196e-4	1.860e-3	1.233e-3	2.119e-3	1.212e-2
1/80	1.100e-4	7.739e-4	6.188e-4	1.060e-3	6.258e-3

Table 5.3: The convergence performance for BEsplit2 method. The time step Δt is set to be equal to mesh size h.

h	$\|u-u_h\|_\infty$	$\|\nabla u-\nabla u_h\|_2$	$\|\phi-\phi_h\|_\infty$	$\|\phi-\phi_h\|_I$	$\|(u_h^f-u_h^p)\cdot\mathbf{n}\|_I$
1/5	3.044e-3	7.789e-2	7.647e-3	1.112e-2	2.284e-1
1/10	4.323e-4	2.259e-2	1.520e-3	2.085e-3	4.795e-2
1/20	5.466e-5	5.193e-3	3.654e-4	4.961e-4	9.849e-3
1/40	7.829e-6	1.270e-3	9.081e-5	1.227e-4	2.487e-3
1/80	1.573e-6	3.187e-4	2.265e-5	3.056e-5	5.273e-4

Table 5.4: The convergence performance for CNsplit method. The time step Δt is set to be equal to mesh size h.

5.4.2 Test 2: Stability in case of small parameters.

In this test, we compare the performance of our proposed methods for uncoupling Stokes-Darcy flows for three cases: small $k_{\min}$ and $O(1)$ S_0, $O(1)$ $k_{\min}$ and small S_0, and small $k_{\min}$ and small S_0. The last case is separated into several sub-cases to distinguish 'extremely small' and 'moderately small' S_0 and $k_{\min}$. Our test here is to check the largest timestep for which the four methods are stable over long time intervals. Since the problem is linear we can take the body force terms to be zero. The true solution decays as $t \to \infty$, so any growth in the approximate solution is an instability. We take the initial condition

$$
\begin{aligned}
u_1(x,y,0) &= (x^2(y-1)^2 + y)\,,\\
u_2(x,y,0) &= \left(-\frac{2}{3}x(y-1)^3 + 2 - \pi\sin(\pi x)\right)\,,\\
p(x,y,0) &= (2-\pi\sin(\pi x))\sin\left(\frac{\pi}{2}y\right)\,,\\
\phi(x,y,0) &= (2-\pi\sin(\pi x))(1-y-\cos(\pi y)).
\end{aligned}
$$

Define the kinetic energy $E^n = \|u_h^n\|_f^2 + \|\phi_h^n\|_p^2$. The final time T_f in our experiment is 10.0 and the system parameters are simply set to be 1.0, except hydraulic conductivity $k_{\min}$ and storativity coefficient S_0. We take the mesh size $h = 1/10$ and run the experiment with different time-step sizes. With each value of Δt, we compute the kinetic energy at final time, i.e., E^N where $N = T_f/\Delta t$. However, we use 10^{250} as a 'cut-off' value for E^n. If E^n exceeds 10^{250} at some n, we stop and output E^n, the kinetic energy at that point. By looking at these figures, we can estimate the largest Δt for which numerical methods is stable.

Since Stokes flows and porous media flows are not typically high velocity flows, and since the domains are large with associated significant costs for subdomain solves, the ability to take large timesteps is desirable. In the stability tests for small parameter $k_{\min}$ or S_0 the three first order methods are superior. They are stable for larger timesteps, as predicted by the theory. The CNsplit method generally requires a much smaller timestep to attain stability. Thus, in some of the figures, the largest timesteps needed for the stability of CNsplit are not shown in some cases. To present the CNsplit case, Figure 5.7 gives a graph showing stability of CNsplit alone with numerous small values of S_0 and $k_{\min}$.

5.5 CONCLUSION

In both our analysis and tests on problems k_{min} and S_0 are small, it seems that stability over long time intervals (and the associated time step restriction) is a key issue in uncoupling the Stokes-Darcy problem. With one small parameter, the first order splitting methods had significant advantages in stability and are a good option when $k_{\min}$ or S_0 is small.

Many other open problems remain. Finding partitioned methods stable for large time steps when both $k_{\min}$, S_0 are small is an open problem. Further, while the first order methods gave acceptable error levels, more accuracy is always desirable. The stability of higher order partitioned methods for large timesteps and small parameters also is also largely an open problem. We have not tried to optimize the dependence of the timestep barriers upon the domain size. This is an important and open problem, especially for domains with large aspect ratios. At this point we do not know if a partitioned method exists with timestep restriction independent of $S_0, k_{\min}, \nu$ and h. If $k_{\min}, \nu \to 0$ the problem reduces to $u_t + C\phi = 0$ and $\phi_t - Cu = 0$ and any such algorithm would be an explicit method for an abstract wave-like equation written as a first order system. The behavior of numerical methods (both partitioned time stepping methods and iterative decoupling methods for use with monolithic time discretizations) in the quasi-static limit (as $S_0 \to 0$) is an open question critical in applications to aquifers since quasi static models are common, e.g., [27] for an example and [96] for a first step to its resolution. In many problems k_{min} and S_0 are both small and the double asymptotics of both parameters is important and open. Since fluid flow acts on different time scales in free flow and in porous media, developing algorithms with good properties that allow different time step sizes in the two domains (multi-rate or asynchronous methods) is an important and largely open challenge.

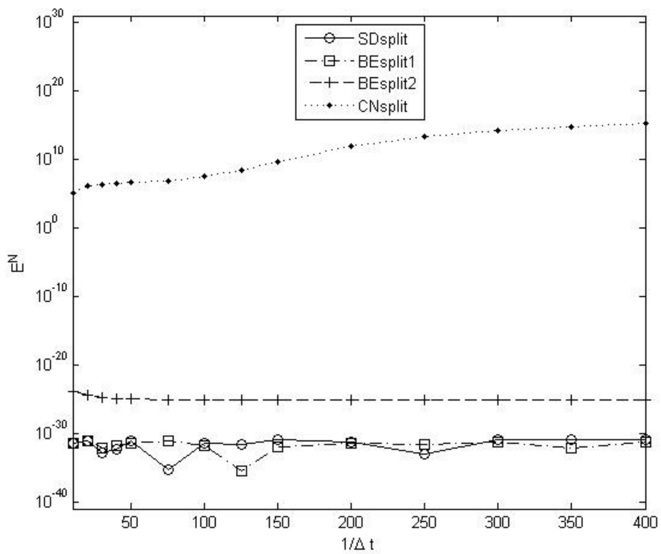

Figure 5.1: E^N using different time step sizes and splitting methods with $k_{\min} = 1$ and $S_0 = 10^{-12}$.

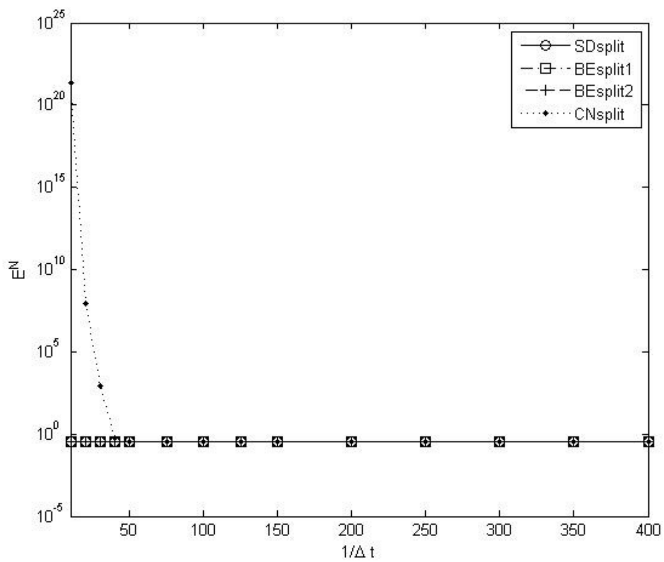

Figure 5.2: E^N using different time step sizes and splitting methods with $k_{\min} = 10^{-12}$ and $S_0 = 1$.

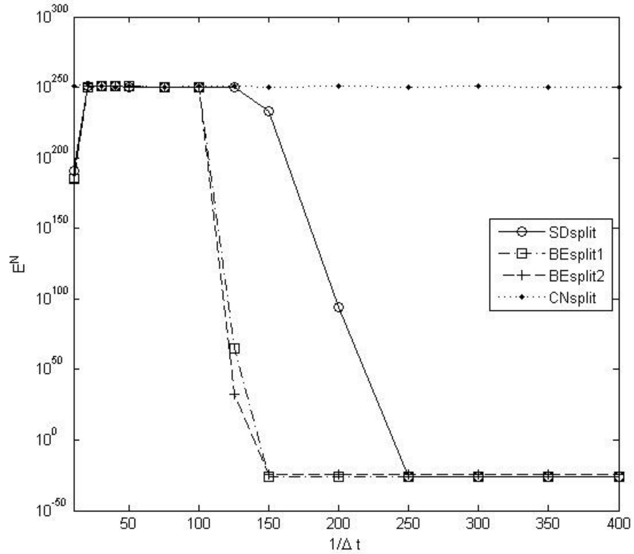

Figure 5.3: E^N using different time step sizes and splitting methods with $k_{\min} = 10^{-3}$ and $S_0 = 10^{-3}$.

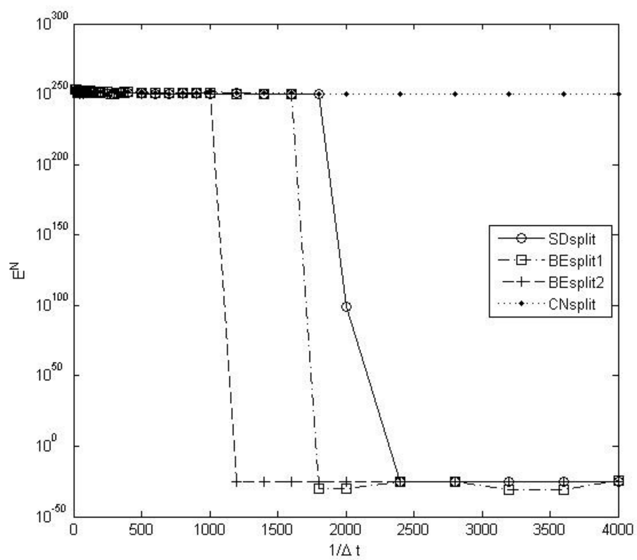

Figure 5.4: E^N using different time step sizes and splitting methods with $k_{\min} = 10^{-4}$ and $S_0 = 10^{-4}$.

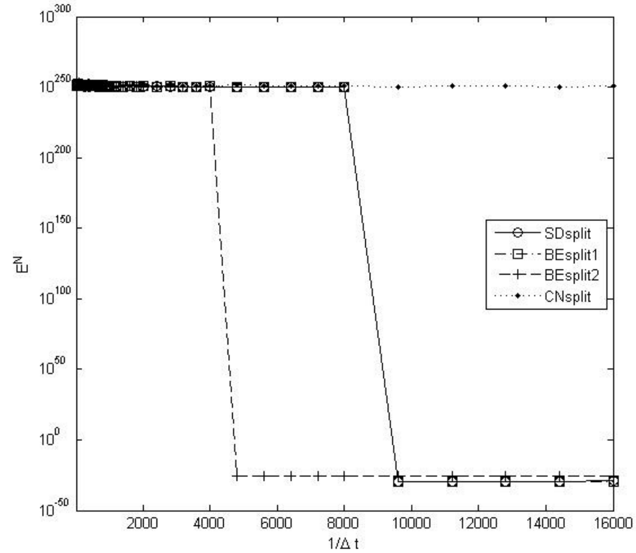

Figure 5.5: E^N using different time step sizes and splitting methods with $k_{\min} = 10^{-4}$ and $S_0 = 10^{-12}$.

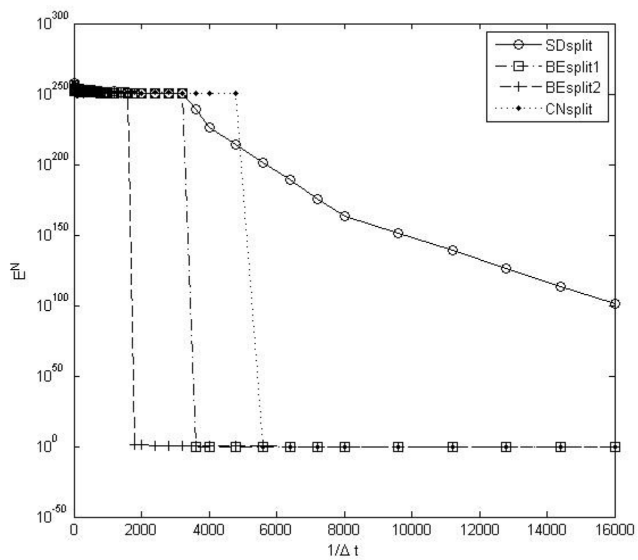

Figure 5.6: E^N using different time step sizes and splitting methods with $k_{\min} = 10^{-12}$ and $S_0 = 10^{-4}$.

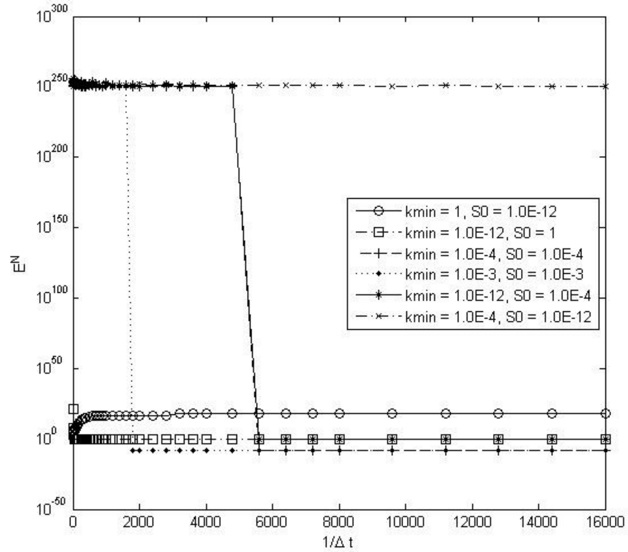

Figure 5.7: Stability of CNsplit at different small values of $k_{\min}$ and S_0.

6.0 CONCLUDING REMARKS AND FUTURE RESEARCH

The major contribution of this work is the development and analysis of partitioned methods for three coupled fluid flow problems:

1. uncoupled variational multiscale stabilization of turbulence flows,
2. partitioned time stepping methods for magnetohydrodynamics flows,
3. partitioned time stepping methods for Stokes-Darcy problems.

Our methods have substantial algorithmic advantage, since they effectively break the complex coupled system into the subproblems and allow the use of optimized and legacy codes. By this way, they help to reduce the technical costs and programming effort. It has been shown that the proposed algorithms are stable and convergent at the optimal rates. In particular, long time and uniform in time stability are obtained for Stokes-Darcy flows, which surpasses previous results. The goal of any uncoupled method is to give results not appreciably worse than the associated fully coupled approach (which is expected to be more accurate). In the numerical experiments presented herein, our methods well meet this goal.

For uncoupling a coupled problem, our methods face some limitations as a trade-off for algorithmic advantage. The time stepping methods normally require time step restrictions for stability. These conditions are particularly troublesome in applications involving small or large physical parameters. We partially address the issue in this thesis; however, schemes with stronger stability properties are still in need in many cases. Also, deriving the exact dependence of the stability and/or error behavior on model parameters remains largely an open question. Certainly, studying higher order accurate uncoupling strategies, or strategies which allow the use of different time step and mesh size for subproblem solvers is another important and promising direction for future works. The following research projects would help develop further computational capabilities for complex flow systems:

1. Studying how to induce VMS stabilization in Step 2 when Step 1 is the result from a *black box* flow code. We need to analyze the algorithm when different meshes are used for Steps 1 and 2 and estimate the extra error caused by interpolating the velocity between the postprocessing step's mesh and the code's mesh.
2. Developing algorithms with higher order time accuracy for MHD flows, still allowing large time steps. Methods with time step restrictions should be considered, focusing on using larger time steps than are currently possible.
3. Developing partitioned algorithms for nonlinear coupling in full MHD flows.
4. Developing algorithms with higher order time accuracy for Stokes-Darcy flows, allowing large time steps when both $k_{\min}$ and S_0 are small.
5. Studying the mass conservation errors across the interface I for the Stokes-Darcy flow. One interesting direction is developing and analyzing the combination of uncoupling schemes and mixed formulations, which are expected to have better conservation properties.
6. It should be checked that the numerical methods in this thesis are adaptable to equations with more realistic physics.

There are many other multiphysics flow models which are widely used in science and technology, but whose computational simulation was not well developed. It is worth studying uncoupling strategies for those models. Here are another problem we are investigating:

6.1 FAST-SLOW WAVE SPLITTING FOR ATMOSPHERIC AND OCEAN CODES

The Earth's atmosphere supports many types of wave motion, which are vastly different in time and length scales: Rossby waves, gravity waves and sound waves. Rossby waves propagate more slowly than gravity waves, which in turn move more slowly than sound waves. If time derivatives in the equations governing atmospheric flow are approximated using explicit finite difference schemes, the maximum stable time step will be limited by the speed of the fastest-moving wave. Since sound waves play no direct role in atmospheric and ocean circulations, they need not be accurately simulated to obtain a good weather forecast. The quality of the weather forecast depends solely on the ability of the model to accurately simulate atmospheric disturbances that evolve on much slower time scales. To obtain a reasonably efficient numerical model for the simulation of atmospheric circulations, it is necessary to circumvent the severe time step restrictions associated with sound wave propagation and bring the maximum stable time step into closer agreement with the time step limitations arising from accuracy considerations, [43].

While fully implicit time differences successfully meet this goal by treating sound waves in a stable manner, they require the solution of a nonlinear algebraic system at each time step and are generally thought to be less efficient than implicit-explicit (IMEX) methods in which only those terms responsible for linear sound wave propagation are evaluated using implicit differences and the remaining terms are integrated using explicit formulas. One of the most common time discretizations in atmospheric and ocean codes is the combination of the Crank-Nicolson and Leap-Frog methods, usually abbreviated as CNLF. The usual description is that implicit CN is used to discretized physical effects corresponding to fast waves and low energy while explicit LF for high energy slow waves. In spite of the importance of the application and the large computational experience with the method CNLF, there has been little analysis of CNLF for the application and beyond root condition stability.

We study to give an analytic, nonlinear energy stability and convergence analysis of CNLF based on a splitting of the NSE + rotation/Coriolis force, a great simplification of the geophysical flow. The timestep restriction from the LF component can still be too restrictive if the normal splitting into fast and slow modes is not perfectly done. We develop a new CNLF stabilization which does not require any timestep condition for stability.

BIBLIOGRAPHY

[1] H. Alfvén, *Existence of electromagnetic-hydrodynamic waves*, Nature, 150 (1942), p. 405.

[2] P. Angot, *Analysis of singular perturbations on the Brinkman problem for fictitious domain models of viscous flows*, Math. Methods Appl. Sci., 22 (1999), pp. 1395–1412.

[3] M. Anitescu, F. Pahlevani, and W. Layton, *Unconditional stability for numerical scheme combining implicit timestepping for local effects and explicit timestepping for nonlocal effects*, Electron. Trans. Numer. Anal., 18 (2004), pp. 174–187 (electronic).

[4] T. Apel and G. Matthies, *Non-conforming, anisotropic, rectangular finite elements of arbitrary order for the Stokes problem*, SIAM J. Numer. Anal., 46 (2008), pp. 1867–1891.

[5] U. M. Ascher, S. J. Ruuth, and B. T. R. Wetton, *Implicit-explicit methods for time-dependent partial differential equations*, SIAM J. Numer. Anal., 32 (1995), pp. 797–823.

[6] W. Bangerth, R. Hartmann, and G. Kanschat, *deal.ii — a general purpose object oriented finite element library*, ACM Trans. Math. Software, 33 (2007).

[7] ——, *deal.ii differential equations analysis library*, tech. report, 2007.

[8] D. Barbato, L. C. Berselli, and C. R. Grisanti, *Analytical and numerical results for the rational large eddy simulation model*, J. Math. Fluid Mech., 9 (2007), pp. 44–74.

[9] L. Barleon, V. Casal, and L. Lenhart, *MHD flow in liquid-metal-cooled blankets*, Fusion Engineering and Design, (1991), pp. 401–412.

[10] Y. Bazilevs, V. Calo, T. Tezduyar, and T. Hughes, *Yzβ discontinuity capturing for advection-dominated processes with application to arterial drug delivery*, Int. J. Methods Fluids, 54 (2007), pp. 593–608.

[11] J. Bear, *Hydraulics of Groundwater*, McGraw-Hill, New York, 1979.

[12] G. Beavers and D. Joseph, *Boundary conditions at a naturally permeable wall*, J. Fluid Mech., 30 (1967), pp. 197–207.

[13] R. Bensow and M. Larson, *Residual based VMS subgrid modeling for vortex flows*, Comput. Methods Appl. Mech. Engrg., 199 (2010), pp. 802–809.

[14] L. Berselli, T. Iliescu, and W. Layton, *Mathematics of large eddy simulation of turbulent flows*, Scientific Computation, Springer-Verlag, Berlin, 2006.

[15] L. C. Berselli, *On the large eddy simulation of the Taylor-Green vortex*, J. Math. Fluid Mech., 7 (2005), pp. S164–S191.

[16] S. C. Brenner and L. R. Scott, *The mathematical theory of finite element methods*, vol. 15 of Texts in Applied Mathematics, Springer-Verlag, New York, 1994.

[17] A. N. Brooks and T. J. Hughes, *Streamline Upwind/Petrov-Galerkin formulations for convection dominated flows with particular emphasis on the incompressible Navier-Stokes equations*, Comp. Meth. Appl. Mech. Engrg., 32 (1982), pp. 199–259.

[18] E. Burman and M. A. Fernández, *Stabilized explicit coupling for fluid-structure interaction using Nitsche's method*, C. R. Math. Acad. Sci. Paris, 345 (2007), pp. 467–472.

[19] ——, *Stabilization of explicit coupling in fluid-structure interaction involving fluid incompressibility*, Comput. Methods Appl. Mech. Engrg., 198 (2009), pp. 766–784.

[20] M. Cai, M. Mu, and J. Xu, *Preconditioning techniques for a mixed Stokes/Darcy model in porous media applications*, J. Comput. Appl. Math., 233 (2009), pp. 346–355.

[21] Y. Cao, M. Gunzburger, X. He, and X. Wang, *Parallel, non-iterative, multi-physics domain decomposition methods for time-dependent Stokes-Darcy systems*, tech. report, 2011.

[22] Y. Cao, M. Gunzburger, X.-M. He, and X. Wang, *Robin-Robin domain decomposition methods for the steady-state Stokes-Darcy system with the Beavers-Joseph interface condition*, Numer. Math., 117 (2010), pp. 601–629.

[23] Y. Cao, M. Gunzburger, X. Hu, F. Hua, X. Wang, and W. Zhao, *Finite element approximations for Stokes-Darcy flow with Beavers-Joseph interface conditions*, SIAM J. Numer. Anal., 47 (2010), pp. 4239–4256.

[24] Y. Cao, M. Gunzburger, F. Hua, and X. Wang, *Coupled Stokes-Darcy model with Beavers-Joseph interface boundary condition*, Commun. Math. Sci., 8 (2010), pp. 1–25.

[25] P. Causin, J. F. Gerbeau, and F. Nobile, *Added-mass effect in the design of partitioned algorithms for fluid-structure problems*, Comput. Methods Appl. Mech. Engrg., 194 (2005), pp. 4506–4527.

[26] A. Çeşmelioğlu and B. Rivière, *Analysis of weak solutions for the fully coupled Stokes-Darcy transport problem*, tech. report, Univ. of Pittsburgh.

[27] ——, *Analysis of time-dependent Navier–Stokes flow coupled with Darcy flow*, J. Numerical Math., 16 (2008), pp. 249–280.

[28] A. Chorin, *Numerical solution for the Navier-Stokes equations*, Math. Comp., 22 (1968), pp. 745–762.

[29] G. Comte-Bellot and S. Corrsin, *Simple Eulerian time correlation of full- and narrow-band velocity signals in grid-generated, 'isotropic' turbulence*, J. Fluid Mech., 48 (1971), pp. 273–337.

[30] J. M. Connors, J. S. Howell, and W. J. Layton, *Partitioned time stepping for a parabolic two domain problem*, SIAM J. Numer. Anal., 47 (2009), pp. 3526–3549.

[31] ——, *Decoupled time stepping methods for fluid-fluid interaction*, SIAM J. Numer. Anal., 50 (2012), pp. 1297–1319.

[32] J. M. Connors and A. Miloua, *Partitioned time discretization for parallel solution of coupled ODE systems*, BIT Numerical Mathematics, (2010), pp. 1–21. 10.1007/s10543-010-0295-z.

[33] M. Crouzeix, *Une méthode multipas implicite-explicite pour l'approximation des équations d'évolution paraboliques*, Numer. Math., 35 (1980), pp. 257–276.

[34] P. A. Davidson, *Magnetohydrodynamics in material processing*, Annu. Rev. Fluid Mech., 31 (1999), pp. 273–300.

[35] ——, *An introduction to magnetohydrodynamics*, Cambridge Texts in Applied Mathematics, Cambridge University Press, Cambridge, 2001.

[36] M. Discacciati, *Domain decomposition methods for the coupling of surface and groundwater flows*, PhD thesis, Ecole Polytechnique Federale de Lausanne, Switzerland, 2004.

[37] ——, *Numerical approximation of a steady MHD problem*, no. 60 in Domain decomposition methods in science and engineering XVII, Springer, Berlin, 2008, pp. 313–320. Lect. Notes Comput. Sci. Eng.

[38] M. Discacciati, E. Miglio, and A. Quarteroni, *Mathematical and numerical models for coupling surface and groundwater flows*, Appl. Numer. Math., 43 (2002), pp. 57–74. 19th Dundee Biennial Conference on Numerical Analysis (2001).

[39] M. Discacciati and A. Quarteroni, *Analysis of a domain decomposition method for the coupling of Stokes and Darcy equations*, in Numerical mathematics and advanced applications, Springer Italia, Milan, 2003, pp. 3–20.

[40] ——, *Convergence analysis of a subdomain iterative method for the finite element approximation of the coupling of Stokes and Darcy equations*, Comput. Vis. Sci., 6 (2004), pp. 93–103.

[41] ——, *Navier-Stokes/Darcy coupling: modeling, analysis, and numerical approximation*, Rev. Mat. Complut., 22 (2009), pp. 315–426.

[42] M. Discacciati, A. Quarteroni, and A. Valli, *Robin-Robin domain decomposition methods for the Stokes-Darcy coupling*, SIAM J. Numer. Anal., 45 (2007), pp. 1246–1268 (electronic).

[43] D. R. Durran, *Numerical Methods for Fluid Dynamics*, vol. 32 of Texts in Applied Mathematics, Springer, 2010.

[44] V. Ervin, W. Layton, and M. Neda, *Numerical analysis of filter-based stabilization for evolution equations*, SIAM J. Numer. Anal., (2012), pp. 2307–2335.

[45] J. Frank, W. Hundsdorfer, and J. Verwer, *Stability of Implicit-Explicit linear multistep methods*, tech. report, Centrum Wiskunde and Informatica (CWI), 1996.

[46] V. Girault and P.-A. Raviart, *Finite element methods for Navier-Stokes equations*, vol. 5 of Springer Series in Computational Mathematics, Springer-Verlag, Berlin, 1986. Theory and algorithms.

[47] V. Girault and L. Scott, *A quasi-local interpolation operator preserving the discrete divergence*, Calcolo, 40 (2003), pp. 1–19.

[48] S. Gottlieb, F. Tone, C. Wang, X. Wang, and D. Wirosoetisno, *Long time stability of a classical efficient scheme for two-dimensional Navier-Stokes equations*, SIAM J. Numer. Anal., 50 (2012), pp. 126–150.

[49] V. Gravemeier, *The variational multiscale method for laminar and turbulent flow*, Arch. Comput. Meth. Engrg., 13 (2006), pp. 249–324.

[50] V. Gravemeier, M. Gee, M. Kronbichler, and W. Wall, *An algebraic variational multiscale-multigrid method for large eddy simulation of turbulent flow*, Comp. Meth. Appl. Mech. Engrg., 199 (2010), pp. 853–864.

[51] J.-L. Guermond, *Stabilization of Galerkin approximations of transport equations by subgrid modeling*, ESAIM: Mathematical Modelling and Numerical Analysis, 33 (1999), pp. 1293–1316.

[52] J. L. Guermond and P. D. Minev, *Mixed finite element approximation of an MHD problem involving conducting and insulating regions: The 3D case*, Numer. Methods Partial Differential Equations, 19 (2003), pp. 709–731.

[53] M. Gunzburger, A. Meir, and J. Peterson, *On the existence, uniqueness, and finite element approximation of solutions of the equations of stationary, incompressible magnetohydrodynamics*, Math. Comp., 56 (1991), pp. 523–563.

[54] M. D. Gunzburger, *Finite Element Methods for Viscous Incompressible Flows - A Guide to Theory, Practices, and Algorithms*, Academic Press, 1989.

[55] H. Hashizume, *Numerical and experimental research to solve MHD problem in liquid-blanket system*, Fusion Engineering and Design, 81 (2006), pp. 1431–1438.

[56] F. Hecht and O. Pironneau, *Freefem++*, webpage: http://www.freefem.org.

[57] J. G. Heywood and R. Rannacher, *Finite-element approximation of the nonstationary Navier-Stokes problem. IV. Error analysis for second-order time discretization*, SIAM J. Numer. Anal., 27 (1990), pp. 353–384.

[58] J. Hietala, K. Vakkilainen, and T. Kairesalo, *Community resistance and change to nutrient enrichment and fish manipulation in a vegetated lake littoral*, Freshwater Biol., 49 (2004), pp. 1525–1537.

[59] H. Holden, K. Karlsen, K.-A. Lie, and N. Risebro, *Splitting methods for Partial Differential Equations with rough solutions*, European Math. Soc., Zurich, 2010.

[60] R. Hoppe, P. Porta, and Y. Vassilevski, *Computational issues related to iterative coupling of subsurface and channel flows*, Calcolo, 44 (2007), pp. 1–20.

[61] T. Hughes, *Multiscale phenomena: Green's functions, the Dirichlet-to-Neumann formulation, subgrid scale models, bubbles, and the origins of stabilized methods*, Comp. Meth. Appl. Mech. Engrg., 127 (1995), pp. 387–401.

[62] T. Hughes, L. Mazzei, and K. Jansen, *Large eddy simulation and the variational multiscale method*, Comput. Visual. Sci., (2000), pp. 47–59.

[63] W. Hundsdorfer and J. Verwer, *Numerical solution of time-dependent advection-diffusion-reaction equations*, Springer, Berlin, 2003.

[64] R. Ingram, *Finite element approximation of non-solenoidal, viscous flows around porous and solid obstacles*, SIAM J. Numer. Anal., 49 (2011), pp. 491–520.

[65] W. Jäger and A. Mikelić, *On the interface boundary condition of Beavers, Joseph, and Saffman*, SIAM J. Appl. Math., 60 (2000), pp. 1111–1127 (electronic).

[66] B. Jiang, *A parallel domain decomposition method for coupling of surface and groundwater flows*, Comput. Methods Appl. Mech. Engrg., 198 (2009), pp. 947–957.

[67] V. John, *Large eddy simulation of turbulent incompressible flows*, vol. 34 of Lecture Notes in Computational Science and Engineering, Springer-Verlag, Berlin, 2004. Analytical and numerical results for a class of LES models.

[68] V. John and A. Kindl, *A variational multiscale method for turbulent flow simulation with adaptive large scale space*, J. Comp. Phy., 229 (2010), pp. 301–312.

[69] V. John and W. J. Layton, *Analysis of numerical errors in large eddy simulation*, SIAM J. Numer. Anal., 40 (2002), pp. 995–1020.

[70] A. Johnson, *Compilation of specific yields for various materials*, US Geological Survey Water Supply Paper 1667-D, (1967).

[71] N. Ju, *On the global stability of a temporal discretization scheme for the Navier-Stokes equations*, IMA J. Numer. Anal., 22 (2002), pp. 577–597.

[72] P. Knobloch, *On a variant of the local projection method stable in the SUPG norm*, Kybernetika, 45 (2009), pp. 634–645.

[73] ——, *On the application of local projection methods to convection-diffusion-reaction problems*, in BAIL Proceedings 2008, Springer-Verlag, Berlin, 2009, pp. 183–194.

[74] L. D. Landau and E. M. Lifshitz, *Electrodynamics of continuous media*, Course of Theoretical Physics, Vol. 8. Translated from the Russian by J. B. Sykes and J. S. Bell, Pergamon Press, Oxford, 1960.

[75] W. Layton, *A connection between subgrid scale eddy viscosity and mixed methods*, Appl. Math. Comput., 133 (2002), pp. 147–157.

[76] W. Layton, *Introduction to the numerical analysis of incompressible viscous flows*, vol. 6 of Computational Science & Engineering, Society for Industrial and Applied Mathematics (SIAM), Philadelphia, PA, 2008. With a foreword by Max Gunzburger.

[77] W. Layton, L. G. Rebholz, and C. Trenchea, *Modular nonlinear filter stabilization of methods for higher Reynolds numbers flow*, Journal of Mathematical Fluid Mechanics, 14 (2012), pp. 325–354.

[78] W. Layton, L. Röhe, and H. Tran, *Explicitly uncoupled variational multiscale stabilization of fluid flow*, Comput. Methods Appl. Mech. Engrg., 200 (2011), pp. 3183–3199.

[79] W. Layton, H. Tran, and C. Trenchea, *Numerical analysis of two partitioned methods for uncoupling evolutionary MHD flows*, submitted (2012).

[80] ——, *Stability of partitioned methods for magnetohydrodynamics flows at small magnetic Reynolds numbers*, Contemp. Math., to appear (2012).

[81] ——, *Analysis of long time stability and errors of two partitioned methods for uncoupling evolutionary groundwater - surface water flows*, SIAM J. Numer. Anal., 51 (2013), pp. 248–272.

[82] W. Layton, H. Tran, and X. Xiong, *Long time stability of four methods for splitting the evolutionary Stokes-Darcy problem into Stokes and Darcy sub-problems*, J. Comput. Appl. Math., 236 (2012), pp. 3198–3217.

[83] W. Layton and C. Trenchea, *Stability of two IMEX methods, CNLF and BDF2-AB2, for uncoupling systems of evolution equations*, Appl. Num. Math., 62 (2012), pp. 112–120.

[84] W. J. Layton, A. J. Meir, and P. G. Schmidt, *A two-level discretization method for the stationary MHD equations*, Electron. Trans. Numer. Anal., 6 (1997), pp. 198–210 (electronic).

[85] W. J. Layton, F. Schieweck, and I. Yotov, *Coupling fluid flow with porous media flow*, SIAM J. Numer. Anal., 40 (2003), pp. 2195–2218.

[86] D. Lilly, *The representation of small-scale turbulence in numerical simulation experiments*, in Proceedings IBM Scientific Computing Symposium on Environmental Sciences, vol. 320, Yorktown Heights, New York, 1967, pp. 195–210.

[87] T. F. Lin, J. B. Gilbert, and R. Kossowsky, *Sea water magnetohydrodynamic propulsion for next-generation undersea vehicles*, ONR annual report for period from Feb. 1, 1989 to Jan. 31, 1990, under contract no. N00014-89-J-1693, NTIS AD Number: A218318, (1990).

[88] G. Lube and M. Olshanskii, *Stable finite element calculations of incompressible flows using the rotation form of convection*, IMA J. Numer. Anal., 22 (2002), pp. 437–461.

[89] G. Lube, G. Rapin, and J. Löwe, *Local projection stabilization for incompressible flows: Equal-order vs. inf-sup stable interpolation*, Electronic Transactions on Numerical Analysis, 32 (2008), pp. 106–122.

[90] G. Marchuk, *Splitting and alternate direction methods*, in Handbook of Numerical Analysis, P. Ciarlet and J. Lions, eds., North Holland, Amsterdam, 1990, pp. 197–464.

[91] G. I. Marchuk, *Splitting Methods*, Nauka, Moscow, 1988.

[92] A. J. Meir, *The equations of stationary, incompressible magnetohydrodynamics with mixed boundary conditions*, Comput. Math. Appl., 25 (1993), pp. 13–29.

[93] A. J. Meir and P. G. Schmidt, *Variational methods for stationary MHD flow under natural interface conditions*, Nonlinear Anal., 26 (1996), pp. 659–689.

[94] ——, *Analysis and numerical approximation of a stationary MHD flow problem with nonideal boundary*, SIAM J. Numer. Anal., 36 (1999), pp. 1304–1332.

[95] E. Miglio, A. Quarteroni, and F. Saleri, *Coupling of free surface flow and groundwater flows*, Comput. & Fluids, 23 (2003), pp. 73–83.

[96] M. Moraiti, *On the quasistatic approximation in the Stokes-Darcy model of groundwatersurface water flows*, Journal of Mathematical Analysis and Applications, 394 (2012), pp. 796–808.

[97] M. Mu and J. Xu, *A two-grid method of a mixed Stokes-Darcy model for coupling fluid flow with porous media flow*, SIAM J. Numer. Anal., 45 (2007), pp. 1801–1813.

[98] M. Mu and X. Zhu, *Decoupled schemes for a non-stationary mixed Stokes-Darcy model*, Math. Comp., 79 (2010), pp. 707–731.

[99] M. Olshanskii and A. Reusken, *Navier-Stokes equations in rotation form: a robust multigrid solver for the velocity problem*, SIAM J. Sci. Comput., 23 (2002), pp. 1682–1706.

[100] ——, *Grad-div stabilization for the Stokes equations*, Math. Comp., 73 (2004), pp. 1699–1718.

[101] L. E. Payne, J. C. Song, and B. Straughan, *Continuous dependence and convergence results for Brinkman and Forchheimer models with variable viscosity*, R. Soc. Lond. Proc. Ser. A Math. Phys. Eng. Sci., 455 (1999), pp. 2173–2190.

[102] L. E. Payne and B. Straughan, *Analysis of the boundary condition at the interface between a viscous fluid and a porous medium and related modelling questions*, J. Math. Pures Appl., 9(77) (1998), pp. 317–354.

[103] J. Peterson, *On the finite element approximation of incompressible flows of an electrically conducting fluid*, Numer. Methods Partial Differential Equations, 4 (1988), pp. 57–68.

[104] P. H. Roberts, *An introduction to magnetohydrodynamics*, Elsevier, USA, 1967.

[105] L. Röhe and G. Lube, *Analysis of a variational multiscale method for Large-Eddy simulation and its application to homogeneous isotropic turbulence*, Comp. Meth. Appl. Mech. Engrg., 199 (2010), pp. 2331–2342.

[106] H.-G. Roos, M. Stynes, and L. Tobiska, *Robust Numerical Methods for Singularly Perturbed Differential Equations*, Springer, Berlin, 2008.

[107] P. Saffman, *On the boundary condition at the interface of a porous medium*, Stud. Appl. Math., 1 (1971), pp. 93–101.

[108] P. G. Schmidt, *A Galerkin method for time-dependent MHD flow with nonideal boundaries*, Commun. Appl. Anal., 3 (1999), pp. 383–398.

[109] L. Shan and H. Zheng, *Partitioned time stepping method for fully evolutionary Stokes-Darcy flow with Beavers-Joseph interface conditions*, SIAM J. Numer. Anal., 51 (2013), pp. 813–839.

[110] L. Shan, H. Zheng, and W. Layton, *Decoupled schemes with different time sizes for the time-dependent Stokes-Darcy model*, tech. report, Univ. Pittsburgh, http://www.math.pitt.edu/technical-reports, 2011.

[111] S. Smolentsev, R. Moreau, L. Bühler, and C. Mistrangelo, *MHD thermofluid issues of liquid-metal blankets: Phenomena and advances*, Fusion Engineering and Design, 85 (2010), pp. 1196–1205.

[112] D. Tafti, *Comparison of some upwind-biased high-order formulations with a second-order central-difference scheme for time integration of the incompressible Navier-Stokes equations*, Comput. & Fluids, 25 (1996), pp. 647–665.

[113] G. Taylor, *On decay of vortices in a viscous fluid*, Phil. Mag., 46 (1923), pp. 671–674.

[114] G. I. Taylor and A. E. Green, *Mechanism of the production of small eddies from large ones*, Proceedings of the Royal Society of London. Series A, Mathematical and Physical Sciences, 158 (1937), pp. 499–521.

[115] F. Tone, *On the long-time h^2-stability of the implicit Euler scheme for the 2D magnetohydrodynamics equations*, J. Sci. Comput., 38 (2009), pp. 331–348.

[116] F. Tone and D. Wirosoetisno, *On the long-time stability of the implicit Euler scheme for the two-dimensional Navier-Stokes equations.*, SIAM J. Numer. Anal., 44 (2006), pp. 29–40.

[117] C. Trenchea, *Unconditional stability of a partitioned IMEX method for magnetohydrodynamics flows*, submitted (2012).

[118] A. Valli, G. Carey, and A. Coutinho, *On decoupled time step/subcycling and iteration strategies for multiphysics problems*, Commun. Numer. Methods Eng., 24 (2008), pp. 1941–1952.

[119] J. Varah, *Stability restrictions on second order, three level finite difference schemes for parabolic equations*, SIAM J. Numer. Anal., 17 (1980), pp. 300–309.

[120] D. Vassilev and I. Yotov, *Domain decomposition for coupled Stokes and Darcy flows*, tech. report, Univ. of Pittsburgh, 2011.

[121] J. Verwer, *Convergence and component splitting for the Crank-Nicolson Leap-Frog integration method*, tech. report, Centrum Wiskunde and Informatica (CWI), 2009.

[122] ——, *Component splitting for semi-discrete Maxwell equations*, BIT Numerical Mathematics, (2010), pp. 1–19. 10.1007/s10543-010-0296-y.

[123] X. Wang, *On the coupled continuum pipe flow model (CCPF) for flows in Karst aquifer*, Discrete Contin. Dyn. Syst. Ser. B, 13 (2010), pp. 489–501.

[124] N. Wilson, A. Labovsky, and C. Trenchea, *High accuracy method for magnetohydrodynamics system in Elsasser variables*, submitted (2013).

[125] N. Winowich and W. Hughes, *A finite element analysis of two dimensional MHD flow*, Liquid-Metal Flows and Magnetohydrodynamics, AIAA, New York, 1983.

[126] N. Yanenko, *The Method of Fractional Steps*, Springer, Berlin, 1971.

[127] G. Yuksel and R. Ingram, *Numerical analysis of a finite element, Crank-Nicolson discretization for MHD flow at small magnetic Reynolds number*, tech. report, University of Pittsburgh, 2011.